# Contents

# Chapter 7

# Hydrologic Processes

## 7.1 INTRODUCTION TO HYDROLOGY

### 7.1.1 What is Hydrology?

The U.S. National Research Council (1991) presented the following definition of hydrology:

> *Hydrology is the science that treats the waters of the Earth, their occurrence, circulation, and distribution, their chemical and physical properties, and their reaction with the environment, including the relation to living things. The domain of hydrology embraces the full life history of water on Earth.*

For purposes of this book we are interested in the engineering aspects of hydrology, or what we might call *engineering hydrology*. From this point of view we are mainly concerned with quantifying amounts of water at various locations (spatially) as a function of time (temporally) for surface water applications. In other words, we are concerned with solving engineering problems using hydrologic principles. This chapter is not concerned with the chemical properties of water and their relation to living things.

Books on hydrology include: Bedient and Huber (1992); Bras (1990); Chow (1964); Chow, Maidment, and Mays (1988); Gupta (1989); Maidment (1993); McCuen (1998); Ponce (1989); Singh (1992); Viessman and Lewis (1996); and Wanielista, Kersten, and Eaglin (1997).

### 7.1.2 The Hydrologic Cycle

The central focus of hydrology is the *hydrologic cycle*, consisting of the continuous processes shown in Figure 7.1.1. Water *evaporates* from the oceans and land surfaces to become water vapor that is carried over the earth by atmospheric circulation. The *water vapor* condenses and *precipitates* on the land and oceans. The precipitated water may be *intercepted* by vegetation, become overland flow over the ground surface, *infiltrate* into the ground, flow through the soil as *subsurface flow*, and discharge as *surface runoff*. Evaporation from the land surface comprises evaporation directly from soil and vegetation surfaces, and *transpiration* through plant leaves. Collectively these processes are called *evapotranspiration*. Infiltrated water may percolate deeper to recharge groundwater and later become *springflow* or *seepage* into streams also to become streamflow.

The hydrologic cycle can be viewed on a global scale as shown in Figure 7.1.2. As discussed by the U.S. National Research Council (1991): "As a global average, only about 57 percent of the precipitation that falls on the land ($P_l$) returns directly to the atmosphere ($E_l$) without reaching the ocean. The remainder is runoff ($R$), which find its way to the sea primarily by rivers but also through subsurface (groundwater) movement and by the calving of icebergs from glaciers and ice shelves

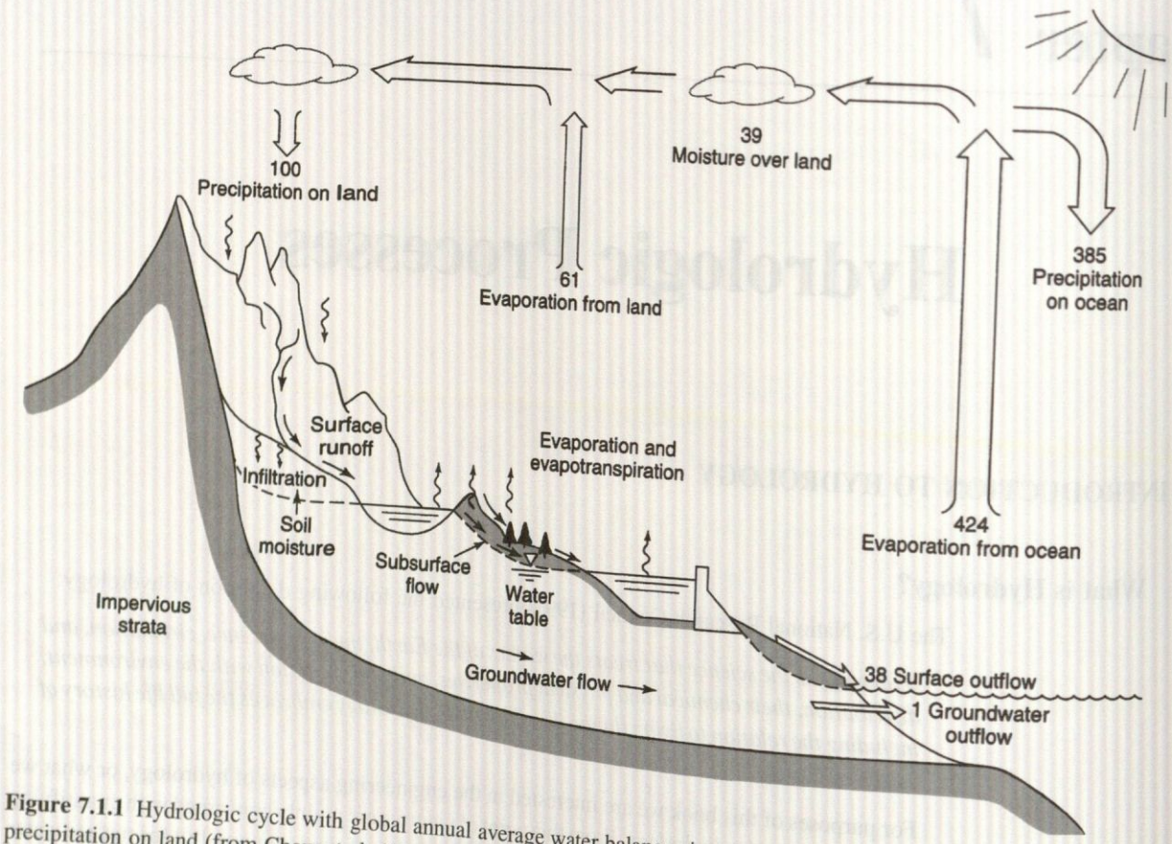


**Figure 7.1.1** Hydrologic cycle with global annual average water balance given in units relative to a value of 100 for the rate of precipitation on land (from Chow et al. (1988)).

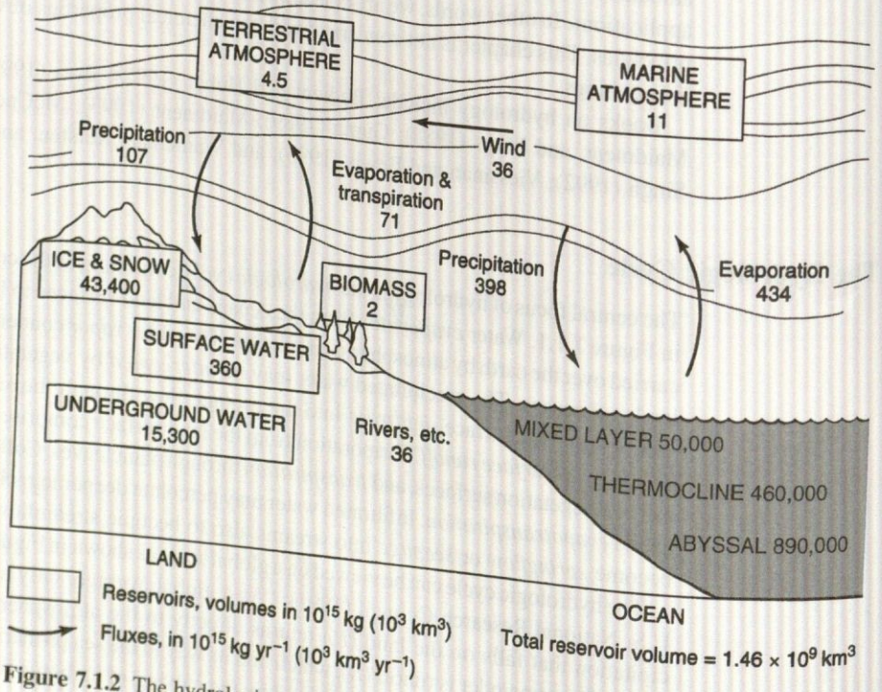


**Figure 7.1.2** The hydrologic cycle at global scale (from U.S. National Research Council (1991)).

(*W*). In this gravitationally powered runoff process, the water may spend time in one or more natural storage reservoirs such as snow, glaciers, ice sheets, lakes, streams, soils and sediments, vegetation, and rock. Evaporation from these reservoirs short-circuits the global hydrologic cycle into subcycles with a broad spectrum of scale. The runoff is perhaps the best-known element of the global hydrologic cycle, but even this is subject to significant uncertainty."

### 7.1.3 Hydrologic Systems

Chow, Maidment, and Mays (1988) defined a *hydrologic system* as a structure or volume in space, surrounded by a boundary, that accepts water and other inputs, operates on them internally, and produces them as outputs. The structure (for surface or subsurface flow) or volume in space (for atmospheric moisture flow) is the totality of the flow paths through which the water may pass as throughput from the point it enters the system to the point it leaves. The boundary is a continuous surface defined in three dimensions enclosing the volume or structure. A *working medium* enters the system as input, interacts with the structure and other media, and leaves as output. Physical, chemical, and biological processes operate on the working media within the system; the most common working media involved in hydrologic analysis are water, air, and heat energy.

The *global hydrologic cycle* can be represented as a system containing three subsystems: the atmospheric water system, the surface water system, and the subsurface water system, as shown in Figure 7.1.3. Another example is the storm-rainfall-runoff process on a watershed, which can be represented as a hydrologic system. The input is rainfall distributed in time and space over the watershed, and the output is streamflow at the watershed outlet. The boundary is defined by the watershed divide and extends vertically upward and downward to horizontal planes.

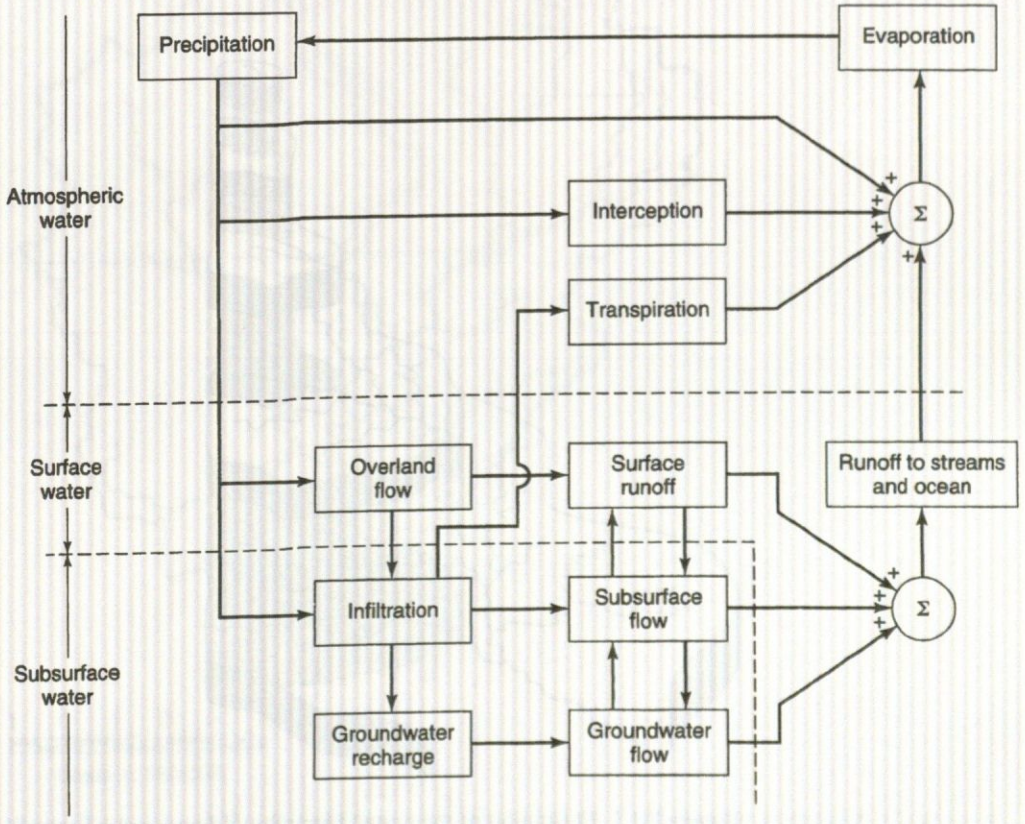


**Figure 7.1.3** Block-diagram representation of the global hydrologic system (from Chow et al. (1988)).

*Drainage basins, catchments,* and *watersheds* are three synonymous terms that refer to the topographic area that collects and discharges surface streamflow through one outlet or mouth. Catchments are typically referred to as small drainage basins, but no specific area limits have been established. Figure 7.1.4 illustrates the drainage basin divide, watershed divide, or catchment divide, which is the line dividing land whose drainage flows toward the given stream from land whose drainage flows away from that stream. Think of drainage basin sizes ranging from the Mississippi

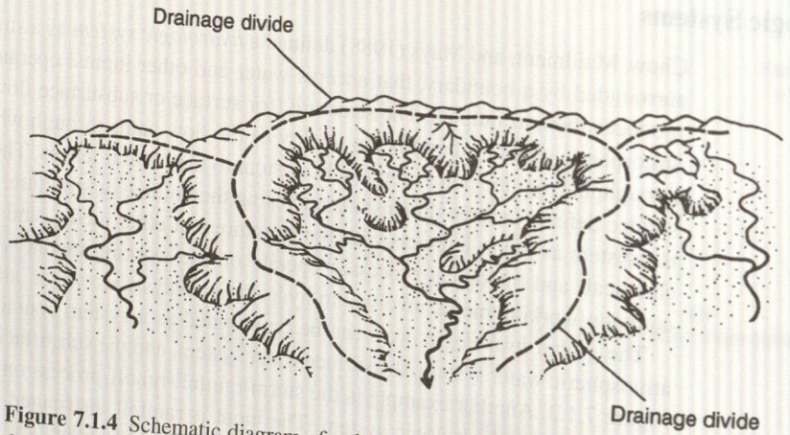


**Figure 7.1.4** Schematic diagram of a drainage basin. The high terrain on the perimeter is the drainage divide (from Marsh (1987)).

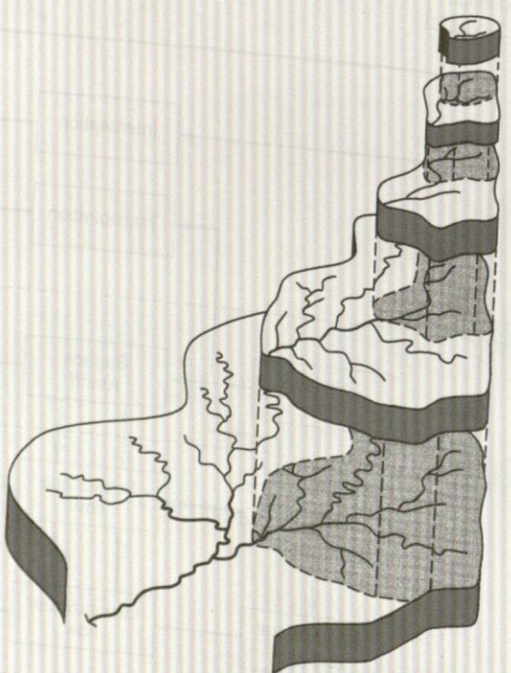

**Figure 7.1.5** Illustration of the nested hierarchy of lower-order basins within a large drainage basin (from Marsh (1987)).

River drainage basin to small urban drainage basins in your local community or some small valley in the countryside near you.

As shown in Figure 7.1.5, drainage basins can be pictured in a pyramidal fashion as the runoffs from smaller basins (subsystems) combine to form larger basins (subsystem in system), and the runoffs from these basins in turn combine to form even larger basins, and so on. Marsh (1987) refers to this mode of organization as a *hierarchy* or *nested hierarchy*, as each set of smaller basins is set inside the next layer. A similar concept is that streams that drain small basins combine to form larger streams, and so on.

Figures 7.1.6–7.1.10 illustrate the hierarchy of the Friends Creek watershed located in the Lake Decatur watershed (drainage area upstream of Decatur, Illinois, on the Sangamon River with a drainage area of 925 $mi^2$ or 2396 $km^2$). Obviously, the Friends Creek watershed can be subdivided into much smaller watersheds. Figure 7.1.8 illustrates the Illinois River basin (29,000 $mi^2$) with the Sangamon River. Figure 7.1.9 illustrates the upper Mississippi River basin (excluding the Missouri River) with the Illinois River. Figure 7.1.10 illustrates the entire Mississippi River basin (1.15 million $mi^2$). This is the largest river basin in the United States, draining about 40 percent of the country. The main stem of the river is about 2400 miles long.

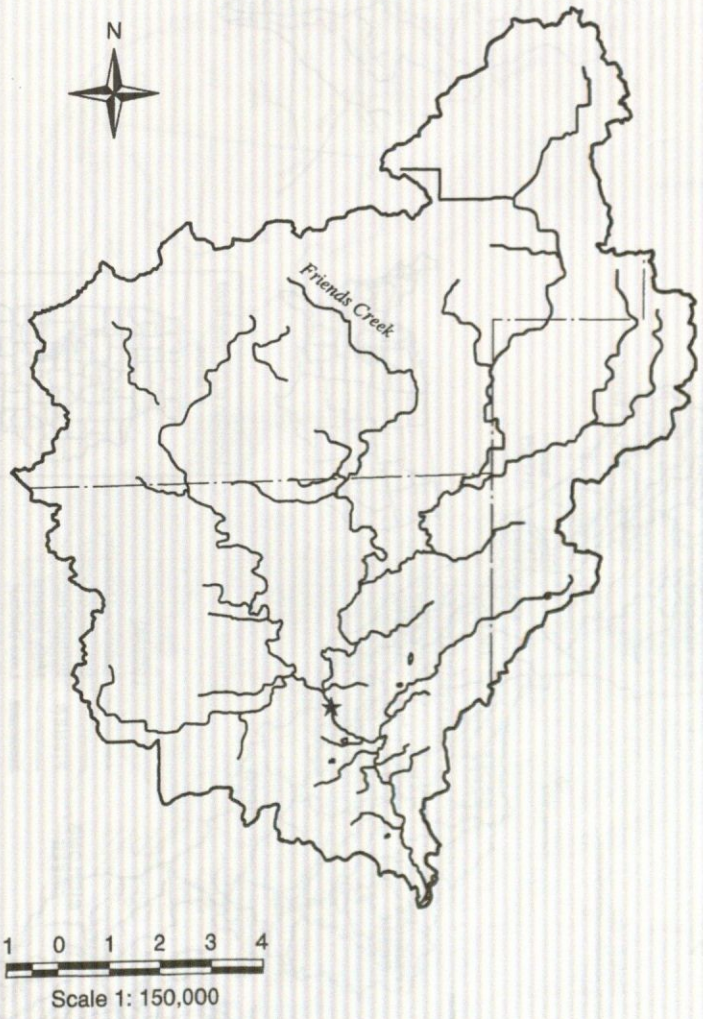


**Figure 7.1.6** Friends Creek watershed, subwatershed of the Lake Decatur watershed. (Courtesy of the Illinois State Water Survey, compiled by Erin Hessler Bauer.)

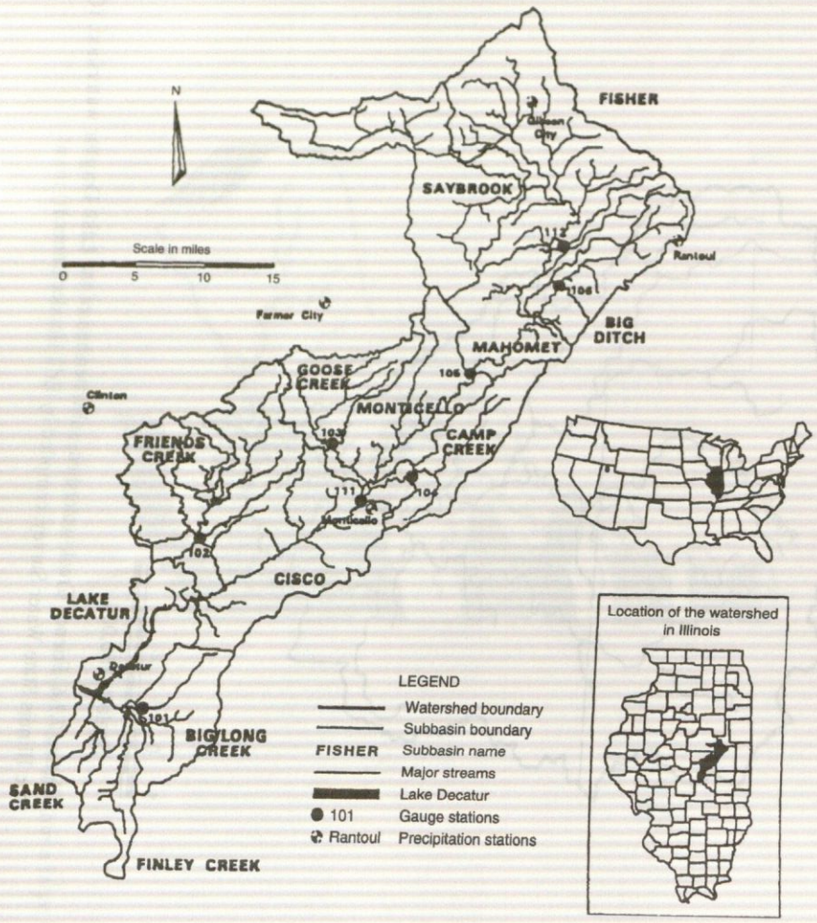


**Figure 7.1.7** Lake Decatur watershed in the upper Sangamon River Basin (upstream of Decatur, Illinois). The location of Friends Creek watershed (Figure 7.1.6) is shown (from Demissee and Keefer (1998)).


**Figure 7.1.8** The Illinois River Basin showing the Sangamon River (from Bhowmik (1998)).

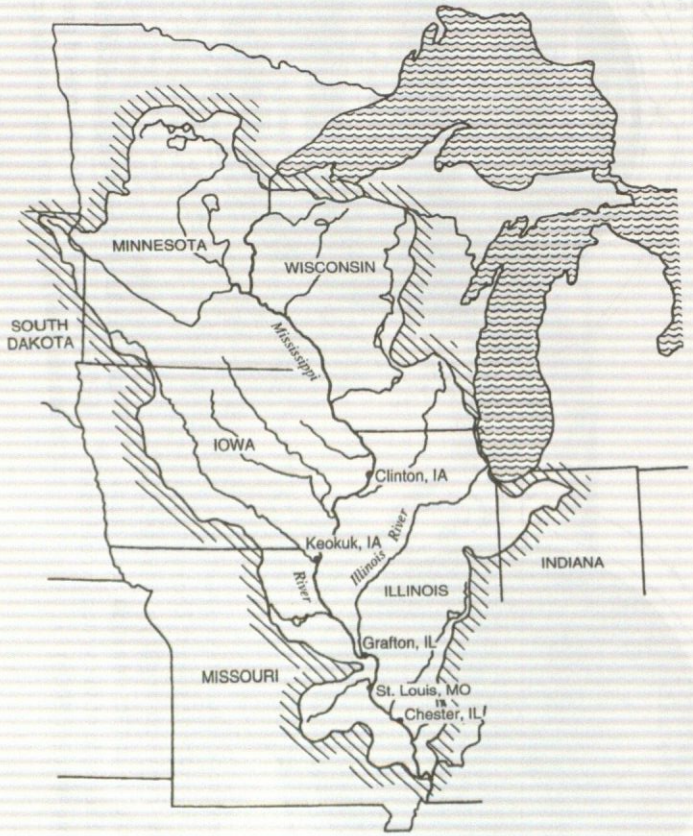


**Figure 7.1.9** The Upper Mississippi River excluding the Missouri River. The location of the Illinois River (Figure 7.1.8) is shown (from Bhowmik (1998)).

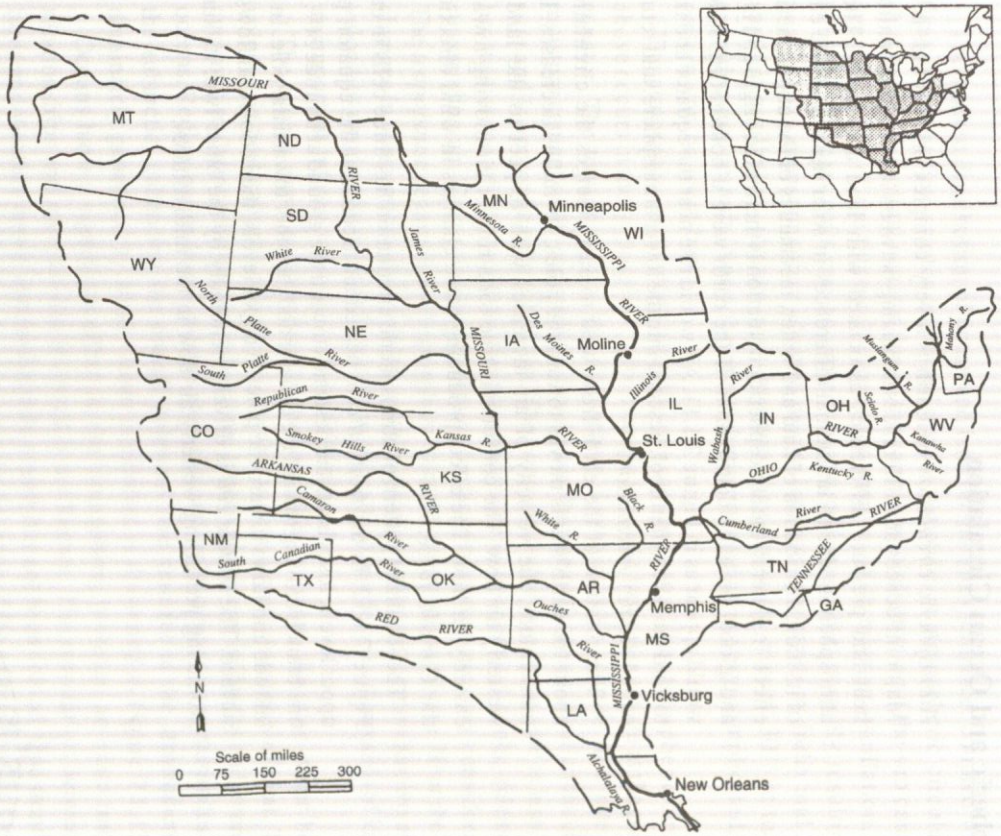


**Figure 7.1.10** The Mississippi River Basin in the United States (from Bhowmik (1998)).

### 7.1.4 Atmospheric and Ocean Circulation

*Atmospheric circulation* on Earth is a very complex process that is influenced by many factors. Major influences are differences in heating between low and high altitudes, the earth's rotation, and heat and pressure differences associated with land and water. The general circulation of the atmosphere is due to latitudinal differences in solar heating of the earth's surface and inclination of its axis, distribution of land and water, mechanics of the atmospheric fluid flow, and the Coriolis effect. In general, the atmospheric circulation is thermal in origin and is related to the earth's rotation and global pressure distribution. If the earth were a nonrotating sphere, atmospheric circulation would appear as in Figure 7.1.11. Air would rise near the equator and travel in the upper atmosphere toward the poles, then cool, descend into the lower atmosphere, and return toward the equator. This is called *Hadley circulation.*

The rotation of the earth from west to east changes the circulation pattern. As a ring of air about the earth's axis moves toward the poles, its radius decreases. In order to maintain angular momentum, the velocity of air increases with respect to the land surface, thus producing a westerly air flow. The converse is true for a ring of air moving toward the equator—it forms an easterly air flow. The effect producing these changes in wind direction and velocity is known as the *Coriolis force.*

The idealized pattern of atmospheric circulation has three cells in each hemisphere, as shown in Figure 7.1.12. In the *tropical cell*, heated air ascends at the equator, proceeds toward the poles at upper levels, loses heat, and descends toward the ground at latitude 30°. Near the ground it branches, one branch moving toward the equator and the other toward the pole. In the *polar cell*, air rises at 60° latitude and flows toward the poles at upper levels, then cools and flows back to 60° near the earth's surface. The *middle cell* is driven frictionally by the other two; its surface flows toward the pole, producing prevailing westerly air flow in the midlatitudes.

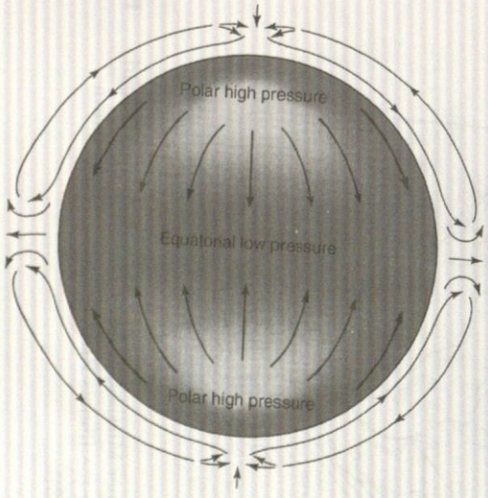


**Figure 7.1.11** Atmospheric circulation pattern that would develop on a nonrotating planet. The equatorial belt would heat intensively and would produce low pressure, which would in turn set into motion a gigantic convection system. Each side of the system would span one hemisphere (from Marsh (1987)).

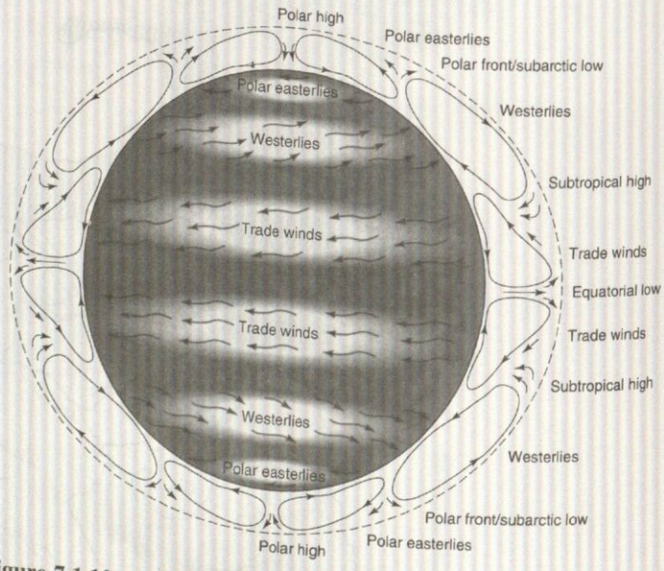


**Figure 7.1.12** Idealized circulation of the atmosphere at the earth's surface, showing the principal areas of pressure and belts of winds (from Marsh (1987)).

The uneven distribution of ocean and land on the earth's surface, coupled with their different thermal properties, creates additional spatial variation in atmospheric circulation. The annual shifting of the thermal equator due to the earth's revolution around the sun causes a corresponding oscillation of the three-cell circulation pattern. With a larger oscillation, exchanges of air between adjacent cells can be more frequent and complete, possibly resulting in many flood years. Also, monsoons may advance deeper into such countries as India and Australia. With a smaller oscillation, intense high pressure may build up around 30° latitude, thus creating extended dry periods. Since the atmospheric circulation is very complicated, only the general pattern can be identified.

The atmosphere is divided vertically into various zones. The atmospheric circulation described above occurs in the *troposphere*, which ranges in height from about 8 km at the poles to 16 km at the equator. The temperature in the troposphere decreases with altitude at a rate varying with the moisture content of the atmosphere. For dry air, the rate of decrease is called the *dry adiabatic lapse rate* and is approximately 9.8°C/km. The *saturated adiabatic lapse rate* is less, about 6.5° C/km, because some of the vapor in the air condenses as it rises and cools, releasing heat into the surrounding air. These are average figures for lapse rates that can vary considerably with altitude. The *tropopause* separates the troposphere from the *stratosphere* above. Near the tropopause, sharp changes in temperature and pressure produce strong narrow air currents known as *jet streams*, with velocities ranging from 15 to 50 m/s (30 to 100 m/h). They flow for thousands of kilometers and have an important influence on air-mass movement.

The oceans exert an important control on global climate. Because water bodies have a high volumetric heat capacity, the oceans are able to retain great quantities of heat. Through wave and current circulation, the oceans redistribute heat to considerable depths and even large areas of the oceans. Redistribution is east-west or west-east and is also across the midaltitudes from the tropics to the subarctic, enhancing the overall poleward beat transfer in the atmosphere. Waves are predominately generated by wind. Ocean circulation is illustrated in Figure 7.1.13.

Oceans have a significant effect on the atmosphere; however, an exact understanding of the relationships and mechanisms involved is not known. The correlation between ocean temperatures and weather trends and midlatitude events has not been solved. One trend is the growth and decline of a warm body of water in the equatorial zone of the eastern Pacific Ocean, referred to as

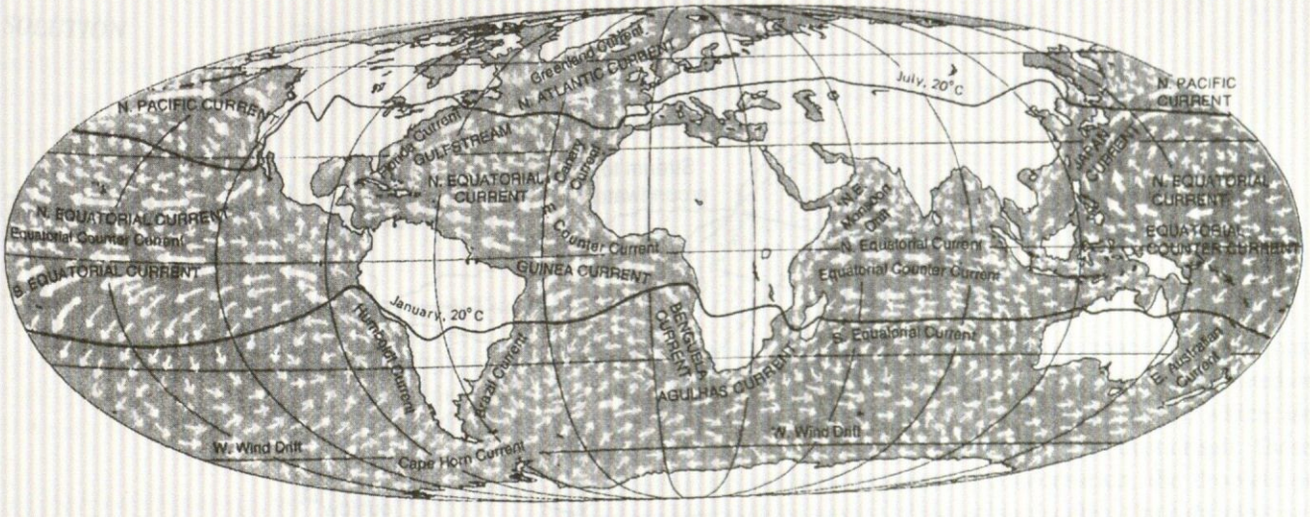


**Figure 7.1.13** The actual circulation of the oceans. Major currents are shown with heavy arrows (from Marsh (1987)).

El Niño (meaning "The Infant" in Spanish, alluding to the Christ Child, because the effect typically begins around Christmas). The warm body of water develops and expands every five years or so off the coast of Peru, initiated by changes in atmospheric pressure resulting in a decline of the easterly trade winds. This reduction in wind reduces resistance, causing the eastwardly equatorial countercurrent to rise. As El Niño builds up, the warm body of water flows out into the Pacific and along the tropical west coast of the Americas, displacing the colder water of the California and Humboldt currents. One of the interesting effects of this weather variation is the South Oscillation, which changes precipitation patterns—resulting in drier conditions in areas of normally little precipitation.

### 7.1.5 Hydrologic Budget

A *hydrologic budget, water budget,* or *water balance* is a measurement of continuity of the flow of water, which holds true for any time interval and applies to any size area ranging from local-scale areas to regional-scale areas or from any drainage area to the earth as a whole. The hydrologists usually must consider an open system, for which the quantification of the hydrologic cycle for that system becomes a mass balance equation in which the change of storage of water ($dS/dt$) with respect to time within that system is equal to the inputs ($I$) to the system minus the outputs ($O$) from the system.

Considering the open system in Figure 7.1.14, the water balance equation can be expressed for the surface water system and the groundwater system in units of volume per unit time separately or, for a given time period and area, in depth.

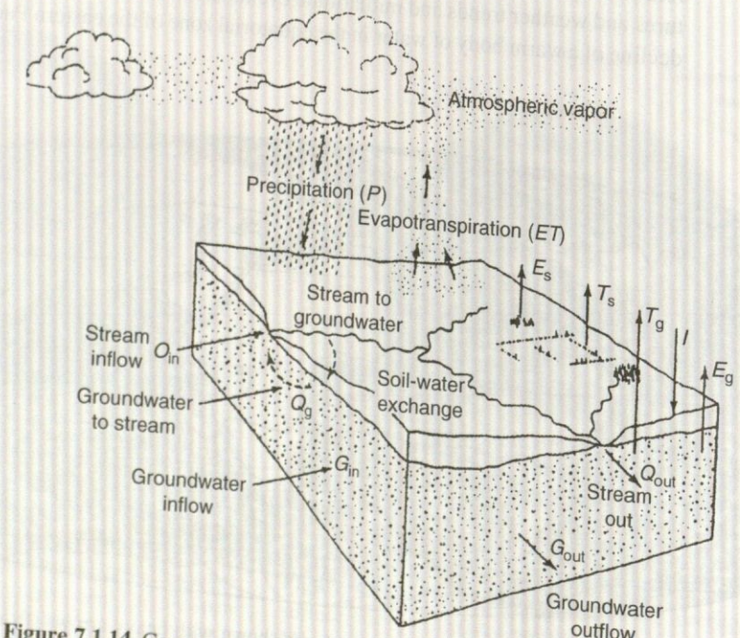


**Figure 7.1.14** Components of hydrologic cycle in an open system: the major inflows and outflows of water from a parcel of land (from Marsh and Dozier (1986)) (Courtesy John Wiley & Sons, Inc.)

***Surface Water System Hydrologic Budget***

$$P + Q_{in} - Q_{out} + Q_g - E_s - T_s - I = \Delta S_s \tag{7.1.1}$$

where $P$ is the precipitation, $Q_{in}$ is the surface water flow into the system, $Q_{out}$ is the surface water flow out of the system, $Q_g$ is the groundwater flow into the stream, $E_s$ is the surface evaporation, $T_s$ is the transpiration, $I$ is the infiltration, and $\Delta S_s$ is the change in water storage of the surface water system.

***Groundwater System Hydrologic Budget***

$$I + G_{in} - G_{out} - Q_g - E_g - T_g = \Delta S_g \tag{7.1.2}$$

where $G_{in}$ is the groundwater flow into the system, $G_{out}$ is the groundwater flow out of the system, and $\Delta S_g$ is the change in groundwater storage. The evaporation, $E_g$, and the transpiration, $T_g$, can be significant if the water table is near the ground surface.

***System Hydrologic Budget***

The system hydrologic budget is developed by adding the above two budgets together:

$$P - (Q_{out} - Q_{in}) - (E_s + E_g) - (T_s + T_g) - (G_{out} - G_{in}) = \Delta(S_s + S_g) \tag{7.1.3}$$

Using net mass exchanges, the above system hydrologic budget can be expressed as

$$P - Q - G - E - T = \Delta S \tag{7.1.4}$$

***EXAMPLE 7.1.1***

During January 1996, the water-budget terms for Lake Annie in Florida included precipitation ($P$) of 1.9 in, evaporation ($E$) of 1.5 in, surface water inflow ($Q_{in}$) of 0 in, surface outflow ($Q_{out}$) of 17.4 in, and change in lake volume ($\Delta S$) of 0 in. Determine the net groundwater flow for January 1996 (the groundwater inflow minus the groundwater outflow).

***SOLUTION***

The water budget equation to define the net groundwater flow for the lake is

$$G = \Delta S - P + E - Q_{in} + Q_{out} = 0 - 1.9 + 1.5 - 0 + 17.4 = 17 \text{ in for January 1996}$$

## 7.2 PRECIPITATION (RAINFALL)

### 7.2.1 Precipitation Formation and Types

Even though precipitation includes rainfall, snowfall, hail, and sleet, our concern in this book will relate almost entirely to rainfall. The formation of water droplets in clouds is illustrated in Figure 7.2.1. *Condensation* takes place in the atmosphere on *condensation nuclei*, which are very small particles ($10^{-3} - 10\,\mu m$) in the atmosphere that are composed of dust or salt. These particles are called *aerosols*. During the initial occurrence of condensation, the droplets or ice particles are very small and are kept aloft by motion of the air molecules. Once droplets are formed they also act as condensation nuclei. These droplets tend to repel one another, but in the presence of an electric field in the atmosphere they attract one another and are heavy enough

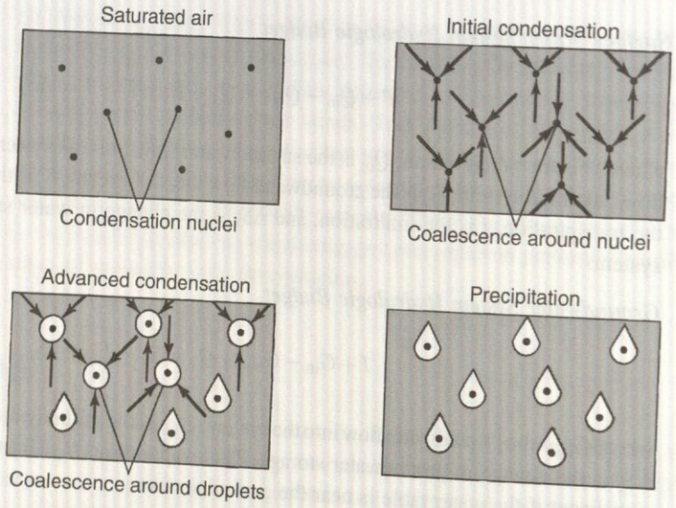


**Figure 7.2.1** Precipitation formation. Water droplets in clouds are formed by nucleation of vapor on aerosols, then go through many condensation-evaporation cycles as they circulate in the cloud, until they aggregate into large enough drops to fall through the cloud base (from Marsh (1987)).

(~0.1 mm) to fall through the atmosphere. Some of the droplets evaporate in the atmosphere, some of the droplets decrease in size by evaporation, and some of the droplets increase in size by impact and aggregation.

Basically, the formation of precipitation requires lifting of an air mass in the atmosphere; it then cools and some of its moisture condenses. There are three main mechanisms of air mass lifting: *frontal lifting*, *orographic lifting*, and *convective lifting*. Frontal lifting (Figure 7.2.2) occurs when warm air is lifted over cooler air by frontal passage, orographic lifting (Figure 7.2.3) occurs when an air mass rises over a mountain range, and convective lifting (Figure 7.2.4) occurs when air is drawn upward by convective action such as a thunderstorm cell.

### 7.2.2 Rainfall Variability

In order to determine the runoff from a watershed and the resulting stream flow, precipitation is one of the primary inputs. Rainfall varies in space and time as a result of the general pattern of atmospheric circulation and local factors. Figure 7.2.5 shows the mean annual precipitation in the United States, and Figure 7.2.6 shows the normal monthly distribution of precipitation in the United States. Figure 7.2.7 shows the mean annual precipitation of the world.

Rainstorms can vary significantly in space and time. *Rainfall hyetographs* are plots of rainfall depth or intensity as a function of time. Figure 7.2.8*a* shows examples of two rainfall hyetographs. Cumulative rainfall hyetographs (rainfall mass curve) can be developed as shown in Figure 7.2.8*b*.

*Isohyets* (contours of constant rainfall) can be drawn to develop isohyetal maps of rainfall depth. *Isohyetal maps* are an interpolation of rainfall data recorded at gauged points. An example is shown in Figure 7.2.9 for the Upper Mississippi River Basin storm of January through July 1993. On a much smaller scale, shown in Figure 7.2.10, is the isohyetal map of the May 24–25, 1981 storm in Austin, Texas.

Figure 7.2.11 illustrates the three methods for determining areal average rainfall using rainfall gauge data. These are the *arithmetic-mean method*, the *Thiessen method*, and the *isohyetal method*.

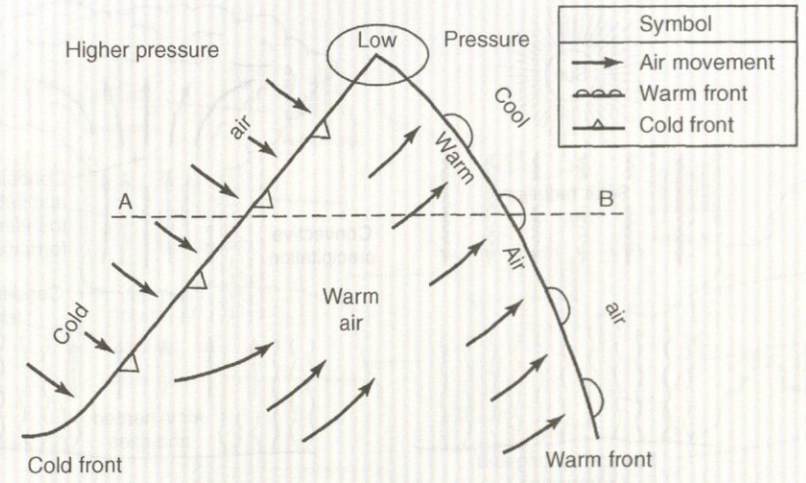


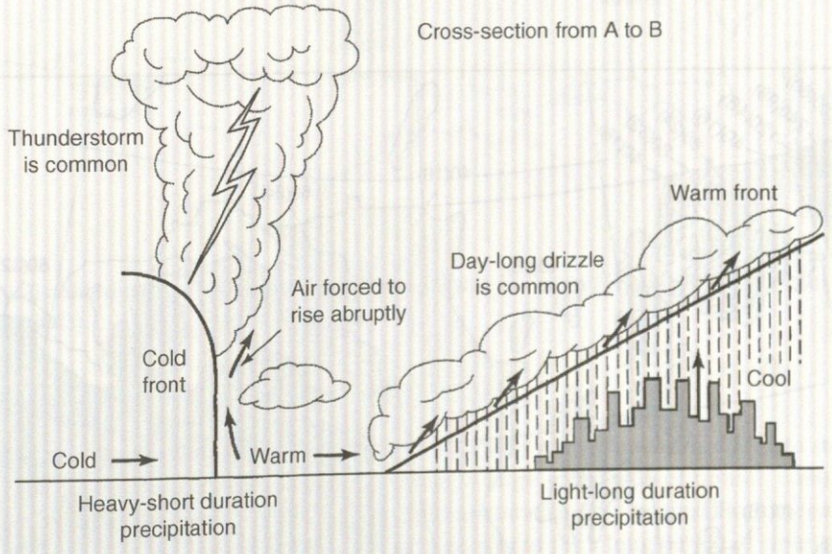


**Figure 7.2.2** Cyclonic storms in midlatitude (from Masch (1984)).

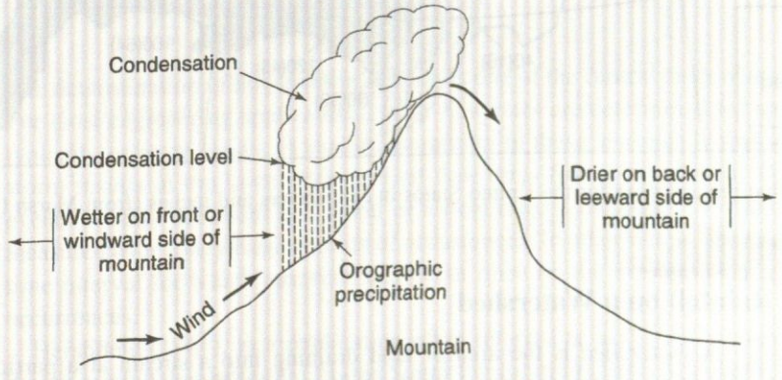


**Figure 7.2.3** Orographic storm (from Masch (1984)).

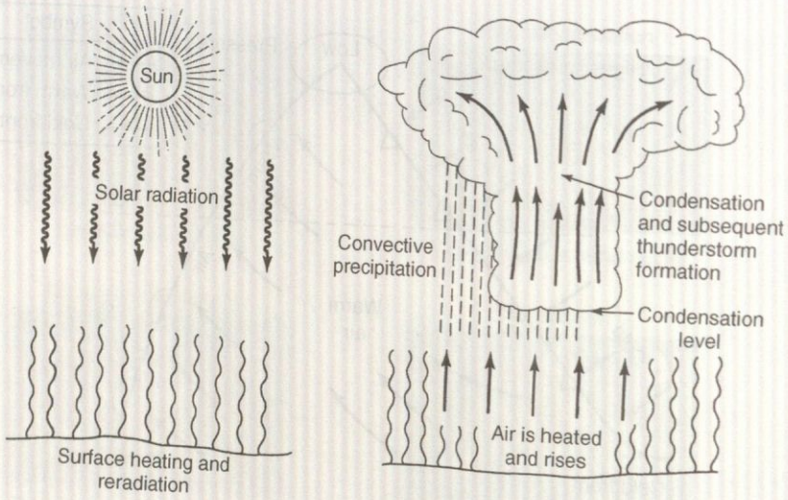


**Figure 7.2.4** Convective storm (from Masch (1984)).

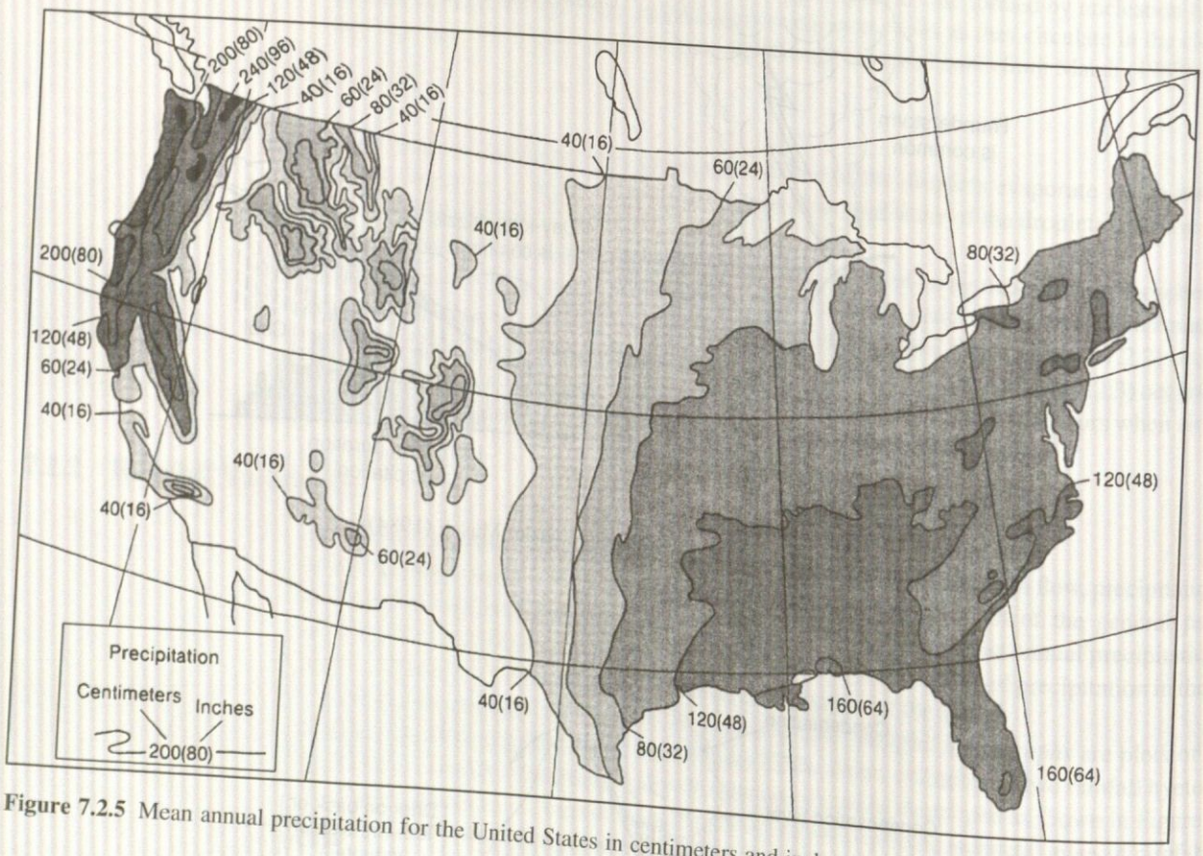


**Figure 7.2.5** Mean annual precipitation for the United States in centimeters and inches (from Marsh (1987)).

### 7.2.3 Disposal of Rainfall on a Watershed

A *watershed* is the area of land draining into a stream at a particular location. The various surface water processes in the hydrologic cycle occur on a watershed. Figure 7.2.12 is a schematic illustration of the disposal of rainfall during a storm on a watershed. This figure

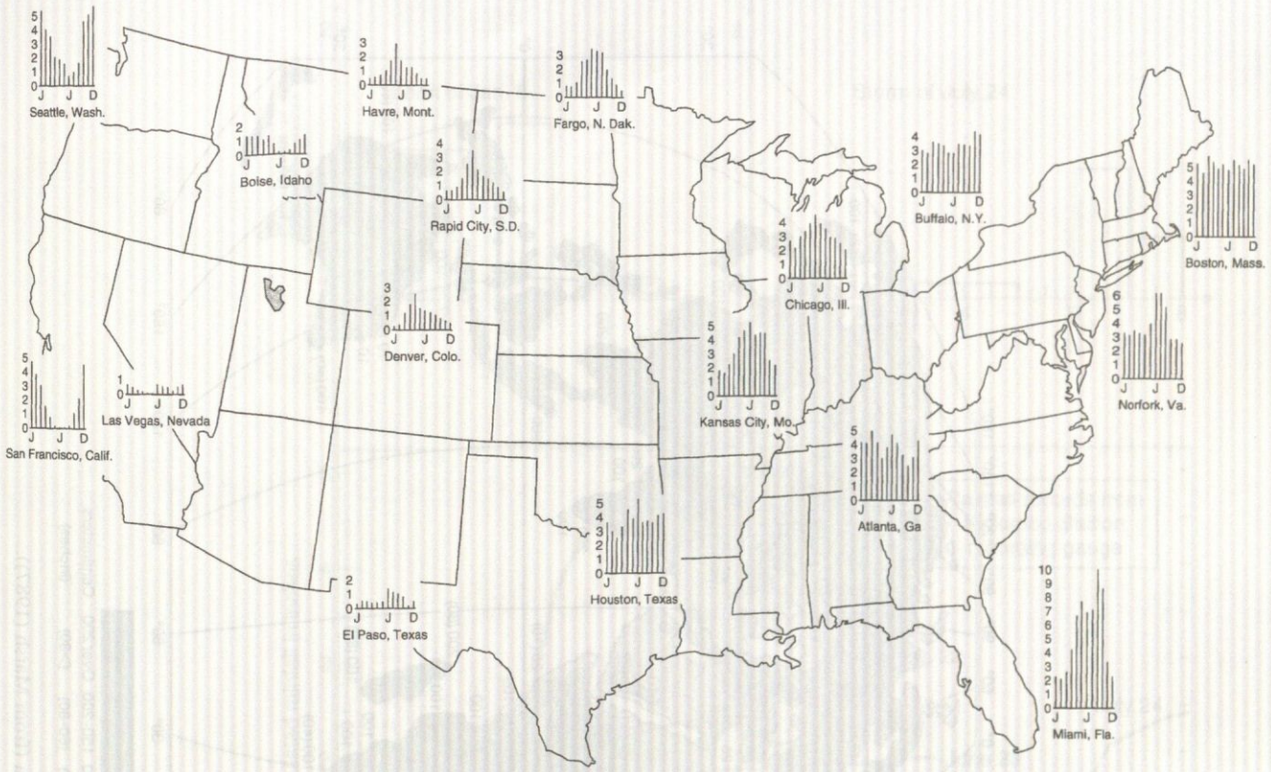


**Figure 7.2.6** Normal monthly distribution of precipitation in the United States in inches (1 in = 254 mm) (from U.S. Environmental Data Services (1968)).

illustrates the rate (as a function of time) at which water flows or is added to storage for each of the processes. At the beginning of a storm, a large proportion of rainfall contributes to *surface storage*, and as water infiltrates, the *soil moisture storage* begins. Both *retention storage* and *detention storage* prevail. Retention storage is held for a long period of time and is depleted by evaporation, whereas detention storage is over a short time and is depleted by flow from the storage location.

### 7.2.4 Design Storms

The determination of flow rates in streams is one of the central tasks of surface water hydrology. For most engineering applications, these flow rates are determined for specified events that are typically extreme events. A major assumption in these analyses is that a certain return period storm results in the same return period flow rates from a watershed. The return period of an event, whether the event is a storm or a flow rate, is the expected value or the average value measured over a very large number of occurrences. In other words, the return period refers to the time interval for which an event will occur once on the average over a very large number of occurrences.

Hershfield (1961), in a publication often referred to as TP-40, presented isohyetal maps of design rainfall depths for the United States for durations from 30 minutes to 24 hours and return periods from 1 to 100 years. The values of rainfall in these isohyetal maps are point precipitation values, which is precipitation occurring at a single point in space (as opposed to areal

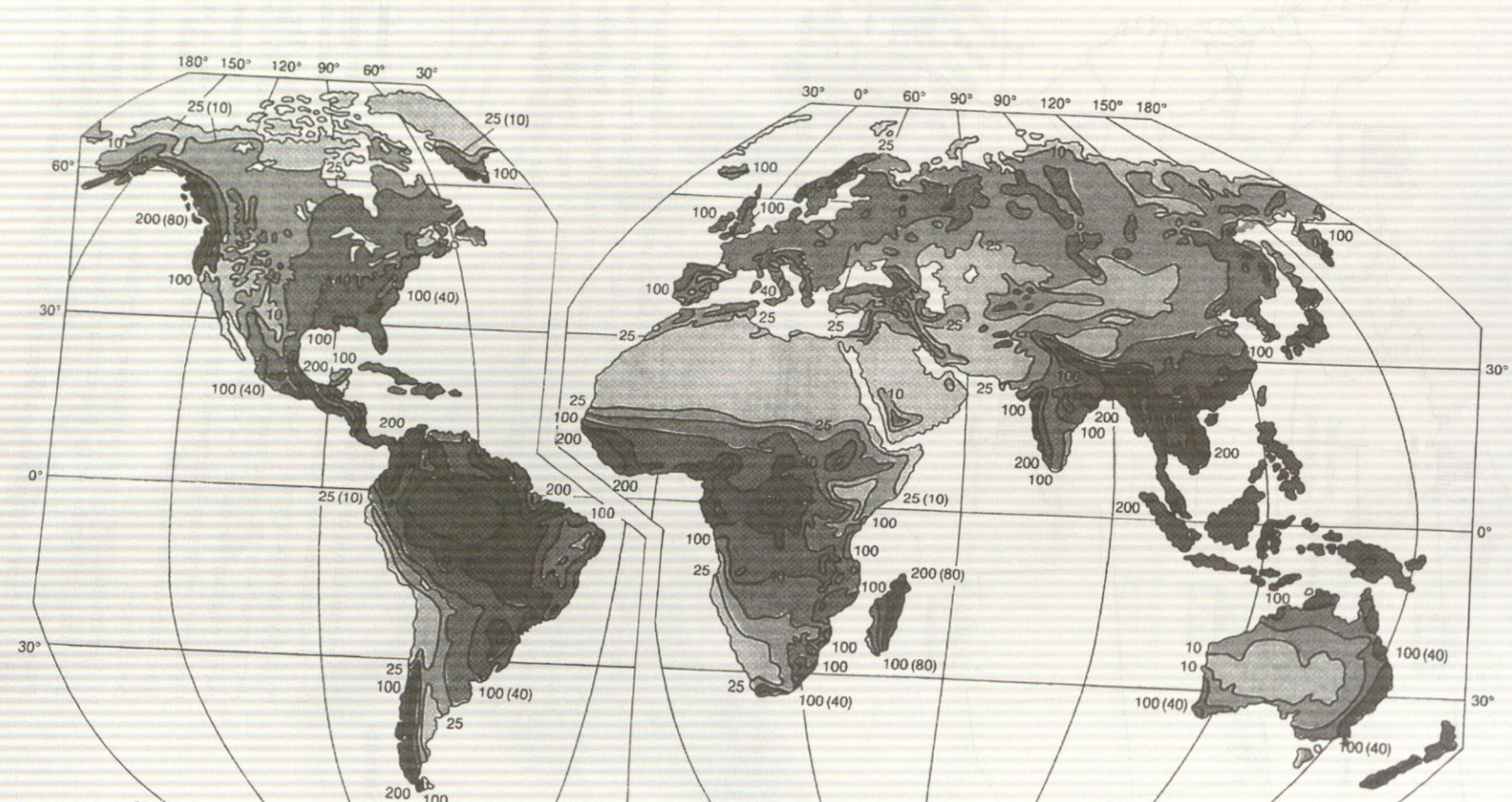


**Figure 7.2.7** Average annual precipitation for the world's land areas, except Antarctica (from Marsh (1987)).

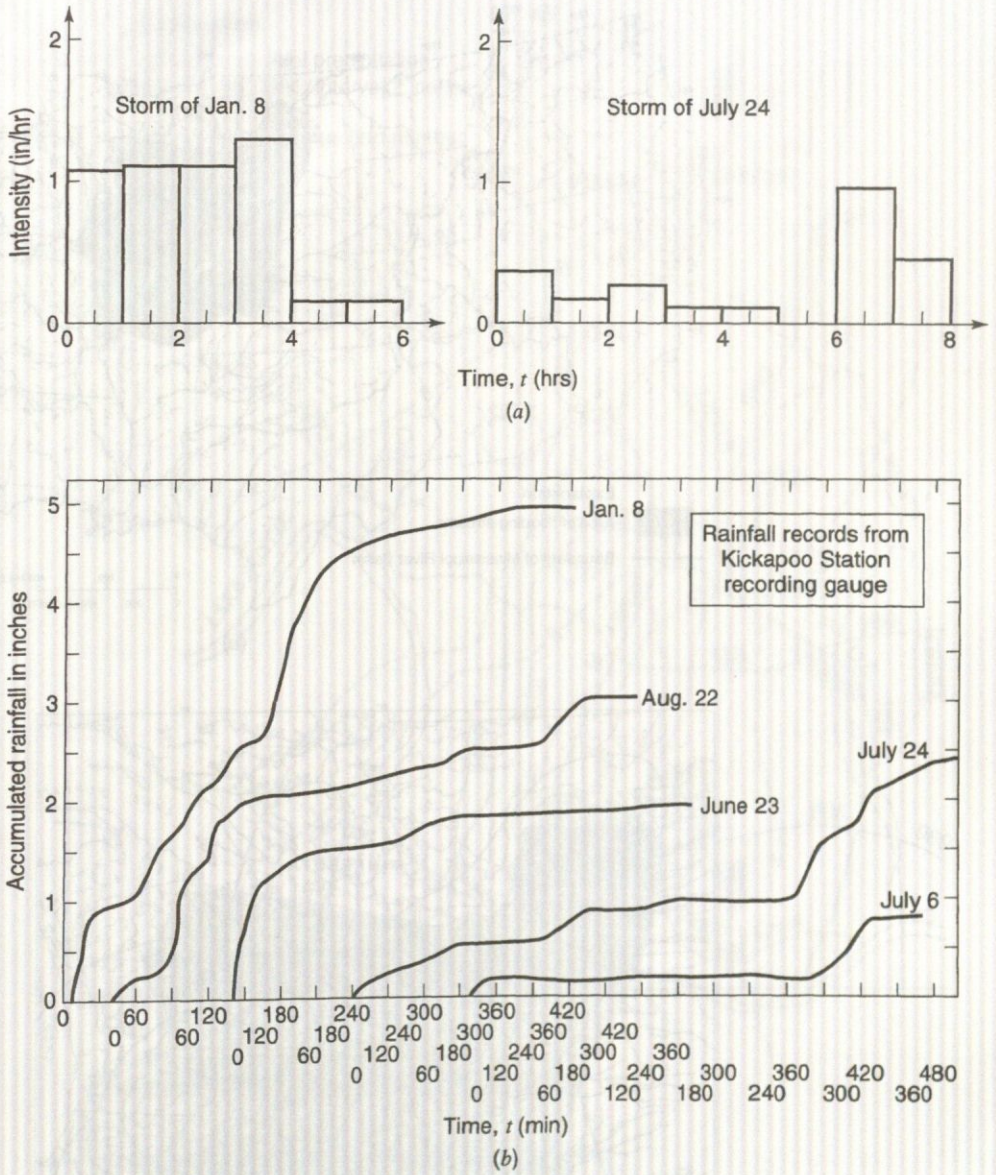


**Figure 7.2.8** (*a*) Rainfall hyetographs for Kickapoo Station; (*b*) Mass rainfall curves (from Masch (1984)).

precipitation, which is over a larger area). Figure 7.2.13 is the isohyetal map for 100-year 24-hour rainfall. A later publication, U.S. Weather Bureau (1964), included maps for durations for 2 to 10 days, in what is referred to as TP-49. Miller et al. (1973) presented isohyetal maps for 6- and 24-hour durations for the 11 mountainous states in the western United States, which supersede the corresponding maps in TP-40.

Frederick et al. (1977), in a publication commonly referred to as HYDRO-35, presented isohyetal maps for events having durations from 5 to 60 minutes. The maps of precipitation depths for 5-, 15-, and 60-minutes durations and return periods of 2 and 100 years for the 37 eastern states are presented in Figures 7.2.14 *a–f*. Depths for a return period are obtained by interpolation from the 5-, 15-, and

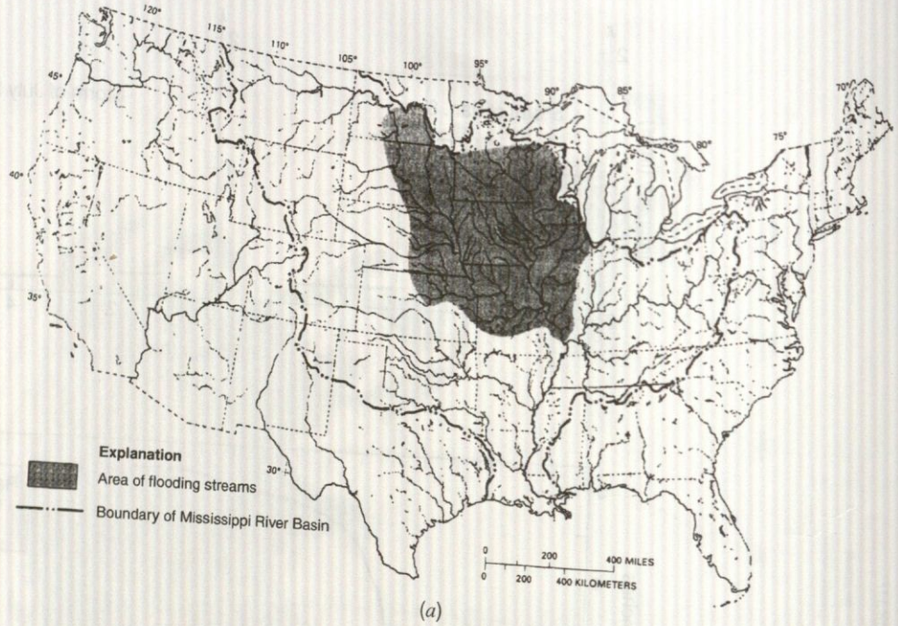


(*a*)

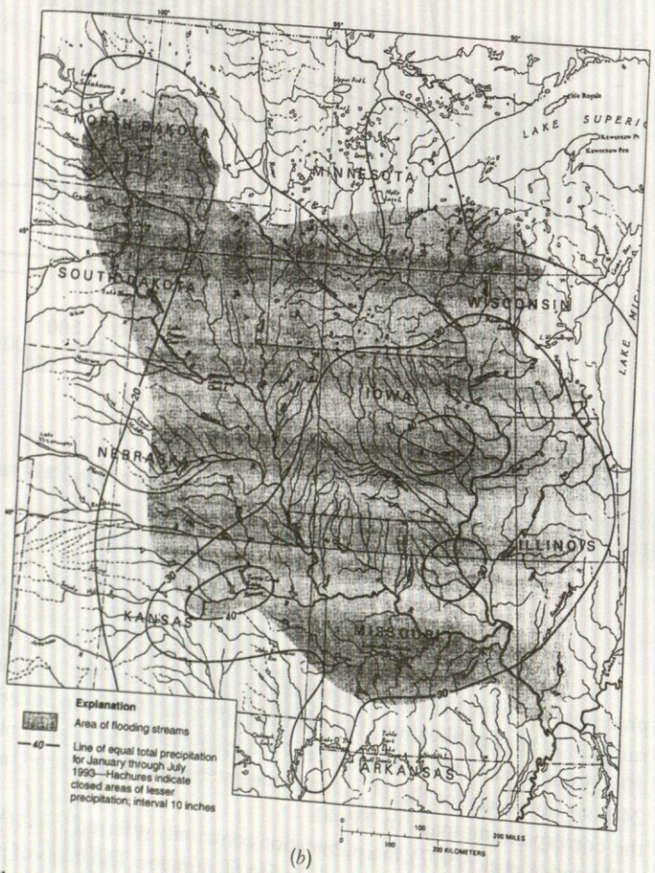


(*b*)

**Figure 7.2.9** (*a*) Mississippi River Basin and general area of flooding streams, June through August 1993 (from Parrett et al. (1993)). (*b*) Areal distribution of total precipitation in the area of flooding in the upper Mississippi River Basin, January through May 1993 (from Parrett et al. (1993)).

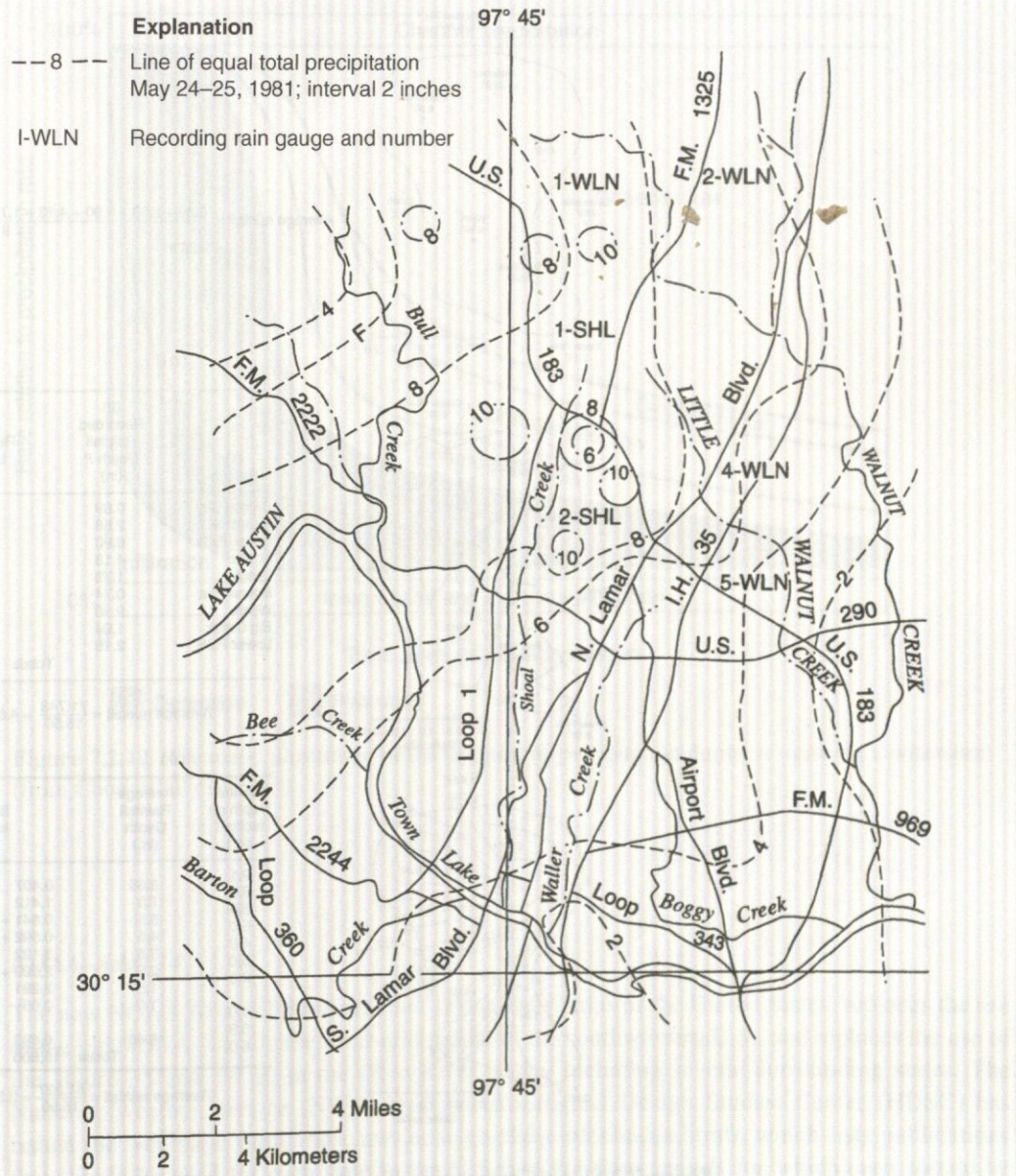


**Figure 7.2.10** Isohyetal map of total precipitation (in) on May 24–25, 1981, based on USGS measurements, the City of Austin network, and unofficial precipitation reports (from Moore et al. (1982)).

60-minute data for the same return period:

$$P_{10\text{min}} = 0.41\,P_{5\text{min}} + 0.59\,P_{15\text{min}} \tag{7.2.1a}$$

$$P_{30\text{min}} = 0.51\,P_{15\text{min}} + 0.49\,P_{60\text{min}} \tag{7.2.1b}$$

To consider return periods other than 2 or 100 years, the following interpolation equation is used:

$$P_{T\,\text{yr}} = aP_{2\text{yr}} + bP_{100\text{yr}} \tag{7.2.2}$$

where the coefficients $a$ and $b$ are found in Table 7.2.1.

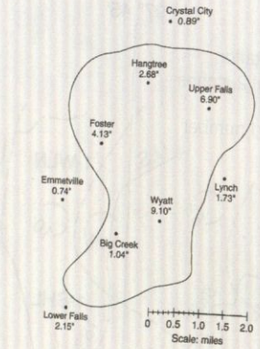


$$\text{Average rainfall} = \frac{0.89 + 2.68 + 6.90 + 4.13 + 1.73 + 0.74 + 1.04 + 9.10 + 2.15}{9} = 3.26 \text{ in}$$

(*a*)

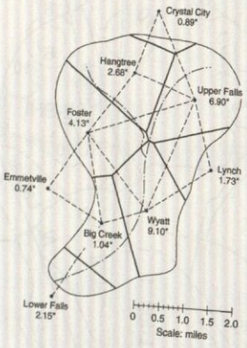


| (1) Station | (2) Recorded Rainfall Depth $P$ (in) | (3) Area $A$ Represented by Station (mi$^2$) | (4) Rainfall Volume (mi$^2$-in) |
|---|---|---|---|
| Crystal City | 0.89 | 0.21 | 0.187 |
| Hangtree | 2.68 | 2.82 | 7.558 |
| Upper Falls | 6.90 | 3.00 | 20.700 |
| Foster | 4.13 | 2.64 | 10.903 |
| Lynch | 1.73 | 1.00 | 1.730 |
| Emmetville | 0.74 | 0 | 0 |
| Wyatt | 9.10 | 2.94 | 26.754 |
| Big Creek | 1.04 | 2.07 | 2.153 |
| Lower Falls | 2.15 | 0.82 | 1.763 |
| | Totals | 15.50 | 71.748 |

$$\text{Average rainfall} = \frac{71.748}{15.50} = 4.63 \text{ in}$$

(*b*)

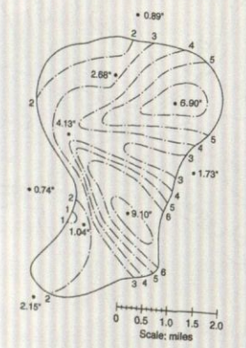


| Rainfall Depth on Isohyet (in.) | Average Rainfall Depth (in.) | Area Between Isohyets (mi$^2$) | Rainfall Volume (mi$^2$-in.) |
|---|---|---|---|
| 9.1 | | | |
| | 8.55 | 0.407 | 3.480 |
| 8.0 | | | |
| | 7.0 | 1.412 | 9.884 |
| 6.0 | | | |
| | 5.5 | 0.841 + 1.375 = 2.216 | 1.219 |
| 5.0 | | | |
| | 4.5 | 0.592 + 1.697 = 2.289 | 10.300 |
| 4.0 | | | |
| | 3.5 | 3.122 | 10.927 |
| 3.0 | | | |
| | 2.5 | 2.599 + 0.431 = 3.030 | 7.575 |
| 2.0 | | | |
| | 1.5 | 2.281 | 3.422 |
| 1.0 | | | |
| | 1.0 | 0.05 | 0.050 |
| 6.9 | | | |
| | 6.45 | 0.693 | 4.470 |
| 6.0 | | | |
| | Totals | 15.500 | 51.327 |

$$\text{Average rainfall} = \frac{51.327}{15.50} = 3.31 \text{ in.}$$

(*c*)

**Figure 7.2.11** (*a*) Computation of areal average rainfall by the arithmetic-mean method for a 24-hr storm. This is the simplest method of determining areal average rainfall. It involves averaging the rainfall depths recorded at a number of gauges. This method is satisfactory if the gauges are uniformly distributed over the area and the individual gauge measurements do not vary greatly about the mean (after Roberson et al. (1998)); (*b*) Computation of areal average rainfall by the Thiessen method for 24-hr storm. This method assumes that at any point in the watershed the rainfall is the same as that at the nearest gauge, so the depth recorded at a given gauge is applied out to a distance halfway to the next station in any direction. The relative weights for each gauge are determined from the corresponding areas of application in a *Thiessen polygon* network, the boundaries of the polygons being formed by the perpendicular bisectors of the lines joining adjacent gauges for $J$ gauges; the area within the watershed assigned to each is $A_j$ and $P_j$ is the rainfall recorded at the $j$th gauge. The areal average precipitation for the watershed is computed by dividing the total rainfall volume by the total watershed area, as shown in the table (after Roberson et al. (1998)). (*c*) Computation of areal average rainfall by the isohyetal method for 24-hr storm. This method connects isoyets, using observed depths at rain gauges and interpolation between adjacent gauges. Where there is a dense network of rain gauges, isohyetal maps can be constructed using computer programs for automated contouring. Once the isohyetal map is constructed, the area $A_j$ between each pair of isohyets within the watershed, is measured and multiplied by the average $P_j$ of the rainfall depths of the two boundary isohyets to compute the areal average precipitation (after Roberson et al. (1998)).

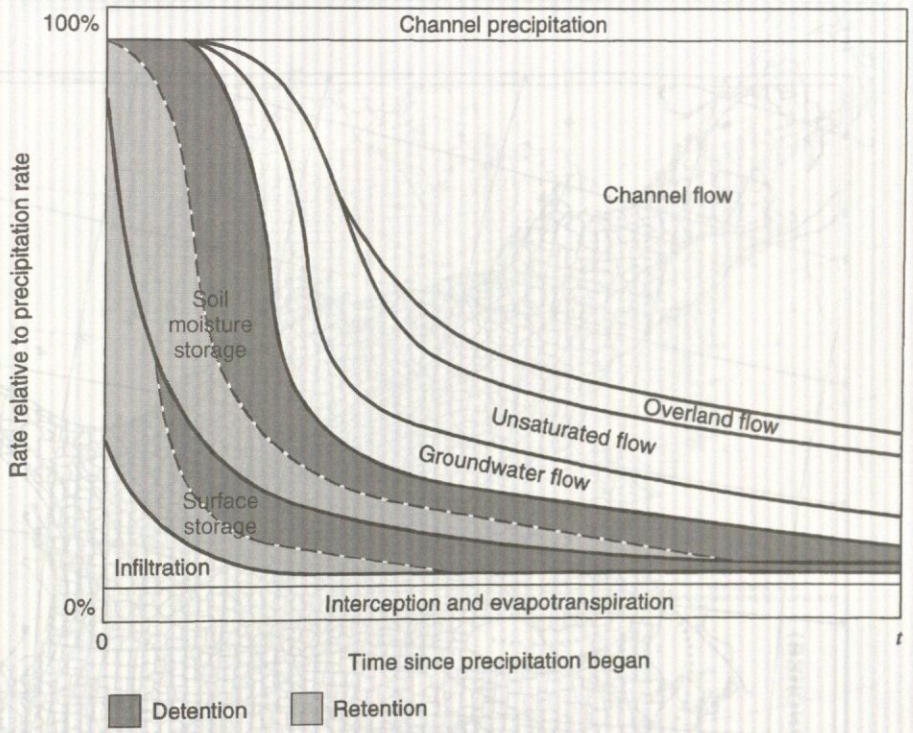


**Figure 7.2.12** Schematic illustration of the disposal of precipitation during a storm on a watershed (from Chow et al. (1988)).

### *NOAA–Atlas 14*

The new NOAA Atlas 14, Precipitation – Frequency Atlas of the United States, replaces the use of the old NOAA Atlas in the semi-arid region of the southwestern U.S., and replaces the use of the Hydro-35 and TP 40 in the Ohio River Valley including several surrounding states. The National Weather Service (NWS) Hydrometeorological Design Studies Center (HDSC) has issued the web page (http://hdsc.nws.noaa.gov/hdsc/pfds/index.html), which lists publications that should be used for each state in the U.S. and the time periods for which each should be used (5 min–60 min, 1 hr–24 hr, and 2-day–10-day periods). The two areas of the U.S. that are most impacted by the new NOAA Atlas 14 are the semi-arid southwest and the Ohio River Valley.

Semi-arid Southwest: NOAA-Atlas 2 is no longer valid for the semi-arid southwest, which includes: Arizona, Nevada, New Mexico, Utah, and Southeast California. For these states, NOAA-Atlas 2 (Volumes 4, 6, 7, 8, and part of 11) has been replaced by NOAA Atlas 14, Volume 1 which is available online: http://www.nws.noaa.gov/oh/hdsc/currentpf.htm

Ohio River Valley: Hydro-35 and Tech Paper No. 40 are no longer valid for most states in the Ohio River Valley and surrounding states, which includes: Delaware, Illinois, Indiana, Kentucky, Maryland, New Jersey, North Carolina, Ohio, Pennsylvania, South Carolina, Tennessee, Virginia, West Virginia, and Washington, DC. For these states, Hydro-35 and Tech Paper-40 have been replaced by NOAA Atlas 14, Volume 2, which is available online: http://www.nws.noaa.gov/oh/hdsc/currentpf.htm

Example point precipitation frequency estimates for two locations are presented in Figure 7.2.15. These are Chicago, Illinois and Phoenix, Arizona.

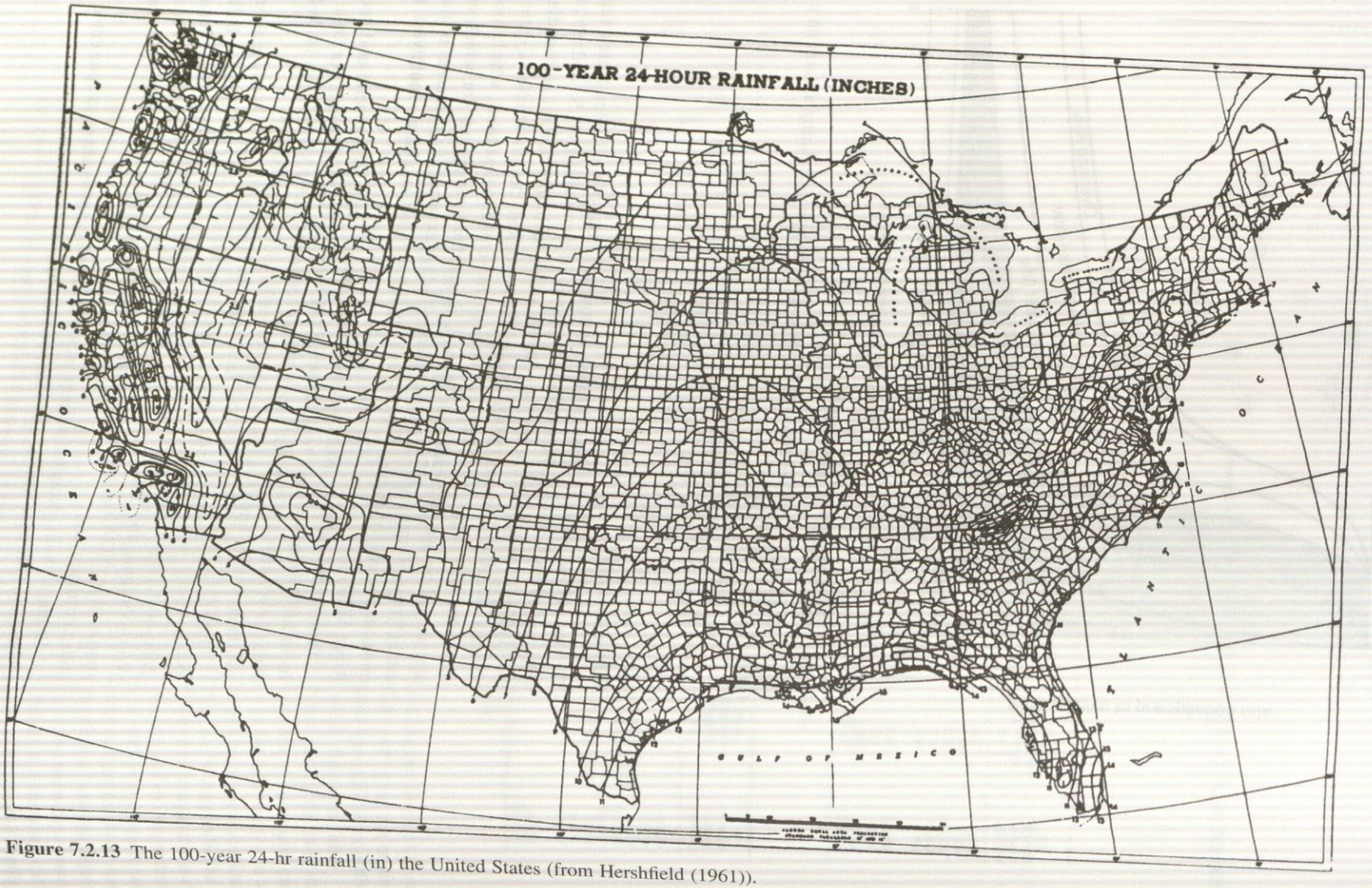


**Figure 7.2.13** The 100-year 24-hr rainfall (in) the United States (from Hershfield (1961)).

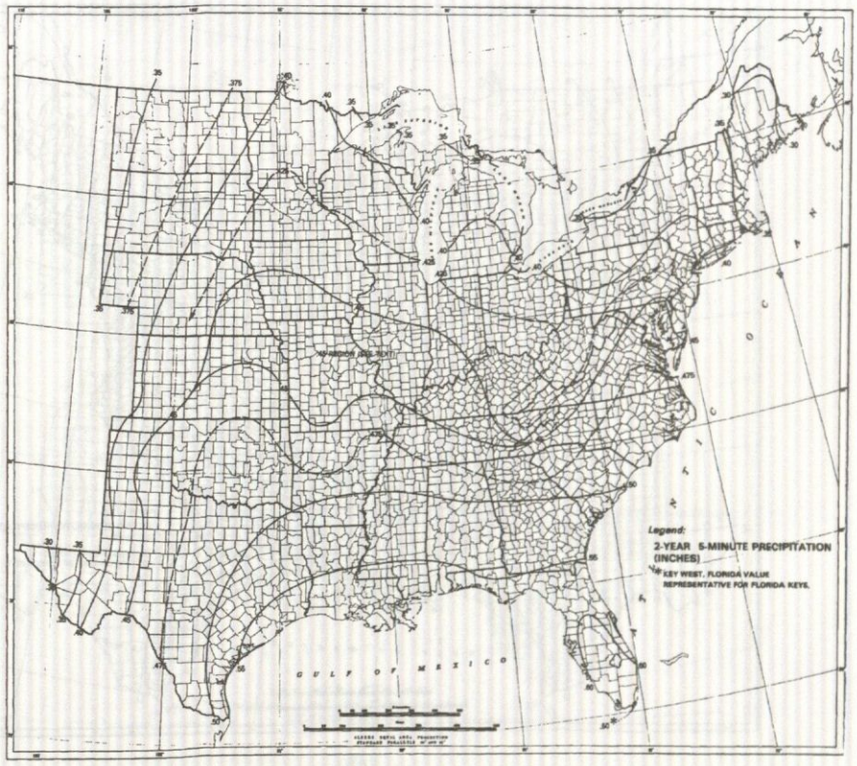


(*a*)

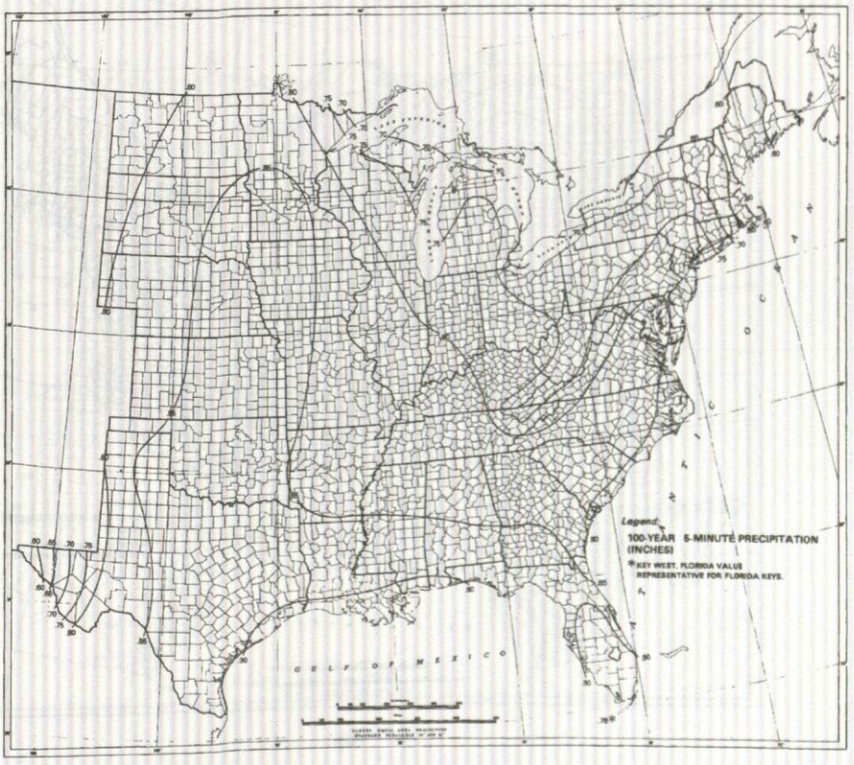


(*b*)

**Figure 7.2.14** (*a*) 2-year 5-min precipitation (in) (from Frederick, Meyers, and Auciello (1977)). (*b*) 100-year 5-min precipitation (in) (from Frederick, Meyers, and Auciello (1977)). (*c*) 2-year 15-min precipitation (in) (from Frederick, Meyers, and Auciello (1977)). (*d*) 100-year 15-min precipitation (in) (from Frederick, Meyers, and Auciello (1977)). (*e*) 2-year 60-min precipitation (in) (from Frederick, Meyers, and Auciello (1977)). (*f*) 100-year 60-min precipitation (in) (from Frederick, Meyers, and Auciello (1977)).


(*c*)

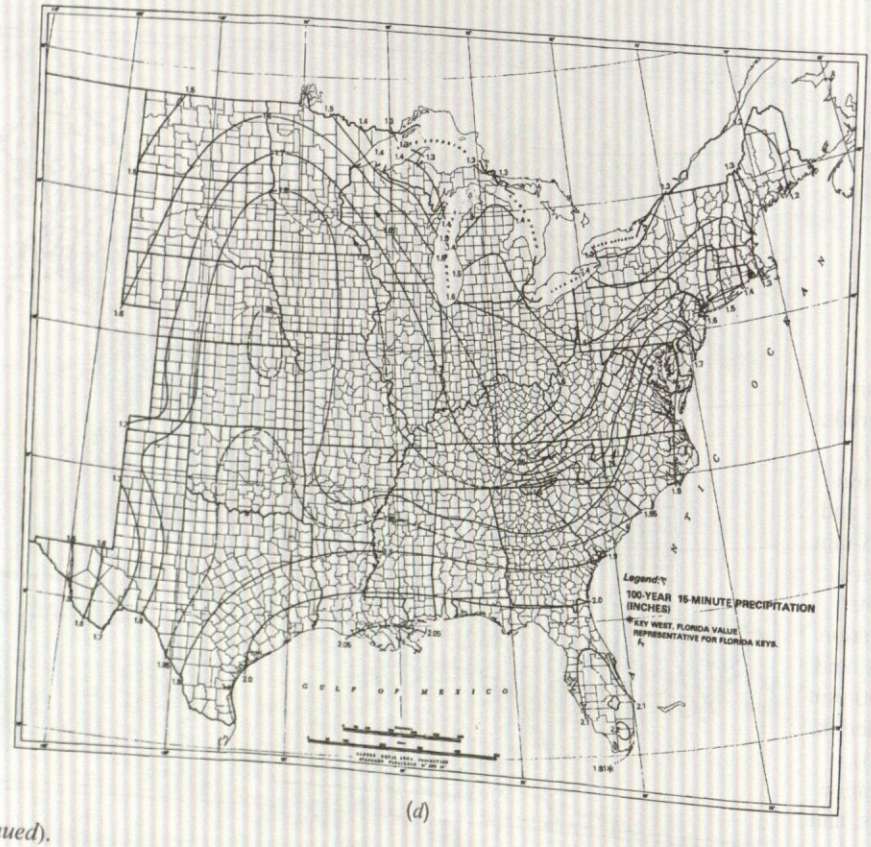


(*d*)

**Figure 7.2.14** (*Continued*).

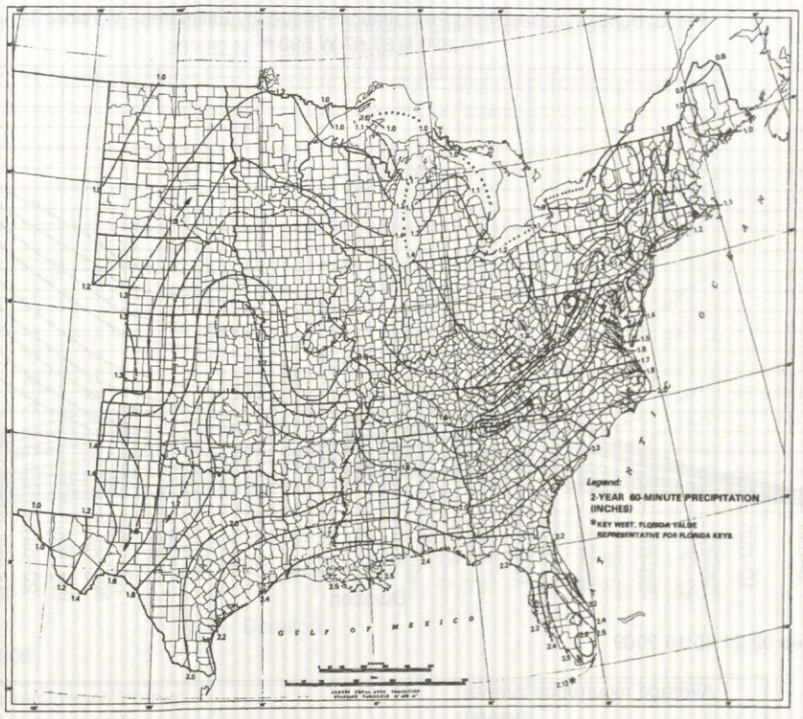


(*e*)

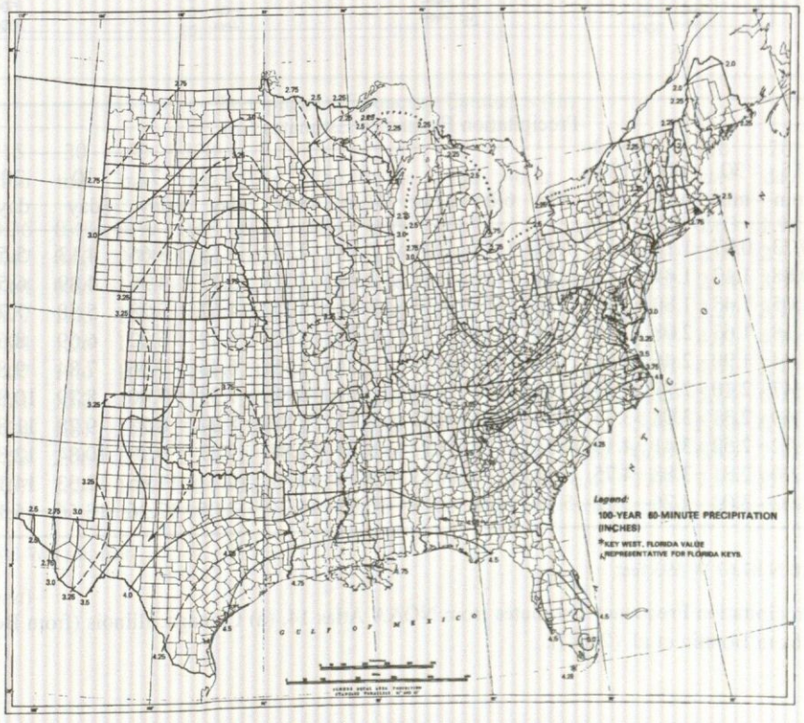


(*f*)

**Figure 7.2.14** (*Continued*)

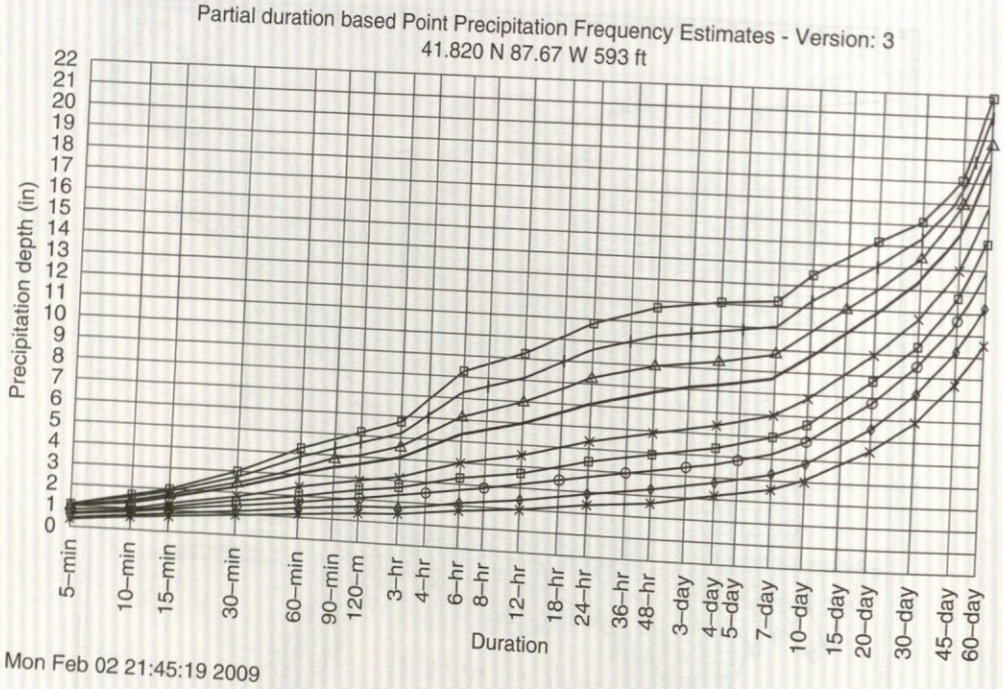


| ARI (years) | Precipitation Frequency Estimates (in) | | | | | | | | | | | | | | | | | |
|---|---|---|---|---|---|---|---|---|---|---|---|---|---|---|---|---|---|---|
| | 5 min | 10 min | 15 min | 30 min | 60 min | 120 min | 3 hr | 6 hr | 12 hr | 24 hr | 48 hr | 4 day | 7 day | 10 day | 20 day | 30 day | 45 day | 60 day |
| 1 | 0.38 | 0.60 | 0.73 | 0.97 | 1.18 | 1.38 | 1.48 | 1.77 | 2.04 | 2.39 | 2.74 | 3.15 | 3.66 | 4.13 | 5.55 | 6.96 | 8.73 | 10.4 |
| 2 | 0.46 | 0.71 | 0.88 | 1.17 | 1.44 | 1.68 | 1.81 | 2.16 | 2.48 | 2.91 | 3.32 | 3.77 | 4.36 | 4.89 | 6.56 | 8.20 | 10.24 | 12.2 |
| 5 | 0.55 | 0.85 | 1.05 | 1.43 | 1.80 | 2.12 | 2.30 | 2.78 | 3.17 | 3.72 | 4.21 | 4.67 | 5.28 | 5.88 | 7.73 | 9.49 | 11.65 | 13.9 |
| 10 | 0.62 | 0.96 | 1.18 | 1.63 | 2.08 | 2.47 | 2.68 | 3.30 | 3.75 | 4.39 | 4.93 | 5.40 | 6.02 | 6.69 | 8.64 | 10.46 | 12.69 | 15.2 |
| 25 | 0.71 | 1.09 | 1.34 | 1.90 | 2.46 | 2.94 | 3.21 | 4.05 | 4.58 | 5.37 | 5.99 | 6.46 | 7.06 | 7.84 | 9.88 | 11.70 | 13.95 | 16.7 |
| 50 | 0.78 | 1.19 | 1.47 | 2.10 | 2.77 | 3.33 | 3.64 | 4.70 | 5.28 | 6.20 | 6.88 | 7.33 | 7.90 | 8.79 | 10.85 | 12.62 | 14.87 | 17.9 |
| 100 | 0.85 | 1.28 | 1.60 | 2.31 | 3.08 | 3.73 | 4.09 | 5.40 | 6.05 | 7.10 | 7.83 | 8.27 | 8.78 | 9.78 | 11.82 | 13.49 | 15.71 | 18.9 |
| 200 | 0.93 | 1.39 | 1.72 | 2.52 | 3.41 | 4.15 | 4.57 | 6.17 | 6.89 | 8.10 | 8.88 | 9.27 | 9.70 | 10.84 | 12.80 | 14.34 | 16.50 | 19.9 |
| 500 | 1.03 | 1.52 | 1.90 | 2.81 | 3.88 | 4.75 | 5.24 | 7.31 | 8.13 | 9.58 | 10.41 | 10.77 | 11.06 | 12.33 | 14.12 | 15.42 | 17.47 | 21.1 |
| 1000 | 1.11 | 1.62 | 2.02 | 3.04 | 4.26 | 5.22 | 5.78 | 8.29 | 9.18 | 10.83 | 11.71 | 12.05 | 12.26 | 13.56 | 15.15 | 16.20 | 18.15 | 21.9 |

(a) Chicago, Ilinois 41.820 N 87.67 W 593 feet

**Figure 7.2.15** Point Precipitation Frequency Estimates from NOAA Atlas 14, (a) Chicago, Illinois (from Bonnin et al. (2004)); (b) Phoenix, Arizona (from Bonnin et al. (2004)).

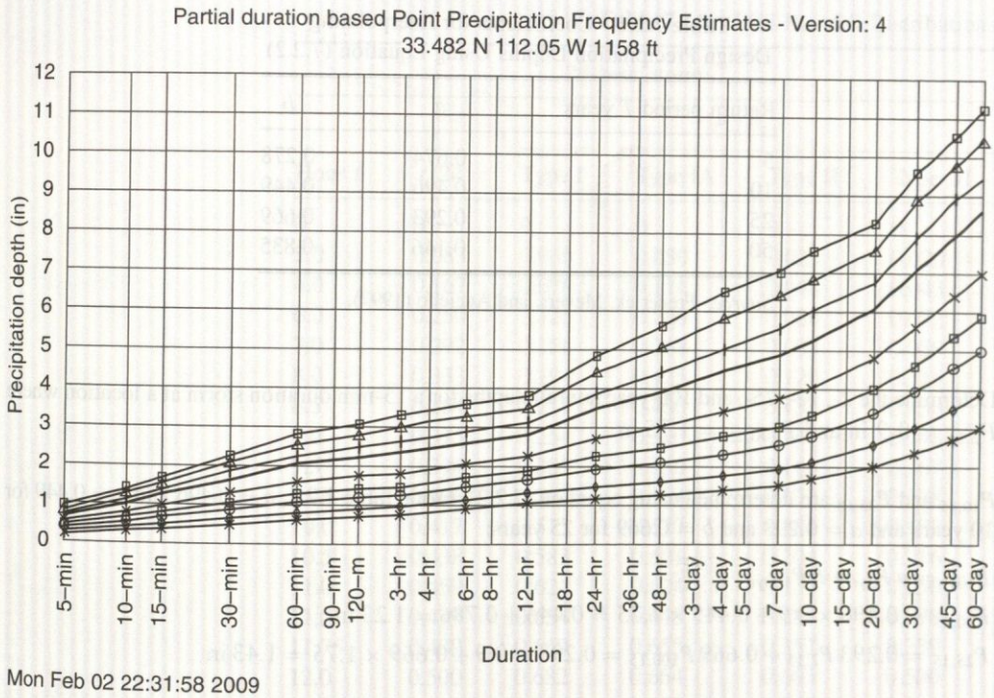


Precipitation Frequency Estimates (in)

| ARI (years) | 5 min | 10 min | 15 min | 30 min | 60 min | 120 min | 3 hr | 6 hr | 12 hr | 24 hr | 48 hr | 4 day | 7 day | 10 day | 20 day | 30 day | 45 day | 60 day |
|---|---|---|---|---|---|---|---|---|---|---|---|---|---|---|---|---|---|---|
| 1 | 0.19 | 0.29 | 0.36 | 0.48 | 0.59 | 0.68 | 0.72 | 0.88 | 0.99 | 1.14 | 1.23 | 1.36 | 1.50 | 1.63 | 1.98 | 2.31 | 2.67 | 2.95 |
| 2 | 0.25 | 0.38 | 0.47 | 0.63 | 0.78 | 0.88 | 0.93 | 1.11 | 1.26 | 1.45 | 1.57 | 1.74 | 1.91 | 2.08 | 2.54 | 2.97 | 3.44 | 3.80 |
| 5 | 0.34 | 0.51 | 0.64 | 0.86 | 1.06 | 1.18 | 1.22 | 1.43 | 1.60 | 1.88 | 2.06 | 2.29 | 2.52 | 2.74 | 3.35 | 3.91 | 4.53 | 4.99 |
| 10 | 0.41 | 0.62 | 0.77 | 1.03 | 1.27 | 1.41 | 1.46 | 1.68 | 1.86 | 2.22 | 2.45 | 2.74 | 3.01 | 3.27 | 3.96 | 4.62 | 5.33 | 5.85 |
| 25 | 0.50 | 0.76 | 0.94 | 1.26 | 1.56 | 1.72 | 1.78 | 2.03 | 2.22 | 2.69 | 3.00 | 3.37 | 3.71 | 4.01 | 4.79 | 5.57 | 6.38 | 6.97 |
| 50 | 0.57 | 0.86 | 1.07 | 1.44 | 1.78 | 1.96 | 2.04 | 2.30 | 2.50 | 3.06 | 3.44 | 3.88 | 4.26 | 4.61 | 5.42 | 6.30 | 7.16 | 7.79 |
| 100 | 0.64 | 0.97 | 1.21 | 1.62 | 2.01 | 2.20 | 2.32 | 2.58 | 2.78 | 3.45 | 3.89 | 4.42 | 4.85 | 5.24 | 6.05 | 7.05 | 7.95 | 8.62 |
| 200 | 0.71 | 1.08 | 1.34 | 1.81 | 2.24 | 2.45 | 2.60 | 2.87 | 3.07 | 3.85 | 4.37 | 5.00 | 5.48 | 5.90 | 6.70 | 7.81 | 8.74 | 9.42 |
| 500 | 0.81 | 1.23 | 1.53 | 2.06 | 2.54 | 2.78 | 2.99 | 3.26 | 3.46 | 4.40 | 5.04 | 5.81 | 6.36 | 6.82 | 7.57 | 8.82 | 9.76 | 10.4 |
| 1000 | 0.88 | 1.34 | 1.67 | 2.24 | 2.78 | 3.04 | 3.31 | 3.57 | 3.75 | 4.84 | 5.57 | 6.47 | 7.07 | 7.57 | 8.23 | 9.60 | 10.53 | 11.2 |

(b) Arizona 33.482 N 112.05 W 1158 feet

**Figure 7.2.15** (*Continued*)

**Table 7.2.1** Coefficients for Interpolating Design Precipitation Depths Using Equation (7.2.2)

| Return period $T$ years | $a$ | $b$ |
|---|---|---|
| 5 | 0.674 | 0.278 |
| 10 | 0.496 | 0.449 |
| 25 | 0.293 | 0.669 |
| 50 | 0.146 | 0.835 |

*Source:* Frederick, Meyers, and Auciello (1997).

***EXAMPLE 7.2.1*** Determine the 2-, 10-, 25-, and 100-year rainfall depths for a 15-min duration storm at a location where $P_{2,15} = 0.9$ in and $P_{100,15} = 1.75$ in.

***SOLUTION*** $P_{10,15}$ and $P_{25,15}$ are determined using equation (7.2.2). From Table 7.2.1, $a = 0.496$ and $b = 0.449$ for 10 years and $a = 0.293$ and $b = 0.669$ for 25 years:

$$P_{10\text{yr}} = a\,P_{2\text{yr}} + b\,P_{100\text{yr}}$$

$$P_{10,15} = 0.496 \times 0.9 + 0.449 \times 1.75 = 0.446 + 0.786 = 1.23 \text{ in}$$

$$P_{25,15} = 0.293\,P_{2,15} + 0.669\,P_{100,15} = 0.293 \times 0.9 + 0.669 \times 1.75 = 1.43 \text{ in}$$

### *IDF Relationships*

In hydrologic design projects, particularly urban drainage design, the use of *intensity-duration-frequency* relationships is recommended. *Intensity* refers to rainfall intensity (depth per unit time), and in some cases depths are used instead of intensity. *Duration* refers to rainfall duration, and *frequency* refers to *return periods*, which is the expected value of the *recurrence interval* (time between occurrences). See Chapter 10 for more details. The intensity-duration-frequency (IDF) relationships are also referred to as *IDF curves*. IDF relationships have also been expressed in equation form, such as

$$i = \frac{c}{T_d^e + f} \tag{7.2.3}$$

where $i$ is the design rainfall intensity in inches per hour, $T_d$ is the duration in minutes, and $c$, $e$, and $f$ are coefficients that vary for location and return period. Other forms of these IDF equations include the return period, such as

$$i = \frac{cT^m}{T_d + f} \tag{7.2.4}$$

and

$$i = \frac{cT^m}{T_d^e + f} \tag{7.2.5}$$

where $T$ is the return period. In Chapter 15, these IDF equations are used in urban drainage design. Chow et al. (1988) describe in detail how to derive the coefficients for these relationships using rainfall data.

### *Synthetic Storm Hyetograph*

In many types of hydrologic analysis, such as *rainfall-runoff analysis*, to determine the runoff (discharge) from a watershed the time sequence of rainfall is needed. In such cases it is standard practice to use a *synthetic storm hyetograph*. The United States Department of Agriculture Soil Conservation Service (1973, 1986) developed synthetic storm hyetographs for 6- and 24-hr storms in

***EXAMPLE 7.***

**Table 7.2.2** SCS Rainfall Distributions

| 24-hour storm | | | | | | 6-hour storm | | |
|---|---|---|---|---|---|---|---|---|
| | | $P_t/P_{24}$ | | | | | | |
| Hour $t$ | $t/24$ | Type I | Type IA | Type II | Type III | Hour $t$ | $t/6$ | $P_t/P_6$ |
| 0 | 0 | 0 | 0 | 0 | 0 | 0 | 0 | 0 |
| 2.0 | 0.083 | 0.035 | 0.050 | 0.022 | 0.020 | 0.60 | 0.10 | 0.04 |
| 4.0 | 0.167 | 0.076 | 0.116 | 0.048 | 0.043 | 1.20 | 0.20 | 0.10 |
| 6.0 | 0.250 | 0.125 | 0.206 | 0.080 | 0.072 | 1.50 | 0.25 | 0.14 |
| 7.0 | 0.292 | 0.156 | 0.268 | 0.098 | 0.089 | 1.80 | 0.30 | 0.19 |
| 8.0 | 0.333 | 0.194 | 0.425 | 0.120 | 0.115 | 2.10 | 0.35 | 0.31 |
| 8.5 | 0.354 | 0.219 | 0.480 | 0.133 | 0.130 | 2.28 | 0.38 | 0.44 |
| 9.0 | 0.375 | 0.254 | 0.520 | 0.147 | 0.148 | 2.40 | 0.40 | 0.53 |
| 9.5 | 0.396 | 0.303 | 0.550 | 0.163 | 0.167 | 2.52 | 0.42 | 0.60 |
| 9.75 | 0.406 | 0.362 | 0.564 | 0.172 | 0.178 | 2.64 | 0.44 | 0.63 |
| 10.0 | 0.417 | 0.515 | 0.577 | 0.181 | 0.189 | 2.76 | 0.46 | 0.66 |
| 10.5 | 0.438 | 0.583 | 0.601 | 0.204 | 0.216 | 3.00 | 0.50 | 0.70 |
| 11.0 | 0.459 | 0.624 | 0.624 | 0.235 | 0.250 | 3.30 | 0.55 | 0.75 |
| 11.5 | 0.479 | 0.654 | 0.645 | 0.283 | 0.298 | 3.60 | 0.60 | 0.79 |
| 11.75 | 0.489 | 0.669 | 0.655 | 0.357 | 0.339 | 3.90 | 0.65 | 0.83 |
| 12.0 | 0.500 | 0.682 | 0.664 | 0.663 | 0.500 | 4.20 | 0.70 | 0.86 |
| 12.5 | 0.521 | 0.706 | 0.683 | 0.735 | 0.702 | 4.50 | 0.75 | 0.89 |
| 13.0 | 0.542 | 0.727 | 0.701 | 0.772 | 0.751 | 4.80 | 0.80 | 0.91 |
| 13.5 | 0.563 | 0.748 | 0.719 | 0.799 | 0.785 | 5.40 | 0.90 | 0.96 |
| 14.0 | 0.583 | 0.767 | 0.736 | 0.820 | 0.811 | 6.00 | 1.0 | 1.00 |
| 16.0 | 0.667 | 0.830 | 0.800 | 0.880 | 0.886 | | | |
| 20.0 | 0.833 | 0.926 | 0.906 | 0.952 | 0.957 | | | |
| 24.0 | 1.000 | 1.000 | 1.000 | 1.000 | 1.000 | | | |

*Source:* U.S. Department of Agriculture Soil Conservation Service (1973, 1986).

the United States. These are presented in Table 7.2.2 and Figure 7.2.16 as cumulative hyetographs. Four 24-hr duration storms, Type I, IA, II, and III, were developed for different geographic locations in the U.S., as shown in Figure 7.2.17. Types I and IA are for the Pacific maritime climate, which has wet winters and dry summers. Type III is for the Gulf of Mexico and Atlantic coastal areas, which have tropical storms resulting in large 24-hour rainfall amounts. Type II is for the remainder of the United States.

In the midwestern part of the United States the Huff (1967) temporal distribution of storms is widely used for heavy storms on areas ranging up to 400 $mi^2$. Time distribution patterns were developed for four probability groups, from the most severe (first quartile) to the least severe (fourth quartile). Figure 7.2.18*a* shows the probability distribution of first-quartile storms. These curves are smooth, reflecting average rainfall distribution with time; they do not exhibit the burst characteristics of observed storms. Figure 7.2.18*b* shows selected histograms of first-quartile storms for 10-, 50-, and 90-percent cumulative probabilities of occurrence, each illustrating the percentage of total storm rainfall for 10 percent increments of the storm duration. The 50 percent histogram represents a cumulative rainfall pattern that should be exceeded in about half of the storms. The 90 percent histogram can be interpreted as a storm distribution that is equaled or exceeded in 10 percent or less of the storms.

***EXAMPLE 7.2.2***

Using equation (7.2.3), compute the design rainfall intensities for a 10-year return period, 10-, 20-, and 60-min duration storms for $c = 62.5$, $e = 0.89$, and $f = 9.10$.

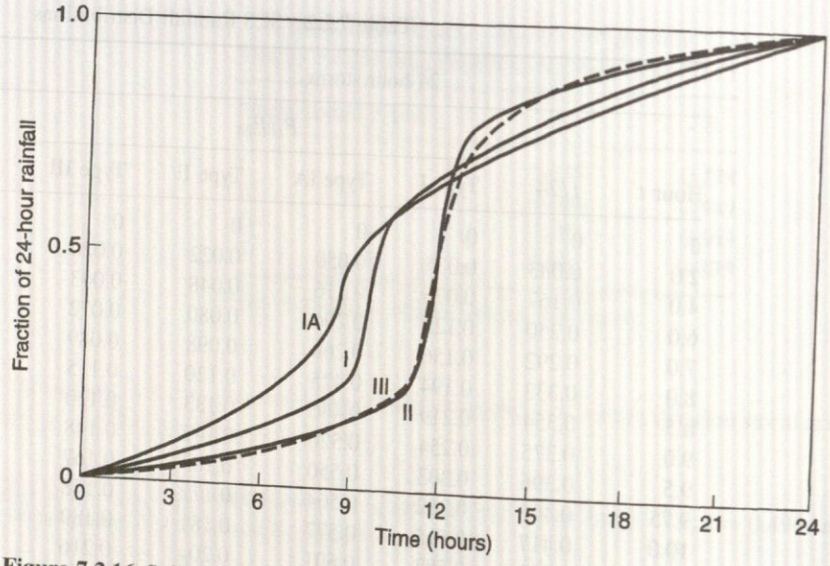


**Figure 7.2.16** Soil Conservation Service 24-hour rainfall hyetographs (from U.S. Department of Agriculture Soil Conservation Service (1986)).


**Figure 7.2.17** Location within the United States for application of the SCS 24-hour rainfall hyetographs (from U.S. Department of Agriculture Soil Conservation Service (1986)).

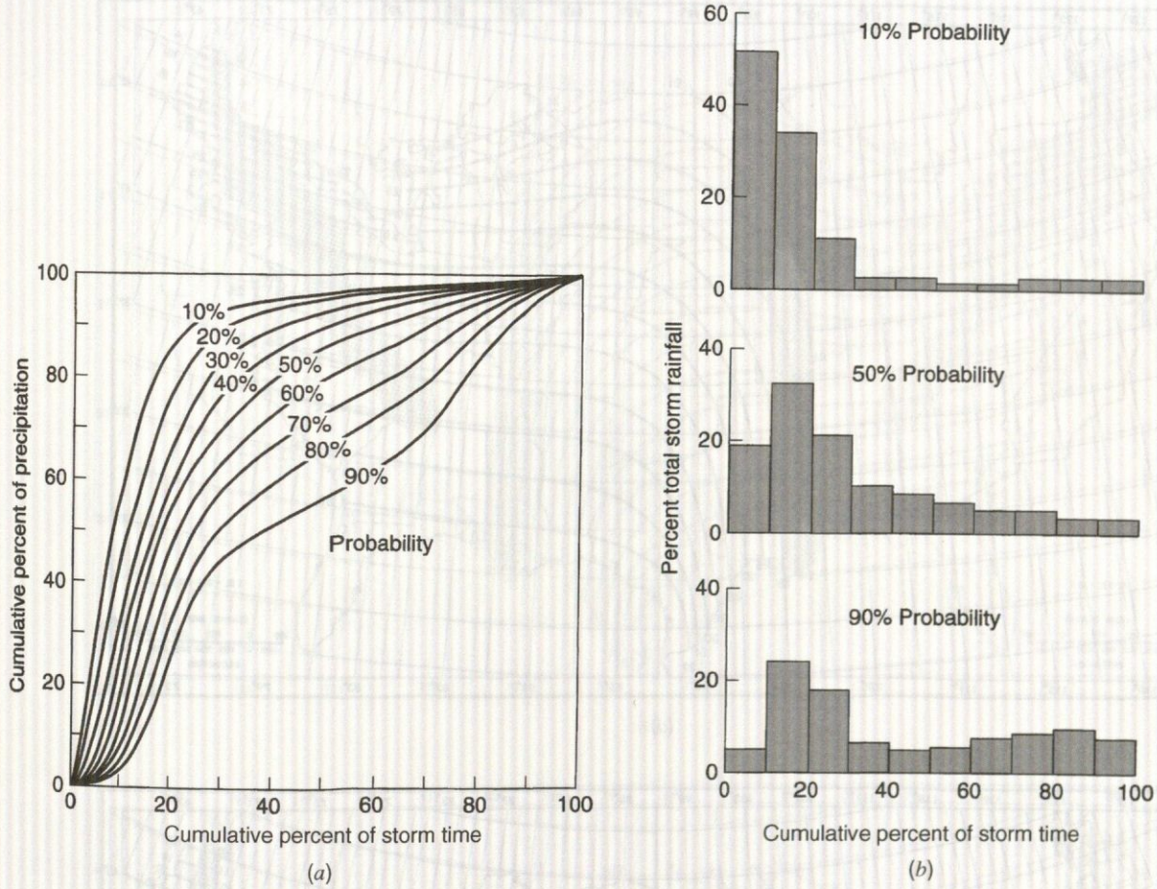


**Figure 7.2.18** (*a*) Time distribution of first-quartile storms. The probability shown is the chance that the observed storm pattern will lie to the left of the curve; (*b*) Selected histograms for first-quartile storms (from Huff (1967)).

***SOLUTION*** The rainfall intensity duration frequency relationship is then

$$i = \frac{62.5}{T_d^{0.89} + 9.10}$$

For $T_d = 10$ min, $i = \dfrac{62.5}{10^{0.89} + 9.10} = 3.71$ in/hr. For $T_d = 20$ min, $i = 2.66$ in/hr, and for $T_d = 60$ min, $i = 1.32$ in/hr.

### 7.2.5 Estimated Limiting Storms

*Estimated limiting values* (ELVs) are used for the design of water control structures such as the spillways on large dams. Of particular interest are the *probable maximum precipitation* (PMP) and the *probable maximum storm* (PMS). These are used to derive a *probable maximum flood* (PMF). PMP is a depth of precipitation that is the estimated limiting value of precipitation, defined as the estimated greatest depth of precipitation for a given duration that is physically possible and reasonably characteristic over a particular geographical region at a certain time of year (Chow et al., 1988). Schreiner and Riedel (1978) presented generalized PMP charts for the United States east of the 105th meridian HMR 51. The all-seasons (any time of the year) estimates of PMP are presented in maps as a function of storm area (ranging from 10 to 20,000 $mi^2$) and storm durations ranging from 6 to 72 hours, as shown in Figure 7.2.19. For regions west of the 105th meridian, the diagram in Figure 7.2.20 shows the appropriate U.S. National Weather Service

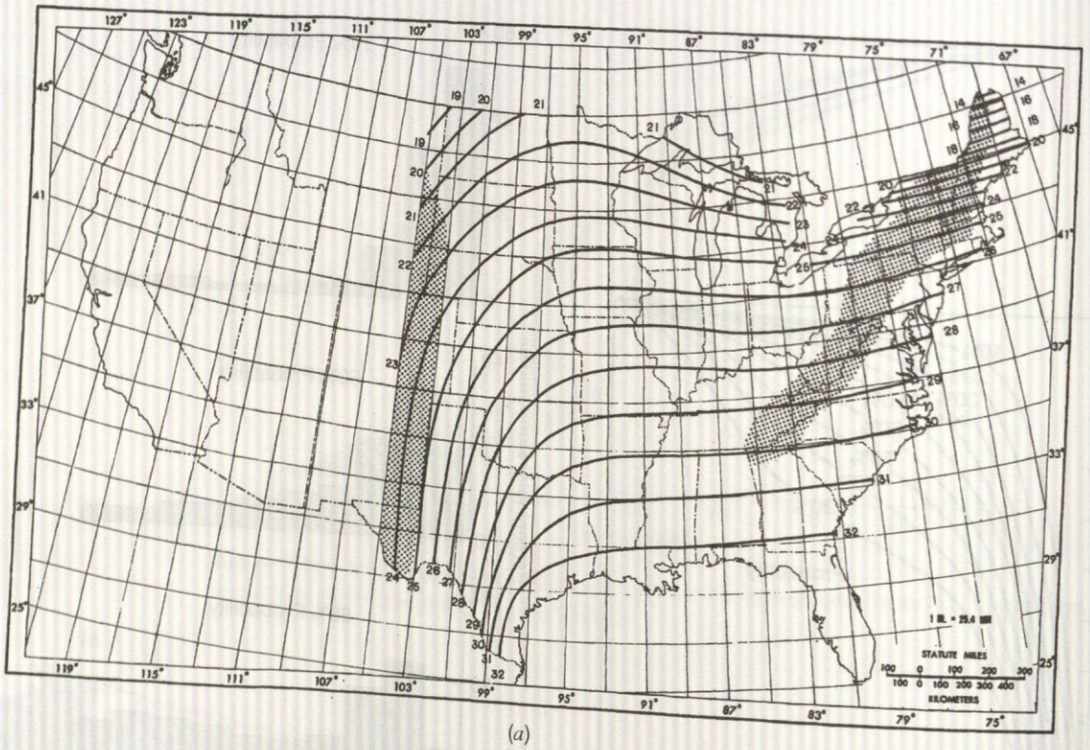


(*a*)

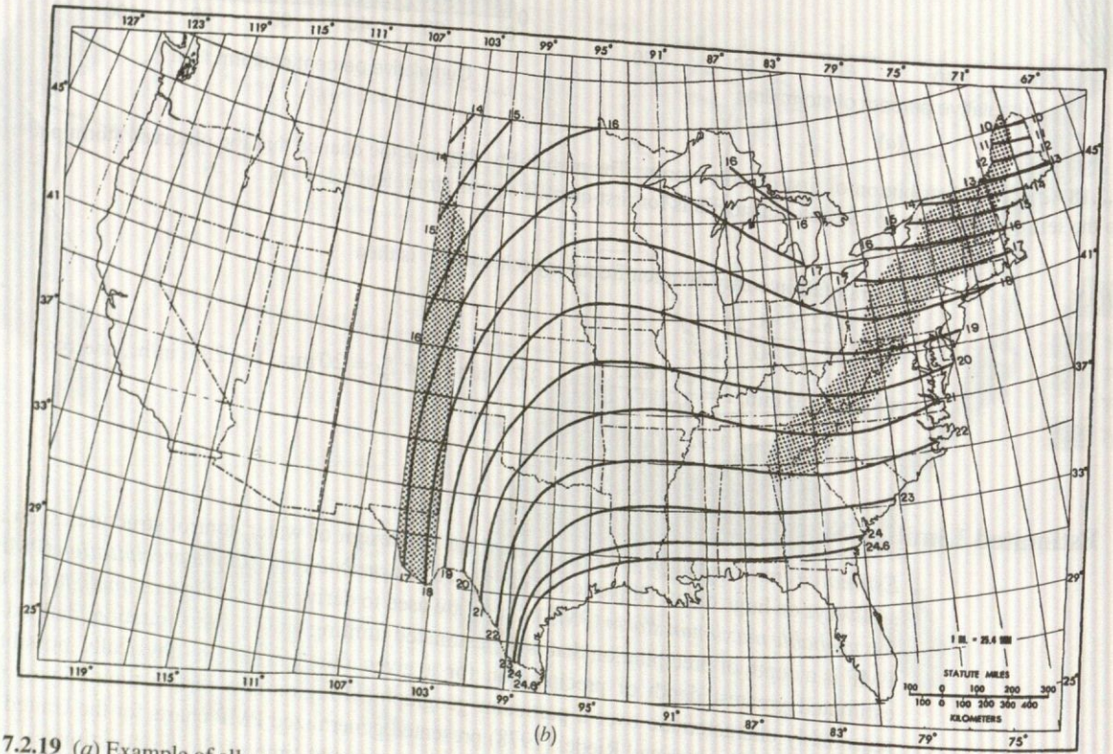


(*b*)

**Figure 7.2.19** (*a*) Example of all-season PMP (in) for 6 hr, 10 mi$^2$ (from Schreiner and Riedel, 1978); (*b*) Example of all-season PMP (in) for 6 hr, 200 mi$^2$ (from Schreiner and Riedel, 1978).

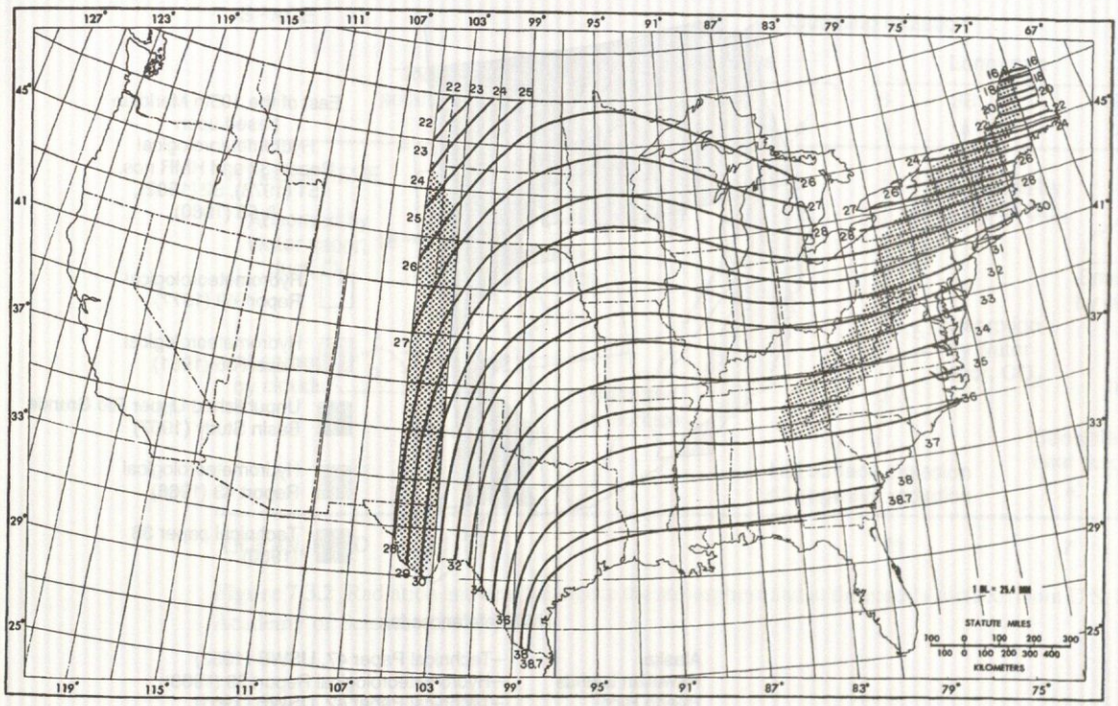


(*c*)

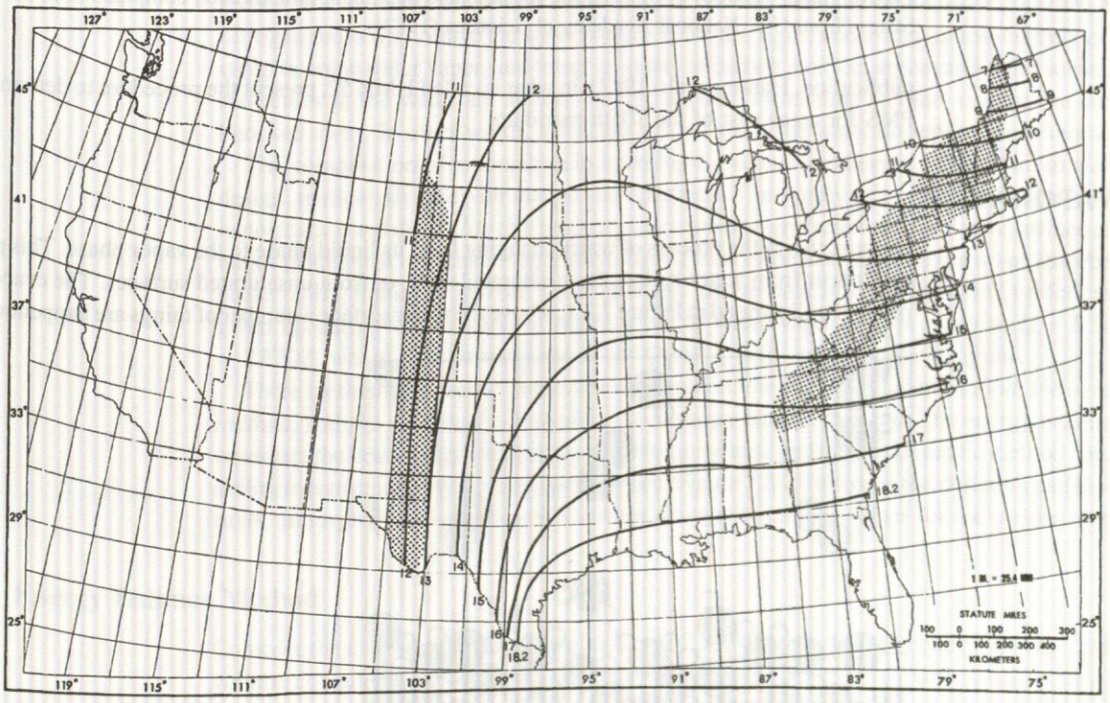


(*d*)

**Figure 7.2.19** (*Continued*) (*c*) Example of all-season PMP (in) for 12 hr, 10 mi$^2$ (from Schreiner and Riedel, 1978); (*d*) Example of all-season PMP (in) for 6 hr, 1000 mi$^2$ (from Schreiner and Riedel, 1978).

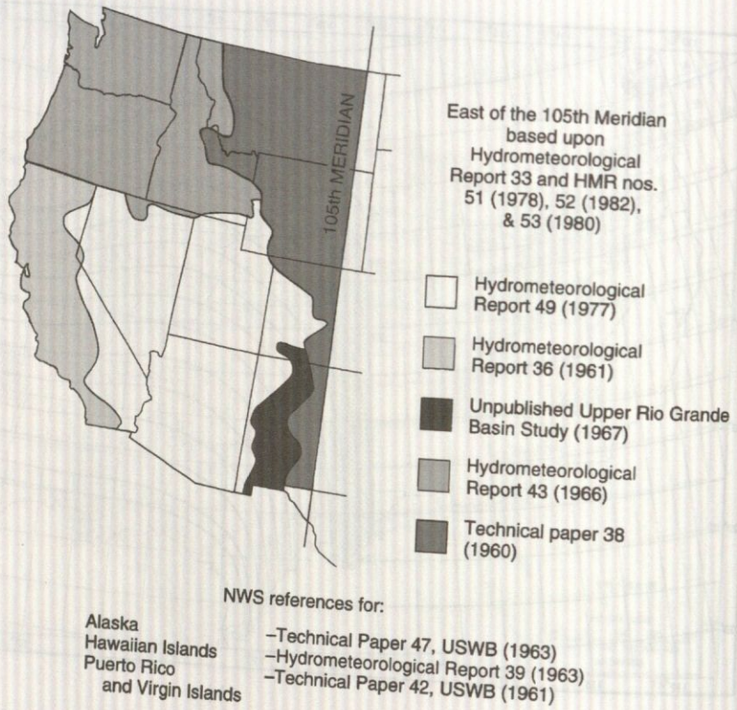


**Figure 7.2.20** Sources of information for probable maximum precipitation computation in the United States (from U.S. National Academy of Sciences (1983)).

publication. Hansen et al. (1982), in what is called HMR 52, present the procedure to determine the PMS for areas east of the 105th meridian.

## 7.3 EVAPORATION

*Evaporation* is the process of water changing from its liquid phase to the vapor phase. This process may occur from water bodies, from saturated soils, or from unsaturated surfaces. The evaporation process is illustrated in Figure 7.3.1. Above the water surface a number of things are happening. First

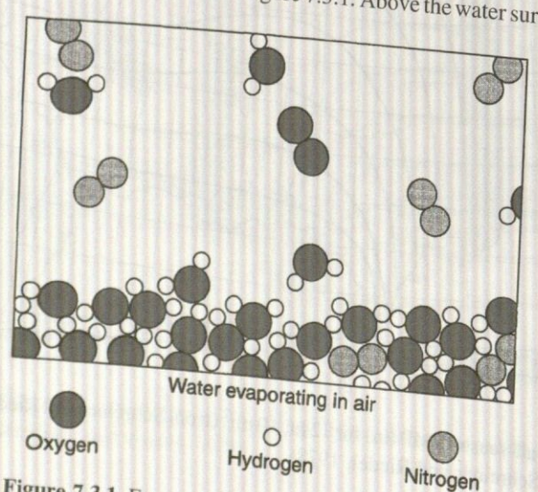


**Figure 7.3.1** Evaporation (magnified one billion times) (from Feynman et al. (1963)).

### 7.3.1 Energy Bala

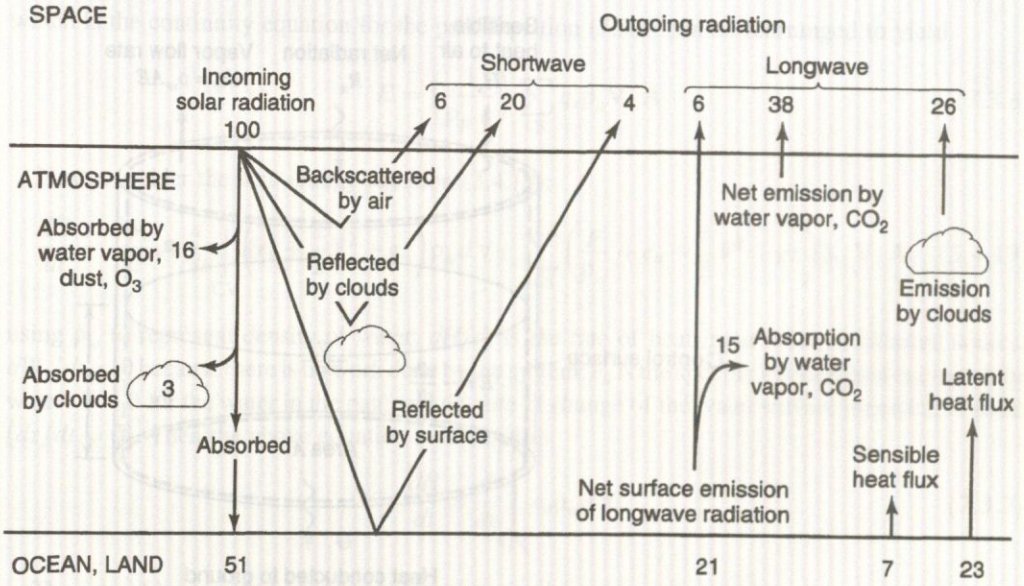


**Figure 7.3.2** Radiation and heat balance in the atmosphere and at the earth's surface (from U.S. National Academy of Sciences (1975)).

of all, there are water molecules in the form of *water vapor*, which are always found above liquid water. In addition, there are some other molecules: (a) two oxygen atoms stuck together by themselves, forming an *oxygen molecule*, and (b) two nitrogen atoms stuck together, forming a nitrogen molecule. Above the water surface is the air, a gas, consisting almost entirely of nitrogen, oxygen, some water vapor, and lesser amounts of carbon dioxide, argon, and other substances. The molecules in the water are always moving around. From time to time, one on the surface gets knocked away. In other words, molecule by molecule, the water disappears or evaporates.

The computation of evaporation in hydrologic analysis and design is important in water supply design, particularly reservoir design and operation. The supply of energy to provide *latent heat of vaporization* and the *ability to transport water vapor away* from the evaporative surface are the two major factors that influence evaporation. *Latent heat* is the heat that is given up or absorbed when a phase (solid, liquid, or gaseous state) changes. *Latent heat of vaporization* ($l_v$) refers to the heat given up during vaporization of liquid water to water vapor, and is given as $l_v = 2.501 \times 10^6 - 2370T$, where $T$ is the temperature in °C and $l_v$ is in joules (J) per kilogram.

Three methods are used to determine evaporation: *the energy balance method, the aerodynamic method*, and *the combined aerodynamic and energy balance method*. The energy balance method considers the heat energy balance of a hydrologic system, and the aerodynamic method considers the ability to transport away from an open surface. Figure 7.3.2 illustrates the radiation and heat balance in the atmosphere and at the earth's surface along with relative values for the various components.

## Energy Balance Method

Consider the evaporation pan shown in Figure 7.3.3 with the defined control volume. This control volume contains water in both the liquid phase and the vapor phase, with densities of $\rho_w$ and $\rho_a$, respectively. The continuity equation must be written for both phases. For the liquid phase, the extensive property $B = m$ (mass of liquid water), the intensive property $\beta = 1$, and $dB/dt = \dot{m}_v$, which is the mass flow rate of evaporation. Continuity for the liquid phase is then

$$-\dot{m}_v = \frac{d}{dt}\int_{CV} \rho_w d\forall + \sum_{CS} \rho_w \mathbf{V}\cdot\mathbf{A} \qquad (7.3.1)$$

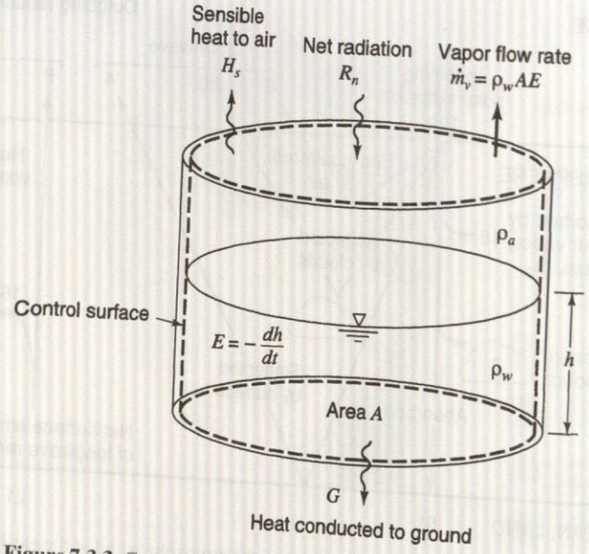


**Figure 7.3.3** Control volume defined for continuity and energy equation development for an evaporation pan (from Chow et al. (1988)).

Because the pan has impermeable sides, there is no flow of liquid water across the control surface, so $\sum_{CS} \rho_w \mathbf{V} \cdot \mathbf{A} = 0$.

The rate of change of storage is

$$\frac{d}{dt} \int_{CV} \rho_w d\forall = \rho_w A \frac{dh}{dt} \tag{7.3.2}$$

where $A$ is the cross-sectional area of the pan and $h$ is the depth of water. Substituting equation (7.3.2) into (7.3.1) gives

$$-\dot{m}_v = \rho_w A \frac{dh}{dt} \tag{7.3.3a}$$

or

$$\dot{m}_v = \rho_w AE \tag{7.3.3b}$$

where $E = -dh/dt$ is the evaporation rate.

Considering the vapor phase, the extensive property is $B = m_v$(mass of water vapor), the intensive property is $\beta = q_v$(specific humidity), and $dB/dt = \dot{m}_v$. Continuity for the vapor phase is

$$\dot{m}_v = \frac{d}{dt} \int_{CV} q_v \rho_a d\forall + \sum_{CS} q_v \rho_a \mathbf{V} \cdot \mathbf{A} \tag{7.3.4}$$

Considering steady flow over the pan, the time derivative of water vapor in the control volume is zero, $\frac{d}{dt} \int_{CV} q_v \rho_a d\forall = 0$, and $\dot{m}_v$ from equation (7.3.3) is substituted into equation (7.3.4) to obtain

$$\rho_w AE \sum_{CS} q_v \rho_a \mathbf{V} \cdot \mathbf{A} \tag{7.3.5}$$

which is the continuity equation for the pan. Equation (7.3.5) can be rearranged to yield

$$E = \left(\frac{1}{\rho_w A}\right) \sum_{CS} q_v \rho_a \mathbf{V} \cdot \mathbf{A} \tag{7.3.6}$$

Next, consider the heat energy equation (3.4.19):

$$\frac{dH}{dt} - \frac{dW_s}{dt} = \frac{d}{dt} \int_{CV} \left(e_u + \frac{1}{2}V^2 + gz\right) \rho_w d\forall + \sum_{CS} \left(\frac{p}{\rho_w} + e_u + \frac{1}{2}V^2 + gz\right) \rho_w \mathbf{V} \cdot \mathbf{A} \tag{3.4.19}$$

using $\rho_w$ to represent density of water; $dH/dt$ is the rate of heat input from an external source, $dW_s/dt = 0$ because there is no work done by the system; $e_u$ is the specific internal heat energy of the water; $V = 0$ for the water in the pan; and the rate of change of the water surface elevation is small ($dz/dt = 0$). Then the above equation is reduced to

$$\frac{dH}{dt} = \frac{d}{dt} \int_{CV} e_u \rho_w d\forall \tag{7.3.7}$$

The rate of heat input from external sources can be expressed as

$$\frac{dH}{dt} = R_n - H_s - G \tag{7.3.8}$$

where $R_n$ is the *net radiation flux* (watts per meter squared), $H_s$ is the *sensible heat* to the air stream supplied by the water, and $G$ is the *ground heat flux* to the ground surface. Net radiation flux is the net input of radiation at the surface at any instant. The net radiation flux at the earth's surface is the major energy input for evaporation of water, defined as the difference between the radiation absorbed, $R_i(1 - \alpha)$ (where $R_i$ is the *incident radiation* and $\alpha$ is the fraction of radiation reflected, called the *albedo*), and that emitted. $R_e$:

$$R_n = R_i(1 - \alpha) - R_e \tag{7.3.9}$$

The amount of radiation emitted is defined by the *Stefan–Boltzmann law*

$$R_e = e\sigma T_p^4 \tag{7.3.10}$$

where $e$ is the *emissivity* of the surface, $\sigma$ is the *Stefan-Boltzmann constant* ($5.67 \times 10^{-8}$ W/m$^2 \cdot$ K$^4$), and $T_p$ is the absolute temperature of the surface in degrees Kelvin.

Assuming that the temperature of the water in the control volume is constant in time, the only change in the heat stored within the control volume is the change in the internal energy of the water evaporated $l_v \dot{m}_v$, where $l_v$ is the latent heat of vaporization, so that

$$\frac{d}{dt} \int_{CV} e_u \rho_w d\forall = l_v \dot{m}_v \tag{7.3.11}$$

Substituting equations (7.3.8) and (7.3.11) into (7.3.7) results in

$$R_n - H_s - G = l_v \dot{m}_v \tag{7.3.12}$$

From equation (7.3.3b), $\dot{m}_v = \rho_w AE$. Substituting in (7.3.12) with $A = 1$ m$^2$ and solving for $E$ (to denote energy balance) gives the *energy balance equation for evaporation*,

$$E = \frac{1}{l_v \rho_w}(R_n - H_s - G) \tag{7.3.13}$$

Assuming the sensible heat flux $H_s$ and the ground heat flux $G$ are both zero, then an evaporation rate $E_r$, which is the rate at which all incoming net radiation is absorbed by evaporation, can be

calculated as

$$E_r = \frac{R_n}{l_v \rho_w} \tag{7.3.14}$$

***EXAMPLE 7.3.1***

For a particular location the average net radiation is 185 W/m$^2$, air temperature is 28.5°C, relative humidity is 55 percent, and wind speed is 2.7 m/s at a height of 2 m. Determine the open water evaporation rate in mm/d using the energy method.

***SOLUTION***

Latent heat of vaporization in joules (J) per kg varies with $T$ (°C), or $l_v = 2.501 \times 10^6 - 2370T$, so $l_v = 2501 - 2.37 \times 28.5 = 2433$ kJ/kg, $\rho_w = 996.3$ kg/m$^3$. The evaporation rate by the energy balance method is determined using equation (7.3.14) with $R_n = 185$ W/m$^2$:

$$E_r = R_n/(l_v \rho_w) = 185/(2433 \times 10^3 \times 996.3) = 7.63 \times 10^{-8} \text{ m/s} = 6.6 \text{ mm/d}.$$

## 7.3.2 Aerodynamic Method

As mentioned previously, the aerodynamic method considers the ability to transport water vapor away from the water surface; that is, generated by the humidity gradient in the air near the surface and the wind speed across the surface. These processes can be analyzed by coupling the equation for mass and momentum transport in the air. Considering the control volume in Figure 7.3.4, the vapor flux $\dot{m}_v$ passing upward by convection can be defined along with the momentum flux (as a function of the humidity gradient and the wind velocity gradient, respectively) (see Chow et al., 1988). The ratio of the vapor flux and the momentum flux can be used to define the *Thornthwaite–Holzman equation* for vapor transport (Thornthwaite and Holzman, 1939). Chow et al. (1988) present details of this derivation. The final form of the evaporation equation for the aerodynamic method expresses the evaporation rate $E_a$ as a function of the difference of the vapor pressure at the surface $e_{as}$, which is the *saturation vapor pressure* at ambient air temperature (when the rate of evaporation and condensation are equal), and the vapor pressure at a height $z_2$ above the water surface, which is taken as the ambient vapor pressure in air $e_a$.

$$E_a = B(e_{as} - e_a) \tag{7.3.15}$$

where $E_a$ has units of mm/day and $B$ is the vapor transfer coefficient with units of mm/day · Pa, given as

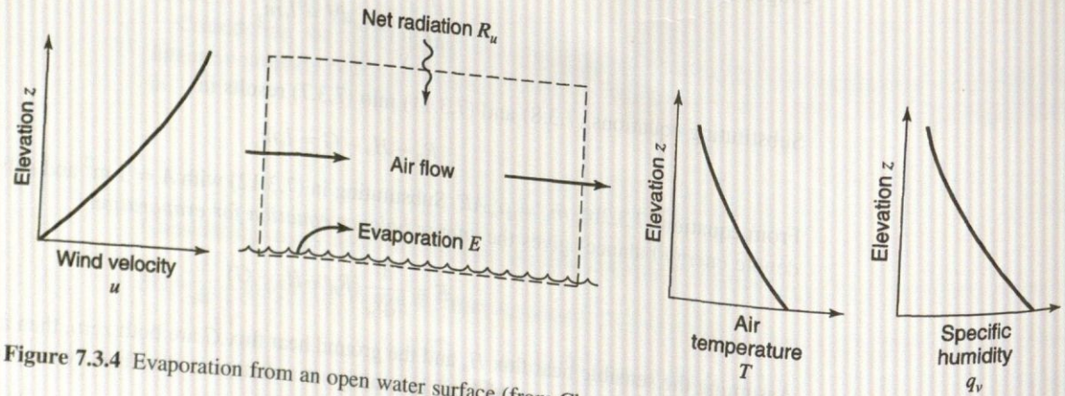


**Figure 7.3.4** Evaporation from an open water surface (from Chow et al. (1988)).

$$B = \frac{0.102u_2}{[\ln(z_2/z_0)]^2} \tag{7.3.16}$$

where $u_2$ is the wind velocity (m/s) measured at height $z_2$ (cm) and $z_0$ is the roughness height (0.01–0.06 cm) of the water surface. The vapor pressures have units of Pa (N/m$^2$). The saturation vapor pressure is approximated as

$$e_{as} = 611 \exp\left(\frac{17.27T}{237.3+T}\right) \tag{7.3.17}$$

and the vapor pressure is

$$e_a = R_h e_{as} \tag{7.3.18}$$

where $T$ is the air temperature in °C and $R_h$ is the relative humidity ($R = e_a/e_{as}$) and ($0 \leq R_h \leq 1$).

***EXAMPLE 7.3.2***

Solve example 7.3.1 using the aerodynamic method, by using a roughness height $z_0 = 0.03$ cm.

***SOLUTION***

From equation (7.3.17), the saturated vapor pressure is

$$e_{as} = 611 \exp[17.27T/(237.3+T)] = 611 \exp[17.27 \times 28.5/(237.3+28.5)]$$
$$= 3893 \text{ Pa}$$

The ambient vapor pressure $e_a$ is determined from equation (7.3.18); for a relative humidity $R_h = 0.55$, $e_a = e_{as} R_h = 3893 \times 0.55 = 2141$ Pa. The vapor transfer coefficient $B$ is given by equation (7.3.16) in which $u_2 = 2.7$ m/s, $z_2 = 2$ m, and $z_0 = 0.03$ cm for an open water surface, so that $B = 0.102u_2/[\ln(zz/z0)]^2 = 0.102 \times 2.7/[\ln(200/0.03)]^2 = 0.0036$ mm/d · Pa; then the evaporation rate by the aerodynamic method is given by equation (7.3.15):

$$E_a = B(e_{as} - e_a) = 0.0036(3893 - 2141) = 6.31 \text{ mm/d}.$$

### 7.3.3 Combined Method

When the energy supply is not limiting, the aerodynamic method can be used, and when the vapor transport is not limiting, the energy balance method can be used. However, both of these factors are not normally limiting, so a combination of these methods is usually required. The combined method equation is

$$E = \left(\frac{\Delta}{\Delta+\gamma}\right)E_r + \left(\frac{\gamma}{\Delta+\gamma}\right)E_a \tag{7.3.19}$$

in which $(\,)E_r$ is the vapor transport term and $(\,)E_a$ is the aerodynamic term. $\gamma$ is the *psychrometric constant* (approximately 66.8 Pa/°C) and $\Delta$ is the *gradient of the saturated vapor pressure curve* $\Delta = de_{as}/dT$ at air temperature $T_\alpha$ given as

$$\Delta = \frac{4098e_{as}}{(237.3+T_\alpha)} \tag{7.3.20}$$

in which $e_{as}$ is the *saturated vapor pressure* (the maximum moisture content the air can hold for a given temperature).

The combination method is best for application to small areas with detailed climatological data including net radiation, air temperature, humidity, wind speed, and air pressure. For very large areas, energy (vapor transport) largely governs evaporation. Priestley and Taylor (1972) discovered that the aerodynamic term in equation (7.3.19) is approximately 30 percent of the energy term, so that

equation (7.3.19) can be simplified to

$$E = 1.3\left(\frac{\Delta}{\Delta+\gamma}\right)E_r \tag{7.3.21}$$

which is known as the *Priestley–Taylor evaporation equation.*

***EXAMPLE 7.3.3*** Solve example 7.3.1 using the combined method.

***SOLUTION***

The gradient of the saturated vapor pressure curve is, from equation (7.3.20),

$$\Delta = 4098e_{as}/(237.3+T)^2 = 4098 \times 3893/(237.3+28.5)^2 = 225.8 \text{ Pa/°C}$$

The psychrometric constant $\gamma$ is approximately 66.8 Pa/°C; then $E_r$ and $E_a$ may be combined according to equation (7.3.19) to give

$$\begin{aligned} E &= \Delta/(\Delta+\gamma)E_r + \gamma/(\Delta+\gamma)E_a \\ &= (225.8/(225.8+66.8))6.6 + (66.8/(225.8+66.8))6.31 = 0.772(6.6) + 0.228(6.31) \\ &= 5.10 + 1.44 = 6.54 \text{ mm/d} \end{aligned}$$

***EXAMPLE 7.3.4*** Solve example 7.3.1 using the Priestley–Taylor method.

***SOLUTION***

The evaporation is computed using equation (7.3.21):

$$\begin{aligned} E &= 1.3\left(\frac{\Delta}{\Delta+\gamma}\right)E_r = 1.3\left(\frac{225.8}{225.8+66.8}\right)6.6 \\ &= 6.62 \text{ mm/d} \end{aligned}$$

## 7.4 INFILTRATION

The process of water penetrating into the soil is *infiltration.* The rate of infiltration is influenced by the condition of the soil surface, vegetative cover, and soil properties including porosity, hydraulic conductivity, and moisture content. In order to discuss infiltration, we must first consider the division of subsurface water (see Figure 6.1.2) and the various subsurface flow processes shown in Figure 7.4.1. These processes are infiltration of water to become *soil moisture, subsurface flow* (unsaturated flow) through the soil, and *groundwater flow* (saturated flow). *Unsaturated flow* refers to flow through a porous medium when some of the voids are occupied by air. *Saturated flow* occurs when the voids are filled with water. The *water table* is the interface between the saturated and unsaturated flow, where atmospheric pressure prevails. Saturated flow occurs below the water table and unsaturated flow occurs above the water table.

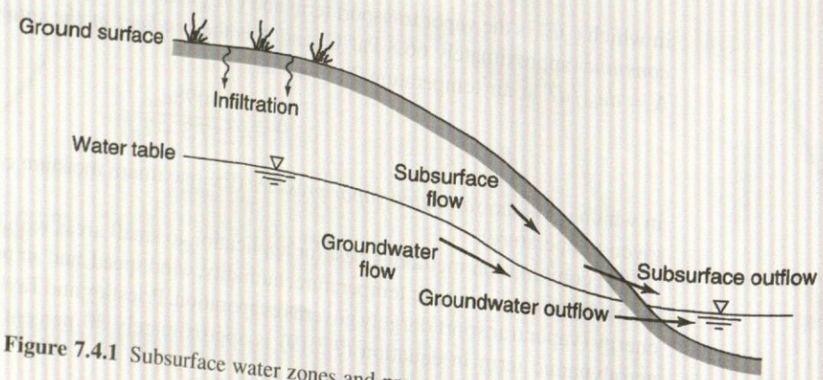


**Figure 7.4.1** Subsurface water zones and processes (from Chow et al. (1988)).

### 7.4.1 Unsaturated Flow

The cross-section through an unsaturated porous medium (Figure 7.4.2*a*) is now used to define *porosity*, $\eta$:

$$\eta = \frac{\text{volume of voids}}{\text{total volume}} \tag{7.4.1}$$

in which $\eta$ is $0.25 < \eta < 0.40$, and the *soil moisture content*, $\theta$,

$$\theta = \frac{\text{volume of water}}{\text{total volume}} \tag{7.4.2}$$

in which $\theta$ is $0 \leq \theta \leq \eta$. For saturated conditions, $\theta = \eta$.

Consider the control volume in Figure 7.4.2*b* for an unsaturated soil with sides of lengths $dx$, $dy$, and $dz$, with a volume of $dxdydz$. The volume of water contained in the control volume is $\theta dxdydz$. Flow through the control volume is defined by the *Darcy flux*, $q = Q/A$, which is the volumetric flow rate per unit of soil area. For this derivation, the horizontal fluxes are ignored and only the vertical ($z$) direction is considered, with $z$ positive upward.

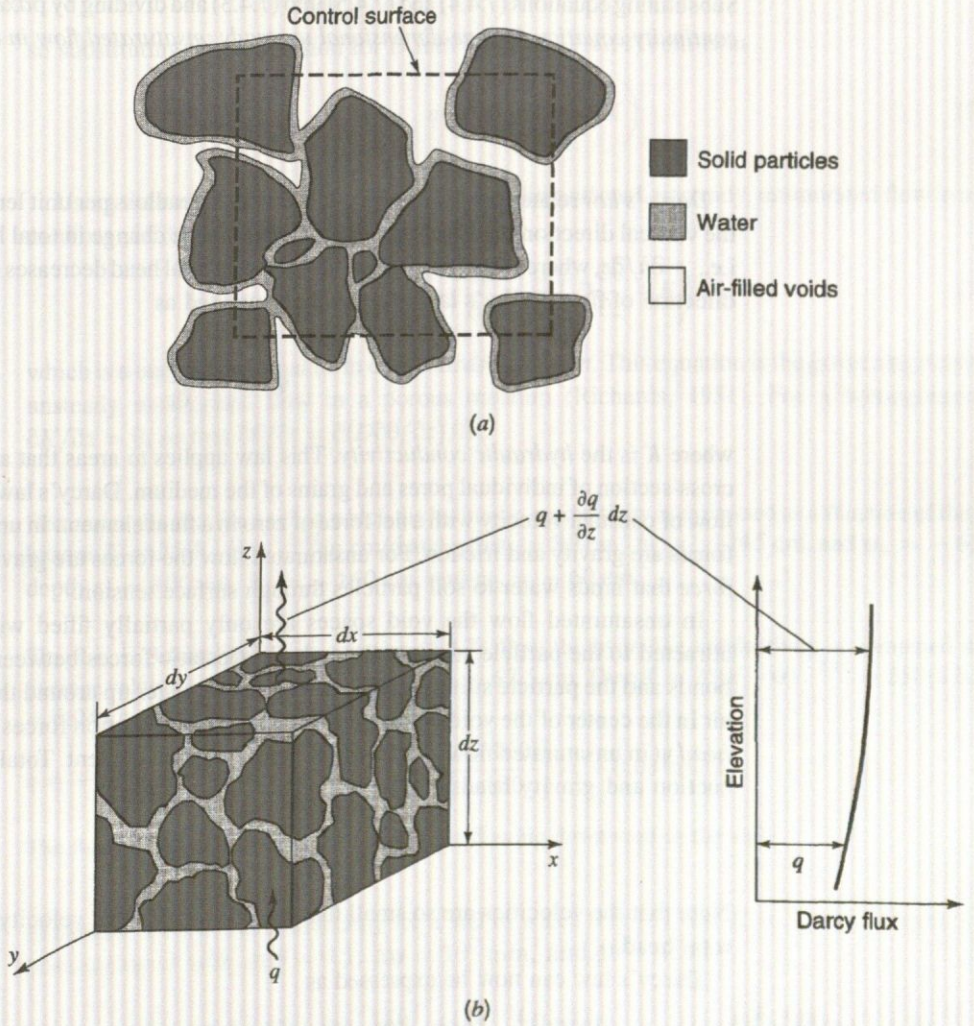


**Figure 7.4.2** (*a*) Cross-section through an unsaturated porous medium; (*b*) Control volume for development of the continuity equation in an unsaturated porous medium (from Chow et al. (1988)).

With the control volume approach, the extensive property $B$ is the mass of soil water, so the intensive property $\beta = dB/dm = 1$ and $dB/dt = 0$, because no phase changes are occurring in water. The general control volume equation for continuity, equation (3.3.1), is applicable:

$$0 = \frac{d}{dt}\int_{CV} \rho \, d\forall + \int_{CS} \rho \mathbf{V} \cdot d\mathbf{A} \tag{7.4.3}$$

The time rate of change of mass stored in the control volume is

$$\frac{d}{dt}\int_{CV} \rho \, d\forall = \frac{d}{dt}(\rho\theta dxdydz) = \rho dxdydz\frac{\partial\theta}{\partial t} \tag{7.4.4}$$

where the density is assumed constant. The net outflow of water is the difference between the volumetric inflow at the bottom ($qdxdy$) and the volumetric outflow at the top $[q + (\partial q/\partial z)dz]dxdy$, so

$$\int_{CV} \rho \mathbf{V} \cdot d\mathbf{A} = \rho\left(q + \frac{\partial q}{\partial z}dz\right)dxdy - \rho q dxdy = \rho dxdydz\frac{\partial q}{\partial z} \tag{7.4.5}$$

Substituting equations (7.4.4) and (7.4.5) into (7.4.3) and dividing by $\rho dxdydz$ results in the following *continuity equation for one-dimensional unsteady unsaturated flow in a porous medium*:

$$\frac{\partial\theta}{\partial t} + \frac{\partial q}{\partial z} = 0 \tag{7.4.6}$$

*Darcy's law* relates the *Darcy flux* $q$ to the rate of headloss per unit length of medium. For flow in the vertical direction the headloss per unit length is the change in total head $\partial h$ over a distance, $\partial z$, i.e., $-\partial h/\partial z$, where the negative sign indicates that total head decreases (as a result of friction) in the direction of flow. Darcy's law can now be expressed as

$$q = -K\frac{\partial h}{\partial z} \tag{7.4.7}$$

where $K$ is the *hydraulic conductivity*. This law applies to areas that are large compared with the cross-section of individual pores and grains of the medium. Darcy's law describes a steady uniform flow of constant velocity with a net force of zero in a fluid element. In unconfined saturated flow, the forces are gravity and friction. For unsaturated flow the forces are gravity, friction, and the *suction force* that binds water to soil particles through surface tension.

In unsaturated flow the void spaces are only partially filled with water, so that water is attracted to the particle surfaces through electrostatic forces between the water molecule polar bonds and the particle surfaces. This in turn draws water up around the particle surfaces, leaving air in the center of the voids. The energy due to the soil suction forces is referred to as the *suction head* $\psi$ in unsaturated flow, which varies with moisture content. Total head is then the sum of the suction and gravity heads:

$$h = \psi + z \tag{7.4.8}$$

Note that the velocities are so small that there is no term for velocity head in this expression for total head.

Darcy's law can now be expressed as

$$q = -K\frac{\partial(\psi + z)}{\partial z} \tag{7.4.9}$$

EXAMPLE 7.4.

SOLUTION

EXAMPLE 7.4.

SOLUTION

Darcy's law was originally conceived for saturated flow and was extended by Richards (1931) to unsaturated flow with the provision that the hydraulic conductivity is a function of the suction head, i.e., $K = K(\psi)$. Also, the hydraulic conductivity can be related more easily to the degree of saturation, so that $K = K(\theta)$. Because the soil suction head varies with moisture content and moisture content varies with elevation, the *suction gradient* can be expanded by using the chain rule to obtain

$$\frac{\partial \psi}{\partial z} = \frac{d\psi}{d\theta}\frac{\partial \theta}{\partial z} \tag{7.4.10}$$

in which $\partial\theta/\partial z$ is the *wetness gradient*, and the reciprocal of $d\psi/d\theta$, i.e., $d\theta/d\psi$, is the *specific water capacity*. Now equation (7.4.9) can be modified to

$$q = -K\left(\frac{\partial \psi}{\partial z} + \frac{\partial z}{\partial z}\right) = -K\left(\frac{\partial \psi}{\partial \theta}\frac{\partial \theta}{\partial z} + 1\right) = -\left(K\frac{d\psi}{d\theta}\frac{\partial \theta}{\partial z} + K\right) \tag{7.4.11}$$

The *soil water diffusivity* $D(L^2/T)$ is defined as

$$D = K\frac{d\psi}{d\theta} \tag{7.4.12}$$

so substituting this expression for $D$ into equation (7.4.11) results in

$$q = -\left(D\frac{\partial \theta}{\partial z} + K\right) \tag{7.4.13}$$

Using the continuity equation (7.4.6) for one-dimensional, unsteady, unsaturated flow in a porous medium yields

$$\frac{\partial \theta}{\partial t} = -\frac{\partial q}{\partial z} = \frac{\partial}{\partial z}\left(D\frac{\partial \theta}{\partial z} + K\right) \tag{7.4.14}$$

which is a one-dimensional form of *Richards' equation*. This equation is the governing equation for unsteady unsaturated flow in a porous medium (Richards, 1931). For a homogeneous soil, $\partial K/\partial z = 0$, so that $\partial\theta/\partial t = \partial(D\partial\theta/\partial z)/\partial z$.

***EXAMPLE 7.4.1***

Determine the flux for a soil in which the hydraulic conductivity is expressed as a function of the suction head as $K = 250(-\psi)^{-2.11}$ in cm/d at depth $z_1 = 80$ cm, $h_1 = -145$ cm, and $\psi_1 = -65$ cm at depth $z_2 = 100$ cm, $h_2 = -160$ cm, and $\psi_2 = -60$ cm.

***SOLUTION***

The flux is determined using equation (7.4.7). First the hydraulic conductivity is computed using an average value of $\psi = [-65 + (-60)]/2 = -62.5$ cm. Then $K = 250(-\psi)^{-2.11} = 250(62.5)^{-2.11} = 0.041$ cm/d. The flux is then

$$q = -K\left(\frac{h_1 - h_2}{z_1 - z_2}\right) = -0.041\left[\frac{-145 - (-160)}{-80 - (-100)}\right] = -0.03\ \text{cm/d}$$

The flux is negative because the moisture is flowing downward in the soil.

***EXAMPLE 7.4.2***

Determine the soil water diffusivity for a soil in which $\theta = 0.1$ and $K = 3 \times 10^{-11}$ mm/s from a relationship of $\psi(\theta)$ at $\theta = 0.1$, $\Delta\psi = 10^7$ mm, and $\Delta\theta = 0.35$.

***SOLUTION***

Using equation (7.4.12), the soil water diffusivity is $D = Kd\psi/d\theta = (3 \times 10^{-11}\ \text{mm/s})(10^7\ \text{mm}/0.35) = 8.57 \times 10^{-4}$ mm/s.

### 7.4.2 Green-Ampt Method

Figure 7.4.3 illustrates the distribution of soil moisture within a soil profile during downward movement. These moisture zones are the *saturated zone*, the *transmission zone*, a *wetting zone*, and a *wetting front*. This profile changes as a function of time as shown in Figure 7.4.4.

The *infiltration rate f* is the rate at which water enters the soil surface, expressed in in/hr or cm/hr. The *potential infiltrate rate* is the rate when water is ponded on the soil surface, so if no ponding occurs the actual rate is less than the potential rate. Most infiltration equations describe a potential infiltration rate. *Cumulative infiltration F* is the accumulated depth of water infiltrated, defined mathematically as

$$F(t) = \int_0^t f(\tau)d\tau \tag{7.4.15}$$

and the infiltration rate is the time derivative of the cumulative infiltration given as

$$f(t) = \frac{dF(t)}{dt} \tag{7.4.16}$$

Figure 7.4.5 illustrates a rainfall hyetograph with the infiltration rate and cumulative infiltration curves. (See Section 8.2 for further details on the rainfall hyetograph.)

Green and Ampt (1911) proposed the simplified picture of infiltration shown in Figure 7.4.6. The *wetting front* is a sharp boundary dividing soil with moisture content $\theta_i$ below from saturated soil

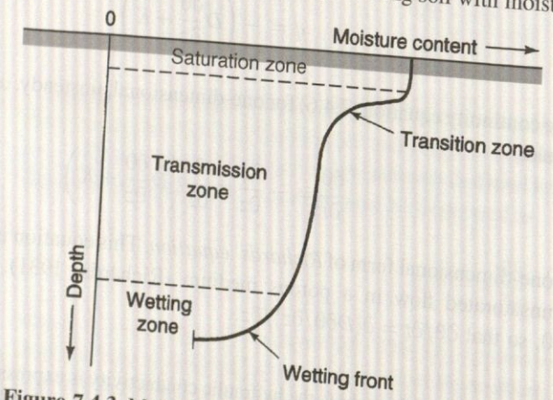


**Figure 7.4.3** Moisture zones during infiltration (from Chow et al. (1988)).

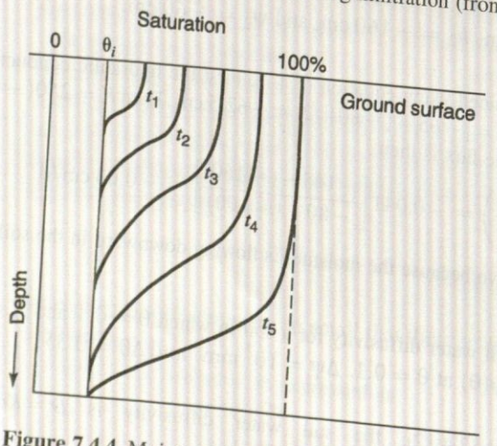


**Figure 7.4.4** Moisture profile as a function of time for water added to the soil surface.

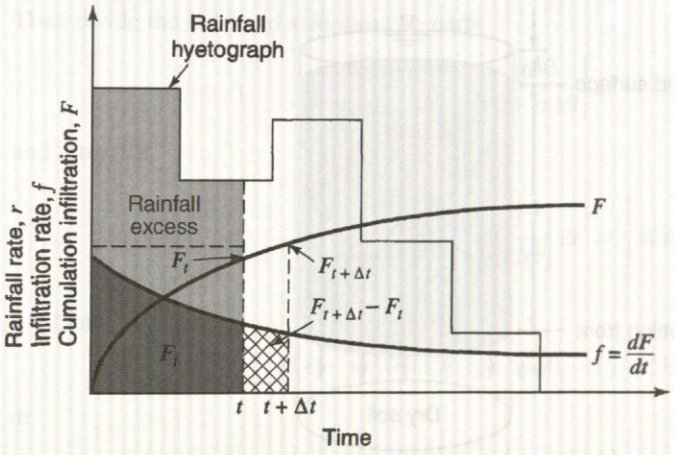


**Figure 7.4.5** Rainfall infiltration rate and cumulative infiltration. The rainfall hyetograph illustrates the rainfall pattern as a function of time. The cumulative infiltration at time $t$ is $F_t$ or $F(t)$ and at time $t+\Delta t$ is $F_{t+\Delta t}$ or $F(t+\Delta t)$ and are computed using equation (7.4.15). The increase in cumulative infiltration from time $t$ to $t+\Delta t$ is $F_{t+\Delta t} - F_t$ or $F(t+\Delta t) - F(t)$, as shown in the figure. Rainfall excess is defined in Chapter 8 as that rainfall that is neither retained on the land surface nor infiltrated into the soil.

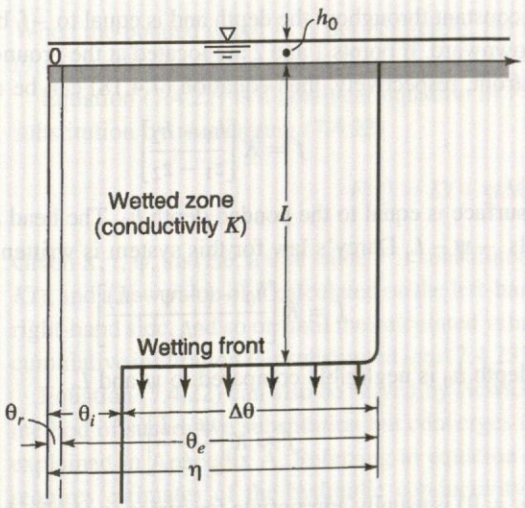


**Figure 7.4.6** Variables in the Green–Ampt infiltration model. The vertical axis is the distance from the soil surface; the horizontal axis is the moisture content of the soil (from Chow et al. (1988)).

with moisture content $\eta$ above. The wetting front has penetrated to a depth $L$ in time $t$ since infiltration began. Water is ponded to a small depth $h_0$ on the soil surface.

Consider a vertical column of soil of unit horizontal cross-sectional area (Figure 7.4.7) with the control volume defined around the wet soil between the surface and depth $L$. For a soil initially of moisture content $\theta_i$ throughout its entire depth, the *moisture content* will increase from $\theta_i$ to $\eta$ (the porosity) as the wetting front passes. The moisture content $\theta$ is the ratio of the volume of water to the total volume within the control surface. $L(\eta - \theta_i)$ is then the increase in the water stored within the control volume as a result of infiltration, through a unit cross-section. By definition this quantity is equal to $F$, the cumulative depth of water infiltrated into the soil, so that

$$F(t) = L(\eta - \theta_i) = L\Delta\theta \tag{7.4.17}$$

where $\Delta\theta = (\eta - \theta_i)$.

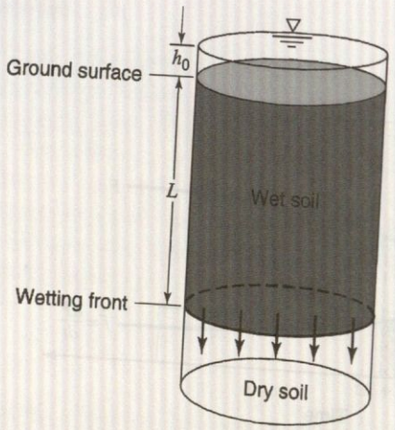


**Figure 7.4.7** Infiltration into a column of soil of unit cross-sectional area for the Green–Ampt model (from Chow et al. (1988)).

Darcy's law may be expressed (using equation (7.4.7)) as

$$q = K\frac{\partial h}{\partial z} = -K\frac{\Delta h}{\Delta z} \tag{7.4.18}$$

The Darcy flux $q$ is constant throughout the depth and is equal to $-f$, because $q$ is positive upward while $f$ is positive downward. If points 1 and 2 are located at the ground surface and just on the dry side of the wetting front, respectively, then equation (7.4.18) can be approximated by

$$f = K\left[\frac{h_1 - h_2}{z_1 - z_2}\right] \tag{7.4.19}$$

The head $h_1$ at the surface is equal to the ponded depth $h_0$. The head $h_2$, in the dry soil below the wetting front, equals $-\psi - L$. Darcy's law for this system is written as

$$f = K\left[\frac{h_0 - (-\psi - L)}{L}\right] \tag{7.4.20a}$$

and if the ponded depth $h_0$ is negligible compared to $\psi$ and $L$,

$$f \approx K\left[\frac{\psi + L}{L}\right] \tag{7.4.20b}$$

This assumption ($h_0 = 0$) is usually appropriate for surface water hydrology problems because it is assumed that ponded water becomes surface runoff.

From equation (7.4.17), the wetting front depth is $L = F/\Delta\theta$, and assuming $h_0 = 0$, substitution into equation (7.4.20) gives

$$f = K\left[\frac{\psi\Delta\theta + F}{F}\right] \tag{7.4.21}$$

Since $f = dF/dt$, equation (7.4.21) can be expressed as a differential equation in the one unknown $F$ as

$$\frac{dF}{dt} = K\left[\frac{\psi\Delta\theta + F}{F}\right]$$

To solve for $F$, cross-multiply to obtain

$$\left[\frac{F}{F + \psi\Delta\theta}\right]dF = K dt$$

Then divide the left-hand side into two parts

$$\left[\frac{F+\psi\Delta\theta}{F+\psi\Delta\theta}-\frac{\psi\Delta\theta}{F+\psi\Delta\theta}\right]dF = Kdt$$

and integrate

$$\int_0^{F(t)}\left[1-\frac{\psi\Delta\theta}{F+\psi\Delta\theta}\right]dF = \int_0^t Kdt$$

to obtain

$$F(t)-\psi\Delta\theta\{\ln[F(t)+\psi\Delta\theta]-\ln(\psi\Delta\theta)\} = Kt \tag{7.4.22a}$$

or

$$F(t)-\psi\Delta\theta\ln\left(1+\frac{F(t)}{\psi\Delta\theta}\right) = Kt \tag{7.4.22b}$$

Equation (7.4.22) is the *Green–Ampt equation* for cumulative infiltration. Once $F$ is computed using equation (7.4.22), the infiltration rate $f$ can be obtained from equation (7.4.21) or

$$F(t) = K\left[\frac{\psi\Delta\theta}{F(t)}+1\right] \tag{7.4.23}$$

When the ponded depth $h_0$ is not negligible, the value of $\psi + h_0$ is substituted for $\psi$ in equations (7.4.22) and (7.4.23).

Equation (7.4.22) is a nonlinear equation in $F$ that can be solved by the method of successive substitution by rearranging (7.4.22)

$$F(t) = Kt+\psi\Delta\theta\ln\left(1+\frac{F(t)}{\psi\Delta\theta}\right) \tag{7.4.24}$$

Given $K$, $t$, $\psi$, and $\Delta\theta$, a trial value $F$ is substituted on the right-hand side (a good trial value is $F = Kt$), and a new value of $F$ calculated on the left-hand side, which is substituted as a trial value on the right-hand side, and so on until the calculated values of $F$ converge to a constant. The final value of cumulative infiltration $F$ is substituted into (7.4.23) to determine the corresponding infiltration rate $f$.

Equation (7.4.22) can also be solved by Newton's method, which is more complicated than the method of successive substitution but converges in fewer iterations. Newton's iteration method is explained in Appendix A. Referring to equation (7.4.24), application of the Green–Ampt model requires estimates of the hydraulic conductivity $K$, the wetting front soil suction bead $\psi$ (see Table 7.4.1), and $\Delta\theta$.

The *residual moisture content* of the soil, denoted by $\theta_r$, is the moisture content after it has been thoroughly drained. The *effective saturation* is the ratio of the available moisture $(\theta-\theta_r)$ to the maximum possible available moisture content $(\eta-\theta_r)$, given as

$$s_e = \frac{\theta-\theta_r}{\eta-\theta_r} \tag{7.4.25}$$

where $\eta-\theta_r$ is called the *effective porosity* $\theta_e$.

The effective saturation has the range $0 \le s_e \le 1.0$, provided $\theta_r \le \theta \le \eta$. For the initial condition, when $\theta = \theta_i$, cross-multiplying equation (7.4.25) gives $\theta_i - \theta_r = s_e\theta_e$, and the change in the moisture content when the wetting front passes is

$$\begin{aligned}\Delta\theta &= \eta-\theta_i = \eta-(s_e\theta_e+\theta_r)\\ \Delta\theta &= (1-s_e)\theta_e\end{aligned} \tag{7.4.26}$$

**Table 7.4.1** Green–Ampt Infiltration Parameters for Various Soil Classes*

| Soil class | Porosity $\eta$ | Effective porosity $\theta_e$ | Wetting front soil suction head $\psi$ (cm) | Hydraulic conductivity $K$ (cm/h) |
|---|---|---|---|---|
| Sand | 0.437 (0.374–0.500) | 0.417 (0.354–0.480) | 4.95 (0.97–25.36) | 11.78 |
| Loamy sand | 0.437 (0.363–0.506) | 0.401 (0.329–0.473) | 6.13 (1.35–27.94) | 2.99 |
| Sandy loam | 0.453 (0.351–0.555) | 0.412 (0.283–0.541) | 11.01 (2.67–45.47) | 1.09 |
| Loam | 0.463 (0.375–0.551) | 0.434 (0.334–0.534) | 8.89 (1.33–59.38) | 0.34 |
| Silt loam | 0.501 (0.420–0.582) | 0.486 (0.394–0.578) | 16.68 (2.92–95.39) | 0.65 |
| Sandy clay loam | 0.398 (0.332–0.464) | 0.330 (0.235–0.425) | 21.85 (4.42–108.0) | 0.15 |
| Clay loam | 0.464 (0.409–0.519) | 0.309 (0.279–0.501) | 20.88 (4.79–91.10) | 0.10 |
| Silty clay loam | 0.471 (0.418–0.524) | 0.432 (0347–0.517) | 27.30 (5.67–131.50) | 0.10 |
| Sandy clay | 0.430 (0.370–0.490) | 0.321 (0.207–0.435) | 23.90 (4.08–140.2) | 0.06 |
| Silty clay | 0.479 (0.425–0.533) | 0.423 (0.334–0.512) | 29.22 (6.13–139.4) | 0.05 |
| Clay | 0.475 (0.427–0.523) | 0.385 (0.269–0.501) | 31.63 (6.39–156.5) | 0.03 |

* The numbers in parentheses below each parameter are one standard deviation around the parameter value given.

*Source:* Rawls, Brakensiek, and Miller (1983).

A logarithmic relationship between the effective saturation $s_e$ and the soil suction head $\psi$ can be expressed by the *Brooks–Corey equation* (Brooks and Corey, 1964):

$$s_e = \left[\frac{\psi_b}{\psi}\right]^{\lambda} \tag{7.4.27}$$

in which $\psi_b$ and $\lambda$ are constants obtained by draining a soil in stages, measuring the values of $s_e$ and $\psi$ at each stage, and fitting equation (7.4.27) to the resulting data.

Brakensiek et al. (1981) presented a method for determining the Green–Ampt parameters using the Brooks–Corey equation. Rawls et al. (1983) used this method to analyze approximately 5000 soil horizons across the United States and determined average values of the Green–Ampt parameters $\eta$, $\theta_e$, $\psi$, and $K$ for different soil classes, as listed in Table 7.4.1. As the soil becomes finer, moving from sand to clay, the wetting front soil suction head increases while the hydraulic conductivity decreases. Table 7.4.1 also lists typical ranges for $\eta$, $\theta_e$, and $\psi$. The ranges are not large for $\eta$ and $\theta_e$, but $\psi$ can vary over a wide range for a given soil. $K$ varies along with $\psi$, so the values given in Table 7.4.1 for both $\psi$ and $K$ should be considered typical values that may show a considerable degree of variability in application (American Society of Agricultural Engineers, 1983; Devanrs and Gifford, 1986).

**Table 7.4.2** Infiltration Computations Using the Green–Ampt Method

| Time $t$ (hr) | 0.0 | 0.1 | 0.2 | 0.3 | 0.4 | 0.5 | 1.0 | 1.5 | 2.0 | 2.5 | 3.0 | 3.5 | 4.0 | 4.5 | 5.0 | 5.5 | 6.0 |
|---|---|---|---|---|---|---|---|---|---|---|---|---|---|---|---|---|---|
| Infiltration rate $f$ (cm/hr) | $\infty$ | 1.78 | 1.20 | 0.97 | 0.84 | 0.75 | 0.54 | 0.44 | 0.39 | 0.35 | 0.32 | 0.30 | 0.28 | 0.27 | 0.26 | 0.25 | 0.24 |
| Infiltration depth $F$ (cm) | 0.00 | 0.29 | 0.43 | 0.54 | 0.63 | 0.71 | 1.02 | 1.26 | 1.47 | 1.65 | 1.82 | 1.97 | 2.12 | 2.26 | 2.39 | 2.51 | 2.64 |

***EXAMPLE 7.4.3***

Use the Green–Ampt method to evaluate the infiltration rate and cumulative infiltration depth for a silty clay soil at 0.1-hr increments up to 6 hr from the beginning of infiltration. Assume an initial effective saturation of 20 percent and continuous ponding.

***SOLUTION***

From Table 7.4.1, for a silty clay soil, $\theta_e = 0.423$, $\psi = 29.22$ cm, and $K = 0.05$ cm/hr. The initial effective saturation is $s_e = 0.2$, so $\Delta\theta = (1 - s_e)$, $\theta_e = (1 - 0.20)0.423 = 0.338$, and $\psi\Delta\theta = 29.22 \times 0.338 = 9.89$ cm. Assuming continuous ponding, the cumulative infiltration $F$ is found by successive substitution in equation (7.4.24):

$$F = Kt + \psi\Delta\theta \ln[1 + F/(\psi\Delta\theta)] = 0.05t + 9.89 \ln[1 + F/9.89]$$

For example, at time $t = 0.1$ hr, the cumulative infiltration converges to a final value $F = 0.29$ cm. The infiltration rate $f$ is then computed using equation (7.4.23):

$$f = K(1 + \psi\Delta\theta/F) = 0.05(1 + 9.89/F)$$

As an example, at time $t = 0.1$ hr, $f = 0.05(1 + 9.89/0.29) = 1.78$ cm/hr. The infiltration rate and the cumulative infiltration are computed in the same manner between 0 and 6 hr at 0.1-hr intervals; the results are listed in Table 7.4.2.

***EXAMPLE 7.4.4***

Ponding time $t_p$ is the elapsed time between the time rainfall begins and the time water begins to pond on the soil surface. Develop an equation for ponding time under a constant rainfall intensity $i$, using the Green–Ampt infiltration equation (see Figure 7.4.8).

***SOLUTION***

The infiltration rate $f$ and the cumulative infiltration $F$ are related in equation (7.4.22). The cumulative infiltration at ponding time $t_p$ is $F_p = it_p$, in which $i$ is the constant rainfall intensity (see Figure 7.4.8). Substituting $F_p = it_p$ and the infiltration rate $f = i$ into equation (7.4.23) yields

$$i = K\left(\frac{\psi\Delta\theta}{it_p} + 1\right)$$

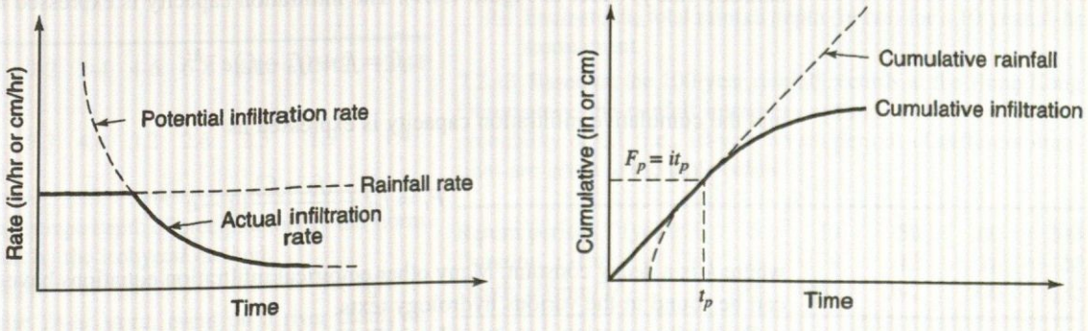


**Figure 7.4.8** Ponding time. This figure illustrates the concept of ponding time for a constant intensity rainfall. Ponding time is the elapsed time between the time rainfall begins and the time water begins to pond on the soil surface.

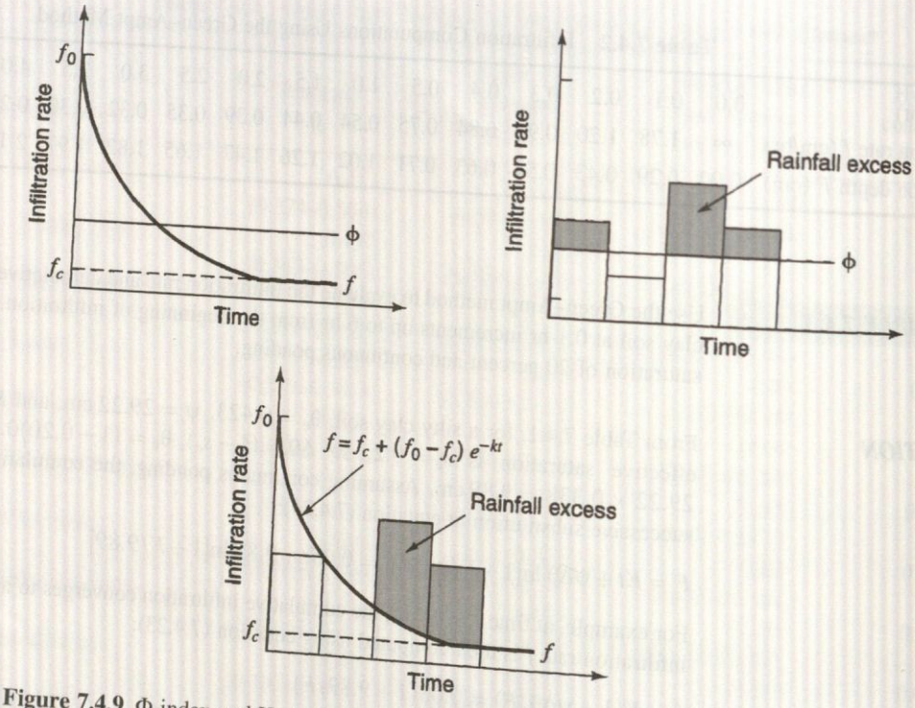


**Figure 7.4.9** Φ-index and Horton's equation.

and solving, we get

$$t_p = \frac{K\psi\Delta\theta}{i(i-K)}$$

which is the ponding time for a constant rainfall intensity.

### 7.4.3 Other Infiltration Methods

The simplest accounting of abstraction is the Φ-*index* (refer to Figure 7.4.9 and Section 8.2), which is a constant rate of abstraction (in/h or cm/h). Other cumulative infiltration and infiltration rate equations include Horton's and the SCS method. Horton's equation (Horton, 1933) is an empirical relation that assumes infiltration begins at some rate $f_o$ and exponentially decreases until it reaches a constant rate $f_c$ (refer to Figure 7.4.9). The infiltration capacity is expressed as

$$f_t = f_c + (f_o - f_c)e^{-kt} \tag{7.4.28}$$

and the cumulative infiltration capacity is expressed as

$$F_t = f_c t + \frac{(f_0 - f_c)}{k}(1 - e^{-kt}) \tag{7.4.29}$$

where $k$ is a decay constant. Many other empirical infiltration equations have been developed that can be found in the various hydrology texts.

Richard's equation can be solved (Philip, 1957, 1969) under less restrictive conditions by assuming that $K$ and $D$ (equation 7.4.14) can vary with moisture content. Philip used the Boltzmann transformation $B(\theta) = zt^{-1/2}$ to convert Richard's equation (7.4.14) into an ordinary differential equation in $B$ and solved to obtain an intimate series for cumulative infiltration $F_t$, approximated as

$$F_t = St^{1/2} + Kt \tag{7.4.30}$$

in which $S$ is the sorptivity, a parameter that is a function of the soil suction potential, and $K$ is the hydraulic conductivity. Differentiating $f(t) = df/dt$, the infiltration rate is defined as

$$f(t) = \frac{1}{2}St^{-1/2} + K \tag{7.4.31}$$

As $t \to \infty$, $f(t) \to K$. The two terms $S$ and $K$ represent the effects of soil suction head and gravity head.

There are many other infiltration methods, including the SCS method described in Sections 8.6–8.8. In summary, the Green–Ampt and the SCS are both used in the U.S. Army Corps of Engineers HEC-1 and HEC-HMS models, and both are used widely in the United States.

## PROBLEMS

7.2.1 Determine the 25-year return period rainfall depth for a 30-min duration in Chicago, Illinois.

7.2.2 Determine the 2-, 10-, 25-, and 100-year precipitation depths for a 15-min duration storm in Memphis, Tennessee.

7.2.3 Determine the 2- and 25-year intensity-duration-frequency curves for Memphis, Tennessee.

7.2.4 Determine the 10- and 50-year intensity-duration-frequency curves for Chicago, Illinois.

7.2.5 Determine the 2-, 5-, 10-, 25-, 50-, and 100-year depths for a 1-hr duration storm in Phoenix, Arizona. Repeat for a 6-hr duration storm.

7.2.6 Develop the Type I, IA, II, and III 24-hour storms for a 24-hour rainfall of 20 in. Plot and compare these storms.

7.2.7 Develop the SCS 6-hr storm for a 6-hr rainfall of 12 in.

7.2.8 Determine the design rainfall intensities (mm/hr) for a 25-year return period, 60-min duration storm using equation (7.2.5) with $c = 12.1$, $m = 0.25$, $e = 0.75$, and $f = 0.125$.

7.2.9 What is the all-season 6-hr PMP (in) for 200 mi$^2$ near Chicago, Illinois?

7.2.10 Tabulated are the data derived from a drainage basin of 21,100 hectares, given the areas covered with each of the rainfall isohyetal lines.

| Interval of isohyets (cm) | 0-2 | 2-4 | 4-6 | 6-8 | 8-10 | 10-42 | 12-44 |
|---|---|---|---|---|---|---|---|
| Enclosed area (hectares × 1000) | 5.3 | 4.4 | 3.2 | 2.6 | 2.3 | 1.9 | 1.4 |

(a) Determine the average depth of precipitation for the storm within the basin by the isohyetal method.
(b) Develop the depth-area relationship based on the data.

7.2.11 For a particular 24-hr storm event on a river basin, an isohyetal map was developed. The corresponding isohyets and area relationship is given in the table below. Based on the given information, (a) develop the depth-area relationship in tabular form for the basin and (b) assuming the maximum point rainfall is 145 mm, estimate the parameters in the following dimensionless depth-area equation that best fit the existing data, $\frac{\bar{P}_A}{P_{\max}} = \exp(-k \times A^n)$, where $\bar{P}_A$ = equivalent uniform rainfall depth for an area of $A$; $P_{\max}$ = maximum point rainfall depth; and $k$ and $n$ = parameters.

| Isohyet (mm) | 130 | 120 | 110 | 100 | 90 |
|---|---|---|---|---|---|
| Incremental area between isohyets (km$^2$) | 143 | 245 | 258 | 290 | 484 |

7.2.12 Based on the 100-year rainfall records at the Hong Kong Observatory, the rainfall intensities with an annual exceedance probability of 0.1 (i.e., 10-yr return period) of different durations are given in the table below.

| Duration, $t_d$ (min) | 15 | 30 | 60 | 120 |
|---|---|---|---|---|
| Intensity, $i$ (mm/h) | 161 | 132 | 103 | 74 |

(a) Determine the least-squares estimates of coefficients $a$ and $c$ in the following rainfall intensity-duration equation and the associated $R^2$ value, $i = \frac{a}{(t_d + 4.5)^c}$, in which $i$ = rainfall intensity (in mm/h) and $t_d$ = storm duration in (minutes).
(b) Estimate the total rainfall depth (in cm) for a 10-year, 4-hr storm event.

7.2.13 Based on the 100-year rainfall records at the Hong Kong Observatory, the rainfall intensities with an annual exceedance probability of 0.1 (i.e., 10-year return period) of different durations are given in the table below.

| Return period, $T$ (year) | 5 | 10 | 50 | 100 | 200 |
|---|---|---|---|---|---|
| Duration, $t_d$ (hr) | 6 | 8 | 12 | 18 | 24 |
| Depth, $d$ (mm/h) | 192 | 255 | 392 | 500 | 622 |

Consider the following empirical model to be used to fit the above rainfall intensity-duration-frequency (IDF) data, $d(T, t_d) = \frac{aT^m}{(t_d + b)^c}$, in which $d$ = rainfall depth (in mm) corres-

ponding to a storm event of return period $T$-year and duration $t_d$-hr.

(a) Describe a least-squares-based procedure to optimally estimate the coefficients a, $b$, $c$, and $m$ in the above rainfall IDF model.

(b) Assuming $b = 4.0$, determine the least-squares estimates of coefficients $a$, $c$, and $m$ in the above rainfall intensity-duration equation and the associated $R^2$ value.

(c) Estimate the average rainfall intensity (in mm/hr) for the 25-year, 4-hr storm event.

7.2.14 Consider a rainfall event having 5-min cumulative rainfall record given below:

| | | | | | | | |
|---|---|---|---|---|---|---|---|
| Time (min) | 0 | 5 | 10 | 15 | 20 | 25 | 30 |
| Cumulative rainfall (mm) | 0 | 7 | 14 | 23 | 34 | 45 | 58 |
| Time (min) | 35 | 40 | 45 | 50 | 55 | 60 | 65 |
| Cumulative rainfall (mm) | 70 | 81 | 91 | 100 | 110 | 119 | 125 |
| Time (min) | 70 | 75 | 80 | 85 | 90 | | |
| Cumulative rainfall (mm) | 131 | 136 | 140 | 140 | 140 | | |

(a) What is the duration of the entire rainfall event and the corresponding total rainfall amount?

(b) Find the rainfall depth hyetograph (in tabular form) with 10-min time interval for the storm event.

(c) Find the maximum 10-min and 20-min average rainfall intensities (in mm/hr) for the storm event.

7.2.15 Based on available rainfall records at a location, the rainfall intensity with an annual exceedance probability of 0.1 (i.e., 10-year return period) of different durations are given in the table below.

| Duration, $t_d$ (min) | 15 | 30 | 60 | 120 |
|---|---|---|---|---|
| Intensity, $i$ (mm/h) | 160 | 132 | 105 | 75 |

(a) Determine the least-squares estimates of coefficients $a$ and $c$ in the following rainfall intensity-duration equation and calculate the corresponding $R^2$ value, $i = \dfrac{a}{(t_d + 4.5)^c}$ in which $i$ = rainfall intensity (in mm/h) and $t_d$ = storm duration (in minutes).

(b) Estimate the total rainfall depth (in mm) for a 10-year, 90-min storm event.

7.2.16 Based on the available rainfall records at the Hong Kong Observatory, the rainfall intensities corresponding to different durations with an annual exceedance probability of 0.1 (i.e. 10-year return period) are given in the table below.

| Duration, $t_d$ (min) | 15 | 30 | 60 | 120 |
|---|---|---|---|---|
| Intensity, $i$ (mm/h) | 161 | 132 | 103 | 74 |

(a) Determine the least-squares estimates of coefficients $a$ and $c$ in the following rainfall intensity-duration equation, $i = \dfrac{a}{(t_d + 45)^c}$ in which $i$ = rainfall intensity (in mm/h) and $t_d$ = storm duration (in minutes).

(b) Estimate the total rainfall depth (in cm) for a 10-year, 4-hr storm event.

7.2.17 An experimental rectangular plot of 10 km × 12 km has five rain gauge stations as shown in the figure. The storm rainfall and coordinates of the stations are given in the table.

| Station | $(x, y)$ | Mean annual rainfall (cm) | Storm rainfall (cm) |
|---|---|---|---|
| A | (1, 3) | 128 | 12.0 |
| B | (8, 11) | 114 | 11.4 |
| C | (3, 10) | 136 | 13.2 |
| D | (5, 8) | 144 | 14.6 |
| E | (7, 5) | 109 | ? |

(a) Estimate the missing rainfall amount at station E.

(b) Based on the position of the five rain gauges, construct the Thiessen polygon for them.

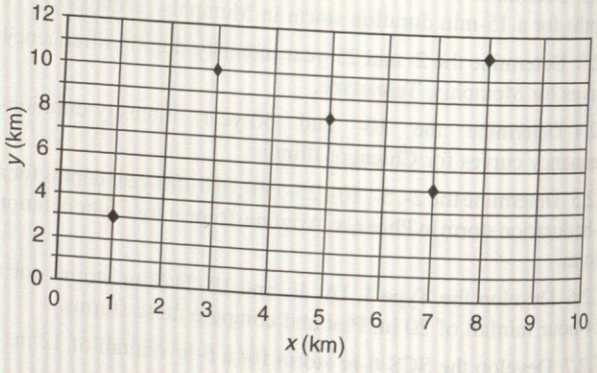


7.3.1 Solve example 7.3.1 for an average net radiation of 92.5 W/m$^2$. Compare the resulting evaporation rate with that in example 7.3.1.

7.3.2 Solve example 7.3.2 for a roughness height $z_0 = 0.04$ cm. Compare the resulting evaporation rate with that in example 7.3.2.

7.3.3 Solve example 7.3.3 for an average net radiation of 92.5 W/m$^2$. Compare the resulting evaporation rate with that in example 7.3.3.

7.3.4 Solve example 7.3.4 for an average net radiation of 92.5 W/m$^2$. Compare the resulting evaporation rate with that in example 7.3.4.

7.3.5 At a certain location during the winter, the average air temperature is 10°C and the net radiation is 40 W/m$^2$ and during the summer the net radiation is 200 W/m$^2$ and the temperature is 25°C Compute the evaporation rates using the Priestley–Taylor method.

7.3.6 The average weather conditions are net radiation = 40 W/m$^2$; air temperature = 28.5° C; relative humidity = 55 percent; and wind speed = 2.7 m/s at a height of 2 m. Calculate the open water evaporation rate in millimeters per day using the energy method, the aerodynamic method, the combination method, and

the Priestley–Taylor method. Assume standard atmospheric pressure is 101 kPa and $z_o$ is 0.03 cm.

7.3.7 A 600-hectare farm land receives annual rainfall of 2500 mm. There is a river flowing through the farm land with inflow rate of 5 $m^3/s$ and outflow rate of 4 $m^3/s$. The annual water storage in the farm land increases by $2.5\times10^6$ $m^3$. Based on the hydrologic budget equation, determine the annual evaporation amount (in mm). [Note: 1 hectare = 10,000 $m^2$]

7.4.1 Determine the infiltration rate and cumulative infiltration curves (0 to 5 h) at 1-hr increments for a clay loam soil. Assume an initial effective saturation of 40 percent and continuous ponding.

7.4.2 Rework problem 7.4.1 using an initial effective saturation of 20 percent.

7.4.3 Rework example 7.4.3 for a sandy loam soil.

7.4.4 Compute the ponding time and cumulative infiltration at ponding for a sandy clay loam soil with a 30-percent initial effective saturation, subject to a rainfall intensity of 2 cm/h.

7.4.5 Rework problem 7.4.4 for a silty clay soil.

7.4.6 Determine the cumulative infiltration and the infiltration rate on a sandy clay loam after 1 hr of rainfall at 2 cm/hr if the initial effective saturation is 25 percent. Assume the ponding depth is negligible in the calculations.

7.4.7 Rework problem 7.4.6 assuming that any ponded water remains stationary over the soil so that the ponded depth must be accounted for in the calculations.

7.4.8 Derive the equation for cumulative infiltration using Horton's equation.

7.4.9 Use the Green–Ampt method to compute the infiltration rate and cumulative infiltration for a silty clay soil ($\eta = 0.479$, $\psi = 29.22$ cm, $K = 0.05$ cm/hr) at 0.25-hr increments up to 4 hr from the beginning of infiltration. Assume an initial effective saturation of 30 percent and continuous ponding.

7.4.10 The parameters for Horton's equation are $f_0 = 3.0$ in/h, $f_c = 0.5$ in/h, and $K = 4.0\,h^{-1}$. Determine the infiltration rate and cumulative infiltration at 0.25-hr increments up to 4 hr from the beginning of infiltration. Assume continuous ponding.

7.4.11 Derive an equation for ponding time using Horton's equation.

7.4.12 Compute the ponding time and cumulative infiltration at ponding for a sandy clay loam soil of 25 percent initial effective saturation for a rainfall intensity of (a) 2 cm/h, (b) 3 cm/h, and (c) 5 cm/h.

7.4.13 Rework problem 7.4.12 considering a silt loam soil.

7.4.14 Consider a soil with porosity $\eta = 0.43$ and suction $\psi = 11.0$ cm. Before the rainfall event, the initial moisture content $\theta_i = 0.3$. It is known that after one hour of rainfall, the total infiltrated water is 2.0 cm.

(a) Determine the hydraulic conductivity in the Green–Ampt infiltration model.
(b) Estimate the potential total infiltration amount 1.5 hr after the beginning of the storm.
(c) Determine the instantaneous potential infiltration rate at $t =$ 1.5 hr.

7.4.15 The following experimental data are obtained from an infiltration study. The objective of the study is to establish a plausible relationship between infiltration rate ($f_t$) and time ($t$).

| Time, $t$ (mm) | 3 | 15 | 30 | 60 | 90 |
|---|---|---|---|---|---|
| Infiltration rate, $f_t$ (cm/hr) | 8.5 | 7.8 | 7.0 | 6.1 | 5.6 |

From the scatter plot of infiltration rate and time, the following relationship between $f_t$ and $t$ is plausible, $f_t = 5.0 + (f_o - 5.0)\exp(-k \times t)$, where $f_o$ is the initial infiltration rate (in cm/hr) and $k$ is the decay constant (in $min^{-1}$).

(a) Determine the values of the two constants, i. e., $f_o$ and $k$, by the least-squares method.
(b) Based on the result in part (a), estimate the infiltration rate at time $t = 150$ min.

7.4.16

(a) For a sandy loam soil, using Green–Ampt equation to calculate the infiltration rate (cm/h) and cumulative infiltration depth (cm) after 1, 60, and 150 min if the effective saturation is 40 percent. Assume a continuously ponded condition.
(b) Take the infiltration rates computed in Part (a) at 1 min and 150 min as the initial and ultimate infiltration rates in Horton's equation, respectively. Determine the decay constant, $k$.
(c) Use the decay constant, $k$, found in Part (b) to compute the cumulative infiltration at $t = 60$ min by Horton's equation.

7.4.17 Assume that ponded surface occurs at the beginning of a storm event.

(a) Calculate the potential infiltration rates (cm/hr) and potential cumulative infiltration depth (cm) by the Green–Ampt model for loamy sand at times 30 and 60 min. The initial effective saturation is 0.2.
(b) Based on the infiltration rates or cumulative infiltration depth computed in Part (a), determine the two parameters $S$ and $K$ in the following Philip two-term infiltration model.

$$F(t) = S\,t^{1/2} + K\,t; \quad f(t) = 0.5\,S\,t^{0.5} + K$$

(c) Based on the $S$ and $K$ computed in Part (b), determine the effective rainfall hyetograph for the following total hyetograph of a storm event.

| Time (min) | 0-30 | 30-60 | 60-90 | 90-120 |
|---|---|---|---|---|
| Intensity (cm/hr) | 8.0 | 15.0 | 5.0 | 3.0 |

(d) Find the value of the Φ-index and the corresponding effective rainfall hyetograph having the total effective rainfall depth obtained in Part (c).

7.4.18 Consider the sandy loam soil with effective porosity $\theta_e = 0.43$, suction $\psi = 11.0$ cm, and hydraulic conductivity $K = 1.1$ cm/h. Before the rainfall event, the initial effective saturation is $S_e = 0.3$. It is known that, after 1 hr of rainfall, the total infiltrated water is 2.0 cm.

(a) Estimate the potential total infiltration amount 1.5 hr after the beginning of the storm event by the Green–Ampt equation.

(b) Also, determine the instantaneous potential infiltration rate at $t = 1.5$ hr.

7.4.19 Considering a plot of land with sandy loam soil, use the Green–Ampt equation to calculate the infiltration rate (cm/h) and cumulative infiltration depth (cm) at $t = 30$ min under the initial degree of saturation of 40 percent and continuously ponding condition. The relevant parameters are: suction head = 6.0 cm; porosity = 0.45; and hydraulic conductivity = 3.00 cm/h.

7.4.20 Suppose that the infiltration of water into a certain type of soil can be described by Horton's equation with the following parameters: initial infiltration rate = 50 mm/h; ultimate infiltration rate = 10 mm/h; and decay constant = 4 $h^{-1}$. A rain storm event has occurred and its pattern is given below.

| Time (min) | 0 | 15 | 30 | 45 | 60 | 75 | 90 |
|---|---|---|---|---|---|---|---|
| Cumu. rain (mm) | 0 | 15 | 25 | 30 | 32 | 33 | 33 |

(a) Determine the effective rainfall intensity hyetograph (in mm/h) from the storm event.

(b) What is the percentage of total rainfall infiltrated into the ground?

(c) What assumption(s) do you use in the Part (a) calculation? Justify them.

7.4.21 Consider a 2-hr storm event with a total rainfall amount of 80 mm. The measured direct runoff volume produced by the storm is 40 mm.

(a) Determine the decay constant $k$ in Horton's infiltration model knowing that the initial and ultimate infiltration rates are 30 mm/hr and 2 mm/hr, respectively.

(b) Use the Horton equation developed in Part (a) to determine the effective rainfall intensity hyetograph for the following storm event.

| Time (min) | 0-10 | 10-20 | 20-30 |
|---|---|---|---|
| Incremental rainfall depth (mm) | 5 | 20 | 10 |

7.4.22 An infiltration study is to be conducted. A quick site investigation indicates that the soil has an effective porosity $\theta_e = 0.40$ and the initial effective saturation $S_e = 0.3$. Also, from the double-ring infiltrometer test, we learn that the cumulative infiltration amounts at $t = 1$ hr and $t = 2$ hr are 1 cm and 1.6 cm, respectively.

(a) It is decided that the Green–Ampt equation is to be used. Determine the parameters suction ($\psi$) and hydraulic conductivity ($K$) from the test data. (You can use an iterative procedure or apply simple approximation using $\ln(1+x) = 2x/(2+x)$ for a direct solution.)

(b) Also, determine the cumulative infiltration and the corresponding instantaneous potential infiltration rate at $t = 3$ hr. (You can use the Newton method to obtain the solution with accuracy within 0.1 mm or the most accurate direct solution approach.)

7.4.23 You are working on a proposal to do some rainfall runoff modeling for a small city nearby. One of the things the city does not have is a hydrology manual. You must decide upon an infiltration methodology for the analysis. You are going to consider methods such as the Φ-index method, empirical methods (such as Horton's and Holtan's), the SCS method, and the Green–Ampt method. Would you choose the Green–Ampt method over the others? Why?

## REFERENCES


American Society of Agricultural Engineers, "Advances in Infiltration," in *Proc. National Conf. on Advances in Infiltration*, Chicago, IL, ASAE Publication 11–83, St. Joseph, MI 1983.

Bedient, P. B., and W. C. Huber, *Hydrology and Floodplain Analysis*, second edition, Addison-Wesley, Reading, MA, 1992.

Bhowmik, N., "River Basin Management: An Integrated Approach" *Water International*, International Water Resources Association, vol. 23, no. 2, pp. 84–90, June 1998.

Bonnin, G. M., D. Martin, B. Lin, T. Parzybok, M. Yekta, and D. Riley, "Precipitation-Frequency Atlas of the United States," NOAA Atlas 14, vol. 2, version 3, NOAA, National Weather Service, Silver Spring, MD, 2004.

Bonnin, G. M., D. Martin, B. Lin, T. Parzybok, M. Yekta, and D. Riley, "Precipitation-Frequency Atlas of the United States," NOAA Atlas 14, vol. 1, version 4, NOAA, National Weather Service, Silver Spring, MD, 2006.

Brakensiek, D. L., R. L. Engleman, and W. J. Rawls, "Variation within Texture Classes of Soil Water Parameters," *Trans. Am. Soc. Agric. Eng.*, vol. 24, no. 2, pp. 335–339, 1981.

Bras, R. L., *Hydrology: An Introduction to Hydrologic Science*, Addison-Wesley, Reading, MA, 1990.

Brooks, R. H., and A. T. Corey, "Hydraulic Properties of Porous Media," *Hydrology Papers*, no. 3, Colorado State University, Fort Collins, CO, 1964.

Chow, V. T., *Handbook of Applied Hydrology*, McGraw Hill, New York 1964.

Chow, V. T., D. R. Maidment, and L. W. Mays, *Applied Hydrology*, McGraw-Hill, New York, 1988.

Demissee, M., and L. Keefer, "Watershed Approach for the Protection of Drinking Water Supplies in Central Illinois," *Water International*. IWRA, vol. 23, no. 4, pp. 272–277, 1998.

Devanrs, M., and G. F. Gifford, "Applicability of the Green and Ampt Infiltration Equation to Rangelands," *Water Resource Bulletin*, vol. 22, no. 1, pp. 19–27, 1986.

Feynman, R. P., R. B. Leighton, and M. Sands, *The Feynman Lecture Notes on Physics*, vol. I, Addison-Wesley, Reading, MA, 1963.

Frederick, R. H., V. A. Meyers, and E. P. Auciello, "Five to 60-Minute Precipitation Frequency for the Eastern and Central United States," NOAA Technical Memo NWS HYDRO-35, National Weather Service, Silver Spring, MD, June 1977.

Green, W. H., and G. A. Ampt, "Studies on Soil Physics. Part I: The Flow of Air and Water Through Soils," *J. Agric. Sci.*, vol. 4, no. 1, pp. 1–24, 1911.

Gupta, R. S., *Hydrology and Hydraulic Systems*, Prentice-Hall, Englewood Cliffs, NJ, 1989.

Hansen, E. M., L. C. Schreiner, and J. F. Miller, "Application of Probable Maximum Precipitation Estimates—United States East of 105th Meridian," NOAA Hydrometeorological Report 52, U.S. National Weather Service, Washington, DC, 1982.

Hershfield, D. M., "Rainfall Frequency Atlas of the United States for Durations from 30 Minutes to 24 Hours and Return Periods from 1 to 100 Years," Tech. Paper 40, U.S. Department of Commerce, Weather Bureau, Washington, DC, 1961.

Horton, R. E., "The Role of Infiltration in the Hydrologic Cycle," *Trans. Am. Geophysical Union*, vol. 14, pp. 446–460, 1933.

Huff, F. A., "Time Distribution of Rainfall in Heavy Storms," *Water Resources Research*, vol. 3, no. 4, pp. 1007–1019, 1967.

Maidment, D. R. (editor-in-chief), *Handbook of Hydrology*, McGraw-Hill, New York, 1993.

Marsh, W. M., *Earthscape: A Physical Geography*, John Wiley & Sons, New York, 1987.

Marsh, W. M., and J. Dozier, *Landscape: An Introduction to Physical Geography*, John Wiley & Sons, New York, 1986.

Masch, F. D., *Hydrology*, Hydraulic Engineering Circular No. 19, FHWA-10-84-15. Federal Highway Administration, U.S. Department of the Interior, McLean, VA, 1984.

McCuen, R. H., *Hydrologic Analysis and Design*, 2nd edition Prentice-Hall. Englewood Cliffs, NJ, 1998.

Miller J. F., R. H. Frederick, and R. J. Tracey, *Precipitation Frequency Atlas of the Coterminous Western United States (by States)*, NOAA Atlas 2, 11 vols., National Weather Service, Silver Spring, MD, 1973.

Moore, W. L., E. Cook, R. S. Gooch, and C. F. Nordin, Jr., "The Austin, Texas, Flood of May, 24-25, 1981," National Research Council, Committee on Natural Disasters, Commission on Engineering and Technical Systems National Academy Press, Washington, DC, 1982.

Parrett, C., N. B. Melcher, and R. W. James, Jr., "Flood Discharges in the Upper Mississippi River Basin," in *Floods in the Upper Mississippi River Basin,"* U.S. Geological Survey Circular, 1120-A U.S. Government Printing Office, Washington, DC, 1993.

Philip, J. R., "Theory of Infiltration: 1. The Infiltration Equation and Its Solution," *Soil Science* 83, pp. 345–357, 1957.

Philip, J. R., "The Theory of Infiltration," in *Advances in Hydro Sciences*, edited by V. T. Chow, vol. 5, pp. 215–296, 1969.

Ponce, V. M., *Engineering Hydrology: Principles and Practices*, Prentice-Hall, Englewood Cliffs, NJ, 1989.

Priestley, C. H. B., and R. J. Taylor, "On the Assessment of Surface Heat Flux and Evaporation Using Large-Scale Parameter," *Monthly Weather Review*, vol. 100, pp. 81–92, 1972.

Rawls, W. J., D. L. Brakensiek, and N. Miller, "Green-Ampt Infiltration Parameters from Soils Data," *J. Hydraulic Div., ASCE*, vol. 109, no. 1, pp. 62–70, 1983.

Richards, L. A., "Capillary Conduction of Liquids Through Porous Mediums," *Physics*, vol. 1, pp. 318–333, 1931.

Roberson, J. A., J. J. Cassidy, and M. H. Chaudhry, *Hydraulic Engineering*, 2nd edition, John Wiley & Sons, New York, 1998.

Schreiner, L. C., and J. T. Riedel, Probable Maximum Precipitation Estimates, United States East of the 105th Meridian, NOAA Hydrometeorological Report no. 51, National Weather Service, Washington, DC, June 1978.

Singh, V. P., *Elementary Hydrology*, Prentice-Hall, Englewood Cliffs, NJ, 1992.

Thornthwaite, C. W., and B. Holzman, "The Determination of Evaporation from Land and Water Surface," *Monthly Weather Review*, vol. 67, pp. 4–11, 1939.

U.S. Army Corps of Engineers, Hydrologic Engineering Center, HEC-1, *Flood Hydrograph Package*, User's Manual, Davis, CA, 1990.

U.S. Department of Agriculture Soil Conservation Service, *A Method far Estimating Volume and Rate of Runoff in Small Watersheds*, Tech. Paper 149, Washington, DC, 1973.

U.S. Department of Agriculture Soil Conservation Service, *Urban Hydrology for Small Watersheds*, Tech. Release no. 55, Washington, DC, 1986.

U.S. Department of Commerce, *Probable Maximum Precipitation Estimates, Colorado River and Great Basin Drainages*, Hydrometeorological Report no 49, NOAA, National Weather Service, Silver Spring, MD, 1977.

U.S. Environmental Data Services, *Climate Atlas of the US.*, U.S. Environment Printing Office, Washington, DC, pp. 43–44, 1968.

U.S. National Academy of Sciences, *Understanding Climate Change*, National Academy Press, Washington, DC, 1975.

U.S. National Academy of Sciences, *Safety of Existing Dams; Evaluation and Improvement*, National Academy Press, Washington, DC, 1983.

U.S. National Research Council, *Global Change in the Geosphere-Biosphere*, National Academy Press, Washington, DC, 1986.

U.S. National Research Council, Committee on Opportunities in the Hydrologic Science, Water Science and Technology Board, *Opportunities in the Hydrologic Sciences*, National Academy Press, Washington, DC, 1991.

U.S. Weather Bureau, *Two- to Ten-Day Precipitation for Return Periods of 2 to 100 Years in the Contiguous United States*, Tech. Paper 49, Washington, DC, 1964.

Viessman, W. Jr., and G. L. Lewis, *Introduction to Hydrology*, 4th edition, Harper and Row, New York, 1996.

Wanielista, M., R. Kersten, and R. Eaglin, *Hydrology: Water Quantity and Quality Control*, John Wiley & Sons, New York, 1997.

# Chapter 8

# Surface Runoff

## 8.1 DRAINAGE BASINS AND STORM HYDROGRAPHS

### 8.1.1 Drainage Basins and Runoff

As defined in Chapter 7, *drainage basins, catchments*, and *watersheds* are three synonymous terms that refer to the topographic area that collects and discharges surface streamflow through one outlet or mouth. The study of topographic maps from various physiographic regions reveals that there are several different types of drainage patterns (Figure 8.1.1). *Dendritic patterns* occur where rock and weathered mantle offer uniform resistance to erosion. Tributaries branch and erode headward in a random fashion, which results in slopes with no predominant direction or orientation. *Rectangular*

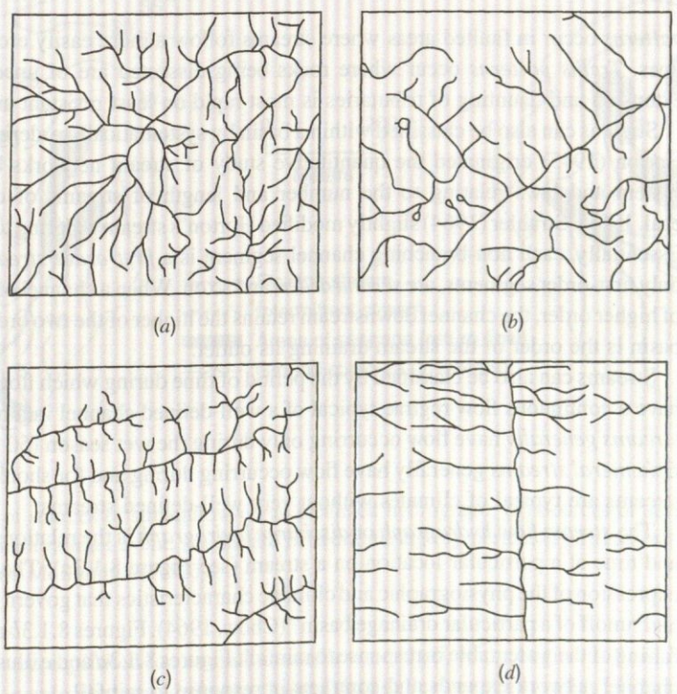


**Figure 8.1.1** Common drainage patterns: (*a*) Dendritic; (*b*) Rectangular; (*c*) Trellis on folded terrain; (*d*) Trellis on mature, dissected coastal plain (from Hewlett and Nutter (1969)).

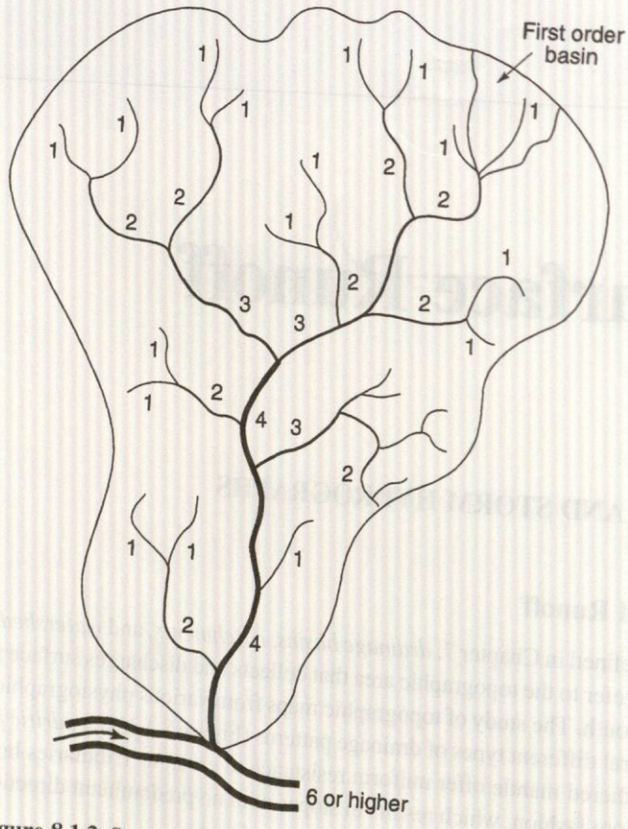


**Figure 8.1.2** Stream orders (from Hewlett and Nutter (1969)).

*patterns* occur in faulted areas where streams follow a more easily eroded fractured rock in fault lines. *Trellis patterns* occur where rocks being dissected are of unequal resistance so that the extension and daunting of tributaries is most rapid on least resistant areas.

Streams can also be classified within a basin by systematically ordering the network of branches. Horton (1945) originated the quantitative study of stream networks by developing an ordering system and laws relating to the number and length of streams of different order (see Chow, et al. 1988). Strahler (1964) slightly modified Horton's stream ordering to that shown in Figure 8.1.2. Essentially, each non-branching channel segment is a *first-order stream*. Streams, which receive only first-order segments, are *second order*, and so on. When a channel of lower order joins a channel of higher order, the channel downstream retains the higher of the two orders. The order of a drainage basin is the order of the stream draining its outlet.

Streams can also be classified by the period of time during which flow occurs. *Perennial streams* have a continuous flow regime typical of a well-defined channel in a humid climate. *Intermittent streams generally* have flow occurring only during the wet season (50 percent of the time or less). *Ephemeral streams* generally have flow occurring during and for short periods after storms. These streams are typical of climates without very well-defined streams.

The *stream flow hydrograph* or *discharge hydrograph* is the relationship of flow rate (discharge) and time at a particular location on a stream (see Figure 8.1.3*a*). The *hydrograph* is "an integral expression of the physiographic and climatic characteristics that govern the relation between rainfall and runoff of a particular drainage basin" (Chow, 1964). Figures 8.1.3*b* and *c* illustrate the rising and falling of the water table in response to rainfall. Figures 8.1.3*d* and *e* illustrate that the flowing stream channel network expands and contracts in response to rainfall.

The spatial and temporal variations of rainfall and the concurrent variation of the abstraction processes define the runoff characteristics from a given storm. When the local abstractions have been

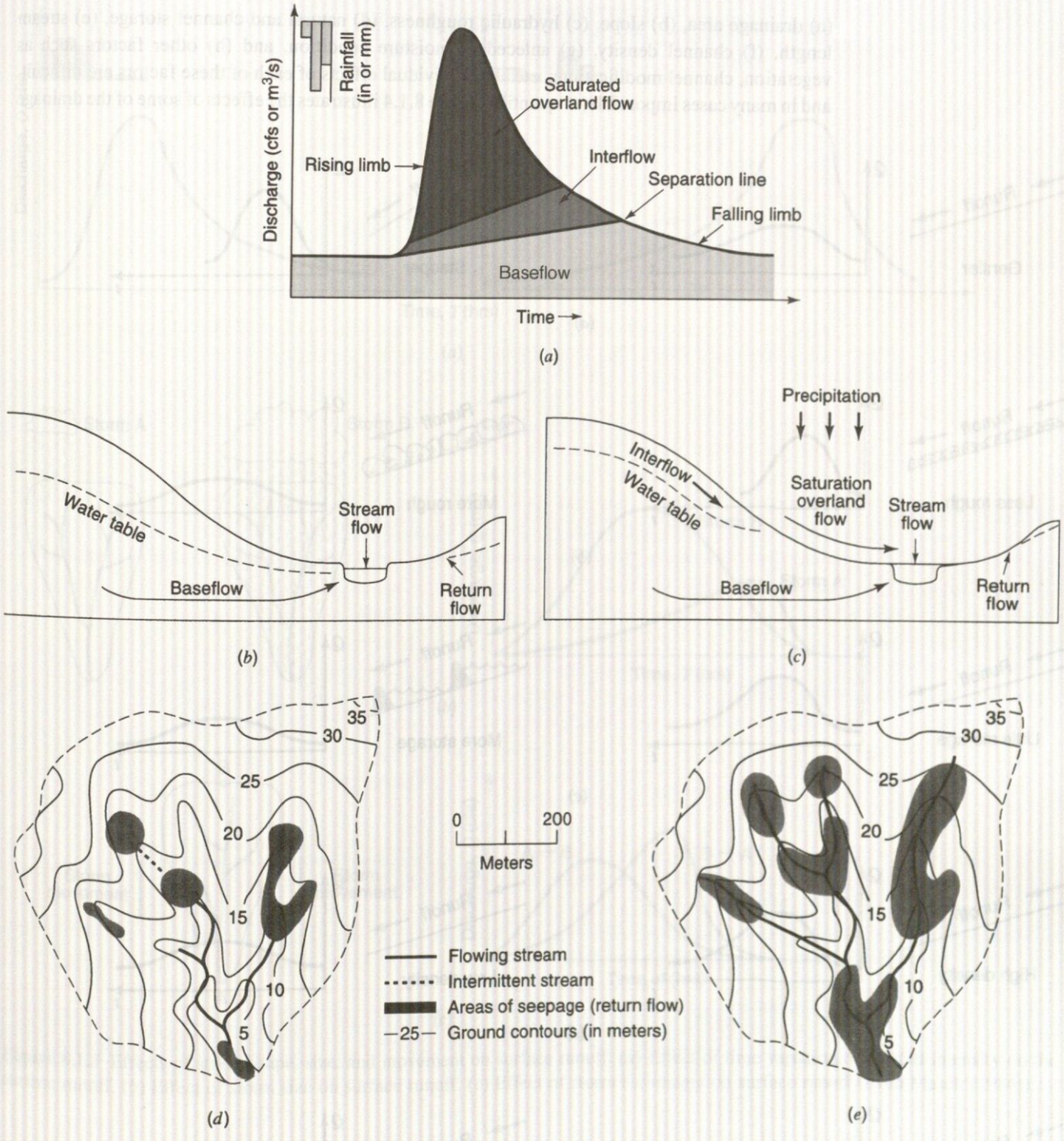


**Figure 8.1.3** (*a*) Separatism of sources of streamflow on an idealized hydrograph; (*b*) Sources of streamflow on a hillslope profile during a dry period; (*c*) During a rainfall event; (*d*) Stream network during dry period; (*e*) Stream network extended during and after rainfall (from Mosley and McKerchar (1993)).

accomplished for a small area of a watershed, water begins to flow overland as *overland flow* and eventually into a drainage channel (in a gulley or stream valley). When this occurs, the hydraulics of the natural drainage channels have a large influence on the runoff characteristics from the watershed. Some of the factors that determine the hydraulic character of the natural drainage system include:

(a) drainage area, (b) slope, (c) hydraulic roughness, (d) natural and channel storage, (e) stream length, (f) channel density, (g) antecedent moisture condition, and (h) other factors such as vegetation, channel modifications, etc. The individual effects of each of these factors are difficult, and in many cases impossible, to quantify. Figure 8.1.4 illustrates the effects of some of the drainage

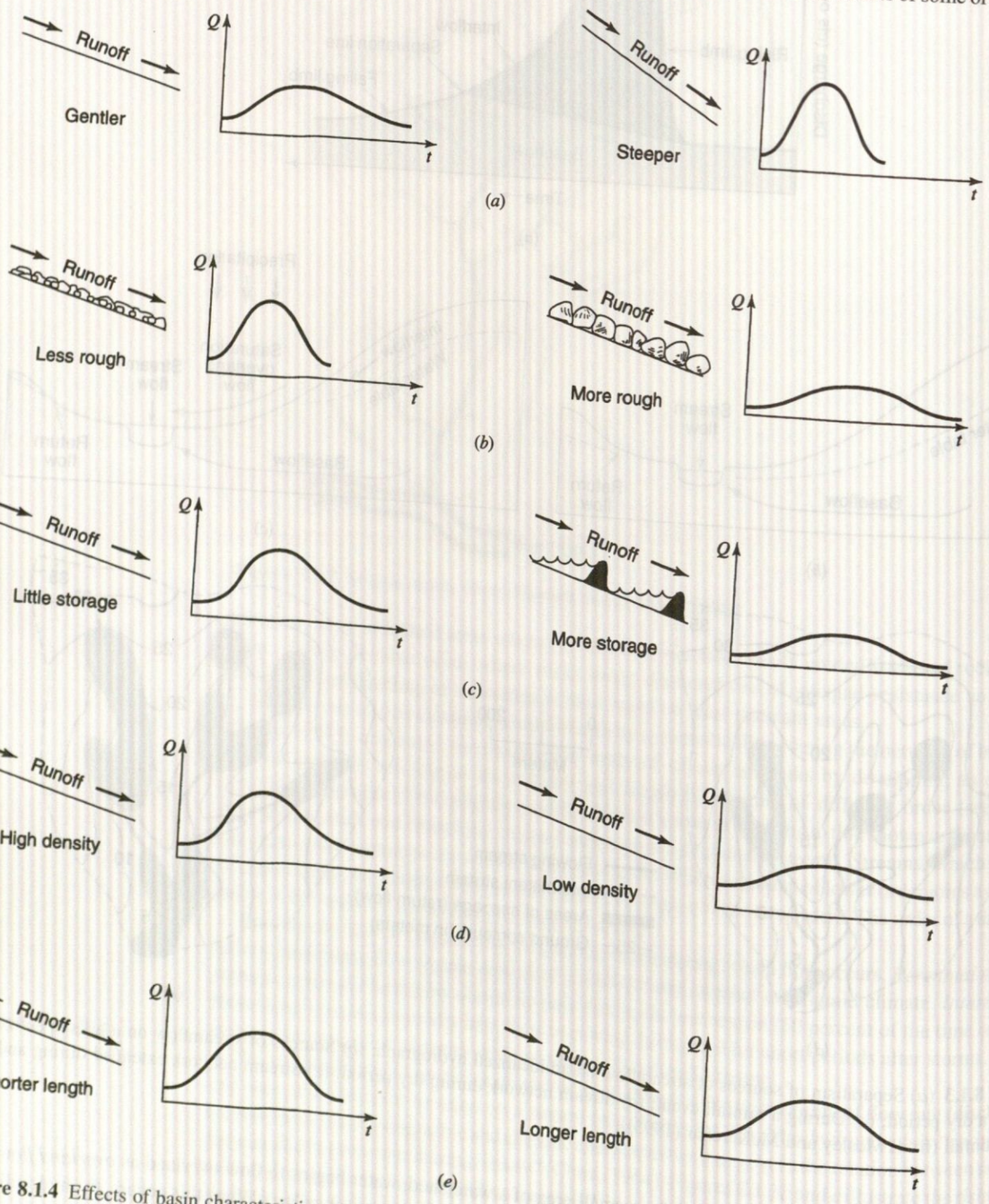


**Figure 8.1.4** Effects of basin characteristics on the flood hydrograph. (*a*) Relationship of slope to peak discharge. (*b*) Relationship of hydraulic roughness to runoff. (*c*) Relationship of storage to runoff. (*d*) Relationship of drainage density to runoff. (*e*) Relationship of channel length to runoff (from Masch (1984)).

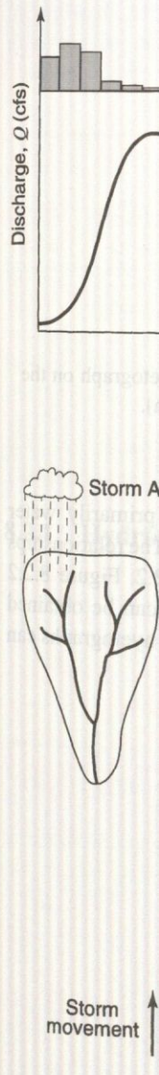


**Figure 8.1.5** Effe
surface runoff. (*b*)

8.2 HYDRO

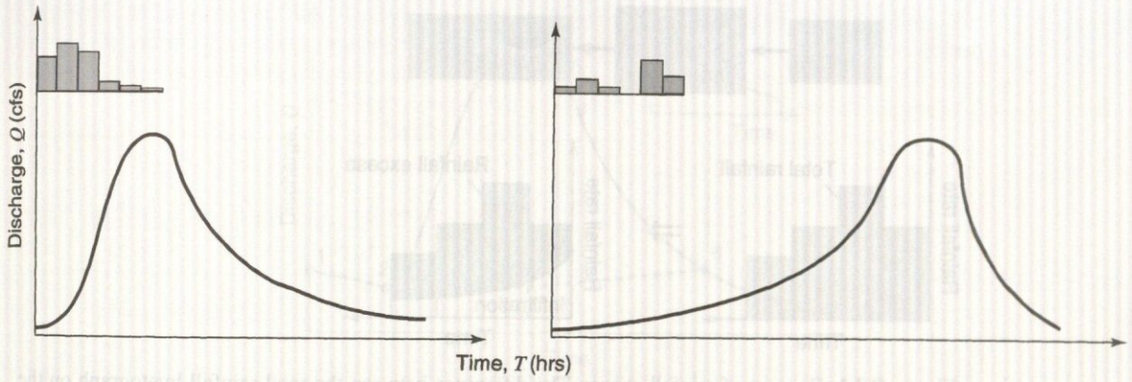


(a)

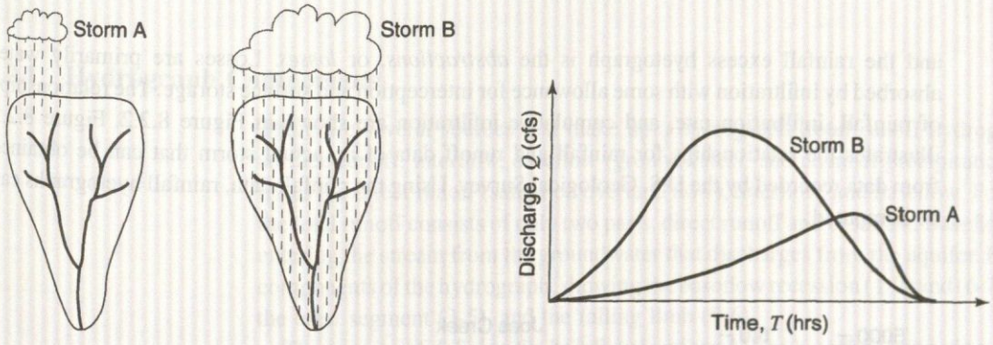


(b)

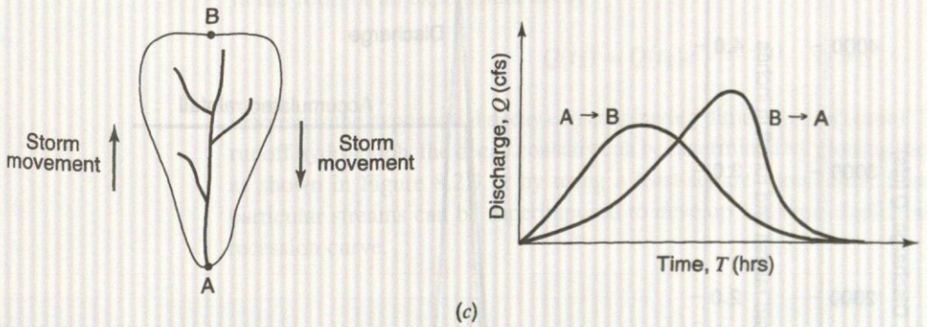


(c)

**Figure 8.1.5** Effects of storm shape, size, and movement on surface runoff. (*a*) Effect of time variation of rainfall intensity on the surface runoff. (*b*) Effect of storm size on surface runoff. (*c*) Effect of storm movement on surface runoff (from Masch (1984)).

basin characteristics on the surface runoff (discharge hydrographs) and Figure 8.1.5 illustrates the effects of storm shape, size, and movement on surface runoff.

## 8.2 HYDROLOGIC LOSSES, RAINFALL EXCESS, AND HYDROGRAPH COMPONENTS

*Rainfall excess*, or *effective rainfall*, is that rainfall that is neither retained on the land surface nor infiltrated into the soil. After flowing across the watershed surface, rainfall excess becomes direct runoff at the watershed outlet. The graph of rainfall excess versus time is the rainfall excess hyetograph. As shown in Figure 8.2.1, the difference between the observed total rainfall hyetograph

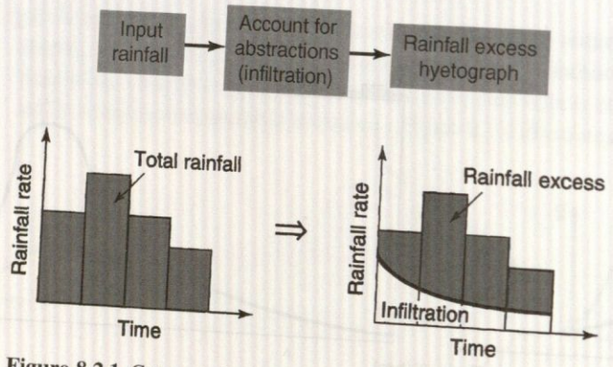


**Figure 8.2.1** Concept of rainfall excess. The difference between the total rainfall hyetograph on the left and the total rainfall excess hyetograph on the right is the abstraction (infiltration).

and the rainfall excess hyetograph is the *abstractions*, or *losses*. Losses are primarily water absorbed by infiltration with some allowance for interception and surface storage. The relationships of rainfall, infiltration rate, and cumulative infiltration are shown in Figure 8.2.2. Figure 8.2.2 illustrates the relationships for rainfall and runoff data of an actual storm that can be obtained from data recorded by the U.S. Geological Survey. Using the rainfall data, rainfall hyetographs can be computed.

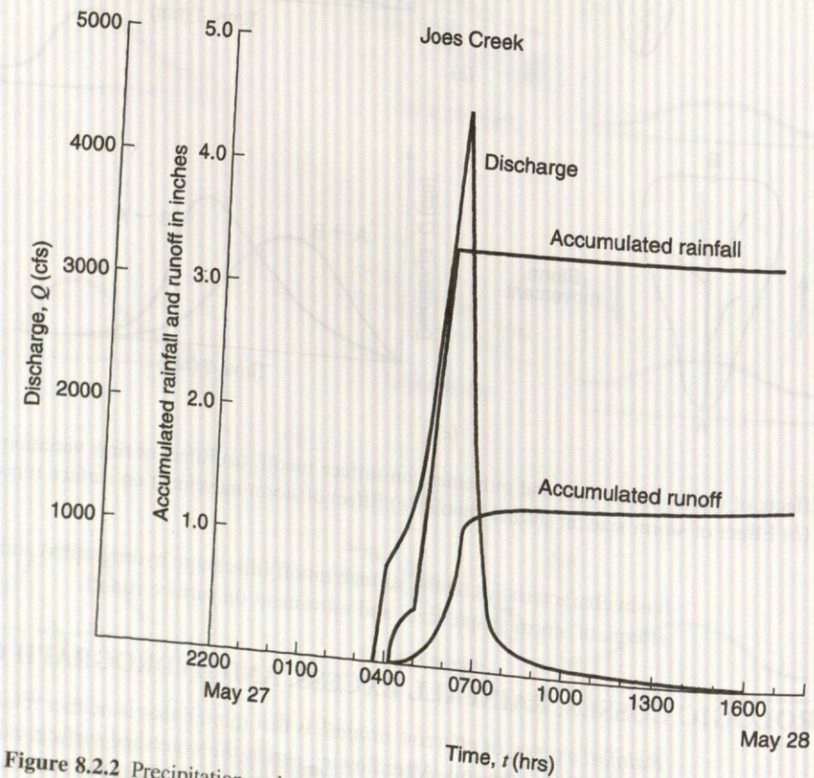


**Figure 8.2.2** Precipitation and runoff data for Joes Creek, storm of May 27–28, 1978 (from Masch (1984)).

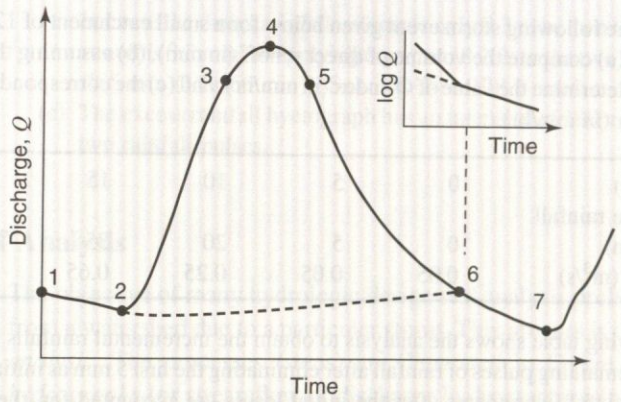


**Figure 8.2.3** Components of a streamflow hydrograph: (1-2) baseflow recession; (2-3) rising limb; (3-5) crest segment; (4) peak; (5-6) falling limb; and (6-7) baseflow recession.

### 8.2.1 Hydrograph Components

There are several sources that make up a hydrograph (total runoff hydrograph) including direct surface runoff, interflow, baseflow (groundwater), and channel precipitation. Figure 8.1.3*a* illustrates the direct runoff (saturated overland flow), interflow, and baseflow. For hydrologic purposes, the total runoff consists of only two parts, direct runoff and baseflow. Baseflow is the result of water entering the stream from the groundwater that discharges from the aquifer. Figure 8.2.3 defines the components of the hydrograph, showing the baseflow recession (1-2) and (6-7), the rising limb (2-3), the crest segment (3-5), and the falling limb (5-6).

The process of defining the baseflow is referred to as baseflow separation. A number of baseflow separation methods have been suggested. Baseflow recession curves (Figure 8.2.3) can be described in the form of an exponential decay

$$Q(t_2) = Q(t_2)e^{-k(t_2-t_1)}, \quad t_2 > t_1 \tag{8.2.1}$$

where $k$ is the exponential decay constant having dimensions of $(\text{time})^{-1}$. With a known streamflow runoff hydrograph, the decay constant can be determined by plotting the curve of log $Q$ versus time as shown in Figure 8.2.3 or by using a least-squares procedure. Baseflow recession curves for particular streams can be superimposed to develop a normal depletion curve or master baseflow recession curve.

### 8.2.2 Φ-Index Method

The Φ-index is a constant rate of abstractions (in/hr or cm/hr) that can be used to approximate infiltration. Using an observed rainfall pattern and the resulting known volume of direct runoff, the Φ-index can be determined. Using the known rainfall pattern, Φ is determined by choosing a time interval $\Delta t$, identifying the number of rainfall intervals $N$ of rainfall that contribute to the direct runoff volume, and then subtracting $\Phi \cdot \Delta t$ from the observed rainfall in each time interval. The values of Φ and $N$ will need to be adjusted so that the volume of direct runoff ($r_d$) and excess rainfall are equal

$$r_d = \sum_{n=1}^{N} (R_n - \Phi \cdot \Delta t) \tag{8.2.2}$$

where $R_n$ is the observed rainfall (in or cm) in time interval $n$.

***EXAMPLE 8.2.1***

Consider the following storm event given below for a small catchment of 120 hectares. For a baseflow of 0.05 $m^3/s$, (a) compute the volume of direct runoff (in mm), (b) assuming the initial losses (abstractions) are 5 mm, determine the value of $\Phi$-index (in mm/hr), and (c) the corresponding effective rainfall intensity hyetograph (in mm/hr).

| Time (min) | 0 | 5 | 10 | 15 | 20 | 25 | 30 |
|---|---|---|---|---|---|---|---|
| Cumulative rainfall Depth (mm) | 0 | 5 | 20 | 35 | 45 | | |
| Discharge ($m^3/s$) | 0.05 | 0.05 | 0.25 | 0.65 | 0.35 | 0.15 | 0.05 |

***SOLUTION***

The following table shows the analysis to obtain the incremental rainfalls and rainfall intensities. There are three remaining pulses of rainfall after eliminating the first 5 mm as initial abstractions. For each of the first two rainfall increments after the initial losses are accounted for, the incremental rainfall volume is $\Phi \cdot \Delta t = \Phi(5 \text{ min})(1 \text{ hr}/60 \text{ min}) = 15$ mm, so solving $\Phi = 180$ mm/hr. For the third interval, $\Phi \cdot \Delta t = \Phi(5 \text{ min})(1 \text{ hr}/60 \text{ min}) = 10$, so the rainfall intensity is 120 mm/hr.

| Time (min) | Discharge ($m^3$/sec) | Direct runoff ($m^3$/sec) | Cumulative rainfall (mm) | Incremental rainfall (mm) | Rainfall intensity (mm/hr) |
|---|---|---|---|---|---|
| 0 | 0.05 | 0 | 0 | | |
| 5 | 0.05 | 0 | 5 (initial loss) | 0 | |
| 10 | 0.25 | 0.20 | 20 | 15 | 180 |
| 15 | 0.65 | 0.60 | 35 | 15 | 180 |
| 20 | 0.35 | 0.30 | 45 | 10 | 120 |
| 25 | 0.15 | 0.10 | | | |
| 30 | 0.05 | 0 | | | |

**(a)** The direct runoff volume = (0.2 + 0.6 + 0.3 + 0.1) $m^2$/sec (5 min.) (60 sec/min) = 360 $m^3$, which converts to $r_d = 360\ m^3/(120 \text{ hectares} \times 10{,}000\ m^2/\text{hectare}) = 0.3$ mm.

**(b)** There are three pulses of rainfall after eliminating the first 5 mm as initial abstractions. Considering the two largest rainfall pulses, the rainfall volume above the 120 mm/hr level is 10 mm, and

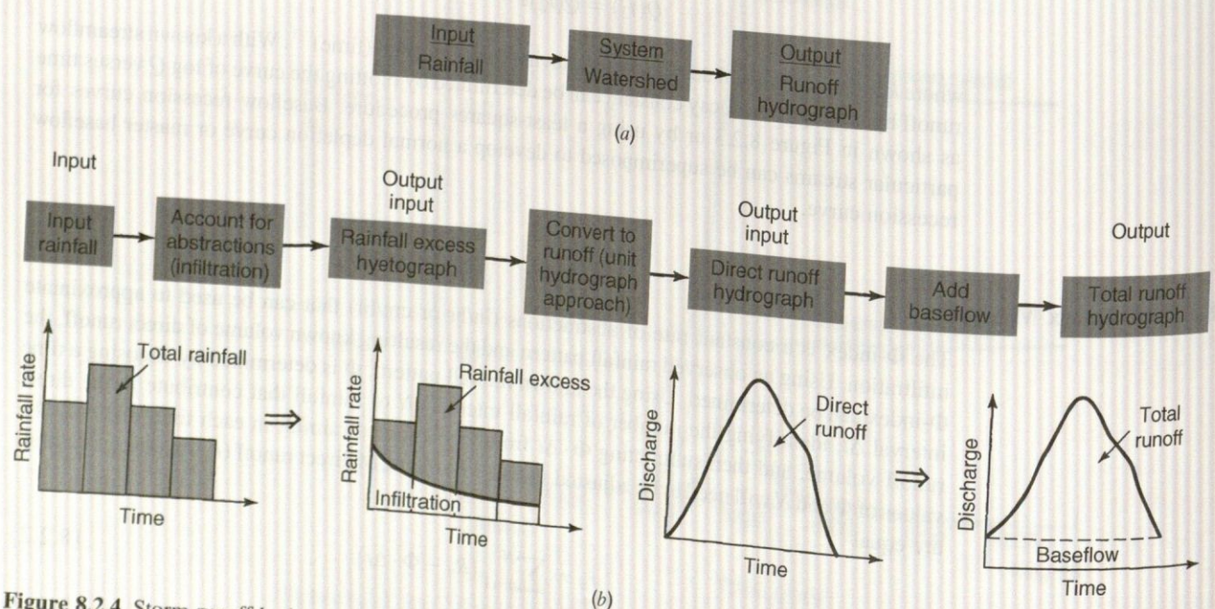


**Figure 8.2.4** Storm runoff hydrographs. (*a*) Rainfall-runoff modeling; (*b*) Steps to define storm runoff.

because the direct rainfall volume is only 0.3 mm, then $\Phi$ is above the 120 mm/hr level. The direct runoff is 0.3 mm, so applying equation (8.2.2) to the two largest pulses, $r_d = 0.3$ mm $= 2[(15$ mm $- \Phi(5$ min$)(1$ hr/60 min$)]$. Solving, $\Phi = 178.2$ mm/hr.

(c) The excess rainfall hyetograph has an intensity of 180 mm/hr − 178.2 mm/hr = 1.8 mm/hr for the two rainfall pulses.

### 8.2.3 Rainfall-Runoff Analysis

The objective of many hydrologic design and analysis problems is to determine the surface runoff from a watershed due to a particular storm. This process is commonly referred to as *rainfall-runoff analysis*. The processes (steps) are illustrated in Figure 8.2.4 to determine the *storm runoff hydrographs* (or streamflow or discharge hydrograph) using the unit hydrograph approach.

## 8.3 RAINFALL-RUNOFF ANALYSIS USING UNIT HYDROGRAPH APPROACH

The objective of *rainfall-runoff analysis* is to develop the runoff hydrograph as illustrated in Figure 8.2.4*a*, where the system is a watershed or river catchment, the input is the rainfall hyetograph, and the output is the runoff or discharge hydrograph. Figure 8.2.4*b* defines the processes (steps) to determine the runoff hydrograph from the rainfall input using the *unit hydrograph approach*.

A *unit hydrograph* is the direct runoff hydrograph resulting from 1 in (or 1 cm in SI units) of excess rainfall generated uniformly over a drainage area at a constant rate for an effective duration. The unit hydrograph is a simple linear model that can be used to derive the hydrograph resulting from any amount of excess rainfall. The following basic assumptions are inherent in the unit hydrograph approach:

1. The excess rainfall has a constant intensity within the effective duration.
2. The excess rainfall is uniformly distributed throughout the entire drainage area.
3. The base time of the direct runoff hydrograph (i.e., the duration of direct runoff) resulting from an excess rainfall of given duration is constant.
4. The ordinates of all direct runoff hydrographs of a common base time are directly proportional to the total amount of direct runoff represented by each hydrograph.
5. For a given watershed, the hydrograph resulting from a given excess rainfall reflects the unchanging characteristics of the watershed.

The following *discrete convolution equation* is used to compute direct runoff hydrograph ordinates $Q_n$, given the rainfall excess values $P_m$ and given the unit hydrograph ordinates $U_{n-m+1}$ (Chow et al., 1988):

$$Q_n = \sum_{m=1}^{n \le M} P_m U_{n-m+1} \quad \text{for } n = 1, 2, \ldots, N \tag{8.3.1}$$

where $n$ represents the direct runoff hydrograph time interval and $m$ represents the precipitation time interval ($m = 1, \ldots, n$).

The reverse process, called *deconvolution*, is used to derive a unit hydrograph given data on $P_m$ and $Q_n$. Suppose that there are $M$ pulses of excess rainfall and $N$ pulses of direct runoff in the storm considered; then $N$ equations can be written for $Q_n$, $n = 1, 2 \ldots, N$, in terms of $N - M + 1$ unknown values of the unit hydrograph, as shown in Table 8.3.1. Figure 8.3.1 diagramatically illustrates the calculation and the runoff contribution by each rainfall input pulse.

Once the unit hydrograph has been determined, it may be applied to find the direct runoff and streamflow hydrographs for given storm inputs. When a rainfall hyetograph is selected, the abstractions are subtracted to define the excess rainfall hyetograph. The time interval used in

**Table 8.3.1** The Set of Equations for Discrete Time Convolution

$$
\begin{aligned}
Q_1 &= P_1U_1 \\
Q_2 &= P_2U_1 + P_1U_2 \\
Q_3 &= P_3U_1 + P_2U_2 + P_1U_3 \\
&\cdots \\
Q_M &= P_MU_1 + P_{M-1}U_2 + \cdots + P_1U_M \\
Q_{M+1} &= 0 + P_MU_2 + \cdots + P_2U_M + P_1U_{M+1} \\
&\cdots \\
Q_{N-1} &= 0 + 0 + \cdots + 0 + 0 + \cdots + P_MU_{N-M} + P_{M-1}U_{N-M+1} \\
Q_N &= 0 + 0 + \cdots + 0 + 0 + \cdots + 0 + P_MU_{N-M+1}
\end{aligned}
$$

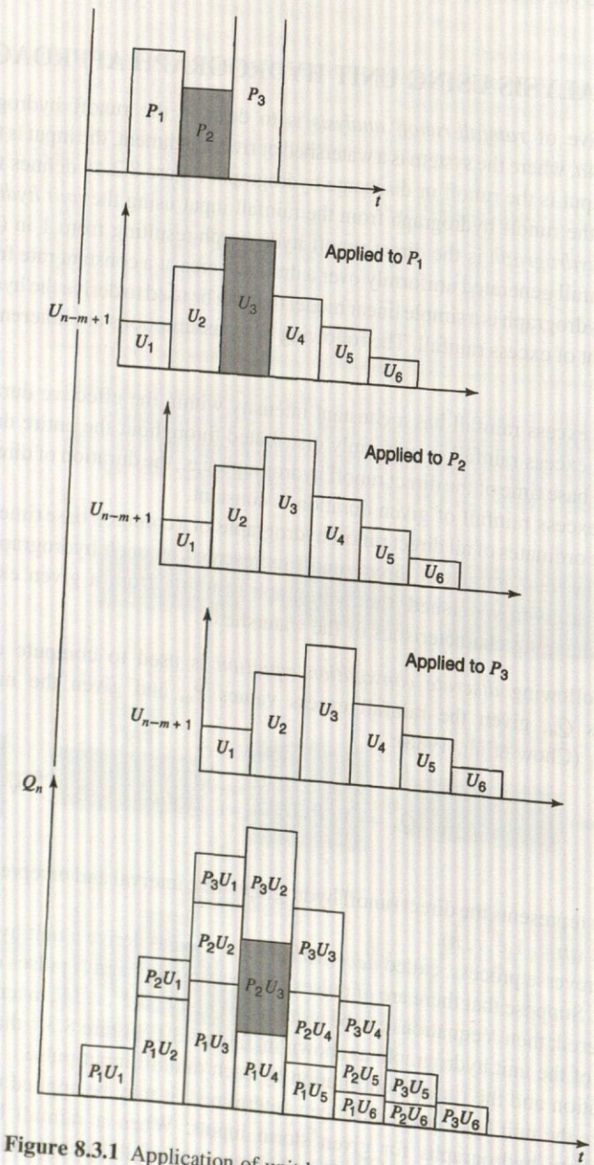


**Figure 8.3.1** Application of unit hydrograph to rainfall input.

***EXAMPLE 8.3.1***

***SOLUTION***

defining the excess rainfall hyetograph ordinates must be the same as that for which the unit hydrograph is specified.

***EXAMPLE 8.3.1***

The 1-hr unit hydrograph for a watershed is given below. Determine the runoff from this watershed for the storm pattern given. The abstractions have a constant rate of 0.3 in/h.

| Time (h) | 1 | 2 | 3 | 4 | 5 | 6 |
|---|---|---|---|---|---|---|
| Precipitation (in) | 0.5 | 1.0 | 1.5 | 0.5 | | |
| Unit hydrograph (cfs) | 10 | 100 | 200 | 150 | 100 | 50 |

***SOLUTION***

The calculations are shown in Table 8.3.2. The 1-hr unit hydrograph ordinates are listed in column 2 of the table; there are $L = 6$ unit hydrograph ordinates, where $L = N - M + 1$. The number of excess rainfall intervals is $M = 4$. The excess precipitation 1-hr pulses are $P_1 = 0.2$ in, $P_2 = 0.7$ in, $P_3 = 1.2$ in, and $P_4 = 0.2$ in, as shown at the top of the table. For the first time interval $n = 1$, the discharge is computed using equation (8.3.1):

$$Q_1 = P_1 U_1 = 0.2 \times 10 = 2 \text{ cfs}$$

For the second time interval, $n = 2$,

$$Q_2 = P_1 U_2 + P_2 U_1 = 0.2 \times 100 + 0.7 \times 10 = 27 \text{ cfs}$$

and similarly for the remaining direct runoff hydrograph ordinates. The number of direct runoff ordinates is $N = L + M - 1 = 6 + 4 - 1 = 9$; i.e., there are nine nonzero ordinates, as shown in Table 8.3.2. Column 3 of Table 8.3.2 contains the direct runoff corresponding to the first rainfall pulse, $P_1 = 0.2$ in, and column 4 contains the direct runoff from the second rainfall pulse, $P_2 = 0.2$ in, etc. The direct runoff hydrograph, shown in column 7 of the table, is obtained, from the principle of superposition, by adding the values in columns 3–6.

**Table 8.3.2** Calculation of the Direct Runoff Hydrograph

| (1) | (2) | (3) | (4) | (5) | (6) | (7) |
|---|---|---|---|---|---|---|
| | | Total precipitation (in) | | | | |
| | | 0.5 | 1 | 1.5 | 0.5 | |
| Time (hr) | Unit hydrograph (cfs/in) | Excess precipitation (in) | | | | Direct runoff (cfs) |
| | | 0.2 | 0.7 | 1.2 | 0.2 | |
| 0 | 0 | 0 | 0 | | | 0 |
| 1 | 10 | 2 | 0 | 0 | | 2 |
| 2 | 100 | 20 | 7 | 0 | 0 | 27 |
| 3 | 200 | 40 | 70 | 12 | 0 | 122 |
| 4 | 150 | 30 | 140 | 120 | 2 | 292 |
| 5 | 100 | 20 | 105 | 240 | 20 | 385 |
| 6 | 50 | 10 | 70 | 180 | 40 | 300 |
| 7 | 0 | 0 | 35 | 120 | 30 | 185 |
| 8 | | | 0 | 60 | 20 | 80 |
| 9 | | | | 0 | 10 | 10 |
| 10 | | | | | 0 | 0 |

***EXAMPLE 8.3.2***

Determine the 1-hr unit hydrograph for a watershed using the precipitation pattern and runoff hydrograph below. The abstractions have a constant rate of 0.3 in/hr, and the baseflow of the stream is 0 cfs.

| Time (h) | 1 | 2 | 3 | 4 | 5 | 6 | 7 | 8 | 9 | 10 |
|---|---|---|---|---|---|---|---|---|---|---|
| Precipitation (in) | 0.5 | 1.0 | 1.5 | 0.5 | | | | | | |
| Runoff (cfs) | 2 | 27 | 122 | 292 | 385 | 300 | 185 | 80 | 10 | 0 |

***SOLUTION***

Using the deconvolution process, we get $Q_1 = P_1 U_1$

so that for $P_1 = 0.5 - 0.3 = 0.2$ in and $Q_1 = 2$ cfs,

$U_1 = Q_1/P_1 = 2/0.2 = 10$ cfs.

$Q_2 = P_1 U_2 + P_2 U_1$, so that

$U_2 = (Q_2 - P_2 U_1)/P_1$

where

$P_2 = 1.0 - 0.3 = 0.7$ in and $Q_2 = 27$ cfs.

$U_2 = (27 - 0.7(10))/0.2 = 100$ cfs and

$Q_3 = P_1 U_3 + P_2 U_2 + P_3 U_1$

then

$U_3 = (Q_3 - P_2 U_2 - P_3 U_1)/P_1$, so that

$U_3 = (122 - 0.7(100) - 1.2(10))/0.2 = 200$ cfs.

The rest of the unit hydrograph ordinates can be calculated in a similar manner.

## 8.4 SYNTHETIC UNIT HYDROGRAPHS

### 8.4.1 Snyder's Synthetic Unit Hydrograph

When observed rainfall-runoff data are not available for unit hydrograph determination, a *synthetic unit hydrograph* can be developed. A unit hydrograph developed from rainfall and streamflow data in a watershed applies only to that watershed and to the point on the storm where the streamflow data were measured. Synthetic unit hydrograph procedures are used to develop unit hydrographs for other locations on the stream in the same watershed or other watersheds that are of similar character.

One of the most commonly used synthetic unit hydrograph procedures is Snyder's synthetic unit hydrograph. This method relates the time from the centroid of the rainfall to the peak of the unit hydrograph to geometrical characteristics of the watershed. To determine the regional parameters $C_t$ and $C_p$, one can use values of these parameters determined from similar watersheds. $C_t$ can be determined from the relationship for the *basin lag*:

$$t_p = C_1 C_t (L \cdot L_c)^{0.3} \tag{8.4.1}$$

where $C_1$, $L$, and $L_c$ are defined in Table 8.4.1. Solving equation (8.4.1) for $C_t$ gives

$$C_t = \frac{t_p}{C_1 (L \cdot L_c)^{0.3}} \tag{8.4.2}$$

To compute $C_t$ for a gauged basin, $L$ and $L_c$ are determined for the gauged watershed and $t_p$ from the derived unit hydrograph for the gauged basin.

To compute the other required parameter $C_p$, the expression for peak discharge of the standard unit hydrograph can be used:

$$Q_p = \frac{C_2 C_p A}{t_p} \tag{8.4.3}$$

or for a unit discharge (discharge per unit area)

$$q_p = \frac{C_2 C_p}{t_p} \tag{8.4.4}$$

Solving equation (8.4.4) for $C_p$ gives

$$C_p = \frac{q_p t_p}{C_2} \tag{8.4.5}$$

This relationship can be used to solve for $C_p$ for the ungauged watershed, knowing the terms in the right-hand side. Table 8.4.1 defines the steps for this procedure.

Section 8.8 discusses the SCS-unit hydrograph procedure.

***EXAMPLE 8.4.1***

A watershed has a drainage area of 5.42 mi$^2$; the length of the main stream is 4.45 mi, and the main channel length from the watershed outlet to the point opposite the center of gravity of the watershed is 2.0 mi. Using $C_t = 2.0$ and $C_p = 0.625$, determine the standard synthetic unit hydrograph for this basin. What is the standard duration? Use Snyder's method to determine the 30-min unit hydrograph parameter.

***SOLUTION***

For the standard unit hydrograph, equation (8.4.1) gives

$$t_p = C_1 C_t (L L_c)^{0.3} = 1 \times 2 \times (4.45 \times 2)^{0.3} = 3.85 \text{ hr}$$

The standard rainfall duration $t_r = 3.85/5.5 = 0.7$ hr. For a 30-min unit hydrograph, $t_R = 30 \text{ min} = 0.5$ hr. The basin lag $t_{pR} = t_p - (t_r - t_R)/4 = 3.85 - (0.7 - 0.5)/4 = 3.80$ hr. The peak flow for the required unit hydrograph is $= q_p t_p / t_{pR}$, and substituting equation (8.4.4) in the previous equation, $q_{pR} = q_p t_p / t_{pR} = (C_2 C_p / t_p) t_p / t_{pR} = C_2 C_p / t_{pR}$, so that $q_{pR} = 640 \times 0.625/3.80 = 105.26$ cfs $(\text{in} \cdot \text{mi}^2)$, and the peak discharge is $Q_{pR} = q_{pR} A = 105.26 \times 5.42 = 570$ cfs/in.

The widths of the unit hydrograph are computed next. At 75 percent of the peak discharge, $W_{75} = C_{W_{75}} q_{pR}^{-1.08} = 440 \times 105.26^{-1.08} = 2.88$ hr. At 50 percent of the peak discharge, $W_{50} = C_{W_{50}} q_{pR}^{-1.08} = 770 \times 105.26^{-1.08} = 5.04$ hr.

The base time $t_b$ may be computed assuming a triangular shape. This, however, does not guarantee that the volume under the unit hydrograph corresponds to 1 in (or 1 cm, for SI units) of excess rainfall. To overcome this, the value of $t_b$ may be exactly computed taking into account the values of $W_{50}$ and $W_{75}$ by solving the equation in step 5 of Table 8.4.1 for $t_b$:

$$t_b = 2581\, A/Q_{pR} - 1.5\, W_{50} - W_{75}$$

so that, with $A = 5.42$ mi$^2$, $W_{50} = 5.04$ hr, $W_{75} = 2.88$ hr, and $Q_{pR} = 570$ cfs/in, $T_b = 2581(5.42)/570 - 1.5 \times 5.04 - 2.88 = 14.1$ hr.

## 8.4.2 Clark Unit Hydrograph

The Clark unit hydrograph procedure (Clark, 1945) is based upon using a time-area relationship of the watershed that defines the cumulative area of the watershed contributing runoff to the watershed outlet as a function of time. Ordinates of the time-area relationship are converted to a volume of runoff per second for an excess (1 cm or 1 in) and interpolated to the given time interval to define a

**Table 8.4.1** Steps to Compute Snyder's Synthetic Unit Hydrograph

**Step 0** Measured information from topography map of watershed

- $L$ = main channel length in mi (km)
- $L_c$ = length of the main stream channel from outflow point of watershed to a point opposite the centroid of the watershed in mi (km)
- $A$ = watershed area in mi$^2$ (km$^2$)

Regional parameters $C_t$ and $C_p$ determined from similar watersheds.

**Step 1** Determine time to peak ($t_p$) and duration ($t_r$) of the standard unit hydrograph:

$$t_p = C_1 C_t (L \cdot L_c)^{0.3} \quad \text{(hours)}$$
$$t_r = t_p / 5.5 \quad \text{(hours)}$$

where $C_1 = 1.0$ (0.75 for SI units)

**Step 2** Determine the time to peak $t_{pR}$ for the desired duration $t_R$:

$$t_{pR} = t_p + 0.25(t_R - t_r) \quad \text{(hours)}$$

**Step 3** Determine the peak discharge, $Q_{pR}$, in cfs/in ((m$^3$/s)/cm in SI units)

$$Q_{pR} = \frac{C_2 C_p A}{t_{pR}}$$

where $C_2 = 640$ (2.75 for SI units)

**Step 4** Determine the width of the unit hydrograph at $0.5Q_{pR}$ and $0.75Q_{pR}$. $W_{50}$ is the width at 50% of the peak given as

$$W_{50} = \frac{C_{50}}{(Q_{pR}/A)^{1.08}}$$

where $C_{50} = 770$ (2.14 for SI units). $W_{75}$ is the width at 75% of the peak given as

$$W_{75} = \frac{C_{75}}{(Q_{pR}/A)^{1.08}}$$

where $C_{75} = 440$ (1.22 for SI units)

**Step 5** Determine the base, $T_b$, such that the unit hydrograph represents 1 in (1 cm in SI units) of direct runoff volume:

$$1 \text{ in} = \left[\left(\frac{W_{50}+T_b}{2}\right)(0.5Q_{pR}) + \left(\frac{W_{75}+W_{50}}{2}\right)(0.25Q_{pR}) + \frac{1}{2}W_{75}(0.25Q_{pR})\right]\left(\text{hr} \times \frac{\text{ft}^3}{\text{sec}}\right)$$
$$\left(\frac{1}{A(\text{mi})^2} \times \frac{1 \text{ mi}^2}{(5{,}280)^2 \text{ ft}^2} \times \frac{12 \text{ in}}{\text{ft}} \times \frac{3{,}600 \text{ sec}}{\text{hr}}\right)$$

Solving for $T_b$, we get

$$T_b = 2{,}581\frac{A}{Q_{pR}} - 1.5W_{50} - W_{75}$$

for $A$ in mi$^2$, $Q_{pR}$ in cfs, $W_{50}$ and $W_{75}$ in hours.

**Step 6** Define known points of the unit hydrograph. $\left(T_p = t_{pR} + \frac{t_R}{2}\right)$

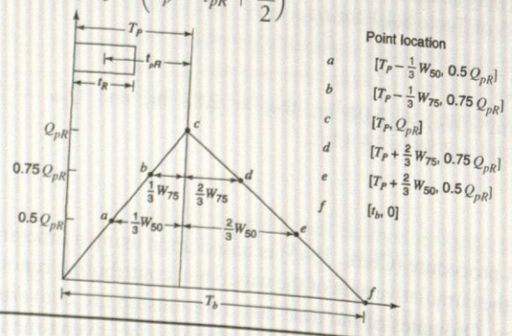


| | Point location |
|---|---|
| a | $[T_p - \frac{1}{3}W_{50},\ 0.5\,Q_{pR}]$ |
| b | $[T_p - \frac{1}{3}W_{75},\ 0.75\,Q_{pR}]$ |
| c | $[T_p, Q_{pR}]$ |
| d | $[T_p + \frac{2}{3}W_{75},\ 0.75\,Q_{pR}]$ |
| e | $[T_p + \frac{2}{3}W_{50},\ 0.5\,Q_{pR}]$ |
| f | $[t_b, 0]$ |

translation hydrograph. The assumption is a pure translation of the rainfall excess without storage effects of the watershed to define a translation hydrograph. This translation hydrograph is routed through a linear reservoir ($S = RQ$) in order to simulate the effects of storage of the watershed, where $R$ is the storage coefficient. The resulting routed hydrograph for the instantaneous excess is averaged to produce the unit hydrograph for the excess (1 cm or 1 inch) occurring in the given time interval.

Synthetic time-area relationships can be expressed in the following form such as that used by the U.S. Army Corps of Engineers (1990)

$$A/A_c = 1.414(t/T_c)^{1.5} \qquad \text{for } 0 \le t/T_c \le 0.5 \tag{8.4.6a}$$

and

$$A/A_c = 1 - 1.414(1 - t/T_c)^{1.5} \quad \text{for } 0.5 \le t/T_c \le 1.0 \tag{8.4.6b}$$

where $A$ is the contributing area at time $t$, $A_c$ is the total watershed area, and $T_c$ is the time of concentration of the watershed area. Some investigators such as Ford et al. (1980) indicate that a detailed time-area curve usually is not necessary for accurate synthetic unit hydrograph estimation. A comparison of the HEC (Hydrologic Engineering Center) default relation found in HEC-1 and HEC-HMS to that used in Phoenix, Arizona is given in Table 8.4.2.

The average instantaneous flow over time interval $t$ to $t + \Delta t$, defining the translation hydrograph is denoted as $I_{ave,t}$. To compute $I_{ave,t}$, assuming a pure translation over a $\Delta t$ hr time period, the flowing equations are used. For 1 cm (0.01 m), the $I_{ave,t}$ in $m^3/s$ is expressed as

$$I_{ave,t} = (0.01\text{ m})(\Delta A\text{ km}^2)(10^6\text{ m}^2/\text{km}^2)(1/\Delta t\text{ hr})(1\text{ hr}/3600\text{ sec}) \tag{8.4.7}$$

where $\Delta A$ is the incremental area in $km^2$ between runoff isochrones (lines of equal runoff at a certain time) and $\Delta t$ is the time increment in hours. For 1 in in the $I_{ave,t}$ in $ft^3/s$ is expressed as

$$I_{ave,t} = (1\text{ in})(1\text{ ft}/12\text{ in})(\Delta A\text{ mi}^2)(5280\text{ ft}^2/\text{mi}^2)(1/\Delta t\text{ hr})(1\text{ hr}/3600\text{ sec}) \tag{8.4.8}$$

Storage effects in the watershed are incorporated by routing the translation hydrograph through a linear reservoir using the continuity equation

$$I_{ave,t} - 0.5(Q_t + Q_{t+\Delta t}) = (S_t + S_{t+\Delta t})/\Delta t \tag{8.4.9}$$

**Table 8.4.2** Synthetic Dimensionless Time-Area Relations

| | Contributing area, as a percent of total area | | |
|---|---|---|---|
| Time as a percent of $T_c$ | Urban* watersheds | Natural* watersheds | HEC default |
| 0 | 0 | 0 | 0.0 |
| 10 | 5 | 3 | 4.5 |
| 20 | 16 | 5 | 12.6 |
| 30 | 30 | 8 | 23.2 |
| 40 | 65 | 12 | 35.8 |
| 50 | 77 | 20 | 50.0 |
| 60 | 84 | 43 | 64.2 |
| 70 | 90 | 75 | 76.8 |
| 80 | 94 | 90 | 87.4 |
| 90 | 97 | 96 | 95.5 |
| 100 | 100 | 100 | 100 |

*Flood Control District of Maricopa County, Phoenix, AZ (1995)

$I_{ave,t}$ is the average instantaneous inflow over time interval $t$ to $t + \Delta t$, defining the translation hydrograph, $Q$ is the outflow from the linear reservoir, and $S$ is the storage in the linear reservoir. In the linear reservoir assumption, storage $S_t$ is assumed to be linearly proportional to $Q_t$

$$S_t = RQ_t \tag{8.4.10}$$

in which $R$ is the proportionality constant (watershed storage coefficient) with units of time. Combining equations (8.4.9) and (8.4.10) the routing equation is

$$Q_{t+\Delta t} = CI_{ave,t} + (1 - C)Q_t \tag{8.4.11}$$

where $I_{ave,t}$ is the average translated runoff (inflow rate to the linear reservoir) during time increment, and

$$C = 2\,\Delta t/(2R + \Delta t) \tag{8.4.12}$$

The discharge, $Q_t$, from the linear reservoir now includes the effects of the storage of the watershed. This hydrograph is an instantaneous (duration = 0 hr) unit hydrograph, which is converted to the desired unit hydrograph of duration $\tau$ by averaging the ordinates over the time interval

$$U_\tau(t) = 0.5[Q_t + Q_{t-\tau}] \tag{8.4.13}$$

The above equations are the basis for the Clark unit hydrograph procedure.

***EXAMPLE 8.4.2***

A small watershed has an area of 10 km$^2$ and a time of concentration of 1.5 hr. The watershed storage coefficient is 0.75 hr. The time-area relationship is the HEC default values in Table 8.4.2. Compute the 1-hr unit hydrograph for this small watershed. Use a time interval of 0.5-hr for the computations.

***SOLUTION***

First the incremental areas of the watershed are determined using the HEC time-area relationship in Table 8.4.2. The translation hydrograph is then computed by applying equation (8.4.7) to each $\Delta A$. Next the translation hydrograph is routed through a linear reservoir using the given watershed storage coefficient. Compute the routing coefficient $C = 2(0.5)/[2(0.75) + 0.5] = 0.5$, so the linear reservoir routing equation is $Q_{t+\Delta t} = 0.5I_{ave,t} + (1 - 0.5)Q_t = 0.5I_{ave,t} + 0.5Q_t$. The unit hydrograph ordinates are computed using equation (8.4.13) with $\tau = 1$ hr. For example, the unit hydrograph ordinate for time 0.5 hr is $(0 + 7.56)/2 = 3.78$ m$^3$/s, for time 1.0 hr is $(0 + 16.4)/2 = 8.20$ m$^3$/s and for 1.5 hr is $(7.56 + 15.8)/2 = 11.7$ m$^3$/s.

| $t$ (hr) | $t/T_c$ | $A/A_c$ | $A$ (km$^2$) | $\Delta A$ (km$^2$) | $I_{ave,t}$ (m$^3$/s) | $Q_{t+\Delta t}$ (m$^3$/s) | $U_\tau(t)$ (m$^3$/s) |
|---|---|---|---|---|---|---|---|
| 0.0 | | | | | | | 0.0 |
| 0.5 | 0.333 | 0.272 | 2.72 | 2.72 | 15.1 | 7.56 | 3.78 |
| 1.0 | 0.667 | 0.728 | 7.28 | 4.56 | 25.3 | 16.4 | 8.20 |
| 1.5 | 1.0 | 1.0 | 10.0 | 2.72 | 15.1 | 15.8 | 11.7 |
| 2.0 | | | | | 0.0 | 7.89 | 12.2 |
| 2.5 | | | | | | 3.94 | 9.86 |
| 3.0 | | | | | | 1.97 | 4.93 |
| 3.5 | | | | | | 0.986 | 2.46 |
| 4.0 | | | | | | 0.493 | 1.23 |
| 4.5 | | | | | | 0.247 | 0.616 |
| 5.0 | | | | | | 0.123 | 0.308 |

## 8.5 S-HYDRO

***EXAMPLE 8.5.1***

***SOLUTION***

The use of the model HEC-HMS (HEC-1) requires the time of concentration, $T_c$, and the storage coefficient $R$. Various locations have developed relationships for these parameters to make the methods more accurate and easier to use. Straub et al. (2000) developed the following equations for small rural watersheds (0.02-2.3 mi$^2$) in Illinois

$$T_c = 1.54L^{0.875} S_o^{-0.181} \tag{8.4.14}$$

and

$$R = 16.4L^{0.342} S_o^{-0.790} \tag{8.4.15}$$

where $L$ is the stream length measured along the main channel from the watershed outlet to the watershed divide in miles, and $S_o$ is the main-channel slope determined from elevations at points that represent 10 and 85 percent of the distance along the channel from the watershed outlet to the watershed divide in ft/mi.

Others have used time of concentration equations that have included additional parameters. For example Phoenix, Arizona (Flood Control District of Maricopa County) uses the following time of concentration equations developed by Papadakis and Kazan (1987) for urban areas

$$T_c = 11.4L^{0.50} K_b^{0.52} S_o^{-0.31} i^{-0.38} \tag{8.4.16}$$

where $T_c$ is the time of concentration in hours, $L$ is the length of the longest flow path in miles, $K_b$ is a watershed resistance coefficient ($K_b = -0.00625 \log A + 0.04$) for commercial and residential areas, $A$ is the watershed area in acres, $S$ is the slope of the flow path in ft/mi, and $i$ is the rainfall intensity in in/hr. The storage coefficient is

$$R = 0.37T_c^{1.11} A^{-0.57} L^{0.80} \tag{8.4.17}$$

where $A$ is the watershed area in mi$^2$.

## .5 S-HYDROGRAPHS

In order to change a unit hydrograph from one duration to another, the *S-hydrograph method*, which is based on the principle of superposition, can be used. An S-hydrograph results theoretically from a continuous rainfall excess at a constant rate for an indefinite period. This curve (see Figure 8.5.1) has an S-shape with the ordinates approaching the rate of rainfall excess at the time of equilibrium.

Basically the S-curve (hydrograph) is the summation of an infinite number of $t_R$ duration unit hydrographs, each lagged from the preceding one by the duration of the rainfall excess, as illustrated in Figure 8.5.2.

A unit hydrograph for a new duration $t'_R$ is obtained by: (1) lagging the S-hydrograph (derived with the $t_R$ duration unit hydrographs) by the new (desired) duration $t'_R$, (2) *subtracting* the two S-hydrographs from one another, and (3) *multiplying* the resulting hydrograph ordinates by the ratio $t_R/t'_R$. Theoretically the S-hydrograph is a smooth curve because the input rainfall excess is assumed to be a constant, continuous rate. However, the numerical processes of the procedures may result in an undulatory form that may require smoothing or adjustment of the S-hydrograph.

**XAMPLE 8.5.1** Using the 2-hr unit hydrograph in Table 8.5.1, construct a 4-hr unit hydrograph (adapted from Sanders (1980)).

**OLUTION** See the computations in Table 8.5.1.

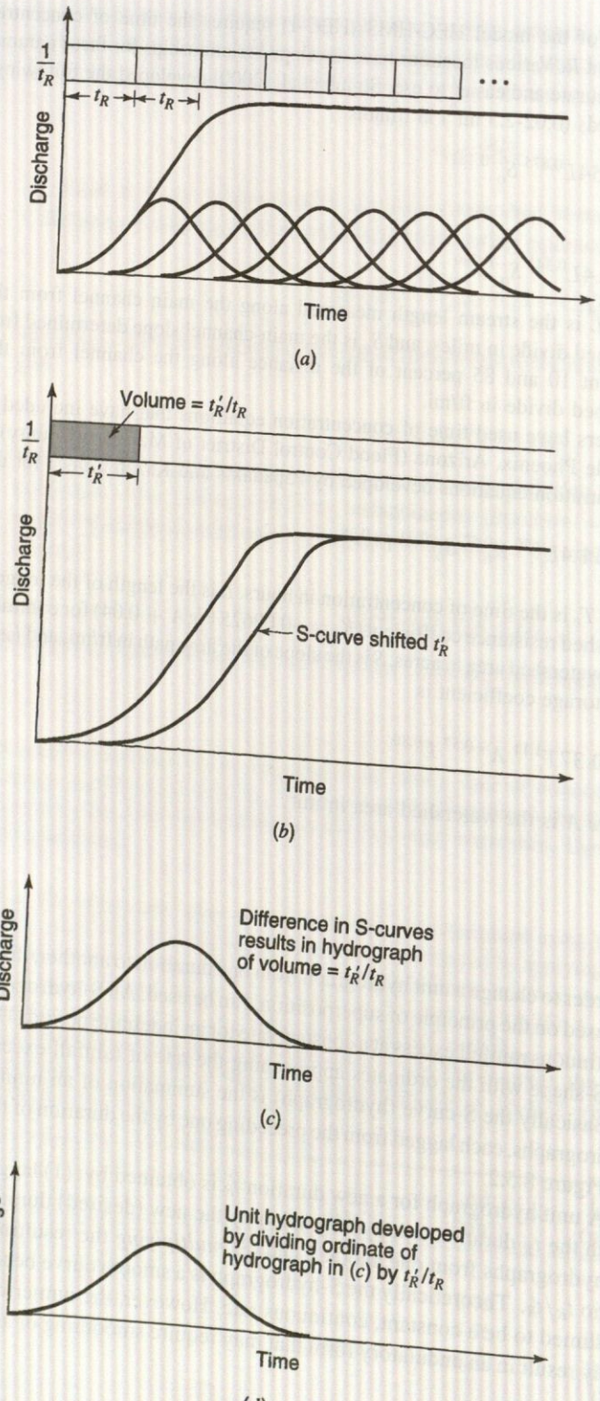


**Figure 8.5.1** Development of a unit hydrograph for duration $t'_R$ from a unit hydrograph for duration $t_R$.

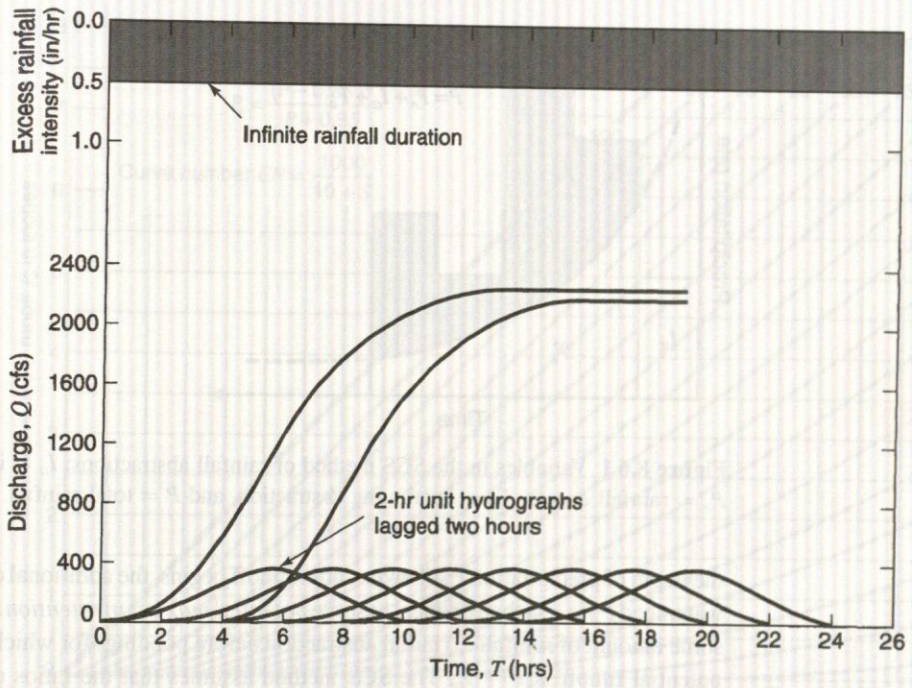


**Figure 8.5.2** Graphical illustration of the S-curve construction (from Masch (1984)).

**Table 8.5.1** S-Curve Determined from a 2-hr Unit Hydrograph to Estimate a 4-hr Unit Hydrograph

| Time (hr) | 2-hr unit hydrograph (cfs/in) | Lagged 2-hr unit hydrograph (cfs/in) | | S-curve | Lagged S-curve | 4-hr hydrograph | 4-hr-unit hydrograph (cfs/in) |
|---|---|---|---|---|---|---|---|
| 0 | 0 | | | 0 | — | 0 | 0 |
| 2 | 69 | 0 | | 69 | — | 69 | 34 |
| 4 | 143 | 69 | 0 ... | 212 | 0 | 212 | 106 |
| 6 | 328 | 143 | 69 ... | 540 | 69 | 471 | 235 |
| 8 | 389 | 328 | 143 ... | 929 | 212 | 717 | 358 |
| 10 | 352 | 389 | 328 | 1281 | 540 | 741 | 375 |
| 12 | 266 | 352 | 389 | 1547 | 929 | 618 | 309 |
| 14 | 192 | 266 | 352 | 1739 | 1281 | 458 | 229 |
| 16 | 123 | 192 | . | 1862 | 1547 | 315 | 158 |
| 18 | 84 | 123 | . | 1946 | 1739 | 207 | 103 |
| 20 | 49 | 84 | . | 1995 | 1862 | 133 | 66 |
| 22 | 20 | 49 | . | 2015 | 1946 | 69 | 34 |
| 24 | 0 | 20 | . | *2015 | 1995 | 20 | 10 |
| 26 | 0 | 0 | . ... | *2015 | 2015 | 0 | 0 |

*Adjusted values

*Source:* Sanders (1980).

## NRCS (SCS) RAINFALL-RUNOFF RELATION

The U.S. Department of Agriculture Soil Conservation Service (SCS) (1972), now the National Resources Conservation Service (NRCS), developed a rainfall-runoff relation for watershed. For the storm as a whole, the depth of excess precipitation or direct runoff $P_e$ is always less than or equal to

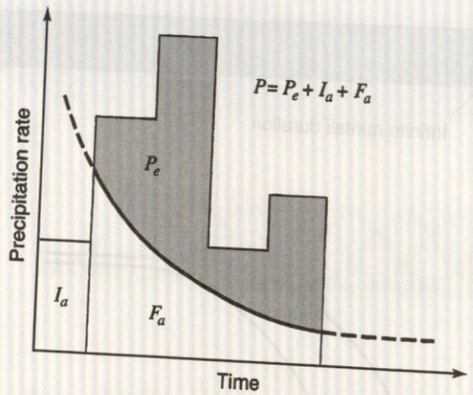


**Figure 8.6.1** Variables in the SCS method of rainfall abstractions: $I_a$ = initial abstraction, $P_e$ = rainfall excess, $F_a$ = continuing abstraction, and $P$ = total rainfall.

the depth of precipitation $P$; likewise, after runoff begins, the additional depth of water retained in the watershed $F_a$ is less than or equal to some *potential maximum retention* $S$ (see Figure 8.6.1). There is some amount of rainfall $I_a$ (initial abstraction before ponding) for which no runoff will occur, so the potential runoff is $P - I_a$. The SCS method assumes that the ratios of the two actual to the two potential quantities are equal, that is,

$$\frac{F_a}{S} = \frac{P_e}{P - I_a} \quad \frac{\text{Actual}}{\text{Potential}} \tag{8.6.1}$$

From continuity,

$$P = P_e + I_a + F_a \tag{8.6.2}$$

so that combining equations (8.6.1) and (8.6.2) and solving for $P_e$ gives

$$P_e = \frac{(P - I_a)^2}{P - I_a + S} \tag{8.6.3}$$

which is the basic equation for computing the depth of excess rainfall or direct runoff from a storm by the SCS method.

From the study of many small experimental watersheds, an empirical relation was developed for $I_a$:

$$I_a = 0.2S \tag{8.6.4}$$

so that equation (8.6.3) is now expressed as

$$P_e = \frac{(P - 0.2S)^2}{P + 0.8S} \tag{8.6.5}$$

Empirical studies by the SCS indicate that the potential maximum retention can be estimated as

$$S = \frac{1000}{CN} - 10 \tag{8.6.6}$$

where $CN$ is a runoff curve number that is a function of land use, antecedent soil moisture, and other factors affecting runoff and retention in a watershed. The curve number is a dimensionless number defined such that $0 \leq CN \leq 100$. For impervious and water surfaces $CN = 100$; for natural surfaces $CN < 100$.

## 8.7 CURVE NUM

### 8.7.1 Antecedent

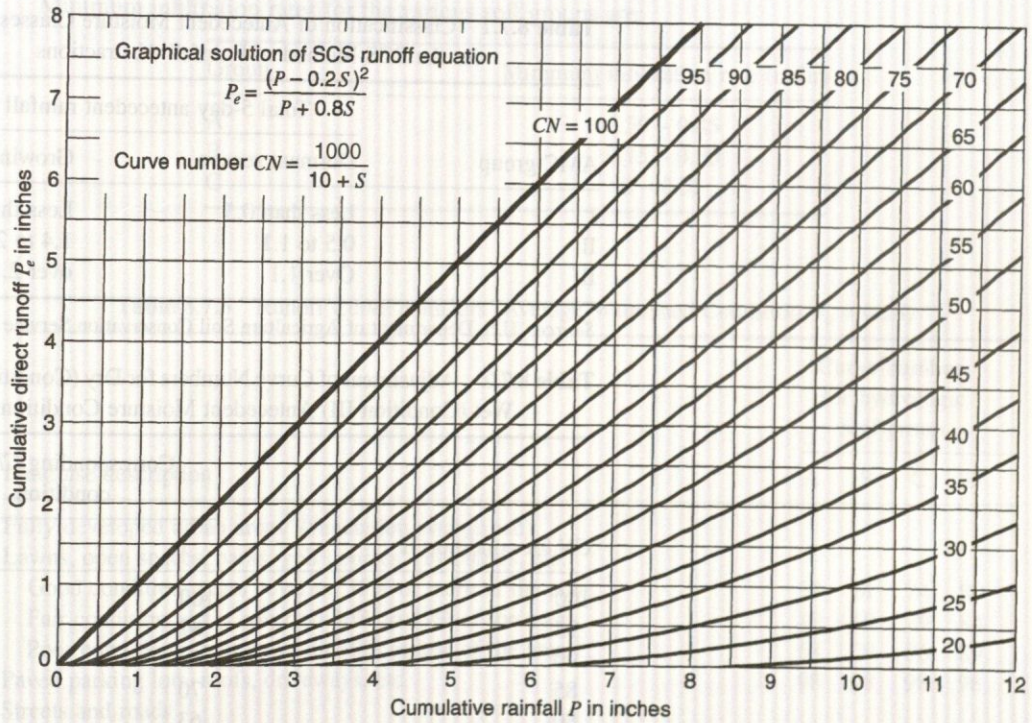


**Figure 8.6.2** Solution of the SCS runoff equations (from U.S. Department of Agriculture Soil Conservation Service (1972)).

The SCS rainfall-runoff relation (equation (8.6.5)) can be expressed in graphical form using the curve numbers as illustrated in Figure 8.6.2. Equation (8.6.5) or Figure 8.6.2 can be used to estimate the volume of runoff when the precipitation volume $P$ and the curve number $CN$ are known.

## 7 CURVE NUMBER ESTIMATION AND ABSTRACTIONS

### 7.1 Antecedent Moisture Conditions

The curve numbers shown in Figure 8.6.2 apply for normal *antecedent moisture conditions* (AMC II). Antecedent moisture conditions are grouped into three categories:

AMC I—Low moisture
AMC II—Average moisture condition, normally used for annual flood estimates
AMC III—High moisture, heavy rainfall over the preceding few days

For dry conditions (AMC I) or wet conditions (AMC III), equivalent curve numbers can be computed using

$$CN(\mathrm{I}) = \frac{4.2CN(\mathrm{II})}{10 - 0.058CN(\mathrm{II})} \tag{8.7.1}$$

and

$$CN(\mathrm{III}) = \frac{23CN(\mathrm{II})}{10 + 0.13CN(\mathrm{II})} \tag{8.7.2}$$

The range of antecedent moisture conditions for each class is shown in Table 8.7.1. Table 8.7.2 lists the adjustment of curve numbers to conditions I and III for known II conditions.

**Table 8.7.1** Classification of Antecedent Moisture Classes (AMC) for the SCS Method of Rainfall Abstractions

| | Total 5-day antecedent rainfall (in) | |
|---|---|---|
| AMC group | Dormant season | Growing season |
| I | Less than 0.5 | Less than 1.4 |
| II | 0.5 to 1.1 | 1.4 to 2.1 |
| III | Over 1.1 | over 2.1 |

*Source:* U.S. Department of Agriculture Soil Conservation Service (1972).

**Table 8.7.2** Adjustment of Curve Numbers for Dry (Condition I) and Wet (Condition III) Antecedent Moisture Conditions

| | Corresponding *CN* for condition | |
|---|---|---|
| *CN* for condition II | I | III |
| 100 | 100 | 100 |
| 95 | 87 | 99 |
| 90 | 78 | 98 |
| 85 | 70 | 97 |
| 80 | 63 | 94 |
| 75 | 57 | 91 |
| 70 | 51 | 87 |
| 65 | 45 | 83 |
| 60 | 40 | 79 |
| 55 | 35 | 75 |
| 50 | 31 | 70 |
| 45 | 27 | 65 |
| 40 | 23 | 60 |
| 35 | 19 | 55 |
| 30 | 15 | 50 |
| 25 | 12 | 45 |
| 20 | 9 | 39 |
| 15 | 7 | 33 |
| 10 | 4 | 26 |
| 5 | 2 | 17 |
| 0 | 0 | 0 |

*Source:* U.S. Department of Agriculture Soil Conservation Service (1972).

### 8.7.2 Soil Group Classification

Curve numbers have been tabulated by the Soil Conservation Service on the basis of soil type and land use in Table 8.7.3. The four soil groups in Table 8.7.3 are described as:

Group A: Deep sand, deep loess, aggregated silts
Group B: Shallow loess, sandy loam
Group C: Clay loams, shallow sandy loam, soils low in organic content, and soils usually high in clay
Group D: Soils that swell significantly when wet, heavy plastic clays, and certain saline soils

The values of *CN* for various land uses on these soil types are given in Table 8.7.3. For a watershed made up of several soil types and land uses, a composite *CN* can be calculated.

Minimum infiltration rates for the various soil groups are:

| Group | Minimum infiltration rate (in/hr) |
|---|---|
| A | 0.30 – 0.45 |
| B | 0.15 – 0.30 |
| C | 0 – 0.05 |

**Table 8.7.3** Runoff Curve Numbers (Average Watershed Condition, $I_a = 0.2S$)

| Land use description | | | Curve numbers for hydrologic soil group | | | |
|---|---|---|---|---|---|---|
| | | | A | B | C | D |
| Fully developed urban areas[a] (vegetation established) | | | | | | |
| Lawns, open spaces, parks, golf courses, cemeteries, etc. | | | | | | |
| Good condition; grass cover on 75% or more of the area | | | 39 | 61 | 74 | 80 |
| Fair condition; grass cover on 50% to 75% of the area | | | 49 | 69 | 79 | 84 |
| Poor condition; grass cover on 50% or less of the area | | | 68 | 79 | 86 | 89 |
| Paved parking lots, roofs, driveways, etc. | | | 98 | 98 | 98 | 98 |
| Streets and roads | | | | | | |
| Paved with curbs and storm sewers | | | 98 | 98 | 98 | 98 |
| Gravel | | | 76 | 85 | 89 | 91 |
| Dirt | | | 72 | 82 | 87 | 89 |
| Paved with open ditches | | | 83 | 89 | 92 | 93 |
| | Average % impervious[b] | | | | | |
| Commercial and business areas | 85 | | 89 | 92 | 94 | 95 |
| Industrial districts | 72 | | 81 | 88 | 91 | 93 |
| Row houses, town houses, and residential with lot sizes 1/8 acre or less | 65 | | 77 | 85 | 90 | 92 |
| Residential: average lot size | | | | | | |
| 1/4 acre | 38 | | 61 | 75 | 83 | 87 |
| 1/3 acre | 30 | | 57 | 72 | 81 | 86 |
| 1/2 acre | 25 | | 54 | 70 | 80 | 85 |
| 1 acre | 20 | | 51 | 68 | 79 | 84 |
| 2 acre | 12 | | 46 | 65 | 77 | 82 |
| Developing urban areas[c] (no vegetation established) | | | | | | |
| Newly graded area | | | 77 | 86 | 91 | 94 |
| | Cover | | | | | |
| Land use | Treatment of practice | Hydrologic condition[d] | | | | |
| Cultivated agricultural land | | | | | | |
| Fallow | Straight row | | 77 | 86 | 91 | 94 |
| | Conservation tillage | Poor | 76 | 85 | 90 | 93 |
| | Conservation tillage | Good | 74 | 83 | 88 | 90 |
| Row crops | Straight row | Poor | 72 | 81 | 88 | 91 |
| | Straight row | Good | 67 | 78 | 85 | 89 |
| | Conservation tillage | Poor | 71 | 80 | 87 | 90 |

(*Continued*)

**Table 8.7.3** (*Continued*)

| Cover | | Hydrologic condition[d] | Curve numbers for hydrologic soil group | | | |
|---|---|---|---|---|---|---|
| Land use | Treatment of practice | | A | B | C | D |
| | Conservation tillage | Good | 64 | 75 | 82 | 85 |
| | Contoured | Poor | 70 | 79 | 84 | 88 |
| | Contoured | Good | 65 | 75 | 82 | 86 |
| | Contoured and conservation tillage | Poor | 69 | 78 | 83 | 87 |
| | | Good | 64 | 74 | 81 | 85 |
| | Contoured and terraces | Poor | 66 | 74 | 80 | 82 |
| | Contoured and terraces | Good | 62 | 71 | 78 | 81 |
| | Contoured and terraces and conservation tillage | Poor | 65 | 73 | 79 | 81 |
| Small grain | Straight row | Good | 61 | 70 | 77 | 80 |
| | Straight row | Poor | 65 | 76 | 84 | 88 |
| | Conservation tillage | Good | 63 | 75 | 83 | 87 |
| | Conservation tillage | Poor | 64 | 75 | 83 | 86 |
| | Contoured | Good | 60 | 72 | 80 | 84 |
| | Contoured | Poor | 63 | 74 | 82 | 85 |
| | Contoured and conservation tillage | Good | 61 | 73 | 81 | 84 |
| | Contoured and terraces | Poor | 62 | 73 | 81 | 84 |
| | Contoured and terraces | Good | 60 | 72 | 80 | 83 |
| | Contoured and terraces and conservation tillage | Poor | 61 | 72 | 79 | 82 |
| | | Good | 59 | 70 | 78 | 81 |
| Close-seeded legumes or rotation meadow | Straight row | Poor | 66 | 77 | 85 | 89 |
| | Straight row | Good | 58 | 72 | 81 | 85 |
| | Contoured | Poor | 64 | 75 | 83 | 85 |
| | Contoured | Good | 55 | 69 | 78 | 83 |
| | Contoured and terraces | Poor | 63 | 73 | 80 | 83 |
| | Contoured and terraces | Good | 51 | 67 | 76 | 80 |
| Noncultivated agricultural land, pasture or range | No mechanical treatment | Poor | 68 | 79 | 86 | 89 |
| | No mechanical treatment | Fair | 49 | 69 | 79 | 84 |
| | No mechanical treatment | Good | 39 | 61 | 74 | 80 |
| | Contoured | Poor | 47 | 67 | 81 | 88 |
| | Contoured | Fair | 25 | 59 | 75 | 83 |
| | Contoured | Good | 6 | 35 | 70 | 79 |
| Meadow | | — | 30 | 58 | 71 | 78 |
| Forested—grass or orchards—evergreen or deciduous | | Poor | 55 | 73 | 82 | 86 |
| | | Fair | 44 | 65 | 76 | 82 |
| Brush | | Good | 32 | 58 | 72 | 79 |
| | | Poor | 48 | 67 | 77 | 83 |
| Woods | | Good | 20 | 48 | 65 | 73 |
| | | Poor | 45 | 66 | 77 | 83 |
| | | Fair | 36 | 60 | 73 | 79 |
| Farmsteads | | Good | 25 | 55 | 70 | 77 |
| Forest-range | | — | 59 | 74 | 82 | 86 |
| Herbaceous | | | | | | |
| | | Poor | | 79 | 86 | 92 |
| | | Fair | | 71 | 80 | 89 |
| | | Good | | 61 | 74 | 84 |

**Table 8.7.3** (*Continued*)

| Land use | Cover: Treatment of practice | Hydrologic condition[d] | Curve numbers for hydrologic soil group: A | B | C | D |
|---|---|---|---|---|---|---|
| Oak–aspen | | Poor | | 65 | 74 | |
| | | Fair | | 47 | 57 | |
| | | Good | | 30 | 41 | |
| Juniper–grass | | Poor | | 72 | 83 | |
| | | Fair | | 58 | 73 | |
| | | Good | | 41 | 61 | |
| Sage–grass | | Poor | | 67 | 80 | |
| | | Fair | | 50 | 63 | |
| | | Good | | 35 | 48 | |

[a]For land uses with impervious areas, curve numbers are computed assuming that 100% of runoff from impervious areas is directly connected to the drainage system. Pervious areas (lawn) are considered to be equivalent to lawns in good condition and the impervious areas have a *CN* of 98.

[b]Includes paved streets.

[c]Use for the design of temporary measures during grading and construction. Impervious area percent for urban areas under development vary considerably. The user will determine the percent impervious. Then using the newly graded area *CN* and Figure 8.7.1*a* or *b*, the composite *CN* can be computed for any degree of development.

[d]For conservation tillage in poor hydrologic condition, 5 percent to 20 percent of the surface is covered with residue (less than 750-lb/acre row crops or 300-lb/acre small grain).

For conservation tillage in good hydrologic condition, more than 20 percent of the surface is covered with residue (greater than 750-lb/acre row crops or 300-lb/acre small grain).

[e]Close-drilled or broadcast.

For noncultivated agricultural land:

Poor hydrologic condition has less than 25 percent ground cover density.

Fair hydrologic condition has between 25 percent and 50 percent ground cover density.

Good hydrologic condition has more than 50 percent ground cover density.

For forest–range:

Poor hydrologic condition has less than 30 percent ground cover density.

Fair hydrologic condition has between 30 percent and 70 percent ground cover density.

Good hydrologic condition has more than 70 percent ground cover density.

*Source:* U.S. Department of Agriculture Soil Conservation Service (1986).

### 8.7.3 Curve Numbers

Table 8.7.3 gives the curve numbers for average watershed conditions, $I_a = 0.2S$, and antecedent moisture condition II. For watersheds consisting of several subcatchments with different *CN*s, the area-averaged composite *CN* can be computed for the entire watershed. This analysis assumes that the impervious areas are directly connected to the watershed drainage system (Figure 8.7.1*a*). If the percent imperviousness is different from the value listed in Table 8.7.3 or if the impervious areas are not directly connected, then Figures 8.7.1*a* or *b*, respectively, can be used. The pervious *CN* used in these figures is equivalent to the open-space *CN* in Table 8.7.3. If the total impervious area is less than 30 percent, Figure 8.7.1*b* is used to obtain a composite *CN*. For natural desert landscaping and newly graded areas, Table 8.7.3 gives only the *CN*s for pervious areas.

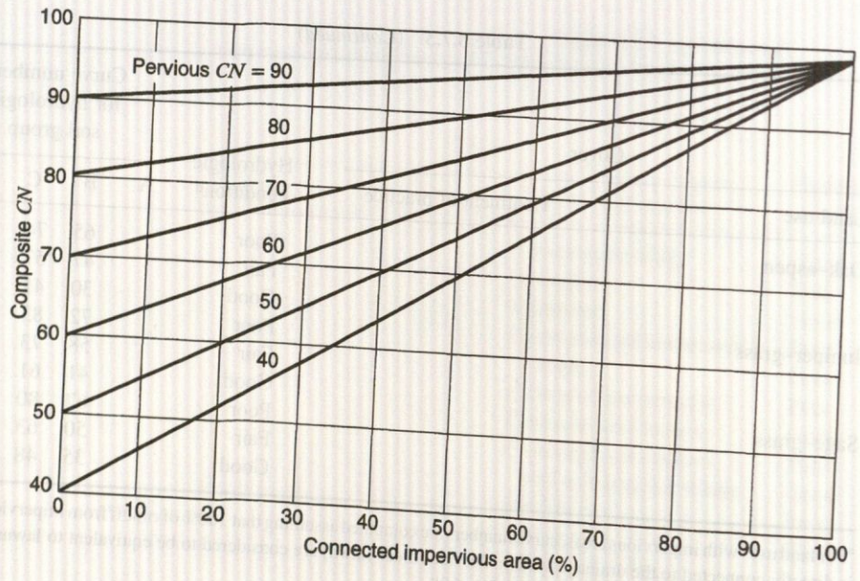


(*a*)

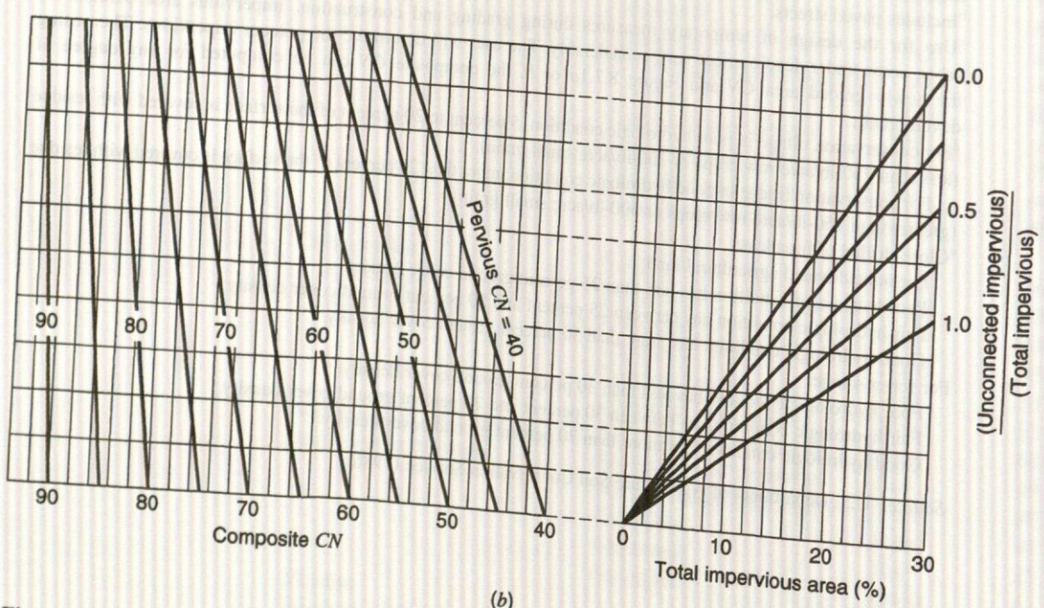


(*b*)

**Figure 8.7.1** Relationships for determining composite *CN*. (*a*) Connected impervious area; (*b*) Unconnected impervious area (from U.S. Department of Agriculture Soil Conservation Service (1986)).

***EXAMPLE 8.7.1*** Determine the weighted curve numbers for a watershed with 40 percent residential (1/4-acre lots), 25 percent open space, good condition, 20 percent commercial and business (85 percent impervious), and 15 percent industrial (72 percent impervious), with corresponding soil groups of C, D, C, and D.

***SOLUTION*** The corresponding curve numbers are obtained from Table 8.7.3:

| Land use (%) | Soil group | Curve number |
|---|---|---|
| 40 | C | 83 |
| 25 | D | 80 |
| 20 | C | 94 |
| 15 | D | 93 |

The weighted curve number is

$$\begin{aligned} CN &= 0.40(83)+0.25(80)+0.20(94)+0.15(93) \\ &= 33.2+20+18.8+13.95 \\ &= 85.95(\text{use } 86) \end{aligned}$$

***EXAMPLE 8.7.2***

The watershed in example 8.7.1 experienced a rainfall of 6 in. What is the runoff volume?

***SOLUTION***

Using equation (8.6.5), $P_e$ = runoff volume is

$$P_e = \frac{(P-0.2S)^2}{P+0.8S}$$

where $S$ is computed with the weighted curve number of 86 from example 8.7.1:

$$S = \frac{1000}{86} - 10 = 1.63$$

So

$$\begin{aligned} P_e &= \frac{[6-0.2(1.63)]^2}{6+0.8(1.63)} = \frac{32.19}{7.3} \\ &= 4.41 \text{ in of runoff} \end{aligned}$$

***EXAMPLE 8.7.3***

For the watershed in examples 8.7.1 and 8.7.2, the 6-in rainfall pattern was 2 in the first hour, 3 in the second hour, and 1 in the third hour. Determine the cumulative rainfall and cumulative rainfall excess as functions of time.

***SOLUTION***

The initial abstractions are computed as $I_a = 0.2S$ with $S = 1.63$ from example 8.7.2, so $I_a = 0.2(1.63) =$ 033 in. The remaining losses for time period (the first hour) are computed using the following equation, derived by combining equations (8.6.1) and (8.6.2):

$$F_{a,t} = \frac{S(P_t - I_a)}{P_t - I_a + S} = \frac{1.63(P_t - 0.33)}{P_t - 0.33 + 1.63} = \frac{1.63(P_t - 0.33)}{P_t + 1.3}$$

$$F_{a,1} = \frac{1.63(2-0.33)}{2+1.3} = 0.82 \text{ in}$$

The total loss for the first hour is 0.33 + 0.82 = 1.15 in, and the excess is

$$P_{e1} = P_1 - I_a - F_{a,1} = 2 - 0.33 - 0.82 = 0.85 \text{ in}$$

For the second hour, $P_t = 2+3 = 5$ in, so

$$F_{a,2} = \frac{1.63(5-0.33)}{5+1.3} = 1.21 \text{ in}$$

and the cumulative rainfall excess is $P_{e_2} = 5 - 0.33 - 1.21 = 3.46$ in.

For the third hour, $P_3 = 2+3+1 = 6$ in, so

$$F_{a,3} = \frac{1.63(6-0.33)}{6+1.3} = 1.27 \text{ in}$$

and $P_{e_3} = 6 - 0.33 - 1.27 = 4.40$ in (which compares well with the results of example 8.7.2).

The results are summarized below, along with the rainfall excess hyetograph.

| Time (h) | Cumulative rainfall $P_t$ (in) | Cumulative abstractions $I_a$ (in) | Cumulative abstractions $F_{a,t}$ (in) | Cumulative rainfall excess $P_e$ (in) | Rainfall excess hyetograph (in) |
|---|---|---|---|---|---|
| 1 | 2 | 0.33 | 0.82 | 0.85 | 0.85 |
| 2 | 5 | 0.33 | 1.21 | 3.46 | 2.61 |
| 3 | 6 | 0.33 | 1.27 | 4.40 | 0.94 |

## 8.8 NRCS (SCS) UNIT HYDROGRAPH PROCEDURE

The SCS dimensionless unit hydrograph and mass curve are shown in Figure 8.8.1 and tabulated in Table 8.8.1. The SCS dimensionless equivalent triangular unit hydrograph is also shown in Figure 8.8.1. The following section discusses how to develop a unit hydrograph from these dimensionless unit hydrographs.

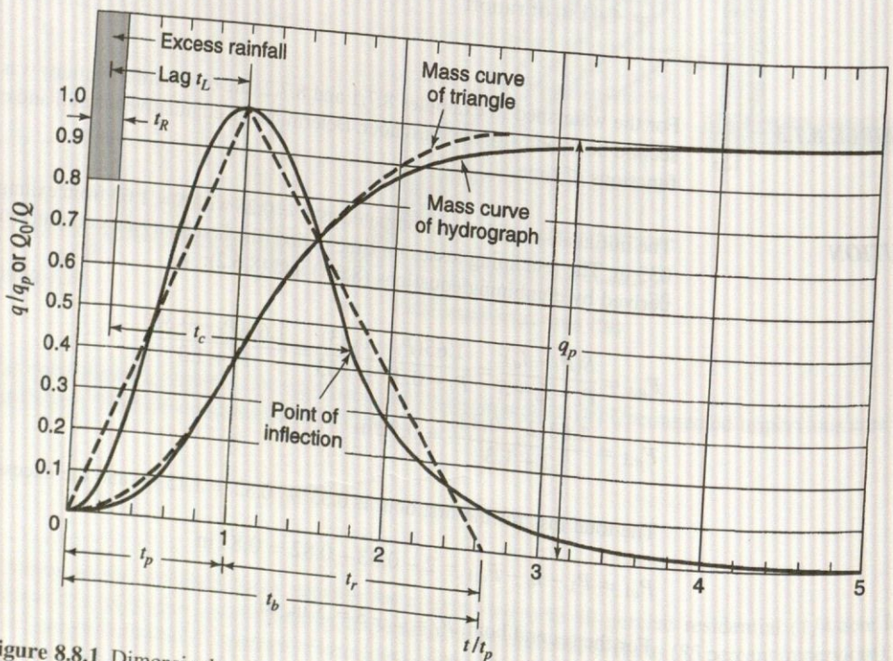


**Figure 8.8.1** Dimensionless curvilinear unit hydrograph and equivalent triangular hydrograph (from U.S. Department of Agriculture Soil Conservation Service (1986)).

### 8.8.1 Time of

**Table 8.8.1** Ratios for Dimensionless Unit Hydrograph and Mass Curve

| Time ratios $t/t_p$ | Discharge ratios $q/q_p$ | Mass curve ratios $Q_a/Q$ |
|---|---|---|
| 0 | 0.000 | 0.000 |
| 0.1 | 0.030 | 0.001 |
| 0.2 | 0.100 | 0.006 |
| 0.3 | 0.190 | 0.012 |
| 0.4 | 0.310 | 0.035 |
| 0.5 | 0.470 | 0.065 |
| 0.6 | 0.660 | 0.107 |
| 0.7 | 0.820 | 0.163 |
| 0.8 | 0.930 | 0.228 |
| 0.9 | 0.990 | 0.300 |
| 1.0 | 1.000 | 0.375 |
| 1.1 | 0.990 | 0.450 |
| 1.2 | 0.930 | 0.522 |
| 1.3 | 0.860 | 0.589 |
| 1.4 | 0.780 | 0.650 |
| 1.5 | 0.680 | 0.700 |
| 1.6 | 0.560 | 0.751 |
| 1.7 | 0.460 | 0.790 |
| 1.8 | 0.390 | 0.822 |
| 1.9 | 0.330 | 0.849 |
| 2.0 | 0.280 | 0.871 |
| 2.2 | 0.207 | 0.908 |
| 2.4 | 0.147 | 0.934 |
| 2.6 | 0.107 | 0.953 |
| 2.8 | 0.077 | 0.967 |
| 3.0 | 0.055 | 0.977 |
| 3.2 | 0.040 | 0.984 |
| 3.4 | 0.029 | 0.989 |
| 3.6 | 0.021 | 0.993 |
| 3.8 | 0.015 | 0.995 |
| 4.0 | 0.011 | 0.997 |
| 4.5 | 0.005 | 0.999 |
| 5.0 | 0.000 | 1.000 |

*Source:* U.S. Department of Agriculture Soil Conservation Service (1972).

### 8.8.1 Time of Concentration

The *time of concentration* for a watershed is the time for a particle of water to travel from the hydrologically most distant point in the watershed to a point of interest, such as the outlet of the watershed. SCS has recommended two methods for time of concentration, the *lag method* and the *upland*, or *velocity method.*

The lag method relates the *time lag* ($t_L$), defined as the time in hours from the center of mass of the rainfall excess to the peak discharge, to the slope ($Y$) in percent, the hydraulic length ($L$) in feet, and the potential maximum retention ($S$), expressed as

$$t_L = \frac{L^{0.8}(S+1)^{0.7}}{1900Y^{0.5}} \tag{8.8.1}$$

The SCS uses the following relationship between the time of concentration ($t_c$) and the lag ($t_L$):

$$t_c = \frac{5}{3} t_L \tag{8.8.2}$$

or

$$t_c = \frac{L^{0.8}(S+1)^{0.7}}{1140Y^{0.5}} \tag{8.8.3}$$

where $t_c$ is in hours. Refer to Figure 8.8.1 to see the SCS definition of $t_c$ and $t_L$.

The velocity (upland) method is based upon defining the time of concentration as the ratio of the hydraulic flow length ($L$) to the velocity ($V$):

$$t_c = \frac{L}{3600V} \tag{8.8.4}$$

where $t_c$ is in hours, $L$ is in feet, and $V$ is in ft/s. The velocity can be estimated knowing the land use and the slope in Figure 8.8.2. Alternatively, we can think of the concentration as being the sum of

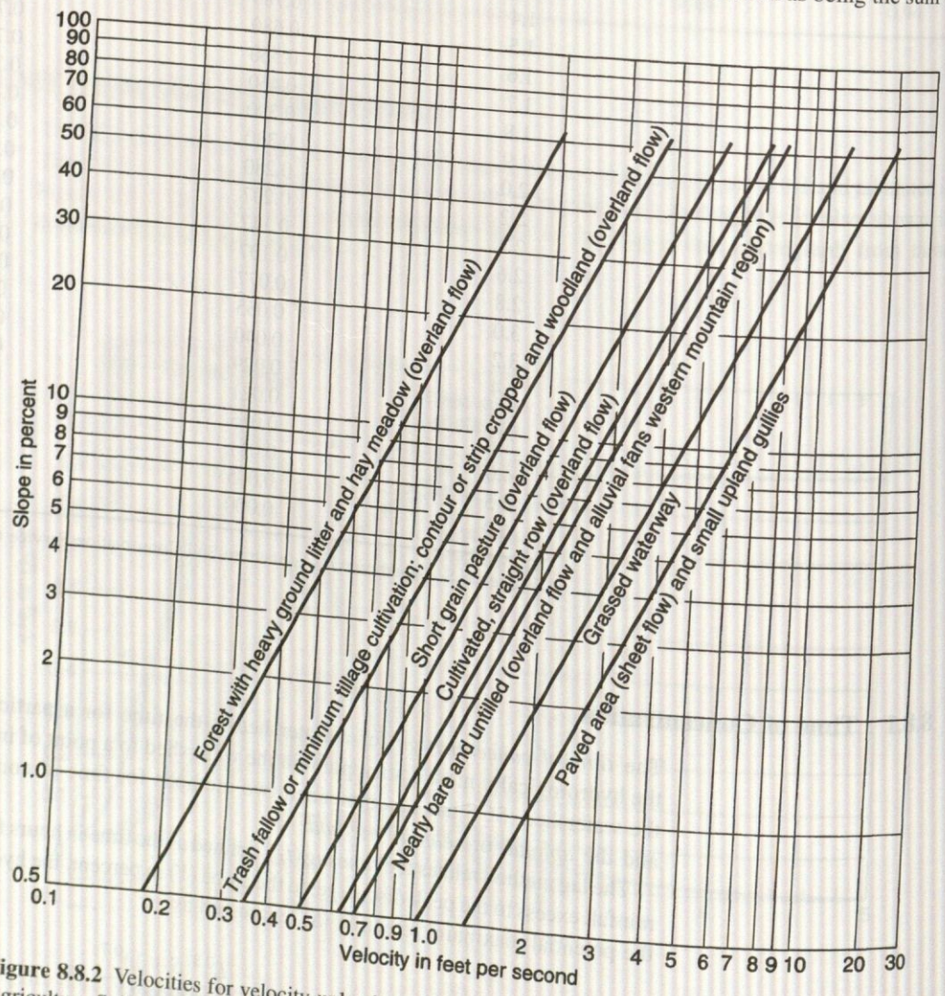


**Figure 8.8.2** Velocities for velocity upland method of estimating $t_c$ (from U.S. Department of Agriculture Soil Conservation Service (1986)).

8.8.2 Time to

8.8.3 Peak Dis

travel times for different segments

$$t_c = \frac{1}{3600}\sum_{i=1}^{k}\frac{L_i}{V_i} \tag{8.8.5}$$

for $k$ segments, each with different land uses.

### 8.8.2 Time to Peak

Time to peak ($t_p$) is the time from the beginning of rainfall to the time of the peak discharge (Figure 8.8.1)

$$t_p = \frac{t_R}{2} + t_L \tag{8.8.6}$$

where $t_p$ is in hours, $t_R$ is the duration of the rainfall excess in hours, and $t_L$ is the lag time in hours. The SCS recommends that $t_R$ be 0.133 of the time of concentration of the watershed, $t_c$:

$$t_R = 0.133t_c \tag{8.8.7}$$

and because $t_L = 0.6t_c$ by equation (8.8.2), then by equation (8.8.6) we get

$$\begin{aligned} t_p &= \frac{0.133t_c}{2} + 0.6t_c \\ t_p &= 0.67t_c \end{aligned} \tag{8.8.8}$$

### 8.8.3 Peak Discharge

The area of the unit hydrograph equals the volume of direct runoff $Q$, which was estimated by equation (8.6.5). With the equivalent triangular dimensionless unit hydrograph of the curvilinear dimensionless unit hydrograph in Figure 8.8.1, the time base of the dimensionless triangular unit hydrograph is 8/3 of the time to peak $t_p$, as compared to $5t_p$ for the curvilinear. The areas under the rising limb of the two dimensionless unit hydrographs are the same (37 percent).

Based upon geometry (Figure 8.8.1), we see that

$$Q = \frac{1}{2}q_p(t_p + t_r) \tag{8.8.9}$$

for the direct runoff $Q$, which is 1 in where $t_r$ is the recession time of the dimensionless triangular unit hydrograph and $q_p$ is the peak discharge. Solving equation (8.8.9) for $q_p$ gives

$$q_p = \frac{Q}{t_p}\left[\frac{2}{1 + t_r/t_p}\right] \tag{8.8.10}$$

Letting $K = \left[\dfrac{2}{1 + t_r/t_p}\right]$, then

$$q_p = \frac{KQ}{t_p} \tag{8.8.11}$$

where $Q$ is the volume, equals to 1 in for a unit hydrograph.

The above equation can be modified to express $q_p$ in $ft^3/sec$, $t_p$ in hours, and $Q$ in inches:

$$q_p = 645.33K\frac{AQ}{t_p} \tag{8.8.12}$$

The factor 645.33 is the rate necessary to discharge 1 in of runoff from 1 $mi^2$ in 1 hr. Using $t_r = 1.67t_p$ gives $K = [2/(1 + 1.67)] = 0.75$; then equation (8.8.12) becomes

$$q_p = \frac{484AQ}{t_p} \tag{8.8.13}$$

For SI units,

$$q_p = \frac{2.08AQ}{t_p} \tag{8.8.14}$$

where $A$ is in square kilometers.

The steps in developing a unit hydrograph are:

Step 1 Compute the time of concentration using the lag method (equation (8.8.3)) or the velocity method (equation (8.8.4) or (8.8.5)).

Step 2 Compute the time to peak $t_p = 0.67t_c$ (equation (8.8.8)) and then the peak discharge $q_p$ using equation (8.8.13) or (8.8.14).

Step 3 Compute time base $t_b$ and the recession time $t_r$:

Triangular hydrograph: $t_b = 2.67t_p$

Curvilinear hydrograph: $t_b = 5t_p$

$t_r = t_b - t_p$

Step 4 Compute the duration $t_R = 0.133\ t_c$ and the lag $t_L = 0.6\ t_c$ by using equations (8.8.7) and (8.8.2), respectively.

Step 5 Compute the unit hydrograph ordinates and plot. For the triangular only $t_p$, $q_p$, and $t_r$ are needed. For the curvilinear, use the dimensionless ratios in Table 8.8.1.

***EXAMPLE 8.8.1***

For the watershed in example 8.7.1, determine the triangular SCS unit hydrograph. The average slope of the watershed is 3 percent and the area is 3.0 $mi^2$. The hydraulic length is 1.2 mi.

***SOLUTION***

Step 1 The time of concentration is computed using equation (8.8.1), with S = 1.63 from example 8.7.2:

$$t_L = \frac{(6336)^{0.8}(1.63+1)^{0.7}}{1900\sqrt{3}} = 0.66 \text{ hr}$$

and $t_c = \frac{5}{3}t_L = 1.1$ hr

Step 2 The time to peak $t_p = 0.67t_c = 0.67(1.1) = 0.74$ hr.

Step 3 The time base is $t_b = 2.67t_p = 1.97$ hr.

Step 4 The duration is $t_R = 0.133t_c = 0.133(1.1) = 0.15$ hr, and $t_L$ is 0.66 hr.

Step 5 The peak is (for $Q = 1$ in)

$$q_p = \frac{484AQ}{t_p} = \frac{484(3)(1)}{0.74} = 1962 \text{ cfs.}$$

In summary, the triangular unit hydrograph has a peak of 1962 cfs at the time to peak of 0.74 hr with a time base of 1.97 hr. This is a 0.15-hr duration unit hydrograph.

## 8.9 KINEMATIC-WAVE OVERLAND FLOW RUNOFF MODEL

*Hortonian overland flow* occurs when the rainfall rate exceeds the infiltration capacity and sufficient water ponds on the surface to overcome surface tension effects and fill small depressions. Overland flow is surface runoff that occurs in the form of sheet flow on the land surface without concentrating

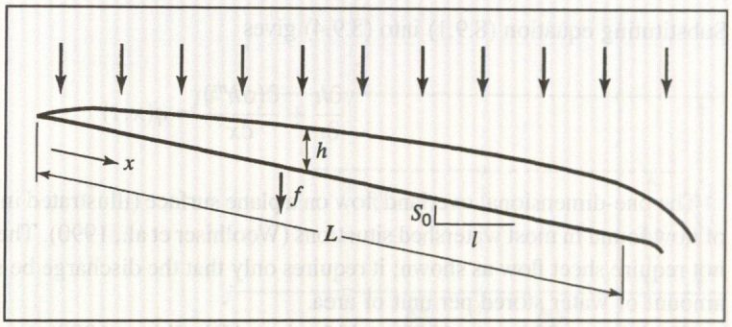


**Figure 8.9.1** Definition sketch of overland flow on a plane as a one-dimensional flow (from Woolhiser et al. (1990)).

in clearly defined channels (Ponce, 1989). For the purposes of rainfall-runoff analysis, this flow can be viewed as a one-dimensional flow process (Figure 8.9.1) in which the flux is proportional to some power of the storage per unit area, expressed as (Woolhiser et al., 1990):

$$Q = \alpha h^m \tag{8.9.1}$$

where $Q$ is the discharge per unit width, $h$ is the storage of water per unit area (or depth if the surface is a plane), and $\alpha$ and $m$ are parameters related to slope, surface roughness, and whether the flow is laminar or turbulent.

The mathematical description of overland flow can be accomplished through the continuity equation in one-dimensional form and a simplified form of the momentum equation. This model is referred to as the *kinematic wave model. Kinematics* refers to the study of motion exclusive of the influence of mass and force. A *wave* is a variation in flow, such as a change in flow rate or water surface elevation. *Wave celerity* is the velocity with which this variation travels. *Kinematic waves* govern flow when inertial and pressure forces are negligible.

The *kinematic wave equations* (also see Chapter 9) for a one-dimensional flow are expressed as follows:

Continuity:

$$\frac{\partial A}{\partial t} + \frac{\partial Q}{\partial x} = q(x,t) \tag{8.9.2}$$

Momentum:

$$S_0 - S_f = 0 \tag{8.9.3}$$

where $A$ is the cross-sectional area of flow, $Q$ is the discharge, $t$ is time, $x$ is the spatial coordinate, $q(x, t)$ is the lateral inflow rate, $S_0$ is the overland flow slope, and $S_f$ is the friction slope.

Equation (8.9.3) indicates that the gravity and friction forces are balanced, so that flow does not accelerate appreciably. The inertial (local and convective acceleration) term and pressure term are neglected in the kinematic wave model (refer to Section 9.4). Eliminating these terms eliminates the mechanism to describe backwater effects and flood wave peak attenuation.

Considering that $h$ is the storage per unit area or depth, then $A = h$, so that equation (8.9.2) becomes

$$\frac{\partial h}{\partial t} + \frac{\partial Q}{\partial x} = q(x,t) \tag{8.9.4}$$

Substituting equation (8.9.1) into (8.9.4) gives

$$\frac{\partial h}{\partial t} + \frac{\partial(\alpha h^m)}{\partial x} = q(x,t) \tag{8.9.5}$$

The one-dimensional overland flow on a plane surface (illustrated in Figure 8.9.1) is not the type of flow found in most watershed situations (Woolhiser et al., 1990). The kinematic assumption does not require sheet flow as shown; it requires only that the discharge be some unique function of the amount of water stored per unit of area.

Woolhiser and Liggett (1967) and Morris and Woolhiser (1980) showed that the kinematic-wave formulation is an excellent approximation for most overland flow conditions. Keep in mind that these equations are a simplification of the Saint-Venant equations (see Chapter 9).

The kinematic-wave equation (8.9.5) for overland flow can be solved numerically using a four-point implicit method where the finite-difference approximations for the spatial and temporal derivatives are, respectively,

$$\frac{\partial h}{\partial x} = \theta\frac{h_{i+1}^{j+1} - h_i^{j+1}}{\Delta x} + (1-\theta)\frac{h_{i+1}^{j} - h_i^{j}}{\Delta x} \tag{8.9.6}$$

and

$$\frac{\partial h}{\partial t} = \frac{1}{2}\left[\frac{h_i^{j+1} - h_i^{j}}{\Delta t} + \frac{h_{i+1}^{j+1} - h_{i+1}^{j}}{\Delta t}\right]$$

or

$$\frac{\partial h}{\partial t} = \frac{h_i^{j+1} + h_{i+1}^{j+1} - h_i^{j} - h_{i+1}^{j}}{2\Delta t} \tag{8.9.7}$$

and

$$q = \frac{1}{2}(\bar{q}_{i+1} + \bar{q}_i) \tag{8.9.8}$$

where $\theta$ is a weighting parameter for spatial derivative, $\theta = \Delta' t/\Delta t$ (see Figure 8.9.2). The derivative $\partial h/\partial t$ is the average of the temporal derivatives at locations $i$ and $i+1$ or for the midway locations between $i$ and $i+1$, and $\bar{q}_i$ and $\bar{q}_{i+1}$ are the average lateral inflows at $i$ and $i+1$, respectively. Notation for the finite-difference grid is shown in Figure 8.9.2. Substituting these finite difference expressions (8.9.6), (8.9.7), and (8.9.8) into (8.9.5) and simplifying results in the following finite-difference equation:

$$\begin{aligned} &h_{i+1}^{j+1} - h_{i+1}^{j} + h_i^{j+1} - h_i^{j} \\ &+ \frac{2\Delta t}{\Delta x}\left\{\theta\left[\alpha_{i+1}^{j+1}(h_{i+1}^{j+1})^m - \alpha_i^{i+1}(h_i^{j+1})^m\right] + (1-\theta)\left[\alpha_{i+1}^{j}(h_{i+1}^{j})^m - \alpha_i^{j}(h_i^{j})^m\right]\right\} \\ &- \Delta t(\bar{q}_{i+1} + \bar{q}_i) = 0 \end{aligned} \tag{8.9.9}$$

The only unknown in the above equation is $h_{i+1}^{j+1}$, which must be solved by using Newton's method (see Appendix A). Using Manning's equation to express equation (8.9.1), $Q = \alpha h^m$, we

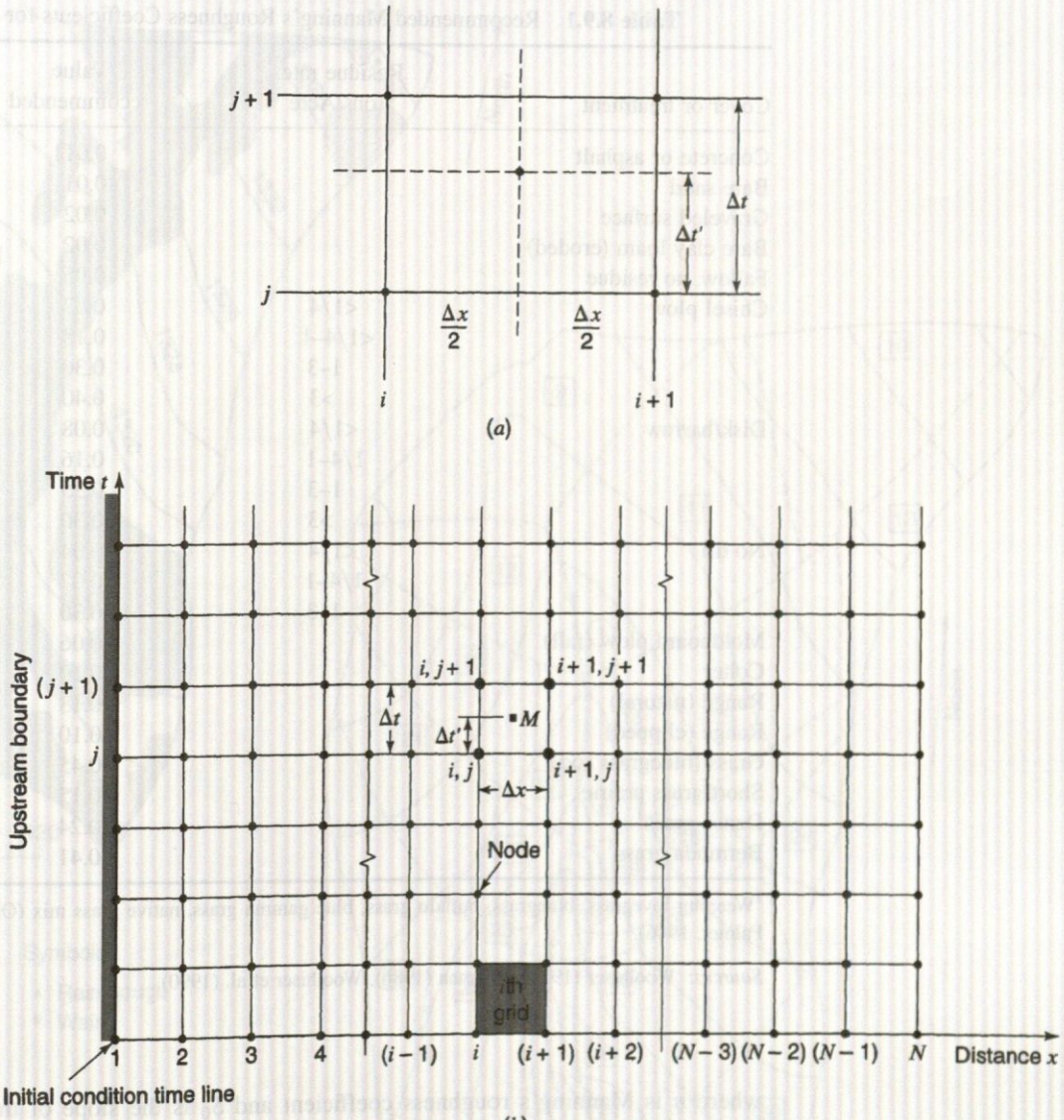


**Figure 8.9.2** The $x$-$t$ solution plane: The finite-difference forms of the Saint-Venant equations are solved at a discrete number of points (values of the independent variables $x$ and $t$) arranged to the time axis represent locations along the plane, and those parallel to the distance axis represent times. (*a*) Four points of finite-difference grid; (*b*) Finite difference grid.

find

$$Q = \left[\frac{1.49S^{1/2}}{n}\right] h^{5/3} \tag{8.9.10}$$

where

$$\alpha = \frac{1.49S_0^{1/2}}{n},\ m = 5/3 \tag{8.9.11}$$

**Table 8.9.1** Recommended Manning's Roughness Coefficients for Overland Flow

| Cover or treatment | Residue rate, Tons/Acre | Value recommended | Range |
|---|---|---|---|
| Concrete or asphalt | | 0.011 | 0.010–0.013 |
| Bare sand | | 0.01 | 0.010–0.016 |
| Graveled surface | | 0.02 | 0.012–0.03 |
| Bare clay loam (eroded) | | 0.02 | 0.012–0.033 |
| Fallow, no residue | | 0.05 | 0.006–0.16 |
| Chisel plow | <1/4 | 0.07 | 0.006–0.17 |
| | <1/4–1 | 0.18 | 0.07–0.34 |
| | 1–3 | 0.30 | 0.19–0.47 |
| | >3 | 0.40 | 0.34–0.46 |
| Disk/harrow | <1/4 | 0.08 | 0.008–0.41 |
| | 1/4–1 | 0.16 | 0.10–0.25 |
| | 1–3 | 0.25 | 0.14–0.53 |
| | >3 | 0.30 | — |
| No till | <1/4 | 0.04 | 0.03–0.07 |
| | 1/4–1 | 0.07 | 0.01–0.13 |
| | 1–3 | 0.30 | 0.16–0.47 |
| Moldboard plow (fall) | | 0.06 | 0.02–0.10 |
| Colter | | 0.10 | 0.05–0.13 |
| Range (natural) | | 0.13 | 0.01–0.32 |
| Range (clipped) | | 0.10 | 0.02–0.24 |
| Grass (bluegrass sod) | | 0.45 | 0.39–0.63 |
| Short grass prairie | | 0.15 | 0.10–0.20 |
| Dense grass[1] | | 0.24 | 0.17–0.30 |
| Bermuda grass[1] | | 0.41 | 0.30–0.48 |

[1]Weeping lovegrass, bluegrass, buffalo grass, blue gamma grass, native grass mix (OK), alfalfa, lespedeza (from Palmer, 1946).

*Sources:* Woolhiser (1975), Engman (1986), Woolhiser et al. (1990).

where $n$ is Manning's roughness coefficient and $S_0$ is the slope of the overland flow plane. Recommended values of Manning's roughness coefficients for overland flow are given in Table 8.9.1. The *time to equilibrium* of a plane of length $L$ and slope $S_0$ can be derived using Manning's equation as

$$t_c = \frac{nL}{1.49 S_0^{1/2} h^{2/3}} \tag{8.9.12}$$

The U.S. Department of Agriculture Agricultural Research Service (Woolhiser et al., 1990) has developed a KINematic runoff and EROSion model referred to as KINEROS. This model is event-oriented, i.e., it is a physically based model describing the processes of interception, infiltration, surface runoff, and erosion from small agricultural and urban watersheds. The model is distributed because flows are modeled for both the watershed and the channel elements, as illustrated in Figures 8.9.3 and 8.9.4. The model is *event-oriented* because it does not have components describing evapotranspiration and soil water movement between storms. In other words, there is no hydrologic balance between storms.

Figures 8.9.3 and 8.9.4 illustrate that the approach to describing a watershed is to divide it into a branching system of channels with plane elements contributing lateral flow to channels. The

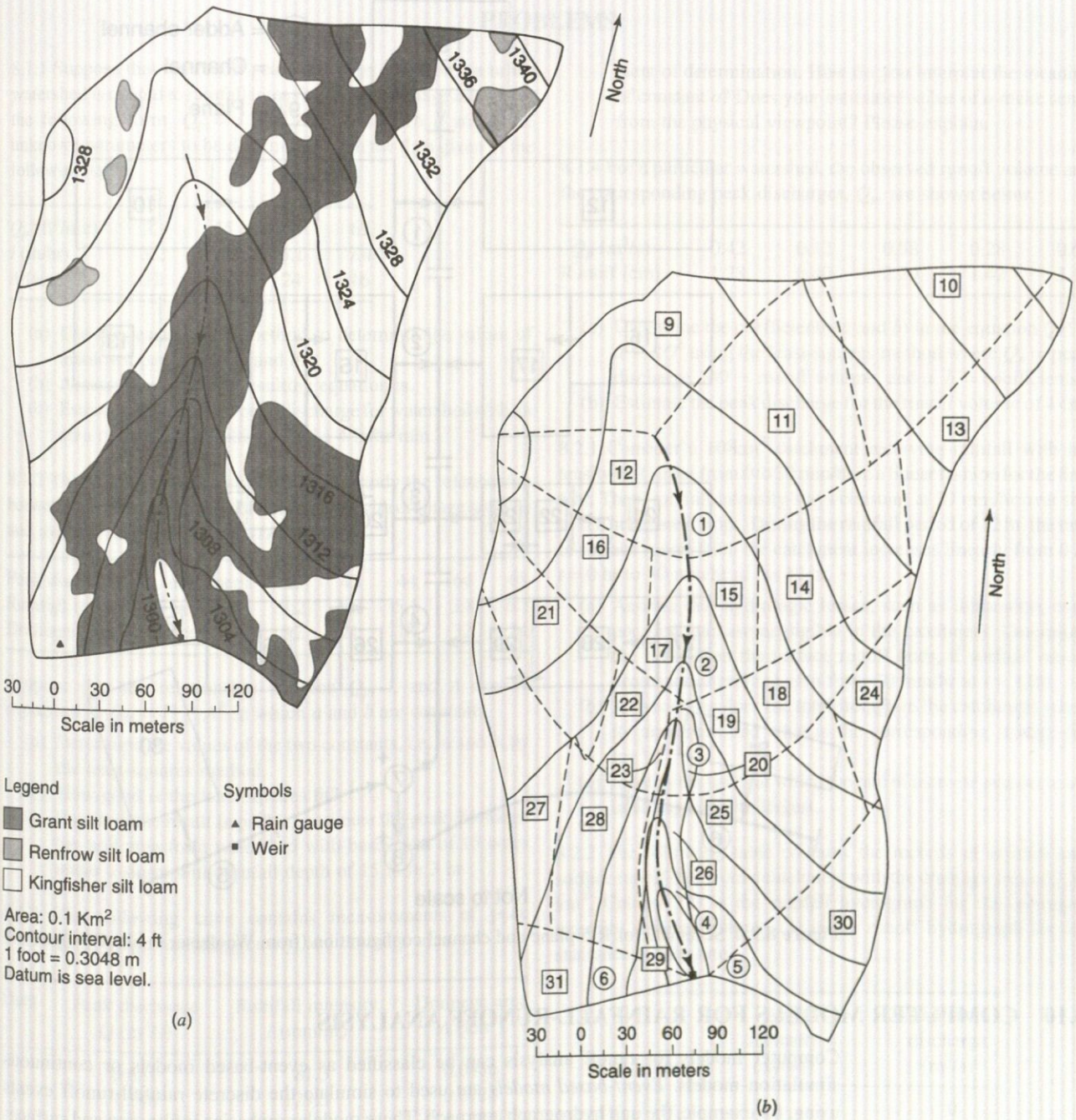


**Figure 8.9.3** R-5 catchment, Chickasha, OK. (*a*) Contour map; (*b*) Division into plane and channel elements (from Woolhiser et al. (1990)).

KINEROS model takes into account interception, infiltration, overland flow routing, channel routing, reservoir routing, erosion, and sediment transport. Overland flow routing has been described in this section. Channel routing is performed using the kinematic-wave approximation described in Chapter 9. The reservoir routing in KINEROS is basically a level-pool routing procedure, as described in Chapter 9.

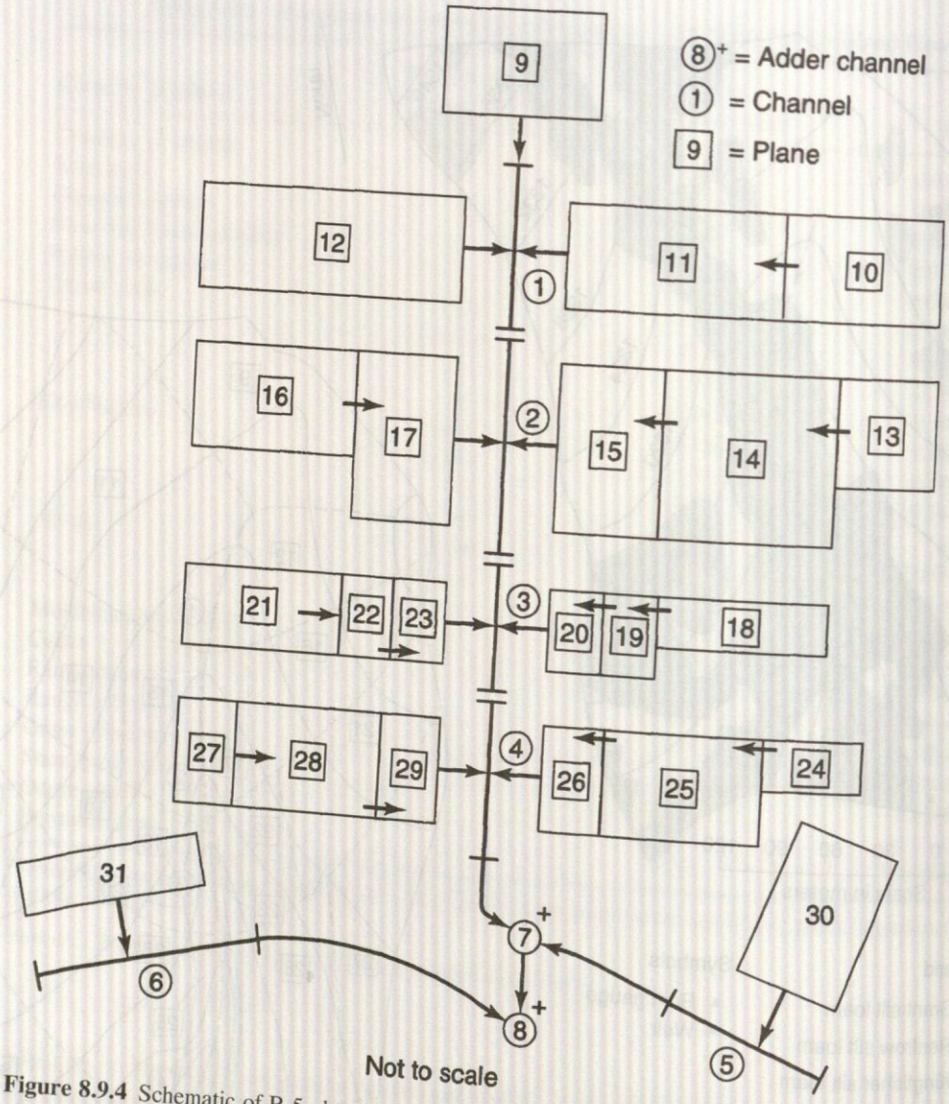


**Figure 8.9.4** Schematic of R-5 plane and channel configuration (from Woolhiser et al. (1990)).

## 8.10 COMPUTER MODELS FOR RAINFALL-RUNOFF ANALYSIS

Computer models for runoff analysis can be classified as event-based models or continuous simulation models. *Event-based models* are used to simulate the discrete rainfall-runoff events using, for example, the unit hydrograph approach. These models emphasize infiltration and surface-runoff components with the objective of determining direct runoff, and are applicable to excess-water flow calculations in cases where direct runoff is the major contributor to streamflow. The HEC-HMS (HEC-1) and the TR-20 and TR-55 models are single-event models. The KINEROS model (Woolhiser et al., 1990) described in the previous section is an overland flow model based on the kinematic-wave routing. This model is a *distributed event-based model*. Other examples include the kinematic-wave model for overland flow routing in the HEC-HMS (HEC-1) model.

*Continuous-simulation models* account for the overall moisture balance of the basin, including moisture accounting between storm events. These models explicitly account for all runoff components including surface flow and indirect runoff such as interflow and baseflow, and are well suited for *long-term runoff forecasting*.

## PROBLEMS

8.1.1 Suppose that the runoff peak discharge ($Q_p$) from an urban watershed is related to rainfall intensity ($I$) and drainage area ($A$) in the following form, $Q_p = a \times I^b \times A^b$, in which $a$ and $b$ are unknown parameters to be determined from the data given in the following table.

| | | | | |
|---|---|---|---|---|
| $Q_p$ (ft$^3$/sec) | 23 | 45 | 68 | 62 |
| $I$ (in/hr) | 3.2 | 4.6 | 6.1 | 7.4 |
| $A$ (acres) | 12 | 21 | 24 | 16 |

(a) Use the least-squares method to determine the values of unknown parameters $a$ and $b$.
(b) Assess how good the resulting equation is.
(c) Estimate the expected peak discharge for watershed with an area of 20 acres resulting from a 4-in/hr rain.

8.1.2 The following data were obtained to study the relationship between peak discharge ($Q_p$) of a watershed with drainage area ($A$) and average rainfall intensity ($I$).

| | | | | | |
|---|---|---|---|---|---|
| Peak discharge ($Q_p$ in ft$^3$/sec) | 23 | 45 | 44 | 64 | 68 |
| Rainfall intensity ($I$ in in/hr) | 3.2 | 4.2 | 5.1 | 3.8 | 6.1 |
| Drainage area ($A$ in acres) | 12 | 21 | 18 | 32 | 24 |

Suppose that the relationship between $Q_p$, $I$, and $A$ can be expressed as $Q_p = I^a \times A^b$ in which $a$ and $b$ are constants.

(a) Determine the values of the two constants, i.e., $a$ and $b$, by the least-squares method.
(b) How good is the least-squares fit?
(c) Based on the result in part (a), estimate the peak discharge per unit area for a watershed with basin area of 15 acres under a storm with rainfall depth of 15 in in 3 hr.

8.1.3 The following table contains measurements of peak discharge, average rainfall intensity, and drainage area.

| Data | Peak discharge $Q$ (m$^3$/s) | Rainfall intensity $I$ (mm/hr) | Drainage area $A$ (km$^2$) |
|---|---|---|---|
| 1 | 0.651 | 81.3 | 0.0486 |
| 2 | 1.246 | 129.5 | 0.0728 |
| 3 | 1.812 | 96.5 | 0.1295 |
| 4 | 1.926 | 154.9 | 0.0971 |

(a) Determine the coefficients $a$ and $b$ in the equation $Q = a \times (I \times A)^b$ using the least-squares method.
(b) Determine the corresponding coefficient of determination and standard error of estimate for part (a).
(c) Physically, when a storm with constant rainfall intensity $I$ continues indefinitely, the term $I \times A$ represents the steady-state peak discharge. Under the steady-state condition, let $b = 1$ in the above equation. Determine the least-squares estimate for the constant $a$ and the corresponding coefficient of determination. How do you interpret the meaning of constant $a$? Does your estimated value of $a$ make sense from the physical viewpoint? Please explain.

8.1.4 For a particular watershed, the observed runoff volume and the corresponding peak discharges, $Q_p$, are shown below.

| | | | | | |
|---|---|---|---|---|---|
| $Q_p$ (m$^3$/s) | 0.42 | 0.12 | 0.58 | 0.28 | 0.66 |
| Runoff (cm) | 1.28 | 0.40 | 2.29 | 1.42 | 3.19 |

(a) Determine the coefficients ($a$ and $b$) in the equation $QP = a \times RO^b$ using the least-squares method where $Q_p$ = peak discharge, $RO$ = runoff volume, and $a$, $b$ = coefficients.
(b) Estimate the peak discharge for the runoff volume of 4 cm.

8.2.1 Consider a 10-km$^2$ catchment receiving rainfall with intensity that varies from 0 to 30 mm/hr in a linear fashion for the first 6 hr. Then, rainfall intensity stays constant at 30 mm/hr over the next 6 hr before it stops. During the rainfall period of 12 hr, the rate of surface runoff from the catchment increases linearly from 0 at $t = 0$ hr to 30 mm/hr at $t = 12$ hr.

(a) Assume that hydrologic losses, such as infiltration, evaporation, etc. are negligible in the catchment. Determine the time when the surface runoff ends, if surface runoff decreases linearly to zero from 30 mm/hr at $t = 12$hr.
(b) At what time does the total storage in the catchment reach its maximum and what is the corresponding storage (in km$^3$)?
(c) Identify the times at which the rate of increase and decrease in storage are the largest.

8.2.2 The following table contains the records of rainfall and surface runoff data from a catchment with the drainage area of 2.25 km$^2$. Column (2) is the rainfall hyetograph for the averaged intensity whereas column (3) is the runoff hydrograph for instantaneous flow rate.

| Time | Avg. intensity (mm/h) | Instantaneous discharge (m$^3$/s) |
|---|---|---|
| 1:00 | | 0 |
| 1:10 | 60 | 12 |
| 1:20 | 150 | 24 |
| 1:30 | 30 | 48 |
| 1:40 | 18 | 30 |
| 1:50 | 60 | 18 |
| 2:00 | 72 | 24 |
| 2:10 | 24 | 30 |
| 2:20 | 12 | 18 |
| 2:30 | | 12 |
| 2:40 | | 6 |
| 2:50 | | 0 |

(a) Determine the rolling-time and clock-time maximum rainfall depth (in mm) for durations of 30 min and 50 min.
(b) Determine the time and the corresponding volume (in $m^3$) when the maximum storage occurs. Assume that the initial storage volume is zero.
(c) Determine the percentage of rainfall volume that becomes the surface runoff.

8.2.3 Based on the table given below showing the hydrograph ordinates at 24-hour intervals, use graph paper to (a) identify the time instant at which the direct runoff ends and (b) determine the recession constant, $k$, in the following equation:

$$Q(t_2) = Q(t_1) \times e^{-k(t_2 - t_1)}$$

in which $t_2 > t_1$ are two time points on the baseflow recession of a hydrograph.

| Time (day) | Flow ($m^3/s$) | Time (day) | Flow ($m^3/s$) |
|---|---|---|---|
| 1 | 6 | 8 | 91 |
| 2 | 970 | 9 | 79 |
| 3 | 707 | 10 | 68 |
| 4 | 400 | 11 | 58 |
| 5 | 254 | 12 | 50 |
| 6 | 162 | 13 | 43 |
| 7 | 121 | 14 | 37 |

8.2.4 The following table contains the records of rainfall and surface runoff data of a particular storm event for a watershed with the drainage area of 8.4 $km^2$.

(a) Determine the maximum rainfall intensity for durations of 30 min, 60 min, and 120 min.
(b) Determine the percentage of total rainfall that is lost from appearing as the surface runoff.
(c) Determine the time period that the storage volume of the water is increasing in the watershed.

| Time of day | Cumulative rainfall (mm) | Instantaneous runoff ($m^3/s$) |
|---|---|---|
| 4:00 | 0 | 0.0 |
| 4:30 | 30 | 0.3 |
| 5:00 | 80 | 4.2 |
| 5:30 | 90 | 11.3 |
| 6:00 | 95 | 13.0 |
| 6:30 | 127 | 34.0 |
| 7:00 | 130 | 45.3 |
| 7:30 | 132 | 21.2 |
| 8:00 | | 9.3 |
| 8:30 | | 4.8 |
| 9:00 | | 2.5 |
| 9:30 | | 1.4 |
| 10:00 | | 0.8 |
| 10:30 | | 0.0 |

8.2.5 The following table contains the records of rainfall and surface runoff data of a storm event for a watershed having the drainage area of 8.0 $km^2$.

(a) Determine the maximum rainfall intensity for durations of 15 min, 30 min, and 60 min.
(b) Determine the percentage of total rainfall that is lost from appearing as the surface runoff.
(c) Determine the time period that the storage volume of the water is increasing in the watershed and the maximum storage volume (in cm).
(d) Determine the $\Phi$ index and the corresponding rainfall excess hyetograph.

| Time | Cumul. rainfall (mm) | Instant. flow rate ($m^3/s$) |
|---|---|---|
| 4:00 | 0 | 0 |
| 4:15 | 15 | 1 |
| 4:30 | 40 | 4 |
| 4:45 | 45 | 11 |
| 5:00 | 48 | 13 |
| 5:15 | 64 | 35 |
| 5:30 | 65 | 45 |
| 5:45 | 66 | 21 |
| 6:00 | 66 | 10 |
| 6:15 | 66 | 5 |
| 6:30 | | 3 |
| 6:45 | | 1 |
| 7:00 | | 0 |

8.2.6 Consider a watershed with drainage area of 1 $km^2$, For a given storm event, the recorded average rainfall intensity and total instantaneous discharge at the outlet of the watershed are listed in the following table. Assume that the baseflow is 1 $m^3/s$ and rainfall amount in the first 30 min is the initial loss.

(a) Determine the total amount of rainfall.
(b) Determine the volume of direct runoff.
(c) Determine the average infiltration *rate*, i.e., $\phi$ index
(d) Determine the rainfall excess *intensity* hyetograph corresponding to the $\phi$ index obtained in (c). Also, what is the duration of rainfall excess hyetograph?

| Time (min) | Intensity (mm/h) | Discharge ($m^3/s$) |
|---|---|---|
| 0 | 10 | 1 |
| 30 | 20 | 1 |
| 60 | 38 | 4 |
| 90 | 26 | 8 |
| 120 | 10 | 6 |
| 150 | 20 | 4 |
| 180 | 24 | 3 |
| 210 | | 1 |

8.2.7 On a particular day in 1990, there was a rainstorm event that produced the following rainfall and runoff on a 36-km$^2$ drainage basin.

| Time (min) | 0 | 15 | 30 | 45 | 60 | 75 | 90 | 105 | 120 |
|---|---|---|---|---|---|---|---|---|---|
| Cumulative rainfall (mm) | 0 | 10 | 50 | 75 | 90 | 100 | | | |
| Instantaneous runoff (m$^3$/s) | 10 | 30 | 160 | 360 | 405 | 305 | 125 | 35 | 10 |

For the above rainstorm event, assume that the baseflow is 10 m$^3$/s.

(a) Find the volume of direct runoff (in mm).
(b) Assuming the initial loss is 10 mm, determine the value of $\phi$ index (in mm/hr) and the corresponding effective rainfall intensity hyetograph (in mm/hr).

8.3.1 Determine the 4-hr unit hydrograph using the following data for a watershed having a drainage area of 200 km$^2$, assuming a constant rainfall abstraction rate and a constant baseflow of 20 m$^3$/s.

| Four-hour period | 1 | 2 | 3 | 4 | 5 | 6 | 7 | 8 | 9 | 10 | 11 |
|---|---|---|---|---|---|---|---|---|---|---|---|
| Rainfall (cm) | 1.0 | 2.5 | 4.0 | 2.0 | | | | | | | |
| Storm flow (m$^3$/s) | 20 | 30 | 60 | 95 | 130 | 170 | 195 | 175 | 70 | 25 | 20 |

8.3.2 Using the unit hydrograph developed in problem 8.3.1, determine the direct runoff from the 200 km$^2$ watershed using the following rainfall excess pattern.

| Four-hour period | 1 | 2 | 3 | 4 |
|---|---|---|---|---|
| Rainfall excess (cm) | 2.0 | 3.0 | 0.0 | 1.5 |

8.3.3 The ordinates at 1-hr intervals of a 1-hr unit hydrograph are 100, 300, 500, 700, 400, 200, and 100 cfs. Determine the direct runoff hydrograph from a 3-hr storm in which 1 in of excess rainfall occurred in the first hour, 2 in the second hour, and 0.5 in the third hour. What is the area of the watershed in mi$^2$?

8.3.4 You are responsible for developing the runoff hydrograph for a watershed that fortunately has gauged information at a very nearby location on the stream. You have obtained information on an actual rainfall-runoff event for this watershed. This information includes the actual rainfall hyetograph and the resulting runoff hydrograph. You have been asked to develop the runoff hydrograph for a design rainfall event. The peak discharge from this new developed storm hydrograph will be used to design a hydraulic structure. You will assume a constant baseflow and a constant rainfall abstraction. Explain the hydrologic analysis procedure that you will use to solve this problem.

8.3.5 Consider a drainage basin with an area of 226.8 km$^2$. From a storm event, the observed cumulative rainfall depth and the corresponding runoff hydrograph are given in the following table. Assume that the baseflow is 10 m$^3$/s.

| Time (hr) | 0 | 3 | 6 | 9 | 12 | 15 | 18 | 21 | 24 | 27 | 30 | 33 | 36 |
|---|---|---|---|---|---|---|---|---|---|---|---|---|---|
| Cumulative rainfall (cm) | 0.0 | 0.5 | 1.5 | 2.5 | 4.5 | 6.5 | 8.0 | 9.5 | | | | | |
| Discharge (m$^3$/s) | 10 | 10 | 30 | 50 | 130 | 175 | 260 | 240 | 220 | 145 | 70 | 40 | 10 |

(a) Determine the value of the $\phi$ index and the corresponding effective rainfall hyetograph.
(b) Set up the system of equations, $Pu = Q$, and solve for the unit hydrograph.

8.3.6 Suppose the 4-hr unit hydrograph for a watershed is

| Time (hr) | 0 | 2 | 4 | 6 | 8 | 10 | 12 |
|---|---|---|---|---|---|---|---|
| UH (m$^3$/s/cm) | 0 | 20 | 50 | 75 | 90 | 40 | 0 |

(a) Determine the 2-hr unit hydrograph.
(b) Suppose that a 10-year design storm has a total effective rainfall of 50 mm and the corresponding hyetograph has a rainfall of 30 mm in the first 2 hr period, no rain in the second period, and 20 mm in the third period. Assuming the baseflow is 10 m$^3$/s, calculate the total runoff hydrograph from this 10-year design storm.

8.3.7 Consider a drainage basin with an area of 151.2 km$^2$. From a storm event, the observed cumulative rainfall depth and the corresponding runoff hydrograph are given in the following table. Assume that the baseflow is 10 m$^3$/s.

| Time (hr) | 0 | 2 | 4 | 6 | 10 | 12 | 14 | 16 | 18 | 20 | 22 | 24 | 26 |
|---|---|---|---|---|---|---|---|---|---|---|---|---|---|
| Cumulative rainfall (cm) | 0.0 | 0.5 | 1.5 | 2.5 | 4.5 | 6.5 | 8.0 | 9.5 | | | | | |
| Instantaneous discharge (m$^3$/s) | 10 | 10 | 30 | 50 | 130 | 175 | 260 | 240 | 220 | 145 | 70 | 40 | 10 |

(a) Determine the value of the $\phi$ index and the corresponding effective rainfall hyetograph.
(b) Set up the system of equations, $Pu = Q$, for deriving the 6-hr unit hydrograph and define the elements in $P$, $u$, and $Q$. Solve for the unit hydrograph.

8.3.8 Suppose the 30-min unit hydrograph for a watershed is

| Time (hr) | 0 | 3 | 6 | 9 | 12 | 15 | 18 | 21 |
|---|---|---|---|---|---|---|---|---|
| UH (m$^3$/s/cm) | 0 | 15 | 45 | 65 | 50 | 25 | 10 | 0 |

(a) Determine the 1-hr unit hydrograph.
(b) A storm has a total depth of 4 cm with an effective rainfall hyetograph of 2 cm in the first 2 hr, 1 cm in the second 2 hr. Assuming the baseflow is 10 m$^3$/s, calculate the total runoff hydrograph from the storm.

8.3.9 The following table lists a 15-min unit hydrograph.

| Time (min) | 0 | 5 | 10 | 15 | 20 | 25 | 30 | 35 | 40 | 45 |
|---|---|---|---|---|---|---|---|---|---|---|
| 15 min UH (m$^3$/s/cm) | 0.0 | 1.5 | 3.5 | 6.0 | 5.5 | 5.0 | 3.0 | 2.0 | 0.5 | 0.0 |

(a) Determine the corresponding area of the drainage basin.
(b) Determine the 10-min unit hydrograph.
(c) Determine the total runoff hydrograph resulting from the following effective rainfall, assuming the base flow is 2 $m^3/s$.

| Time (min) | 0 | 10 | 20 | 30 |
|---|---|---|---|---|
| Cumul. rainfall excess (mm) | 0 | 10 | 30 | 35 |

8.3.10 Consider there are two rain gauges (A and B) in a watershed with an area of 21.6 $km^2$. The cumulative rainfall depths over time for a particular storm event at both rain gauge stations are given in the table below. The storm also produces a runoff hydrograph at the outlet of the watershed, shown in the last row of the table. Assume that the baseflow is 10 $m^3/s$. It is known, by the Thiessen polygon, that the contributing areas for the rain gauges are identical.

| Time (hr) | 0 | 1 | 2 | 3 | 4 | 5 | 6 | 7 | 8 | 9 | 10 |
|---|---|---|---|---|---|---|---|---|---|---|---|
| Cumul. Rainfall at Station A (mm) | 0 | 25 | 80 | 105 | 100 | 140 | 180 | 230 | 230 | | |
| Cumul. rainfall at Station B (mm) | 0 | 15 | 40 | 85 | 130 | 180 | 210 | 230 | 230 | | |
| Instantaneous discharge ($m^3/s$) | 10 | 10 | 30 | 60 | 30 | 40 | 80 | 40 | 30 | 10 | 10 |

(a) Determine the basin-wide representative rainfall hyetograph (in mm/hr) for the storm event. Furthermore, determine the value of $\phi$ index (in mm/hr) and the corresponding effective rainfall hyetograph (in mm/hr).
(b) Set up the system of equations $Pu = Q$.
(c) Solve part (b) *by the least-squares method* for the unit hydrograph. What is the duration of the unit hydrograph obtained?

8.3.11 Consider a drainage basin with an area of 167.95 $km^2$. From a storm event, the observed cumulative rainfall depth and the corresponding runoff hydrograph are given in the following table. Assume that the baseflow is 10 $m^3/s$.

| Time (hr) | 0 | 2 | 4 | 6 | 8 | 10 | 12 | 14 | 16 | 18 | 20 | 22 | 24 |
|---|---|---|---|---|---|---|---|---|---|---|---|---|---|
| Cumulative rainfall (cm) | 0.0 | 0.5 | 1.5 | 2.5 | 4.5 | 6.5 | 8.0 | 9.5 | | | | | |
| Instantaneous discharge ($m^3/s$) | 10 | 10 | 30 | 50 | 130 | 175 | 260 | 240 | 220 | 145 | 70 | 40 | 10 |

(a) Determine the value of the $\phi$ index and the corresponding effective rainfall hyetograph.
(b) Set up the system of equations, $Pu = Q$, for deriving the 4-hr unit hydrograph and define the elements in $P$, $u$, and $Q$.
(c) Solve for the unit hydrograph ordinates.

8.3.12 Consider a drainage basin with an area of 216 $km^2$. From a storm event, the observed cumulative rainfall depth and the corresponding runoff hydrograph are given in the following table. Assume that the baseflow is 20 $m^3/s$.

| Time (hr) | 0 | 6 | 12 | 18 | 24 | 30 |
|---|---|---|---|---|---|---|
| Cumulative rainfall (cm) | 0.0 | 1.5 | 4.5 | 9.5 | | |
| Discharge ($m^3/s$) | 20 | 50 | 160 | 340 | 180 | 20 |

(a) Determine the value of the $\phi$ index and the corresponding effective rainfall hyetograph.
(b) Determine the 6-hr unit hydrograph by the least-squares method.

8.3.13 On a particular date, the measured rainfall and runoff from a drainage basin of 54 ha ($54 \times 10^4$ $m^2$) are listed in the table below.

(a) Assuming that the base flow is 2 $m^3/s$, determine the effective rainfall hyetograph by the $\phi$ index method.
(b) Based on the effective rainfall hyetograph and direct runoff hydrograph obtained in Part (a), use the least-squares method to determine the 15-min unit hydrograph.

| Time (min) | 0 | 15 | 30 | 45 | 60 | 75 |
|---|---|---|---|---|---|---|
| Cumul. rain (mm) | 0 | 5 | 20 | 40 | 50 | |
| Instant. flow ($m^3/s$) | 2 | 6 | 10 | 7 | 3 | 2 |

8.3.14 You have been given information on an actual rainfall-runoff event and asked to develop the runoff hydrograph for another storm hydrograph for the watershed. The following is known:

| Time (hr) | Rainfall (in) | Discharge (cfs) |
|---|---|---|
| 0 | | 10 |
| 1 | 1.1 | 20 |
| 2 | 2.1 | 130 |
| 3 | 0 | 410 |
| 4 | 1.1 | 570 |
| 5 | | 510 |
| 6 | | 460 |
| 7 | | 260 |
| 8 | | 110 |
| 9 | | 60 |
| 10 | | 10 |

A constant base flow of 10 cfs and a uniform rainfall loss of 0.1 in/hr are applicable. Determine the size of the drainage basin. Then determine the direct runoff hydrograph for a 2.0-in excess precipitation for the first hour, no rainfall for the second hour, followed by a 2.0-in excess precipitation for the third hour.

8.4.1 A watershed has a drainage area of 14 $km^2$; the length of the main stream is 7.16 km, and the main channel length from the watershed outlet to the point opposite the center of gravity of the watershed is 3.22 km. Use $C_t = 2.0$ and $C_p = 0.625$ to determine the standard synthetic unit hydrograph for the watershed. What is the standard duration? Use Snyder's method to determine the 30-min unit hydrograph for the watershed.

8.4.2 Watershed A has a 2-hr unit hydrograph with $Q_{pR} = 276$ $m^3/s$, $t_{pR} = 6$ hr, $W_{50} = 4.0$ hr, and $W_{75} = 2$ hr. The watershed area = 259 $km^2$, $L_c = 16.1$ km, and $L = 38.6$ km. Watershed B is assumed to be hydrologically similar with an area of 181 $km^2$, $L = 25.1$ km, and $L_c = 15.1$ km. Determine the 1-hr synthetic unit hydrograph for watershed B. Determine the direct runoff hydrograph for a 2-hr storm that has 1.5 cm of excess rainfall the first hour and 2.5 cm of excess rainfall the second hour.

8.4.3 A watershed has an area of 39.3 $mi^2$ and a main channel length of 18.1 mi, and the main channel length from the watershed outlet to the point opposite the centroid of the watershed is 6.0 mi. The regional parameters are $C_t = 2.0$ and $C_p = 0.6$. Compute the $T_P$, $Q_P$,$W_{50}$, $W_{75}$, and $T_B$ for Snyder's standard synthetic unit hydrograph and the same information for a 3-hr Snyder's synthetic unit hydrograph. Also, what is the duration of the standard synthetic unit hydrograph?

8.4.4 Compute the 3-hr Snyder's synthetic unit hydrograph for the watershed in problem 8.4.3.

8.4.5 You are performing a hydrologic study (rainfall-runoff analysis) for a watershed Z. Unfortunately, there is no gauged data or other hydrologic studies so you do not have a unit hydrograph. However, you do have data for another nearby watershed, known as watershed X, which has gauged information (including the discharge hydrograph for a known rainfall event). What procedure would you use to develop a design runoff hydrograph for a design storm for watershed Z? What are you assuming about the watersheds in this procedure?

8.4.6 You have determined the following from the basin map of a given watershed: $L = 100$ km, $L_c = 50$ km, and drainage area = 2000 $km^2$. From the unit hydrograph developed for the watershed, the following were determined: $t_R = 6$ hr, $t_{pR} = 15$ hr, and the peak discharge = 80 $km^3/s/cm$. Determine the regional parameters used in the Snyder's synthetic unit hydrograph procedure.

8.4.7 Derive a 3-hr unit hydrograph by the Snyder method for a watershed of 54 $km^2$ area. It has a main stream that is 10-km long. The distance measured from the watershed outlet to a point on the stream nearest to the centroid of the watershed is 3.75 km. Take $C_t = 2.0$ and $C_p = 0.65$. Sketch the 3-hr unit hydrograph for the watershed.

8.4.8 Derive a 2-hr unit hydrograph by the Snyder method for a watershed of 50 $km^2$ area. It has a main stream that is 8 km long. The distance measured from the watershed outlet to a point on the stream nearest to the centroid of the watershed is 4 km. Take $C_t = 2.0$ and $C_p = 0.65$. Graph the 2-hr unit hydrograph for the watershed.

8.4.9 Use the Clark unit hydrograph procedure to compute the 1-hr unit hydrograph for a watershed that has an area of 5.0 $km^2$ and a time of concentration of 5.5 hr. The Clark storage coefficient is estimated to be 2.5 hr. Use a 1-hr time interval for the computations. Use the HEC U.S. Army Corps of Engineer synthetic time-area relationship.

8.4.10 Compute the Clark unit hydrograph parameters ($T_c$ and $R$) for a 2.17-$mi^2$ (1389 acre) urban watershed in Phoenix, Arizona that has a flow path of 1.85 mi, a slope of 30.5 ft/mi, and an imperviousness of 21 percent. A rainfall intensity of 2.56 in/hr is to be used. The time of concentration for the watershed is computed using $T_c = 11.4L^{0.50} K_b^{0.52} S^{-0.31} i^{-0.38}$, where $T_c$ is the time of concentration in hours, $L$ is the length of the longest flow path in miles, $K_b$ is a watershed resistance coefficient ($K_b = -0.00625 \log A + 0.04$) for commercial and residential areas, $A$ is the watershed area in acres, $S$ is the slope of the flow path in ft/mi, and $i$ is the rainfall intensity in in/hr. The storage coefficient is $R = 0.37T_c^{1.11} A^{-0.57} L^{0.80}$, where $A$ is the area in $mi^2$.

8.4.11 Compute the 15-min Clark unit hydrograph for the Phoenix watershed in problem 8.4.10.

8.4.12 For the situation in problem 8.4.10, compute the time of concentration. However, now the rainfall intensity is not given, instead use the rainfall intensity duration frequency relation in Figure 7.2.15, with a 25-year return period.

8.4.13 Develop the 15-min Clark unit hydrograph for a 2.17-$mi^2$ (1389 acre) rural watershed that has a flow path of 1.85 mi, a slope of 30.5 ft/mi, and an imperviousness of 21 percent. A rainfall intensity of 2.56 in/hr is to be used. The time of concentration for the watershed is computed using $T_c = 11.4L^{0.50} K_b^{0.52} S^{-0.31} i^{-0.38}$, where $T_c$ is the time of concentration in hours, $L$ is the length of the longest flow path in miles, $K_b$ is a watershed resistance coefficient ($K_b = -0.01375 \log A + 0.08$), $A$ is the watershed area in acres, and $S$ is the slope of the flow path in ft/mi, and $i$ is the rainfall intensity in in/hr.

8.5.1 Using the 4-hr unit hydrograph developed in problem 8.3.1, use the S-curve method to develop the 8-hr unit hydrograph for this 200 $km^2$ watershed.

8.5.2 Using the one-hour unit hydrograph given in problem 8.3.3, develop the 3-hr unit hydrograph using the S-curve method.

8.5.3 Suppose the 4-hr unit hydrograph for a watershed is

| Time (hr) | 0 | 2 | 4 | 6 | 8 | 10 | 12 | 14 |
|---|---|---|---|---|---|---|---|---|
| UH ($m^3/s$/10 mm) | 0 | 15 | 45 | 65 | 50 | 25 | 10 | 0 |

(a) Determine the 2-hr unit hydrograph.
(b) From the frequency analysis, the 10-year 4-hr storm has a total depth of 3 cm with an effective rainfall intensity of 1 cm/hr in the first 2 hr and 0.5 cm/hr in the second 2 hr. Assuming the baseflow is 10 $m^3/s$, calculate the total runoff hydrograph from the 10-year 4-hr storm.

8.5.4 Suppose the 4-hr unit hydrograph for the watershed is

| Time (hr) | 0 | 2 | 4 | 6 | 8 | 10 | 12 | 14 | 16 |
|---|---|---|---|---|---|---|---|---|---|
| UH ($m^3/s$/cm) | 0 | 19 | 38 | 32 | 22 | 13 | 6 | 2 | 0 |

(a) What is the area of the watershed?
(b) Determine the 2-hr unit hydrograph.
(c) Suppose that a 25-year design storm has a total effective rainfall of 7 cm and the corresponding hyetograph has 5 cm in the first 2 hr and 2 cm in the second 2 hr. Assuming the baseflow is 10 $m^3/s$, calculate the total runoff hydrograph from this 25-year design storm.

8.5.5 Suppose the 6-hr unit hydrograph for the watershed is

| Time (hr) | 0 | 3 | 6 | 9 | 12 | 15 | 18 | 21 |
|---|---|---|---|---|---|---|---|---|
| UH ($m^3/s$/cm) | 0 | 15 | 45 | 65 | 50 | 25 | 10 | 0 |

(a) What is the area of the watershed?
(b) Determine the 3-hr unit hydrograph.
(c) Suppose that a 10-year design storm has a total effective rainfall of 6 cm and the corresponding hyetograph has 4 cm in the first 3 hr and 2 cm in the second 3 hr. Assuming the baseflow is 10 $m^3/s$, calculate the total runoff hydrograph from this 10-year design storm.

8.5.6 Suppose the 6-hr unit hydrograph for a watershed is

| Time (hr) | 0 | 3 | 6 | 9 | 12 | 15 | 18 |
|---|---|---|---|---|---|---|---|
| UH ($m^3/s/cm$) | 0 | 60 | 90 | 50 | 30 | 10 | 0 |

(a) Determine the 3-hr unit hydrograph.
(b) Suppose that a 50-year design storm has a total effective rainfall of 9 cm and the corresponding hyetograph has 2 cm in the first 3 hr, 5 cm in the second 3 hr, and 2 cm in the third 3 hr. Assuming the baseflow is 20 $m^3/s$, determine the total runoff hydrograph from this 50-year design storm.

8.5.7 Suppose the 6-hr unit hydrograph for a watershed is

| Time (hr) | 0 | 3 | 6 | 9 | 12 | 15 | 18 | 21 |
|---|---|---|---|---|---|---|---|---|
| UH ($m^3/s/cm$) | 0 | 15 | 45 | 65 | 50 | 25 | 10 | 0 |

(a) Determine the 2-hr unit hydrograph.
(b) Assuming the baseflow is 10 $m^3/s$, calculate the total runoff hydrograph from an effective rainfall hyetograph of 2 cm in the first 2 hr and 1 cm in the second 2 hr.

8.7.1 Determine the weighted curve numbers for a watershed with 60 percent residential (1/4-acre lots), 20 percent open space, good condition, and 20 percent commercial and business (85 percent impervious) with corresponding soil groups of C, D, and C.

8.7.2 Rework example 8.7.1 with corresponding soil groups of B, C, D, and B.

8.7.3 The watershed in problem 8.7.1 experienced a rainfall of 5 in; what is the runoff volume per unit area?

8.7.4 Rework example 8.7.2 with a 7-in rainfall.

8.7.5 Calculate the cumulative abstractions and the excess rainfall hyetograph for the situation in problems 8.7.1 and 8.7.3. The rainfall pattern is 1.5 in during the first hour, 2.5 in during the second hour, and 1.0 in during the third hour.

8.7.6 Calculate the cumulative abstraction and the excess rainfall hyetograph for the situation in problems 8.7.2 and 8.7.4. The rainfall pattern is 2.0 in during the first hour, 3.0 in during the second hour, and 2.0 in during the third hour.

8.7.7 Consider an urban drainage basin having 60 percent soil group B and 40 percent soil group C. The land use pattern is 1/2 commercial area and 1/2 industrial district. Determine the rainfall excess *intensity* hyetograph under the dry antecedent moisture condition (AMC I) from the recorded storm given in problem 8.2.6.

8.7.8 Consider a drainage basin having 60 percent soil group B and 40 percent soil group C. Five years ago, the watershed land use pattern was 1/2 wooded area with good cover and 1/2 pasture with good condition. Now, the land use has been changed to 1/3 wooded area, 1/3 pasture land, and 1/3 residential area (1/4-acre lot). Estimate the volume of increased runoff due to the land use change over the past 5-year period for a storm with 6 in of rainfall under the dry antecedent moisture condition (AMC I).

8.7.9 Refer to problem 8.7.8 for the present watershed land use pattern. Determine the effective rainfall hyetograph for the following storm event using the SCS method under the dry antecedent moisture condition (AMC I). Next determine the value of the $\phi$ index corresponding to the effective rainfall hyetograph.

| Time (h) | 0–0.5 | 0.5–1.0 | 1.0–1.5 | 1.5–2.0 |
|---|---|---|---|---|
| Rainfall intensity (in/h) | 6.0 | 3.0 | 2.0 | 1.0 |

8.7.10 Consider a drainage basin having 60 percent soil group A and 40 percent soil group B. Five years ago, the land use pattern in the basin was 1/2 wooded area with poor cover and 1/2 cultivated land with good conservation treatment. Now, the land use has been changed to 1/3 wooded area, 1/3 cultivated land, and 1/3 commercial and business area. Estimate the increased runoff volume during the dormant season due to the land use change over the past 5-year period for a storm of 350 mm in total depth. This storm depth corresponds to a duration of 6-hr and 100-year return period. The total 5-day antecedent rainfall amount is 30 mm. Note: 1 inch = 25.4 mm.

8.7.11 Consider a drainage basin of 500-ha having hydrologic soil group D. In 1970, the watershed land use pattern was 50% wooded area with good cover, 25% range land with good condition, and 25% residential area (1/4-acre lot). Ten years later, the land use has been changed to 30% wooded area, 20% pasture land, 40% residential area (1/4-acre lot), and 10% commercial and business area.

(a) Compute the weighted curve numbers in 1970 and 1980.
(b) Using the SCS method, estimate the percentage of change (increase or decrease) in runoff volume with respect to year 1970 due to the land use change over the 10-year period for a 2-hr, 50-mm rainfall event under the wet antecedent moisture condition.
(c) Suppose that the 2-hr, 50-mm rainfall event has the following hyetograph. Determine the rainfall excess intensity hyetograph (in mm/hr) and the corresponding incremental infiltration (in mm) over the storm duration under 1980 conditions.

| Time (hr) | 0–0.5 | 0.5–1.0 | 1.0–1.5 | 1.5–2.0 |
|---|---|---|---|---|
| Rainfall intensity (mm/hr) | 4.0 | 50.0 | 30.0 | 16.0 |

8.7.12 Consider a drainage basin of 36 $km^2$ having hydrologic soil group B. In 1970, the watershed land use pattern was 60 percent wooded area with good cover, 25 percent range land with good condition, and 15 percent residential area (1/4-acre lot). Twenty years later (i.e., in 1990), the land use has been changed to 30 percent wooded area with good cover, 20 percent pasture land with good condition, 40 percent residential area (1/4-acre lot), and 10 percent commercial and business area.

On a particular day in 1990, there was a rainstorm event that produced rainfall and runoff recorded in the following table.

| Time (min) | 0 | 15 | 30 | 45 | 60 | 75 | 90 | 105 | 120 |
|---|---|---|---|---|---|---|---|---|---|
| Cumulative rainfall (mm) | 0 | 10 | 50 | 75 | 90 | 100 | | | |
| Instantaneous runoff ($m^3/s$) | 10 | 30 | 160 | 360 | 405 | 305 | 125 | 35 | 10 |

(a) Using the SCS method, estimate the percentage of change (increase or decrease) in runoff volume in 1990 with respect to that of 1970 for the above rainstorm event under the normal antecedent moisture condition.
(b) Under the wet antecedent moisture condition, determine the rainfall excess intensity hyetograph (in mm/hr) and the corresponding incremental infiltration (in mm) over the storm duration for the above rainstorm event under the 1990 conditions.
(c) For a baseflow of 10 $m^3/s$, determine the volume of direct runoff.
(d) Assuming an initial loss of 10 mm, determine the $\Phi$ index (in mm/hr) and the corresponding excess rainfall hyetograph.

8.7.13 Consider a drainage basin with an area of 200 $km^2$. From a storm event, the observed cumulative rainfall depth and the corresponding runoff hydrograph are given in the following table. Assume that the baseflow is 20 $m^3/s$.

| Time (hr) | 0 | 4 | 8 | 12 | 16 | 20 |
|---|---|---|---|---|---|---|
| Cum. rainfall (cm) | 0.0 | 1.6 | 5.5 | 7.5 | 7.5 | 7.5 |
| Discharge ($m^3/s$) | 20 | 40 | 130 | 300 | 155 | 20 |

(a) Determine the effective rainfall hyetograph by the SCS method with a curve number $CN = 85$.
(b) Determine the 4-hr unit hydrograph by the least-squares method.

8.7.14 During a rain storm event, rain gauge at location X broke down and rainfall record was not available. Fortunately, three rain gauges nearby did not have a technical problem and their rainfall readings, along with other information, are provided in the table below.

| Rain gauge | A | B | C | X |
|---|---|---|---|---|
| Event depth (mm) | 40 | 60 | 50 | Missing |
| Distance to gauge X (km) | 10 | 8 | 12 | 0 |
| Elevation (m) | 20 | 50 | 40 | 60 |
| Mean annual rainfall (mm) | 1500 | 2000 | 1800 | 2200 |
| Polygon area ($km^2$) | 10 | 30 | 20 | 40 |

The four rain gauges are located either within or in the neighborhood of a watershed having a drainage area of 100 $km^2$. According to the Thiessen polygon method, the contributing area of each rain gauge is shown in the above table.

For this particular storm event, the duration of the storm is 3 hr and the percentage of rainfall depth in the first hour is 50 percent, in the second hour 30 percent, and in the third hour 20 percent. The watershed largely consists of woods and meadow of good hydrologic condition with soil group B. Among the two land cover types, woods occupy 60 percent of the total area while the meadow makes up the remaining 40 percent.

For this watershed, the 1-hr unit hydrograph resulting from 1 cm of effective rainfall has been derived and is given below:

| Time (hr) | 0 | 1 | 2 | 3 | 4 | 5 |
|---|---|---|---|---|---|---|
| Flow rate ($m^3/s/cm$) | 0 | 10 | 30 | 20 | 10 | 0 |

(a) Select a method to estimate missing rainfall depth at station X by an appropriate method. Explain the reasons why the method is selected.
(b) Determine the basin-wide equivalent uniform rainfall depth and the corresponding hyetograph for this particular storm.
(c) According to part (b), determine the total effective rainfall depth and the corresponding rainfall excess hyetograph for the storm. It is known that a storm occurred 2 days before this particular storm and, therefore, the ground is quite wet.
(d) What is the magnitude of peak runoff discharge produced by this particular storm? It is reasonable to assume that the baseflow is 5 $m^3/s$.

8.7.15 Consider a drainage basin having 60 percent soil group A and 40 percent soil group B. Five years ago, the land use pattern in the basin was 1/2 wooded area with poor cover and 1/2 cultivated land with good conservation treatment. Now the land use has been changed to 1/3 wooded area, 1/3 cultivated land, and 1/3 commercial and business area.

(a) Estimate the increased runoff volume during the dormant season due to the land use change over the past 5-year period for a storm of 35 cm total depth under the dry antecedent moisture condition (AMC I). This storm depth corresponds to a duration of 6-hr and 100-year return period. The total 5-day antecedent rainfall amount is 30 mm. (Note: 1 in = 25.4 mm.)
(b) Under the present watershed land use pattern, find the effective rainfall hyetograph (in cm/hr) for the following storm event using SCS method under the dry antecedent moisture condition (AMC I).

| Time (hr) | 0–0.5 | 0.5–1.0 | 1.0–1.5 | 1.5–2.0 |
|---|---|---|---|---|
| Avg. rainfall intensity (cm/hr) | 16.0 | 9.0 | 5.0 | 3.0 |

8.7.16 Consider a drainage basin having 60 percent soil group B and 40 percent soil group C. Five years ago, the watershed land use pattern was 1/2 wooded area with good cover and 1/2 pasture with good condition. Today, the wooded area and pasture each have been reduced down to 1/3 and the remaining 1/3 of the drainage basin has become a residential area (1/4-acre lot). Consider the rainstorm event having the observed rainfall mass data given below.

| Time (min) | 0 | 30 | 60 | 90 | 120 |
|---|---|---|---|---|---|
| Cumulative Rainfall (mm) | 0 | 152 | 228 | 278 | 304 |

(a) Estimate the increased total runoff volume due to the land use change over the past 5-year period for the above rainstorm event under the dry antecedent moisture condition (AMC I).
(b) Referring to the present watershed land use condition, find the effective rainfall hyetograph (in mm/hr) for the rainstorm event given the above using the SCS method under the dry antecedent moisture condition (AMC I).

8.7.17 Consider a drainage basin of 1,200 hectares having 60 percent soil group B and 40 percent soil group C. Five years ago, the watershed land use pattern was 1/2 wooded area with good cover and 1/2 pasture with good condition. Now the land use has been changed to 1/3 wooded area, 1/3 pasture land, and 1/3 residential area (1/4-acre lot). For a storm event, the cumulative rainfall and the corresponding runoff hydrograph are shown in the following table and figure, respectively. (Note: 1 hectare = 10,000 $m^2$; 1 in = 25.4 mm).

| Time (hr) | 0 | 1 | 2 | 3 | 4 |
|---|---|---|---|---|---|
| Cumulative rainfall (mm) | 0 | 60 | 120 | 160 | 180 |

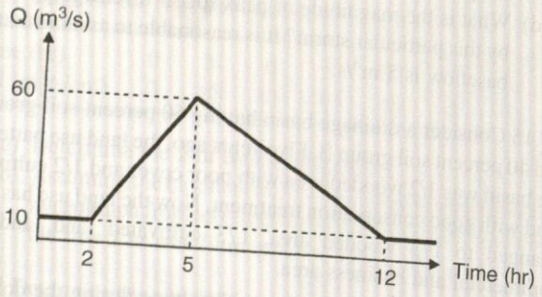


(a) Estimate the increased total runoff volume by the SCS method due to the land use change over the past 5-year period for this storm under the wet antecedent moisture condition.
(b) Find the effective rainfall intensity hyetograph for the storm event using the SCS method under the wet antecedent moisture condition and current land use condition.
(c) Find the value of the $\phi$ index corresponding to the above direct runoff hydrograph assuming the baseflow is 10 $m^3/s$.

8.7.18 Consider a drainage basin having soil group D. The land use pattern in the basin is 1/3 wooded area with good cover, 1/3 cultivated land with conservation treatment, and 1/3 commercial and business area. For the rainstorm event given below, use the SCS method under the dry antecedent moisture condition (AMC I).

(a) Estimate the total volume of effective rainfall (in cm).
(b) Find the effective rainfall hyetograph (in cm/hr) for the following storm event.

| Time (hr) | 0–0.5 | 0.5–1.0 | 1.0–1.5 | 1.5–2.0 |
|---|---|---|---|---|
| Avg. rainfall intensity (cm/hr) | 16.0 | 9.0 | 5.0 | 3.0 |

8.8.1 Develop the SCS triangular unit hydrograph for a 400-acre watershed that has been commercially developed. The flow length is 1,500 ft, the slope is 3 percent, and the soil group is group B.

8.8.2 Prior to development of the 400-acre watershed in problem 8.8.1, the land use was contoured pasture land with fair condition. Compute the SCS triangular unit hydrograph and compare with the one for commercially developed conditions.

8.8.3 Using the watershed defined in problems 8.8.1 and 8.8.2, determine the SCS triangular unit hydrograph assuming residential lot size. Compare with the results in problem 8.8.2.

8.8.4 A 20.7-$km^2$ watershed has a time of concentration of 1.0 hr. Calculate the 10-min unit hydrograph for the watershed using the SCS triangular unit hydrograph method. Determine the direct runoff hydrograph for a 30-min storm having 1.5 cm of excess rainfall in the first 10 min, 0.5 cm in the second 10 min, and 1.0 cm in the third 10 min.

8.9.1 Develop a flowchart of the kinematic overland flow runoff model described in Section 8.9.

8.9.2 Develop the appropriate equations to solve equation (8.9.9) by Newton's method.

8.9.3 Derive equation (8.9.12).

## REFERENCES

Chow, V. T. (editor), *Handbook of Applied Hydrology*, McGraw-Hill, New York, 1964.

Chow, V. T., D. R. Maidment, and L. W. Mays, *Applied Hydrology*, McGraw-Hill, New York, 1988.

Clark, C. O., "Storage and the Unit Hydrograph," *Trans. American Society of Civil Engineers*, Vol. 110, pp. 1419–1488, 1945.

Engman, E. T., "Roughness Coefficients for Routing Surface Runoff", *Journal of Irrigation and Drainage Engineering;* American Society of Civil Engineers, 112(1), pp. 39–53, 1986.

Flood Control District of Maricopa County, *Drainage Design Manual for Maricopa County, Arizona*, Phoenix, AZ, 1995.

Ford, D., E. C. Morris, and A. D. Feldman, "Corps of Engineers' Experience with Automatic Calibration Precipitation-Runoff Model," in *Water and Related Land Resource Systems* edited by Y. Haimes and J. Kindler, p. 467–476, Pergamon Press, New York, 1980.

Hewlett, J. D., and W. L. Nutter, *An Outline of Forest Hydrology*, University of Georgia Press, Athens, GA, 1969.

Horton, R. E., "Erosional Development of Streams and Their Drainage Basins; Hydrological Approach to Quantitative Morphology," *Bull. Geol. Soc. Am.*, vol. 56, pp. 275–370, 1945.

Masch, F. D., *Hydrology*, Hydraulic Engineering Circular No. 19, FHWA-10-84-15, Federal Highway Administration, U.S. Department of the Interior, McLean, VA, 1984.

Morris, E. M., and D. A. Woolhiser, "Unsteady One-Dimensional Flow over a Plane: Partial Equilibrium and Recession Hydrographs," *Water Resources Research*, vol. 16, no. 2, pp. 355–360, 1980.

Mosley, M. P., and A. I. McKerchar, "Streamflow," in *Handbook of Hydrology* (edited by D. R. Maidment), McGraw-Hill, New York, 1993.

Palmer, V. J., "Retardance Coefficients for Low Flow in Channels Lined with Vegetation," *Transactions of the American Geophysical Union*, 27(11), pp. 187–197, 1946.

Papadakis, C. N., and M. N. Kazan, "Time of Concentration in Small, Rural Watersheds," *Proceedings of the Engineering Hydrology Symposium*, ASCE, Williamsburg, Virginia, pp. 633–638, 1987.

Ponce, V. M., *Engineering Hydrology; Principles and Practices*, Prentice-Hall, Englewood Cliffs, NJ, 1989.

Sanders, T. G. (editor), *Hydrology for Transportation Engineers*, U.S. Dept. of Transportation, Federal Highway Administration, 1980.

Strahler, A. N., "Quantitative Geomorphology of Drainage Basins and Channel Networks," section 4-II in *Handbook of Applied Hydrology* (edited by V. T. Chow), McGraw-Hill, New York, 1964.

Straub, T. D., C. S. Melching, and K. E. Kocher, *Equations for Estimating Clark Unit-Hydrograph Parameters for Small Rural Watersheds in Illinois*, U.S. Geological
Report 00-4184, Urbana, IL, 20(

U.S. Army Corps of Engineer
Flood Hydrograph Package, Us

U.S. Department of Agricul
Engineering Handbook, Sectio
ernment Printing Office, Washi

U.S. Department of Agricu
Hydrology for Small Watersh
DC, June, 1986.

Woolhiser, D. A., and J. A. Liggett, "Unsteady, One-Dimensional Flow over a Plane—the Rising Hydrograph," *Water Resources Research*, vol. 3(3), pp. 753–771, 1967.

Woolhiser, D. A., R. E. Smith, and D. C. Goodrich, *KINEROS, A. Kinematic Runoff and Erosion Model: Documentation and User Manual*, U. S. Department of Agricultural Research Service, ARS-77, Tucson, AZ, 1990.

(a) Estimate t
change
even
(b) R

# Chapter 9

# Reservoir and Stream Flow Routing

## 9.1 ROUTING

Figure 9.1.1 illustrates how stream flow increases as the *variable source area* extends into the drainage basin. The variable source area is the area of the watershed that is actually contributing flow to the stream at any point. The variable source area expands during rainfall and contracts thereafter.

*Flow routing* is the procedure to determine the time and magnitude of flow (i.e., the flow hydrograph) at a point on a watercourse from known or assumed hydrographs at one or more points upstream. If the flow is a flood, the procedure is specifically known as flood routing. Routing by lumped system methods is called *hydrologic (lumped) routing*, and routing by distributed systems methods is called *hydraulic (distributed) routing*.

For hydrologic routing, input $I(t)$, output $Q(t)$, and storage $S(t)$ as functions of time are related by the continuity equation (3.3.10)

$$\frac{dS}{dt} = I(t) - Q(t) \tag{9.1.1}$$

Even if an inflow hydrograph $I(t)$ is known, equation (9.1.1) cannot be solved directly to obtain the outflow hydrograph $Q(t)$, because, both $Q$ and $S$ are unknown. A second relationship, or storage function, is required to relate $S$, $I$, and $Q$; coupling the storage function with the continuity equations provides a solvable combination of two equations and two unknowns.

The specific form of the storage function depends on the nature of the system being analyzed. In reservoir routing by the level pool method (Section 9.2), storage is a nonlinear function of $Q$, $S = f(Q)$, and the function $f(Q)$ is determined by relating reservoir storage and outflow to reservoir water level. In the Muskingum method (Section 9.3) for flow routing in channels, storage is linearly related to $I$ and $Q$.

The effect of storage is to redistribute the hydrograph by shifting the centroid of the inflow hydrograph to the position of the outflow hydrograph in a *time of redistribution*. In very long channels, the entire flood wave also travels a considerable distance, and the centroid of its hydrograph may then be shifted by a time period longer than the time of redistribution. This additional time may be considered the *time of translation*. The total time of flood movement between the centroids of the inflow and outflow hydrographs is equal to the sum of the time of redistribution and the time of translation. The process of redistribution modifies the shape of the hydrograph, while translation changes its position.

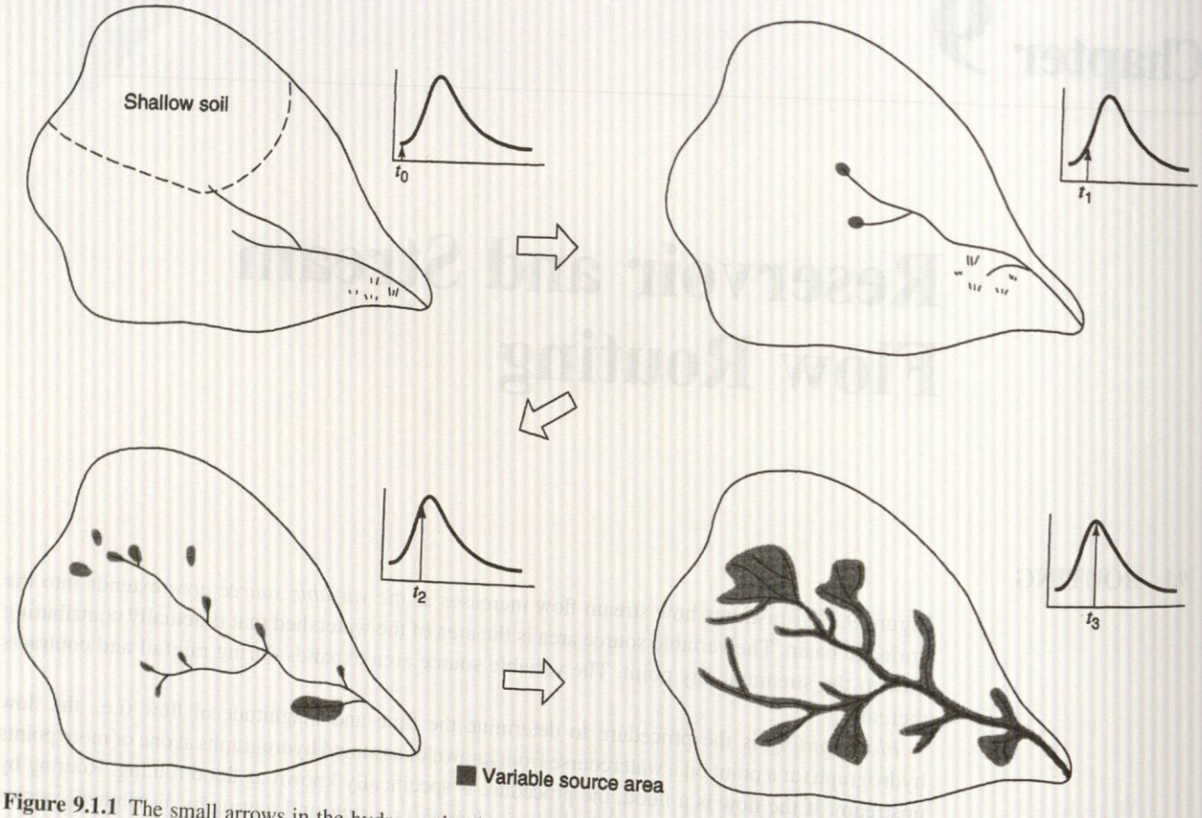


**Figure 9.1.1** The small arrows in the hydrographs show how streamflow increases as the variable source extends into swamps, shallow soils, and ephemeral channels. The process reverses as streamflow declines (from Hewlett (1982)).

## 9.2 HYDROLOGIC RESERVOIR ROUTING

*Level pool routing* is a procedure for calculating the outflow hydrograph from a reservoir assuming a horizontal water surface, given its inflow hydrograph and storage-outflow characteristics. Equation (9.1.1) can be expressed in the infinite-difference form to express the change in storage over a time interval (see Figure 9.2.1) as

$$S_{j+1} - S_j = \frac{I_j + I_{j+1}}{2}\Delta t - \frac{Q_j + Q_{j+1}}{2}\Delta t \tag{9.2.1}$$

The inflow values at the beginning and end of the $j$th time interval are $I_j$ and $I_{j+1}$, respectively, and the corresponding values of the outflow are $Q_j$ and $Q_{j+1}$. The values of $I_j$ and $I_{j+1}$ are prespecified. The values of $Q_j$ and $S_j$ are known at the $j$th time interval from calculations for the previous time interval. Hence, equation (9.2.1) contains two unknowns, $Q_{j+1}$ and $S_{j+1}$, which are isolated by multiplying (9.2.1) through by $2/\Delta t$, and rearranging the result to produce:

$$\left[\frac{2S_{j+1}}{\Delta t} + Q_{j+1}\right] = (I_j + I_{j+1}) + \left[\frac{2S_j}{\Delta t} - Q_j\right] \tag{9.2.2}$$

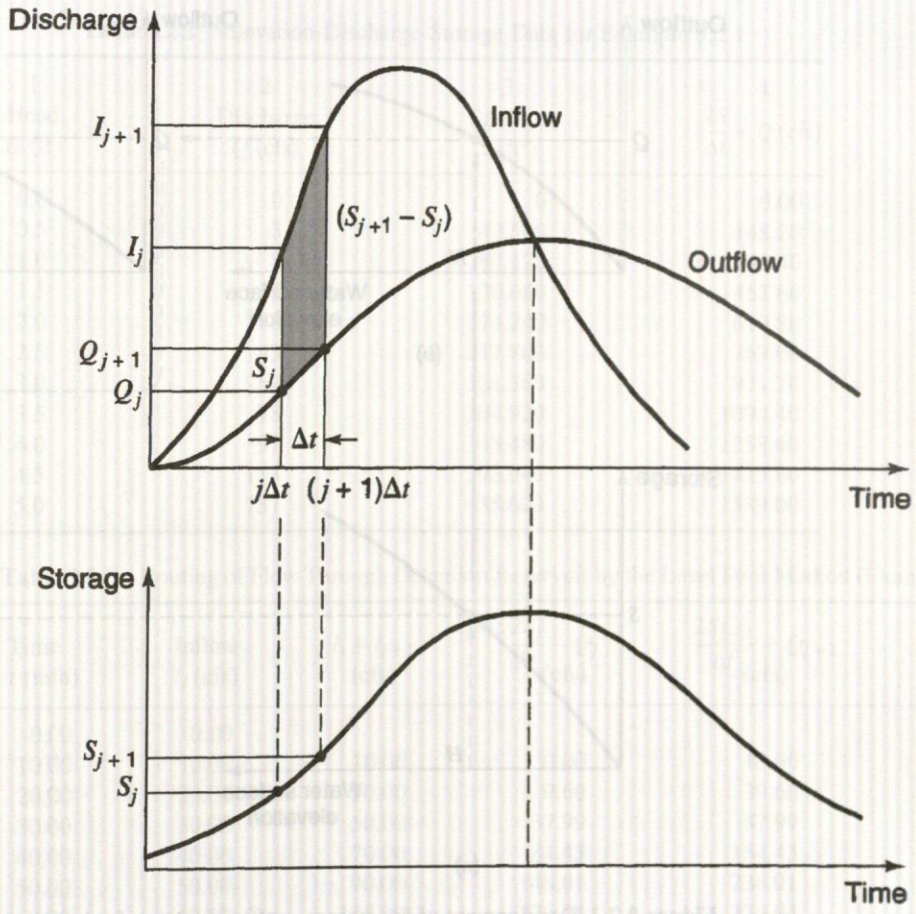


**Figure 9.2.1** Change of storage during a routing period $\Delta t$.

In order to calculate the outflow $Q_{j+1}$, a storage-outflow function relating $2S/\Delta t + Q$ and $Q$ is needed. The method for developing this function using elevation-storage and elevation-outflow relationships is shown in Figure 9.2.2. The relationship between water surface elevation and reservoir storage can be derived by planimetering topographic maps or from field surveys. The elevation-discharge relation is derived from hydraulic equations relating head and discharge for various types of spillways and outlet works. (See Chapter 17.) The value of $\Delta t$ is taken as the time interval of the inflow hydrograph. For a given value of water surface elevation, the values of storage $S$ and discharge $Q$ are determined (parts (*a*) and (*b*) of Figure 9.2.2), and then the value of $2S/\Delta t + Q$ is calculated and plotted on the horizontal axis of a graph with the value of the outflow $Q$ on the vertical axis (part (*c*) of Figure 9.2.2).

In routing the flow through time interval $j$, all terms on the right side of equation (9.2.2) are known, and so the value of $2S_{j+1}/\Delta t + Q_{j+1}$ can be computed. The corresponding value of $Q_{j+1}$ can be determined from the storage-outflow function $2S/\Delta t + Q$ versus $Q$, either graphically or by linear interpolation of tabular values. To set up the data required for the next time interval, the value of $(2S_{j+1}/\Delta t - Q_{j+1})$ is calculated using

$$\left[\frac{2S_{j+1}}{\Delta t} - Q_{j+1}\right] = \left[\frac{2S_{j+1}}{\Delta t} + Q_{j+1}\right] - 2Q_{j+1} \tag{9.2.3}$$

The computation is then repeated for subsequent routing periods.

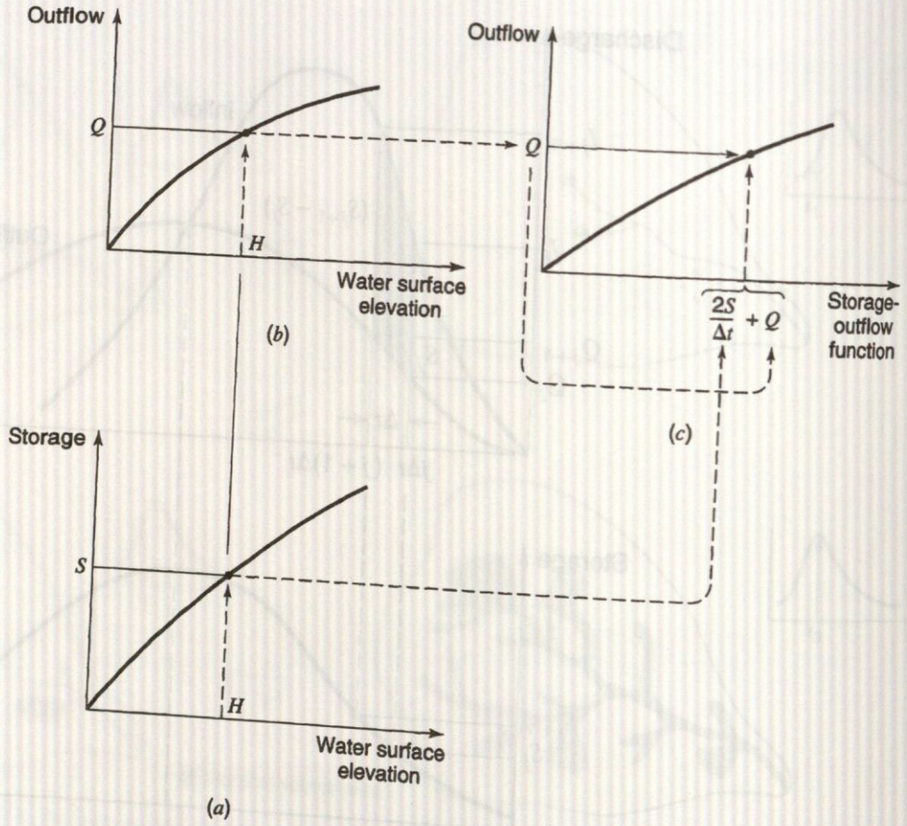


**Figure 9.2.2** Development of the storage-outflow function for level pool routing on the basis of storage-elevation-outflow curves (from Chow et al. (1988)).

***EXAMPLE 9.2.1***

Consider a 2-acre stormwater detention basin with vertical walls. The triangular inflow hydrograph increases linearly from zero to a peak of 60 cfs at 60 min and then decreases linearly to a zero discharge at 180 min. Route the inflow hydrograph through the detention basin using the head-discharge relationship for the 5-ft diameter pipe spillway in columns (1) and (2) of Table 9.2.1. The pipe is located at the bottom of the basin. Assuming the basin is initially empty, use the level pool routing procedure with a 10-min time interval to determine the maximum depth in the detention basin.

***SOLUTION***

The inflow hydrograph and the head-discharge (columns (1) and (2)) and discharge-storage (columns (2) and (3)) relationships are used to determine the routing relationship in Table 9.2.1. A routing interval of 10 min is used to determine the routing relationship $2S/\Delta t + Q$ vs. $Q$, which is columns (2) and (4) in Table 9.2.1. The routing computations are presented in Table 9.2.2. These computations are carried out using equation (9.2.3). For the first time interval, $S_1 = Q_1 = 0$ because the reservoir is empty at $t = 0$; then $(2S_1/\Delta t - Q_1) = 0$. The value of the storage-outflow function at the end of the time interval is

$$\left[\frac{2S_2}{\Delta t} + Q_2\right] = (I_1 + I_2) + \left[\frac{2S_1}{\Delta t} - Q_1\right] = (0 + 10) + 0 = 10$$

The value of $Q_2$ is determined using linear interpolation, so that

$$Q_2 = 0 + \frac{(3-0)}{(148.2-0)}(10-0) = 0.2 \text{ cfs}$$

**Table 9.2.1** Elevation-Discharge-Storage Data for Example 9.2.1

| 1<br>Head<br>$H$ (ft) | 2<br>Discharge<br>$Q$ (cfs) | 3<br>Storage<br>$S$ (ft$^3$) | 4<br>$\frac{2S}{\Delta t} + Q$ (cfs) |
|---|---|---|---|
| 0.0 | 0 | 0 | 0.00 |
| 0.5 | 3 | 43,500 | 148.20 |
| 1.0 | 8 | 87,120 | 298.40 |
| 1.5 | 17 | 130,680 | 452.60 |
| 2.0 | 30 | 174,240 | 610.80 |
| 2.5 | 43 | 217,800 | 769.00 |
| 3.0 | 60 | 261,360 | 931.20 |
| 3.5 | 78 | 304,920 | 1094.40 |
| 4.0 | 97 | 348,480 | 1258.60 |
| 4.5 | 117 | 392,040 | 1423.80 |
| 5.0 | 137 | 435,600 | 1589.00 |

**Table 9.2.2** Routing of Flow Through Detention Reservoir by the Level Pool Method (Example 9.2.1)

| Time<br>$t$ (min) | Inflow<br>$I_j$ (cfs) | $I_j + I_{j+1}$<br>(cfs) | $\frac{2S_j}{\Delta t} - Q_j$ (cfs) | $\frac{2S_{j+1}}{\Delta t} + Q_{j+1}$ (cfs) | Outflow<br>(cfs) |
|---|---|---|---|---|---|
| 0.00 | 0.00 | | | | 0.00 |
| 10.00 | 10.00 | 10.00 | 0.00 | 10.00 | 0.20 |
| 20.00 | 20.00 | 30.00 | 9.60 | 39.60 | 0.80 |
| 30.00 | 30.00 | 50.00 | 37.99 | 87.99 | 1.78 |
| 40.00 | 40.00 | 70.00 | 84.43 | 154.43 | 3.21 |
| 50.00 | 50.00 | 90.00 | 148.01 | 238.01 | 5.99 |
| 60.00 | 60.00 | 110.00 | 226.04 | 336.04 | 10.20 |
| 70.00 | 55.00 | 115.00 | 315.64 | 430.64 | 15.72 |
| 80.00 | 50.00 | 105.00 | 399.21 | 504.21 | 21.24 |
| 90.00 | 45.00 | 95.00 | 461.72 | 556.72 | 25.56 |
| 100.00 | 40.00 | 85.00 | 505.61 | 590.61 | 28.34 |
| 110.00 | 35.00 | 75.00 | 533.93 | 608.93 | 29.85 |
| 120.00 | 30.00 | 65.00 | 549.24 | 614.24 | 30.28 |
| 130.00 | 25.00 | 55.00 | 553.67 | 608.67 | 29.83 |
| 140.00 | 20.00 | 45.00 | 549.02 | 594.02 | 28.62 |
| 150.00 | 15.00 | 35.00 | 536.78 | 571.78 | 26.79 |
| 160.00 | 10.00 | 25.00 | 518.19 | 543.19 | 24.44 |
| 170.00 | 5.00 | 15.00 | 494.30 | 509.30 | 21.66 |
| 180.00 | 0.00 | 5.00 | 465.98 | 470.98 | 18.51 |
| 190.00 | 0.00 | 0.00 | 433.96 | 433.96 | 15.91 |
| 200.00 | 0.00 | 0.00 | 402.14 | 402.14 | 14.05 |
| 210.00 | 0.00 | 0.00 | 374.03 | 374.03 | 12.41 |
| 220.00 | 0.00 | 0.00 | 349.20 | 349.20 | 10.97 |
| 230.00 | 0.00 | 0.00 | 327.27 | 327.27 | 9.69 |
| 240.00 | 0.00 | 0.00 | 307.90 | 307.90 | 8.55 |

With $Q_1 = 0.2$, then $2S_2/\Delta t - Q_2$ for the next iteration is

$$\left[\frac{2S_2}{\Delta t} - Q_2\right] = \left[\frac{2S_2}{\Delta t} + Q_2\right] - 2Q_2 = 10 - 2(0.2) = 9.6 \text{ cfs}$$

The computation now proceeds to the next time interval. Refer to Table 9.2.2 for the remaining computations.

## 9.3 HYDROLOGIC RIVER ROUTING

The *Muskingum method* is a commonly used hydrologic routing method that is based upon a variable discharge-storage relationship. This method models the storage volume of flooding in a river channel by a combination of wedge and prism storage (Figure 9.3.1). During the advance of a flood wave, inflow exceeds outflow, producing a wedge of storage. During the recession, outflow exceeds inflow, resulting in a negative wedge. In addition, there is a prism of storage that is formed by a volume of constant cross-section along the length of prismatic channel.

Assuming that the cross-sectional area of the flood flow is directly proportional to the discharge at the section, the *volume of prism storage* is equal to $KQ$, where $K$ is a proportionality coefficient (approximate as the travel time through the reach), and the *volume of wedge storage* is equal to $KX(I-Q)$, where $X$ is a weighting factor having the range $0 \leq X \leq 0.5$. The total storage is defined as the sum of two components,

$$S = KQ + KX(I - Q) \tag{9.3.1}$$

which can be rearranged to give the storage function for the Muskingum method

$$S = K[XI + (I - X)Q] \tag{9.3.2}$$

and represents a linear model for routing flow in streams.

The value of $X$ depends on the shape of the modeled wedge storage. The value of $X$ ranges from 0 for reservoir-type storage to 0.5 for a full wedge. When $X = 0$, there is no wedge and hence no backwater; this is the case for a level-pool reservoir. In natural streams, $X$ is between 0 and 0.3, with a mean value near 0.2. Great accuracy in determining $X$ may not be necessary because the results of the method are relatively insensitive to the value of this parameter. The parameter $K$ is the time of travel of the flood wave through the channel reach. For hydrologic routing, the values of $K$ and $X$ are assumed to be specified and constant throughout the range of flow.

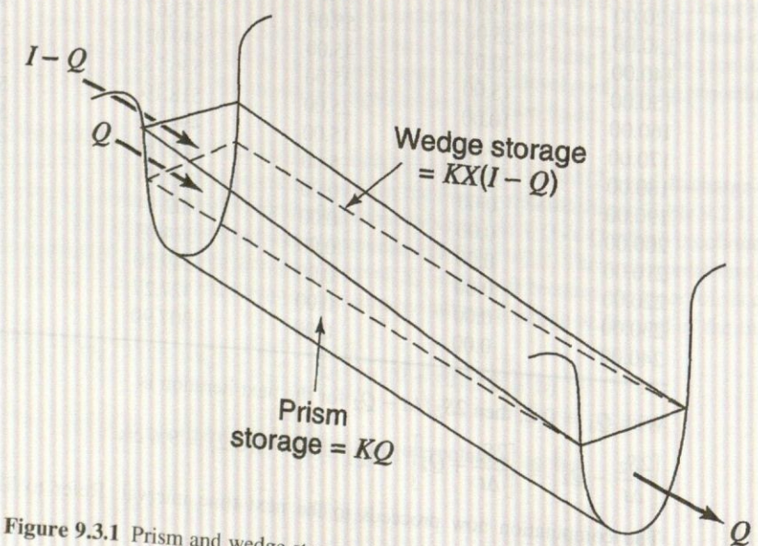


**Figure 9.3.1** Prism and wedge storages in a channel reach.

The values of storage at time $j$ and $j + 1$ can be written, respectively, as

$$S_j = K[XI_j + (1-X)Q_j] \tag{9.3.3}$$

$$S_{j+1} = K[XI_{j+1} + (1-X)Q_{j+1}] \tag{9.3.4}$$

Using equations (9.3.3) and (9.3.4), the change in storage over time interval $\Delta t$ is

$$S_{j+1} - S_j = K\{[XI_{j+1} + (1-X)Q_{j+1}] - [XI_j + (1-X)Q_j]\} \tag{9.3.5}$$

The change in storage can also be expressed using equation (9.2.1). Combining equations (9.3.5) and (9.2.1) and simplifying gives

$$Q_{j+1} = C_1 I_{j+1} + C_2 I_j + C_3 Q_j \tag{9.3.6}$$

which is the routing equation for the Muskingum method, where

$$C_1 = \frac{\Delta t - 2KX}{2K(1-X) + \Delta t} \tag{9.3.7}$$

$$C_2 = \frac{\Delta t + 2KX}{2K(1-X) + \Delta t} \tag{9.3.8}$$

$$C_3 = \frac{2K(1-X) - \Delta t}{2K(1-X) + \Delta t} \tag{9.3.9}$$

Note that $C_1 + C_2 + C_3 = 1$.

The routing procedure can be repeated for several sub-reaches ($N_{\text{steps}}$) so that the total travel time through the reach is $K$. To insure that the method is computationally stable and accurate, the U.S. Army Corps of Engineers (1990) uses the following criterion to determine the number of routing reaches:

$$\frac{1}{2(1-X)} \leq \frac{K}{N_{\text{steps}}\Delta t} \leq \frac{1}{2X} \tag{9.3.10}$$

If observed inflow and outflow hydrographs are available for a river reach, the values of $K$ and $X$ can be determined. Assuming various values of $X$ and using known values of the inflow and outflow, successive values of the numerator and denominator of the following expression for $K$, derived from equations (9.3.5) and (9.2.1), can be computed using

$$K = \frac{0.5\Delta t[(I_{j+1} + I_j) - (Q_{j+1} + Q_j)]}{X(I_{j+1} - I_j) + (1-X)(Q_{j+1} - Q_j)} \tag{9.3.11}$$

The computed values of the numerator (storage) and denominator (weighted discharges) are plotted for each time interval, with the numerator on the vertical axis and the denominator on the horizontal axis. This usually produces a graph in the form of a loop, as shown in Figure 9.3.2. The value of $X$ that produces a loop closest to a single line is taken to be the correct value for the reach, and $K$, according to equation (9.3.11), is equal to the slope of the line. Since $K$ is the time required for the incremental flood wave to traverse the reach, its value may also be estimated as the observed time of travel of peak flow through the reach.

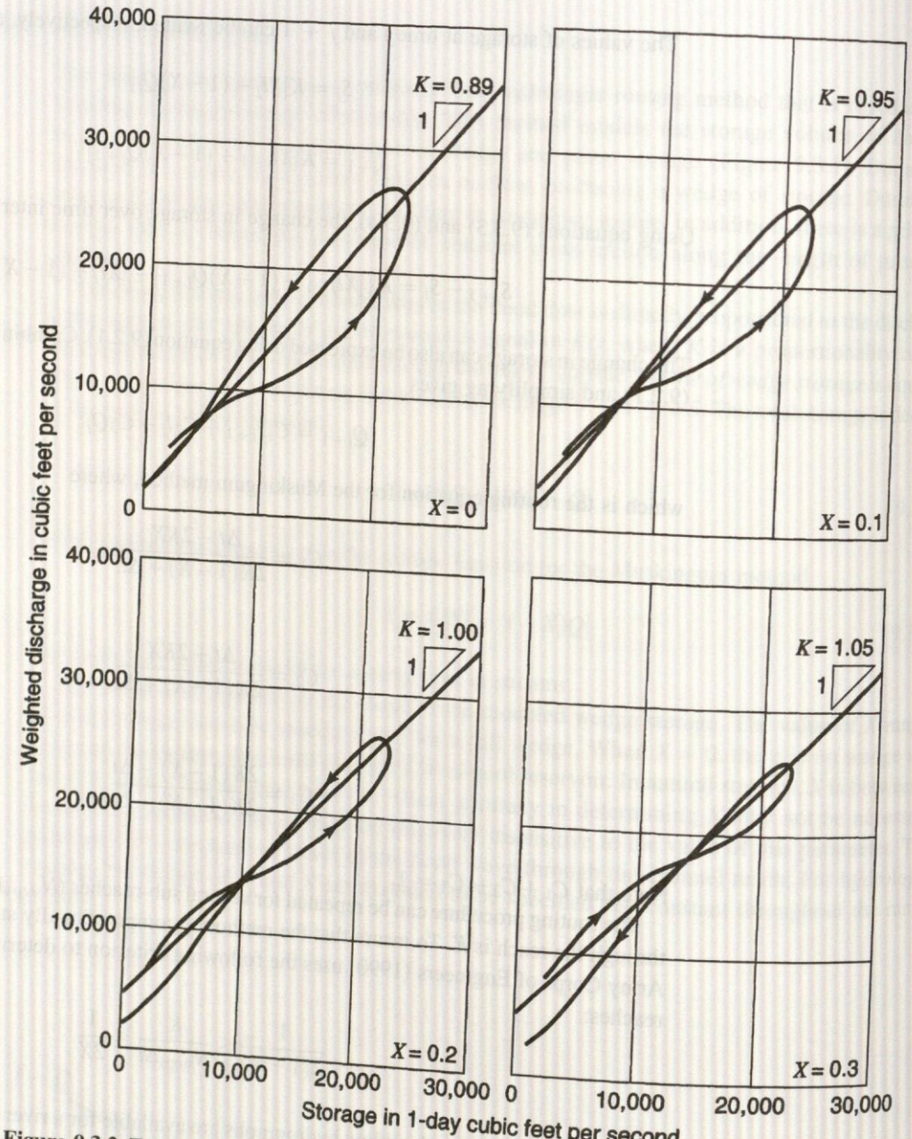


**Figure 9.3.2** Typical valley storage curves (after Cudworth (1989)).

***EXAMPLE 9.3.1***

The objective of this example is to determine $K$ and $X$ for the Muskingum routing method using the February 26 to March 4, 1929 data on the Tuscarawas River from Dover to Newcomerstown. This example is taken from the U.S. Army Corps of Engineers (1960) as used in Cudworth (1989). Columns (2) and (3) in Table 9.3.1 are the inflow and outflow hydrographs for the reach. The numerator and denominator of equation (9.3.11) were computed (for each time period) using four values of $X = 0$, 0.1, 0.2, and 0.3. The accumulated numerators are in column (9) and the accumulated denominators (weighted discharges) are in columns (11), (13), (15), and (17). In Figure 9.3.2, the accumulated numerator (storages) from column (9) are plotted against the corresponding accumulated denominator (weighted discharges) for each of the four $X$ values. According to Figure 9.3.2, the best fit (linear relationship) appears to be for $X = 0.2$, which has a resulting $K = 1.0$. To perform a routing, $K$ should equal $\Delta t$, so that if $\Delta t = 0.5$ day, as in this case, the reach should be subdivided into two equal reaches ($N_{\text{steps}} = 2$) and the value of $K$ should be 0.5 day for each reach.

**Table 9.3.1** Determination of Coefficients $K$ and $X$ for the Muskingum Routing Method. Tuscarawas River, Muskingum Basin, Ohio Reach from Dover to Newcomerstown, February 26 to March 4, 1929

| | | | | | | | | | Values of $D$ and $\Sigma D$ for assumed values of $X$ | | | | | | | |
|---|---|---|---|---|---|---|---|---|---|---|---|---|---|---|---|---|
| | | | | | | | | | $X = 0$ | | $X = 0.1$ | | $X = 0.2$ | | $X = 0.3$ | |
| (1) Date $\Delta t = 0.5$ day | (2) In-flow[1], ft$^3$/s | (3) Out-flow[2], ft$^3$/s | (4) $I_2 + I_1$, ft$^3$/s | (5) $O_2 + O_1$, ft$^3$/s | (6) $I_2 - I_1$, ft$^3$/s | (7) $O_2 - O_1$, ft$^3$/s | (8) $^3N$ | (9) $\Sigma N$ | $^4D$ (10) | $\Sigma D$ (11) | $D$ (12) | $\Sigma D$ (13) | $D$ (14) | $\Sigma D$ (15) | $D$ (16) | $\Sigma D$ (17) |
| 2-26-29 a.m. | 2200 | 2000 | 16,700 | 9000 | 12,300 | 5000 | 1900 | | 5000 | | 5700 | | 6500 | | 7200 | |
| p.m. | 14,500 | 7000 | 42,900 | 18,700 | 13,900 | 4700 | 6100 | 1900 | 4700 | 5000 | 5600 | 5700 | 6500 | 6500 | 7500 | 7200 |
| 2-27-29 a.m. | 28,400 | 11,700 | 60,200 | 28,200 | 3400 | 4800 | 8000 | 8000 | 4800 | 9700 | 4600 | 11,300 | 4500 | 13,000 | 4300 | 14,700 |
| p.m. | 31,800 | 16,500 | 61,500 | 40,500 | −2100 | 7500 | 5200 | 16,000 | 7500 | 14,500 | 6700 | 15,900 | 5600 | 17,500 | 4600 | 19,000 |
| 2-28-29 a.m. | 29,700 | 24,000 | 55,000 | 53,100 | −4400 | 5100 | 500 | 21,200 | 5100 | 22,000 | 4100 | 22,600 | 3200 | 23,100 | 2300 | 23,600 |
| p.m. | 25,300 | 29,100 | 45,700 | 57,500 | −4900 | −700 | −2900 | 21,700 | −700 | 27,100 | −1100 | 26,700 | −1500 | 26,300 | −2000 | 25,900 |
| 3-01-29 a.m. | 20,400 | 28,400 | 36,700 | 52,200 | −4100 | −4600 | −3900 | 18,800 | −4600 | 26,400 | −4600 | 25,600 | −4500 | 24,800 | −4400 | 23,900 |
| p.m. | 16,300 | 23,800 | 28,900 | 43,200 | −3700 | −4400 | −3600 | 14,900 | −4400 | 21,800 | −4300 | 21,000 | −4300 | 20,300 | −4200 | 19,500 |
| 3-02-29 a.m. | 12,600 | 19,400 | 21,900 | 34,700 | −3300 | −4100 | −3200 | 11,300 | −4100 | 17,400 | −4000 | 16,700 | −3900 | 16,000 | −3900 | 15,300 |
| p.m. | 9300 | 15,300 | 16,000 | 26,500 | −2600 | −4100 | −2500 | 8100 | −4100 | 13,300 | −4000 | 12,700 | −3800 | 12,100 | −3600 | 11,400 |
| 3-03-29 a.m. | 6700 | 11,200 | 11,700 | 19,400 | −1700 | −3000 | −1900 | 5500 | −3000 | 9200 | −2800 | 8700 | −2800 | 8300 | −2600 | 7800 |
| p.m. | 5000 | 8200 | 9100 | 14,600 | −900 | −1800 | −1400 | 3600 | −1800 | 6200 | −1700 | 5900 | −1600 | 5500 | −1600 | 5200 |
| 3-04-29 a.m. | 4100 | 6400 | 7700 | 11,600 | −500 | −1200 | −1000 | 2200 | −1200 | 4400 | −1200 | 4200 | −1100 | 3900 | −900 | 3600 |
| p.m. | 3600 | 5200 | 6000 | 9800 | −1200 | −600 | −1000 | 1200 | −600 | 3200 | −600 | 3000 | −700 | 2800 | −800 | 2700 |
| 3-05-29 a.m. | 2400 | 4600 | — | — | — | — | — | 200 | — | 2600 | — | 2400 | — | 2100 | — | 1900 |

[1]Inflow to reach was adjusted to equal volume of outflow.
[2]Outflow is the hydrograph at Newcomerstown.
[3]Numerator, $N$, is $\Delta t/2$, column (4) – column (5).
[4]Denominator, $D$, is column (7) + $X$ [column (6) - column (7)].
Note: From plottings of column (9) versus columns (11), (13), (15), and (17), the plot giving the best fit is considered to define $K$ and $X$.

$$K = \frac{\text{Numerator, } N}{\text{Denominator, } D} = \frac{0.5\Delta t[(I_2 + I_1) - (O_2 + O_1)]}{X(I_2 - I_1) + (1 - X)(O_2 - O_1)}$$

*Source*: Cudworth (1989).

***EXAMPLE 9.3.2*** Route the inflow hydrograph below using the Muskingum method; $\Delta t = 1$ hr, $X = 0.2$, $K = 0.7$ hr.

| Time (hr) | 0 | 1 | 2 | 3 | 4 | 5 | 6 | 7 |
|---|---|---|---|---|---|---|---|---|
| Inflow (cfs) | 0 | 800 | 2000 | 4200 | 5200 | 4400 | 3200 | 2500 |
| Time (hr) | 8 | 9 | 10 | 11 | 12 | 13 | | |
| Inflow (cfs) | 2000 | 1500 | 1000 | 700 | 400 | 0 | | |

$$C_1 = \frac{1.0 - 2(0.7)(0.2)}{2(0.7)(1-0.2)+1.0} = 0.3396$$

$$C_2 = \frac{1.0 + 2(0.7)(0.2)}{2(0.7)(1-0.2)+1.0} = 0.6038$$

$$C_3 = \frac{2(0.7)(1-0.2) - 1.0}{2(0.7)(1-0.2)+1.0} = 0.0566$$

(Adapted from Masch (1984).)

Check to see if $C_1 + C_2 + C_3 = 1$:

$$0.3396 + 0.6038 + 0.0566 = 1$$

Using equation (9.3.6) with $I_1 = 0$ cfs, $I_2 = 800$ cfs, and $Q_1 = 0$ cfs, compute $Q_2$ at $t = 1$ hr:

$$\begin{aligned} Q_2 &= C_1 I_2 + C_2 I_1 + C_3 Q_1 \\ &= (0.3396)(800) + 0.6038(0) + 0.0566(0) \\ &= 272 \text{ cfs } (7.7 \text{ m}^3/\text{s}) \end{aligned}$$

Next compute $Q_3$ at $t = 2$ hr :

$$\begin{aligned} Q_3 &= C_1 I_3 + C_2 I_2 + C_3 Q_2 \\ &= (0.3396)(2000) + 0.6038(800) + 0.0566(272) \\ &= 1{,}178 \text{ cfs } (33 \text{ m}^3/\text{s}) \end{aligned}$$

The remaining computations result in

| Time (hr) | 0 | 1 | 2 | 3 | 4 | 5 | 6 | 7 |
|---|---|---|---|---|---|---|---|---|
| $Q$ (cfs) | 0 | 272 | 1178 | 2701 | 4455 | 4886 | 4020 | 3009 |
| Time (hr) | 8 | 9 | 10 | 11 | 12 | 13 | 14 | 15 |
| $Q$ (cfs) | 2359 | 1851 | 1350 | 918 | 610 | 276 | 16 | 1 |

## 9.4 HYDRAULIC (DISTRIBUTED) ROUTING

*Distributed routing* or *hydraulic routing*, also referred to as *unsteady flow routing*, is based upon the one-dimensional unsteady flow equations referred to as the *Saint-Venant equations*. The hydrologic river routing and the hydrologic reservoir routing procedures presented previously are lumped procedures and compute flow rate as a function of time alone at a downstream location. Hydraulic (distributed) flow routings allow computation of the flow rate and water surface elevation (or depth) as a function of both space (location) and time. The Saint-Venant equations are presented in Table 9.4.1 in both the *velocity-depth (nonconservation) form* and the *discharge-area (conservation) form*.

The momentum equation contains terms for the physical processes that govern the flow momentum. These terms are: the *local acceleration term*, which describes the change in momentum due to the change in velocity over time, the *convective acceleration term*, which describes the change in momentum due to change in velocity along the channel, the *pressure force term*,

### 9.4.1 Unsteady

**Table 9.4.1** Summary of the Saint-Venant Equations*

*Continuity equation*

Conservation form $$\frac{\partial Q}{\partial x} + \frac{\partial A}{\partial t} = 0$$

Nonconservation form $$V\frac{\partial y}{\partial x} + \frac{\partial V}{\partial x} + \frac{\partial y}{\partial t} = 0$$

*Momentum equation*

Conservation form

$$\frac{1}{A}\frac{\partial Q}{\partial t} + \frac{1}{A}\frac{\partial}{\partial x}\left(\frac{Q^2}{A}\right) + g\frac{\partial y}{\partial x} - g(S_0 - S_f) = 0$$

| Local acceleration term | Convective acceleration term | Pressure force term | Gravity force term | Friction force term |
|---|---|---|---|---|

Nonconservation form (unit with element)

$$\frac{\partial V}{\partial t} + V\frac{\partial V}{\partial x} + g\frac{\partial y}{\partial x} - g(S_0 - S_f) = 0$$

Kinematic wave

Diffusion wave

Dynamic wave

*Neglecting lateral inflow, wind shear, and eddy losses, and assuming $\beta = 1$.

$x$ = longitudinal distance along the channel or river, $t$ = time, $A$ = cross-sectional area of flow, $h$ = water surface elevation, $S_f$ = friction slope, $S_0$ = channel bottom slope, $g$ = acceleration due to gravity, $V$ = velocity of flow, and $y$ = depth of flow.

proportional to the change in the water depth along the channel, the gravity force term, proportional to the bed slope $S_0$, and the friction force term, proportional to the friction slope $S_f$. The local and convective acceleration terms represent the effect of inertial forces on the flow.

Alternative distributed flow routing models are produced by using the full continuity equation while eliminating some terms of the momentum equation (refer to Table 9.4.1). The simplest distributed model is the *kinematic wave model*, which neglects the local acceleration, convective acceleration, and pressure terms in the momentum equation; that is, it assumes that $S_0 = S_f$ and the friction and gravity forces balance each other. The *diffusion wave model* neglects the local and convective acceleration terms but incorporates the pressure term. The *dynamic wave model* considers all the acceleration and pressure terms in the momentum equation.

The momentum equation can also be written in forms that take into account whether the flow is steady or unsteady, and uniform or nonuniform, as illustrated in Table 9.4.1. In the continuity equation, $\partial A/\partial t = 0$ for a steady flow, and the lateral inflow $q$ is zero for a uniform flow.

## 4.1 Unsteady Flow Equations: Continuity Equation

The *continuity equation* for an unsteady variable-density flow through a control volume can be written as in equation (3.3.1):

$$0 = \frac{d}{dt}\int_{CV} \rho d\forall + \int_{CS} \rho \mathbf{V} \cdot d\mathbf{A} \qquad (9.4.1)$$

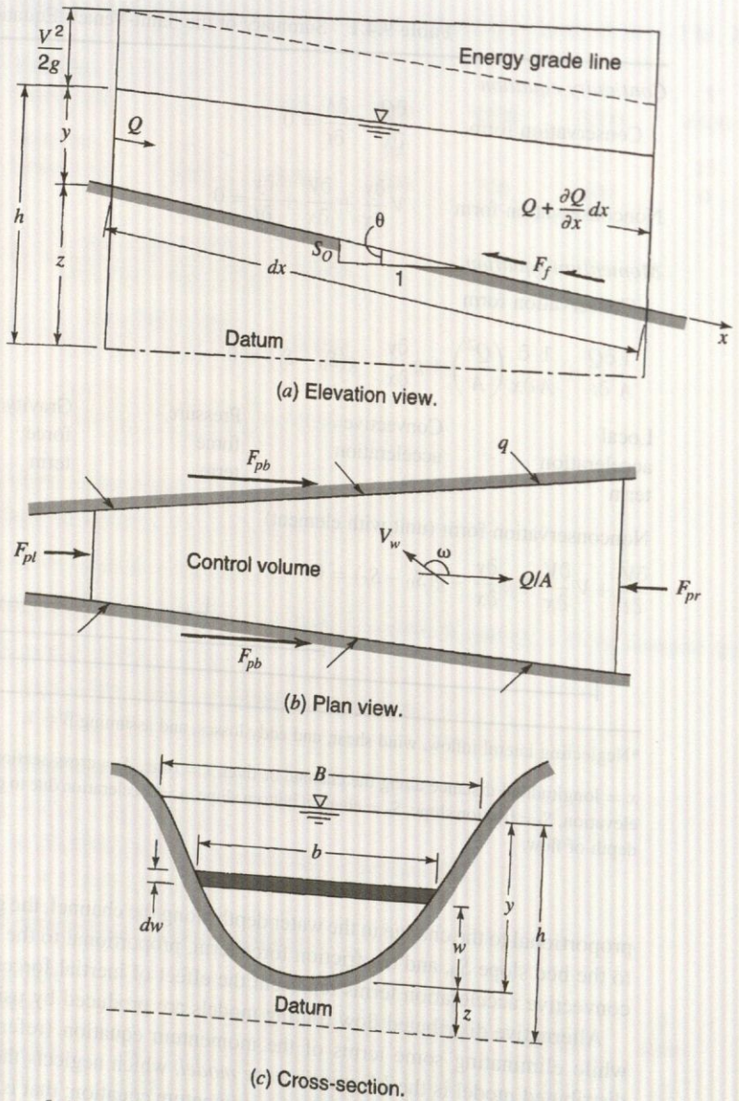


**Figure 9.4.1** An elemental reach of channel for derivation of Sain-Venant equations.

Consider an elemental control volume of length $dx$ in a channel. Figure 9.4.1 shows three views of the control volume: (*a*) an elevation view from the side, (*b*) a plan view from above, and (*c*) a channel cross-section. The inflow to the control volume is the sum of the flow $Q$ entering the control volume at the upstream end of the channel and the lateral inflow $q$ entering the control volume as a distributed flow along the side of the channel. The dimensions of $q$ are those of flow per unit length of channel, so the rate of lateral inflow is $qdx$ and the mass inflow rate is

$$\int_{\text{inlet}} \rho \mathbf{V} \cdot d\mathbf{A} = -\rho(Q + qdx) \tag{9.4.2}$$

This is negative because inflows are considered negative in the control volume approach (Reynolds transport theorem). The mass outflow from the control volume is

$$\int_{\text{outlet}} \rho \mathbf{V} \cdot d\mathbf{A} = \rho\left(Q + \frac{\partial Q}{\partial x} dx\right) \tag{9.4.3}$$

### 9.4.2 Momentu

where $\partial Q/\partial x$ is the rate of change of channel flow with distance. The volume of the channel element is $Adx$, where $A$ is the average cross-sectional area, so the rate of change of mass stored within the control volume is

$$\frac{d}{dt}\int_{CV} \rho \, d\forall = \frac{\partial(\rho A dx)}{\partial t} \tag{9.4.4}$$

where the partial derivative is used because the control volume is defined to be fixed in size (though the water level may vary within it). The net outflow of mass from the control volume is found by substituting equations (9.4.2)–(9.4.4) into (9.4.1):

$$\frac{\partial(\rho A dx)}{dt} - \rho(Q + q dx) + \rho\left(Q + \frac{\partial Q}{\partial x} dx\right) = 0 \tag{9.4.5}$$

Assuming the fluid density $\rho$ is constant, equation (9.4.5) is simplified by dividing through by $\rho dx$ and rearranging to produce the *conservation form* of the continuity equation,

$$\frac{\partial Q}{\partial x} + \frac{\partial A}{\partial t} - q = 0 \tag{9.4.6}$$

which is applicable at a channel cross-section. This equation is valid for a *prismatic* or a *non-prismatic* channel; a prismatic channel is one in which the cross-sectional shape does not vary along the channel and the bed slope is constant.

For some methods of solving the Saint-Venant equations, the *nonconservation form* of the continuity equation is used, in which the average flow velocity $V$ is a dependent variable, instead of $Q$. This form of the continuity equation can be derived for a unit width of flow within the channel, neglecting lateral inflow, as follows. For a unit width of flow, $A = y \times 1 = y$ and $Q = VA = Vy$. Substituting into equation (9.4.6) yields

$$\frac{\partial(Vy)}{\partial x} + \frac{\partial y}{\partial t} = 0 \tag{9.4.7}$$

or

$$V\frac{\partial y}{\partial x} + y\frac{\partial V}{\partial x} + \frac{\partial y}{\partial t} = 0 \tag{9.4.8}$$

### 9.4.2 Momentum Equation

Newton's second law is written in the form of Reynolds transport theorem as in equation (3.5.5):

$$\sum \mathbf{F} = \frac{d}{dt}\int_{CV} \mathbf{V}\rho d\forall + \sum_{CS} \mathbf{V}\rho\mathbf{V}\cdot\mathbf{dA} \tag{9.4.9}$$

This states that the sum of the forces applied is equal to the rate of change of momentum stored within the control volume plus the net outflow of momentum across the control surface. This equation, in the form $\sum F = 0$, was applied to steady uniform flow in an open channel in Chapter 5. Here, unsteady nonuniform flow is considered.

*Forces.* There are five forces acting on the control volume:

$$\sum F = F_g + F_f + F_e + F_p \tag{9.4.10}$$

where $F_g$ is the *gravity force* along the channel due to the weight of the water in the control volume, $F_f$ is the *friction force* along the bottom and sides of the control volume, $F_e$ is the *contraction/*

*expansion force* produced by abrupt changes in the channel cross-section, and $F_p$ is the *unbalanced pressure force* (see Figure 9.4.1). Each of these four forces is evaluated in the following paragraphs.

*Gravity.* The volume of fluid in the control volume is $Adx$ and its weight is $\rho gAdx$. For a small angle of channel inclination $\theta$, $S_0 \approx \sin\theta$ and the gravity force is given by

$$F_g = \rho gAdx \sin\theta \approx \rho gAS_0 dx \tag{9.4.11}$$

where the channel bottom slope $S_0$ equals $-\partial z/\partial x$.

*Friction.* Frictional forces created by the shear stress along the bottom and sides of the control volume are given by $-\tau_0 P dx$, where $\tau_0 = \gamma R S_f = \rho g(A/P)S_f$ is the bed shear stress and $P$ is the wetted perimeter. Hence the friction force is written as

$$F_f = -\rho gAS_f dx \tag{9.4.12}$$

where the friction slope $S_f$ is derived from resistance equations such as Manning's equation.

*Contraction/expansion.* Abrupt contractions or expansions of the channel cause energy losses through eddy motion. Such losses are similar to minor losses in a pipe system. The magnitude of eddy losses is related to the change in velocity head $V^2/2g = (Q/A)^2/2g$ through the length of channel causing the losses. The drag forces creating these eddy losses are given by

$$F_e = -\rho gAS_e dx \tag{9.4.13}$$

where $S_e$ is the eddy loss slope

$$S_e = \frac{K_e}{2g}\frac{\partial(Q/A)^2}{\partial x} \tag{9.4.14}$$

in which $K_e$ is the nondimensional expansion or contraction coefficient, negative for channel expansion (where $\partial(Q/A)^2/\partial x$ is negative) and positive for channel contractions.

*Pressure.* Referring to Figure 9.4.1, the unbalanced pressure force is the resultant of the hydrostatic force on the each side of the control volume. Chow et al. (1988) provide a detailed derivation of the pressure force $F_p$ as simply

$$F_p = \rho gA\frac{\partial y}{\partial x}dx \tag{9.4.15}$$

The sum of the forces in equation (9.4.10) can be expressed, after substituting equations (9.4.11), (9.4.12), (9.4.13), and (9.4.15), as

$$\sum F = \rho AS_0 dx - \rho gAS_f dx - \rho gAS_e dx - \rho gA\frac{\partial y}{\partial x}dx \tag{9.4.16}$$

*Momentum.* The two momentum terms on the right-hand side of equation (9.4.9) represent the rate of change of storage of momentum in the control volume, and the net outflow of momentum across the control surface, respectively.

*Net momentum outflow.* The mass inflow rate to the control volume (equation (9.4.2)) is $-\rho(Q+qdx)$, representing both stream inflow and lateral inflow. The corresponding momentum is computed by multiplying the two mass inflow rates by their respective velocity and a *momentum correction factor* $\beta$:

$$\int_{\text{inlet}} \mathbf{V}\rho\mathbf{V}\,d\mathbf{A} = -\rho(\beta VQ + \beta v_x qdx) \tag{9.4.17}$$

where $-\rho\beta VQ$ is the momentum entering from the upstream end of the channel, and $-\rho\beta v_x qdx$ is the momentum entering the main channel with the lateral inflow, which has a velocity $v_x$ in the $x$

direction. The term $\beta$ is known as the *momentum coefficient* or *Boussinesq coefficient*; it accounts for the nonuniform distribution of velocity at a channel cross-section in computing the momentum. The value of $\beta$ is given by

$$\beta = \frac{1}{V^2 A}\int v^2 dA \tag{9.4.18}$$

where $v$ is the velocity through a small element of area $dA$ in the channel cross-section. The value of $\beta$ ranges from 1.01 for straight prismatic channels to 1.33 for river valleys with floodplains (Chow, 1959; Henderson, 1966).

The momentum leaving the control volume is

$$\int_{\text{outlet}} \mathbf{V}\rho\mathbf{V}\,\mathbf{dA} = \rho\left[\beta VQ + \frac{\partial(\beta VQ)}{\partial x}dx\right] \tag{9.4.19}$$

The net outflow of momentum across the control surface is the sum of equations (9.4.17) and (9.4.19):

$$\int_{\text{CS}} \mathbf{V}\rho\mathbf{V}\,\mathbf{dA} = -\rho(\beta VQ + \beta v_x q dx) + \rho\left[\beta VQ + \frac{\partial(\beta VQ)}{\partial x}dx\right] = -\rho\left[\beta v_x q - \frac{\partial(\beta VQ)}{\partial x}\right]dx \tag{9.4.20}$$

*Momentum storage.* The time rate of change of momentum stored in the control volume is found by using the fact that the volume of the elemental channel is $Adx$, so its momentum is $\rho AdxV$, or $\rho Qdx$, and then

$$\frac{d}{dt}\int_{\text{CV}} \mathbf{V}\rho d\forall = \rho\frac{\partial Q}{\partial x}dx \tag{9.4.21}$$

After substituting the force terms from equation (9.4.16) and the momentum terms from equations (9.4.20) and (9.4.21) into the momentum equation (9.4.9), it reads

$$\rho gAS_0 dx - \rho gAS_f dx - \rho gAS_e dx - \rho gA\frac{\partial y}{\partial x}dx = -\rho\left[\beta v_x q - \frac{\partial(\beta VQ)}{\partial x}\right]dx + \rho\frac{\partial Q}{\partial t}dx \tag{9.4.22}$$

Dividing through by $\rho dx$, replacing $V$ with $Q/A$, and rearranging produces the conservation form of the momentum equation:

$$\frac{\partial Q}{\partial t} + \frac{\partial(\beta Q^2/A)}{\partial t} + gA\left(\frac{\partial y}{\partial x} - S_0 + S_f + S_e\right) - \beta q v_x = 0 \tag{9.4.23}$$

The depth $y$ in equation (9.4.23) can be replaced by the water surface elevation $h$, using

$$h = y + z \tag{9.4.24}$$

where $z$ is the elevation of the channel bottom above a datum such as mean sea level. The derivative of equation (9.4.24) with respect to the longitudinal distance $x$ along the channel is

$$\frac{\partial h}{\partial x} = \frac{\partial y}{\partial x} + \frac{\partial z}{\partial x} \tag{9.4.25}$$

but $\partial z/\partial x = -S_0$, so

$$\frac{\partial h}{\partial x} = \frac{\partial y}{\partial x} - S_0 \tag{9.4.26}$$

The momentum equation can now be expressed in terms of $h$ by using equation (9.4.26) in (9.4.23):

$$\frac{\partial Q}{\partial t} + \frac{\partial(\beta Q^2/A)}{\partial x} + gA\left(\frac{\partial h}{\partial x} + S_f + S_e\right) - \beta q v_x = 0 \tag{9.4.27}$$

The Saint-Venant equations, (9.4.6) for continuity and (9.4.27) for momentum, are the governing equations for one-dimensional, unsteady flow in an open channel. The use of the terms $S_f$ and $S_e$ in equation (9.4.27), which represent the rate of energy loss as the flow passes through the channel, illustrates the close relationship between energy and momentum considerations in describing the flow. Strelkoff (1969) showed that the momentum equation for the Saint-Venant equations can also be derived from energy principles, rather than by using Newton's second law as presented here.

The nonconservation form of the momentum equation can be derived in a similar manner to the nonconservation form of the continuity equation. Neglecting eddy losses, wind shear effect, and lateral inflow, the nonconservation form of the momentum equation for a unit width in the flow is

$$\frac{\partial V}{\partial t} + V\frac{\partial V}{\partial x} + g\left(\frac{\partial y}{\partial x} - S_0 + S_f\right) = 0 \tag{9.4.28}$$

## 9.5 KINEMATIC WAVE MODEL FOR CHANNELS

In Section 8.9, a kinematic wave overland flow runoff model was presented. This is an implicit nonlinear kinematic model that is used in the KINEROS model. This section presents a general discussion of the kinematic wave followed by a brief description of the very simplest linear models, such as those found in the U.S. Army Corps of Engineers HEC-HMS and HEC-1, and the more complicated models such as the KINEROS model (Woolhiser et al., 1990).

*Kinematic waves* govern flow when inertial and pressure forces are not important. Dynamic waves govern flow when these forces are important, as in the movement of a large flood wave in a wide river. In a kinematic wave, the gravity and friction forces are balanced, so the flow does not accelerate appreciably.

For a kinematic wave, the energy grade line is parallel to the channel bottom and the flow is steady and uniform ($S_0 = S_f$) within the differential length, while for a dynamic wave the energy grade line and water surface elevation are not parallel to the bed, even within a differential element.

### 9.5.1 Kinematic Wave Equations

A *wave* is a variation in a flow, such as a change in flow rate or water surface elevation, and the *wave celerity* is the velocity with which this variation travels along the channel. The celerity depends on the type of wave being considered and may be quite different from the water velocity. For a kinematic wave, the acceleration and pressure terms in the momentum equation are negligible, so the wave motion is described principally by the equation of continuity. The name kinematic is thus applicable, as *kinematics* refers to the study of motion exclusive of the influence of mass and force; in *dynamics* these quantities are included.

The kinematic wave model is defined by the following equations.

Continuity:

$$\frac{\partial Q}{\partial x} + \frac{\partial A}{\partial t} = q(x, t) \tag{9.5.1}$$

Momentum:

$$S_0 = S_f \tag{9.5.2}$$

where $q(x, t)$ is the net lateral inflow per unit length of channel.

The momentum equation can also be expressed in the form

$$A = \alpha Q^{\beta} \tag{9.5.3}$$

For example, Manning's equation written with $S_0 = S_f$ and $R = A/P$ is

$$Q = \frac{1.49 S_0^{1/2}}{n P^{2/3}} A^{5/3} \tag{9.5.4}$$

which can be solved for $A$ as

$$A = \left( \frac{n P^{2/3}}{1.49 \sqrt{S_0}} \right)^{3/5} Q^{3/5} \tag{9.5.5}$$

so $\alpha = [n P^{2/3}/(1.49\sqrt{S_0})]^{0.6}$ and $\beta = 0.6$ in this case.

Equation (9.5.1) contains two dependent variables, $A$ and $Q$, but $A$ can be eliminated by differentiating equation (9.5.3):

$$\frac{\partial A}{\partial t} = \alpha \beta Q^{\beta - 1} \left( \frac{\partial Q}{\partial t} \right) \tag{9.5.6}$$

and substituting for $\partial A/\partial t$ in equation (9.5.1) to give

$$\frac{\partial Q}{\partial x} + \alpha \beta Q^{\beta - 1} \left( \frac{\partial Q}{\partial t} \right) = q \tag{9.5.7}$$

Alternatively, the momentum equation could be expressed as

$$Q = aA^{B} \tag{9.5.8}$$

where $a$ and $B$ are defined using Manning's equation. Using

$$\frac{\partial Q}{\partial x} = \frac{dQ}{dA} \frac{\partial A}{\partial x} \tag{9.5.9}$$

the governing equation is

$$\frac{\partial A}{\partial t} + \frac{dQ}{dA} \frac{\partial A}{\partial x} = q \tag{9.5.10}$$

where $dQ/dA$ is determined by differentiating equation (9.5.8):

$$\frac{dQ}{dA} = aBA^{B-1} \tag{9.5.11}$$

and substituting in equation (9.5.10):

$$\frac{\partial A}{\partial t} + aBA^{B-1} \frac{\partial A}{\partial x} = q \tag{9.5.12}$$

The kinematic wave equation (9.5.7) has $Q$ as the dependent variable and the kinematic wave equation (9.5.12) has $A$ as the dependent variable. First consider equation (9.5.7), by taking the logarithm of (9.5.3):

$$\ln A = \ln \alpha + \beta \ln Q \tag{9.5.13}$$

and differentiating

$$\frac{dQ}{Q} = \frac{1}{\beta} \left( \frac{dA}{A} \right) \tag{9.5.14}$$

This defines the relationship between relative errors $dA/A$ and $dQ/Q$. For Manning's equation $\beta < 1$, so that the discharge estimation error would be magnified by the ratio $1/\beta$ if $A$ were the dependent variable instead of $Q$.

Next consider equation (9.5.12); by taking the logarithm of (9.5.8):

$$\ln Q = \ln a + B \ln A$$

$$\frac{dA}{A} = \frac{1}{B}\left(\frac{dQ}{Q}\right) \tag{9.5.15}$$

or

$$\frac{dQ}{Q} = B\left(\frac{dA}{A}\right) \tag{9.5.16}$$

In this case $\beta > 1$, so that the discharge estimation error would be decreased by $B$ if $A$ were the dependent variable instead of $Q$. In summary, if we use equation (9.5.3) as the form of the momentum equation, then $Q$ is the dependent variable with equation (9.5.7) being the governing equation; if we use equation (9.5.8) as the form of the momentum equation, then $A$ is the dependent variable with equation (9.5.12) being the governing equation.

### 9.5.2 U.S. Army Corps of Engineers Kinematic Wave Model for Overland Flow and Channel Routing

The HEC-1 (HEC-HMS) computer program actually has two forms of the kinematic wave. The first is based upon equation (9.5.12) where an explicit finite difference form is used (refer to Figures 9.5.1 and 8.9.2):

$$\frac{\partial A}{\partial t} = \frac{A_{i+1}^{j+1} - A_{i+1}^{j}}{\Delta t} \tag{9.5.17}$$

and

$$\frac{\partial A}{\partial x} = \frac{A_{i+1}^{j} - A_{i}^{j}}{\Delta x} \tag{9.5.18}$$

$$A = \frac{A_{i+1}^{j} + A_{i}^{j}}{2} \tag{9.5.19}$$

$$q = \frac{q_{i+1}^{j+1} + q_{i+1}^{j}}{2} \tag{9.5.20}$$

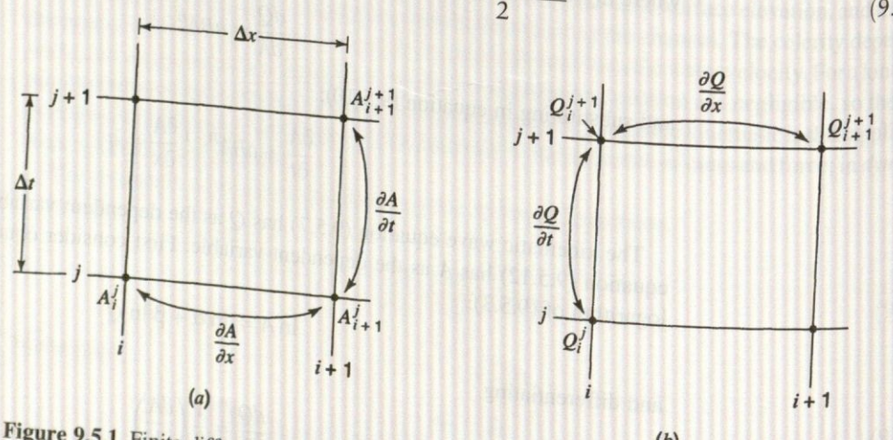


**Figure 9.5.1** Finite difference forms. (*a*) HEC-1 "standard form;" (*b*) HEC-1 "conservation form."

Substituting these finite-difference approximations into equation (9.5.12) gives

$$\frac{1}{\Delta t}(A_{i+1}^{j+1} - A_{i+1}^{j}) + aB\left[\frac{A_{i+1}^{j} + A_{i}^{j}}{2}\right]^{B-1}\left[\frac{A_{i+1}^{j} - A_{i}^{j}}{\Delta x}\right] = \frac{q_{i+1}^{j+1} + q_{i+1}^{j}}{2} \tag{9.5.21}$$

The only unknown in equation (9.5.21) is $A_{i+1}^{j+1}$, so

$$A_{i+1}^{j+1} = A_{i+1}^{j} - aB\left(\frac{\Delta t}{\Delta x}\right)\left[\frac{A_{i+1}^{j} + A_{i}^{j}}{2}\right]^{B-1}(A_{i+1}^{j} - A_{i,j}) + (q_{i+1}^{j+1} + q_{i+1}^{j})\frac{\Delta t}{2} \tag{9.5.22}$$

After computing $A_{i+1}^{j+1}$ at each grid along a time line going from upstream to downstream (see Figure 8.9.2), compute the flow using equation (9.5.8):

$$Q_{i+1}^{j+1} = a(A_{i+1}^{j+1})^{B} \tag{9.5.23}$$

The HEC-1 model uses the above kinematic wave model as long as a stability factor $R < 1$ (Alley and Smith, 1987), defined by

$$R = \frac{a}{q\Delta x}\left[\left(q\Delta t + A_{i}^{j}\right)^{B} - \left(A_{i}^{j}\right)^{B}\right] \text{ for } q > 0 \tag{9.5.24a}$$

$$R = aB(A_{i}^{j})^{B-1}\frac{\Delta t}{\Delta x} \text{ for } q = 0 \tag{9.5.24b}$$

Otherwise the form of equation (9.5.1) is used, where (see Figure 9.5.1)

$$\frac{\partial Q}{\partial x} = \frac{Q_{i+1}^{j+1} - Q_{i}^{j+1}}{\Delta x} \tag{9.5.25}$$

$$\frac{\partial A}{\partial t} = \frac{A_{i}^{j+1} - A_{i}^{j}}{\Delta t} \tag{9.5.26}$$

so

$$\frac{Q_{i+1}^{j+1} - Q_{i}^{j+1}}{\Delta x} + \frac{A_{i}^{j+1} - A_{i}^{j}}{\Delta x} = q \tag{9.5.27}$$

Solving for the only unknown $Q_{i+1}^{j+1}$ yields

$$Q_{i+1}^{j+1} = Q_{i}^{j+1} + q\Delta x - \frac{\Delta x}{\Delta t}(A_{i}^{j+1} - A_{i}^{j}) \tag{9.5.28}$$

Then solve for $A_{i+1}^{j+1}$ using equation (9.5.23):

$$A_{i+1}^{j+1} = \left(\frac{1}{a}Q_{i+1}^{j+1}\right)^{1/B} \tag{9.5.29}$$

The *initial condition* (values of $A$ and $Q$ at time 0 along the grid, referring to Figure 8.9.2) are computed assuming uniform flow or nonuniform flow for an initial discharge. The *upstream boundary* is the inflow hydrograph from which $Q$ is obtained.

The kinematic wave schemes used in the HEC-1 (HEC-HMS) model are very simplified. Chow, et al. (1988) presented both linear and nonlinear kinematic wave schemes based upon the equation (9.5.7) formulation. An example of a more desirable kinematic wave formulation is that by Woolhiser et al. (1990) presented in the next subsection.

### 9.5.3 KINEROS Channel Flow Routing Model

The KINEROS channel routing model uses the equation (9.5.10) form of the kinematic wave equation (Woolhiser et al., 1990):

$$\frac{\partial A}{\partial t} + \frac{dQ}{dA}\frac{\partial A}{\partial x} = q(x, t) \tag{9.5.10}$$

where $q(x, t)$ is the net lateral inflow per unit length of channel. The derivatives are approximated using an implicit scheme in which the spatial and temporal derivatives are, respectively,

$$\frac{\partial A}{\partial x} = \theta\frac{A_{i+1}^{j+1} - A_i^{j+1}}{\Delta x} + (1-\theta)\frac{A_{i+1}^{j} - A_i^{j}}{\Delta x} \tag{9.5.30}$$

$$\frac{dQ}{dA}\frac{\partial A}{\partial x} = \theta\left(\frac{dQ}{dA}\right)^{j+1}\left(\frac{A_{i+1}^{j+1} - A_i^{j+1}}{\Delta x}\right) + (1-\theta)\left(\frac{dQ}{dA}\right)^{j+1}\left(\frac{A_{i+1}^{j} - A_i^{j}}{\Delta x}\right) \tag{9.5.31}$$

and

$$\frac{\partial A}{\partial t} = \frac{1}{2}\left[\frac{A_i^{j+1} - A_i^{j}}{\Delta t} + \frac{A_{i+1}^{j+1} - A_{i+1}^{j}}{\Delta t}\right] \tag{9.5.32}$$

or

$$\frac{\partial A}{\partial t} = \frac{A_i^{j+1} + A_{i+1}^{j+1} - A_i^{j} - A_{i+1}^{j}}{2\Delta t} \tag{9.5.33}$$

Substituting equations (9.5.31) and (9.5.33) into (9.5.10), we have

$$\frac{A_{i+1}^{j+1} - A_{i+1}^{j} + A_i^{j+1} - A_i^{j}}{2\Delta t} + \left\{\theta\left[\left(\frac{dQ}{dA}\right)^{j+1}\left(\frac{A_{i+1}^{j+1} - A_i^{j+1}}{\Delta x}\right)\right] + (1-\theta)\left[\left(\frac{dQ}{dA}\right)^{j+1}\left(\frac{A_{i+1}^{j} - A_i^{j}}{\Delta x}\right)\right]\right\}$$
$$= \frac{1}{2}(q_{i+1}^{j+1} + q_i^{j+1} + q_{i+1}^{j} + q_i^{j}) \tag{9.5.34}$$

The only unknown in this equation is $A_{i+1}^{j+1}$, which must be solved for numerically by use of an iterative scheme such as the Newton-Raphson method (see Appendix A).

Woolhiser et al. (1990) use the following relationship between channel discharge and cross-sectional area, which embodies the kinematic wave assumption:

$$Q = \alpha R^{m-1} A \tag{9.5.35}$$

where $R$ is the hydraulic radius and $\alpha = 1.49S^{1/2}/n$ and $m = 5/3$ for Manning's equation.

### 9.5.4 Kinematic Wave Celerity

Kinematic waves result from changes in $Q$. An increment in flow $dQ$ can be written as

$$dQ = \frac{\partial Q}{\partial x}dx + \frac{\partial Q}{\partial t}dt \tag{9.5.36}$$

Dividing through by $dx$ and rearranging produces:

$$\frac{\partial Q}{\partial x} + \frac{dt}{dx}\frac{\partial Q}{\partial t} = \frac{dQ}{dx} \tag{9.5.37}$$

## 9.6 MUSKIN

Equations (9.5.7) and (9.5.37) are identical if

$$\frac{dQ}{dx} = q \tag{9.5.38}$$

and

$$\frac{dx}{dt} = \frac{1}{\alpha\beta Q^{\beta-1}} \tag{9.5.39}$$

Differentiating equation (9.5.3) and rearranging gives

$$\frac{dQ}{dA} = \frac{1}{\alpha\beta Q^{\beta-1}} \tag{9.5.40}$$

and by comparing equations (9.5.39) and (9.5.40), it can be seen that

$$\frac{dx}{dt} = \frac{dQ}{dA} \tag{9.5.41}$$

or

$$c_k = \frac{dx}{dt} = \frac{dQ}{dA} \tag{9.5.42}$$

where $c_k$ is the kinematic wave celerity. This implies that an observer moving at a velocity $dx/dt = c_k$ with the flow would see the flow rate increasing at a rate of $dQ/dx = q$. If $q = 0$, the observer would see a constant discharge. Equations (9.5.38) and (9.5.42) are the *characteristic equations* for a kinematic wave, two ordinary differential equations that are mathematically equivalent to the governing continuity and momentum equations.

The kinematic wave celerity can also be expressed in terms of the depth $y$ as

$$c_k = \frac{1}{B}\frac{dQ}{dy} \tag{9.5.43}$$

where $dA = Bdy$.

Both kinematic and dynamic wave motion are present in natural flood waves. In many cases the channel slope dominates in the momentum equation; therefore, most of a flood wave moves as a kinematic wave. Lighthill and Whitham (1955) proved that the velocity of the main part of a natural flood wave approximates that of a kinematic wave. If the other momentum terms $\left(\partial V/\partial t,\ V(\partial V/\partial x) \text{ and } (1/g)\partial y/\partial x\right)$ are not negligible, then a dynamic wave front exists that can propagate both upstream and downstream from the main body of the flood wave.

## 9.6 MUSKINGUM–CUNGE MODEL

Cunge (1969) proposed a variation of the kinematic wave method based upon the Muskingum method (see Chapter 8). With the grid shown in Figure 9.6.1, the unknown discharge $Q_{i+1}^{j+1}$ can be expressed using the Muskingum equation $(Q_{j+1} = C_1 I_{j+1} + C_2 I_j + C_3 Q_j)$:

$$Q_{i+1}^{j+1} = C_1 Q_i^{j+1} + C_2 Q_i^j + C_3 Q_{i+1}^j \tag{9.6.1}$$

where $Q_{i+1}^{j+1} = Q_{j+1}$; $Q_i^{j+1} = I_{j+1}$; $Q_i^j = I_j$; and $Q_{i+1}^j = Q_j$. The Muskingum coefficients are

$$C_1 = \frac{\Delta t - 2KX}{2K(1-X) + \Delta t} \tag{9.6.2}$$

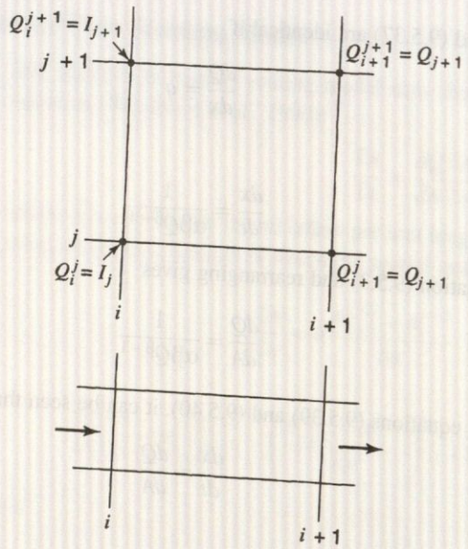


**Figure 9.6.1** Finite-difference grid for the Muskingum–Cunge method.

$$C_2 = \frac{\Delta t + 2KX}{2K(1-X) + \Delta t} \tag{9.6.3}$$

$$C_3 = \frac{2K(1-X) - \Delta t}{2K(1-X) + \Delta t} \tag{9.6.4}$$

Cunge (1969) showed that when $K$ and $\Delta t$ are considered constant, equation (9.6.1) is an approximate solution of the kinematic wave. He further demonstrated that equation (9.6.1) can be considered an approximation of a modified diffusion equation if

$$K = \frac{\Delta x}{c_k} = \frac{\Delta x}{dQ/dA} \tag{9.6.5}$$

and

$$X = \frac{1}{2}\left(1 - \frac{Q}{Bc_k S_0 \Delta x}\right) \tag{9.6.6}$$

where $c_k$ is the celerity corresponding to $Q$ and $B$, and $B$ is the width of the water surface. The value of $\Delta x/(dQ/dA)$ in equation (9.6.5) represents the time propagation of a given discharge along a channel reach of length $\Delta x$. Numerical stability requires $0 \leq X \leq 1/2$. The solution procedure is basically the same as the kinematic wave.

## 9.7 IMPLICIT DYNAMIC WAVE MODEL

The conservation form of the Saint-Venant equations is used because this form provides the versatility required to simulate a wide range of flows from gradual long-duration flood waves in rivers to abrupt waves similar to those caused by a dam failure. The equations are developed from equations (9.4.6) and (9.4.25) as follows.

Weighted four-point finite-difference approximations given by equations (9.7.1)–(9.7.3) are used for dynamic routing with the Saint-Venant equations. The spatial derivatives $\partial Q/\partial x$ and $\partial h/\partial x$ are

estimated between adjacent time lines:

$$\frac{\partial Q}{\partial x} = \theta \frac{Q_{i+1}^{j+1} - Q_i^{j+1}}{\Delta x_i} + (1-\theta)\frac{Q_{i+1}^{j} - Q_i^{j}}{\Delta x_i} \tag{9.7.1}$$

$$\frac{\partial h}{\partial x} = \theta \frac{h_{i+1}^{j+1} - h_i^{j+1}}{\Delta x_i} + (1-\theta)\frac{h_{i+1}^{j} - h_i^{j}}{\Delta x_i} \tag{9.7.2}$$

and the time derivatives are:

$$\frac{\partial (A+A_0)}{\partial t} = \frac{(A+A_0)_i^{j+1} + (A+A_0)_{i+1}^{j+1} - (A+A_0)_i^{j} - (A+A_0)_{i+1}^{j}}{2\Delta t_j} \tag{9.7.3}$$

$$\frac{\partial Q}{\partial t} = \frac{Q_i^{j+1} + Q_{i+1}^{j+1} - Q_i^{j} - Q_{i+1}^{j}}{2\Delta t_j} \tag{9.7.4}$$

The nonderivative terms, such as $q$ and $A$, are estimated between adjacent time lines, using:

$$q = \theta \frac{q_i^{j+1} + q_{i+1}^{j+1}}{2} + (1-\theta)\frac{q_i^{j} + q_{i+1}^{j}}{2} = \theta \overline{q}_i^{j+1} + (1-\theta)\overline{q}_i^{-j} \tag{9.7.5}$$

$$A = \theta \left[\frac{A_i^{j+1} + A_{i+1}^{j+1}}{2}\right] + (1-\theta)\left[\frac{A_i^{j} + A_{i+1}^{j}}{2}\right] = \theta \overline{A}_i^{j+1} + (1-\theta)\overline{A}_i^{-j} \tag{9.7.6}$$

where $\overline{q}_i$ and $\overline{A}_i$ indicate the lateral flow and cross-sectional area averaged over the reach $\Delta x_i$.

The finite-difference form of the continuity equation is produced by substituting equations (9.7.1), (9.7.3), and (9.7.5) into (9.4.6):

$$\begin{aligned} &\theta\left(\frac{Q_{i+1}^{j+1} - Q_i^{j+1}}{\Delta x_i} - \overline{q}_i^{j+1}\right) + (1-\theta)\left(\frac{Q_{i+1}^{j} - Q_i^{j}}{\Delta x_1} - \overline{q}_i^{j}\right) \\ &+ \frac{(A+A_0)_i^{j+1} + (A+A_0)_{i+1}^{j+1} - (A+A_0)_i^{j} - (A+A_0)_{i+1}^{j}}{2\Delta t_j} = 0 \end{aligned} \tag{9.7.7}$$

Similarly, the momentum equation (9.4.27) is written in finite-difference form as:

$$\begin{aligned} &\frac{Q_i^{j+1} + Q_{i+1}^{j+1} - Q_i^{j} - Q_{i+1}^{j}}{2\Delta t_j} \\ &+\theta\left[\frac{(\beta Q^2/A)_i^{j+1} - (\beta Q^2/A)_{i+1}^{j+1}}{\Delta x_i} + g\overline{A}_i^{j+1}\left(\frac{h_{i+1}^{j+1} - h_i^{j+1}}{\Delta x_i} + (\overline{S}_f)_i^{j+1} + (\overline{S}_e)_i^{j+1}\right) - (\overline{\beta q v_x})_i^{j+1}\right] \\ &+(1-\theta)\left[\frac{(\beta Q^2/A)_{i+1}^{j} - (\beta Q^2/A)_{i+1}^{j}}{\Delta x_i} + g\overline{A}_i^{j}\left(\frac{h_{i+1}^{j} - h_i^{j}}{\Delta x_i} + (\overline{S}_f)_i^{j} + (\overline{S}_e)_i^{j}\right) - (\overline{\beta q v_x})_i^{j}\right] = 0 \end{aligned} \tag{9.7.8}$$

The four-point finite-difference form of the continuity equation can be further modified by multiplying equation (9.7.7) by $\Delta x_i$ to obtain

$$\begin{aligned} &\theta\left(Q_{i+1}^{j+1} - Q_i^{j+1} - \overline{q}_i^{j+1}\Delta x_i\right) + (1-\theta)\left(Q_{i+1}^{j} - Q_i^{j} - \overline{q}_i^{j}\Delta x_i\right) \\ &+ \frac{\Delta x_i}{2\Delta t_i}\left[(A+A_0)_i^{j+1} + (A+A_0)_{i+1}^{j+1} - (A+A_0)_i^{j} - (A+A_0)_{i+1}^{j}\right] = 0 \end{aligned} \tag{9.7.9}$$

Similarly, the momentum equation can be modified by multiplying by $\Delta x_i$ to obtain

$$\frac{\Delta x_i}{2\Delta t_j}\left(Q_i^{j+1}+Q_{i+1}^{j+1}-Q_i^j-Q_{i+1}^j\right)$$

$$+\theta\left\{\left(\frac{\beta Q^2}{A}\right)_{i+1}^{j+1}-\left(\frac{\beta Q^2}{A}\right)_i^{j+1}+g\overline{A}_i^{j+1}\left[h_{i+1}^{j+1}-h_i^{j+1}+\left(\overline{S}_f\right)_i^{j+1}+\left(\overline{S}_e\right)_i^{j+1}\Delta x_i\right]-\left(\overline{\beta q v_x}\right)_i^{j+1}\Delta x_i\right\}$$

$$+(1-\theta)\left\{\left(\frac{\beta Q^2}{A}\right)_{i+1}^{j}-\left(\frac{\beta Q^2}{A}\right)_i^{j}+g\overline{A}_i^{j}\left[h_{i+1}^{j}-h_i^{j}+\left(\overline{S}_f\right)_i^{j}\Delta x_i+\left(\overline{S}_e\right)_i^{j}\Delta x_i\right]-\left(\overline{\beta q v_x}\right)_i^{j}\Delta x_i\right\}=0 \tag{9.7.10}$$

where the average values (marked with an overbar) over a reach are defined as

$$\overline{\beta}_i=\frac{\beta_i+\beta_{i+1}}{2} \tag{9.7.11}$$

$$\overline{A}_i=\frac{A_i+A_{i+1}}{2} \tag{9.7.12}$$

$$\overline{B}_i=\frac{B_i+B_{i+1}}{2} \tag{9.7.13}$$

$$\overline{Q}_i=\frac{Q_i+Q_{i+1}}{2} \tag{9.7.14}$$

Also,

$$\overline{R}_i=\overline{A}_i/\overline{B}_i \tag{9.7.15}$$

for use in Manning's equation. Manning's equation may be solved for $S_f$ and written in the form shown below, where the $|Q|Q$ has magnitude $Q^2$ and sign positive or negative depending on whether the flow is downstream or upstream, respectively:

$$\left(\overline{S}_f\right)_i=\frac{\overline{n}_i^2|\overline{Q}_i|\overline{Q}_i}{2.208\overline{A}_i^2\overline{R}_i^{4/3}} \tag{9.7.16}$$

The minor headlosses arising from contraction and expansion of the channel are proportional to the difference between the squares of the downstream and upstream velocities, with a contraction/expansion loss coefficient $K_e$:

$$\left(\overline{S}_e\right)_i=\frac{(K_e)_i}{2g\Delta x_i}\left[\left(\frac{Q}{A}\right)_{i+1}^2-\left(\frac{Q}{A}\right)_i^2\right] \tag{9.7.17}$$

The terms having superscript $j$ in equations (9.7.9) and (9.7.10) are known either from initial conditions or from a solution of the Saint-Venant equations for a previous time line. The terms $g$, $\Delta x_i$, $\beta_i$, $K_e$, $C_w$, and $V_w$ are known and must be specified independently of the solution. The unknown terms are $Q_i^{j+1}$, $Q_{i+1}^{j+1}$, $h_{i+1}^{j+1}$, $A_i^{j+1}$, $A_{i+1}^{j+1}B_i^{j+1}$, and $B_{i+1}^{j+1}$. However, all the terms can be expressed as functions of the unknowns $Q_i^{j+1}$, $Q_{i+1}^{j+1}$, $h_i^{j+1}$, and $h_{i+1}^{j+1}$, so there are actually four unknowns. The unknowns are raised to powers other than unity, so equations (9.7.9) and (9.7.10) are nonlinear equations.

The continuity and momentum equations are considered at each of the $N$-1 rectangular grids shown in Figure 9.7.1 between the upstream boundary at $i = 1$ and the downstream boundary at

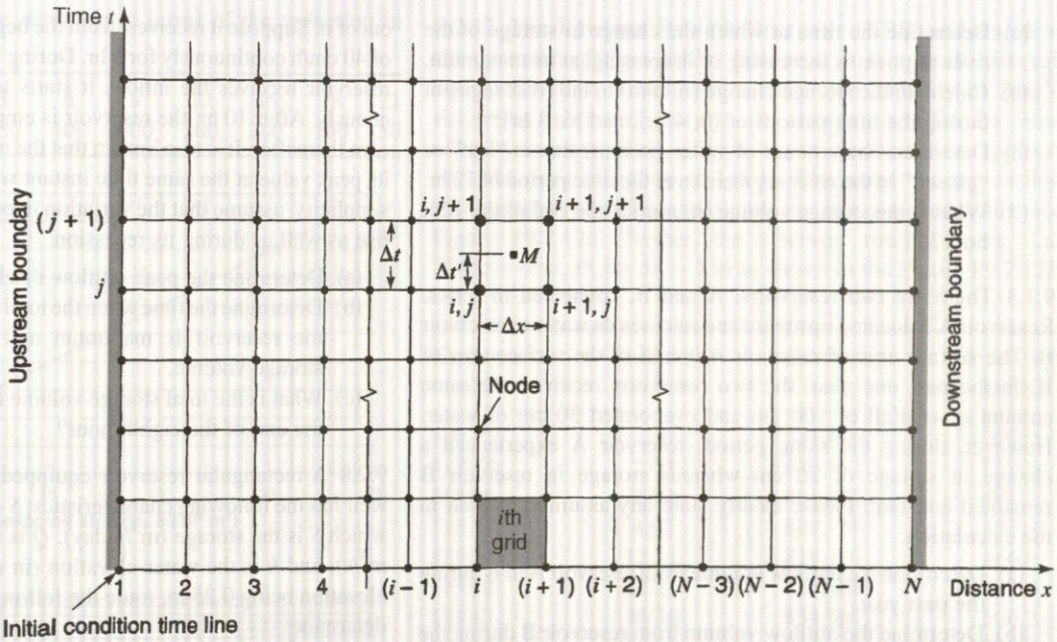


**Figure 9.7.1** The $x$-$t$ solution plane. The finite-difference forms of the Saint–Venant equations are solved at a discrete number of points (values of the independent variables $x$ and $t$) arranged to form the rectangular grid shown. Lines parallel to the time axis represent locations along the channel, and those parallel to the distance axis represent times (from Fread (1974)).

$i = N$. This yields $2N$-2 equations. There are two unknowns at each of the $N$ grid points ($Q$ and $h$), so there are $2N$ unknowns in all. The two additional equations required to complete the solution are supplied by the upstream and downstream boundary conditions. The upstream boundary condition is usually specified as a known inflow hydrograph, while the downstream boundary condition can be specified as a known stage hydrograph, a known discharge hydrograph, or a known relationship between stage and discharge, such as a rating curve. The U.S. National Weather Service FLDWAV model (hsp.nws.noaa.gov/oh/hrl/rvmech) uses the above to describe the implicit dynamic wave model formulation.

## PROBLEMS

9.1.1 Consider a river segment with the surface area of 5 km$^2$. For a given flood event, the measured time variation of inflow rate (called inflow hydrograph) at the upstream section of the river segment and the outflow hydrograph at the downstream section are shown in Figure P9.1.1. Assume that the initial storage of water in the river segment is 10 mm in depth.

(a) Determine the time at which the change in storage of the river segment is increasing, decreasing, and at its maximum.
(b) Calculate the storage change (in mm) in the river segment during the time periods of [0, 4 hr], and [6, 8 hr].
(c) Determine the amount of water (in mm) that is 'lost' or 'gained' in the river segment over the time period of 12 hours.
(d) What is the storage volume (in mm) at the end of the twelfth hour?

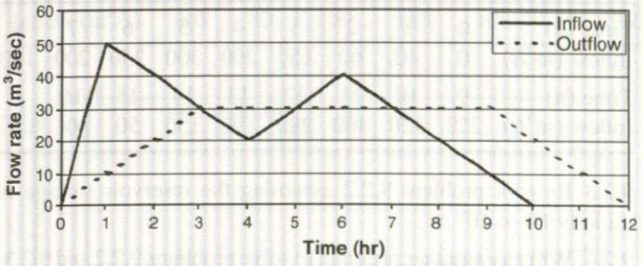


**Figure P9.1.1**

9.1.2 Consider a river segment with the surface area of 5 km$^2$. For a given flood event, the measured time variation of inflow rate (called inflow hydrograph, in m$^3$/sec) at the upstream section of the river segment and the outflow hydrograph at the downstream section are shown in Figure P9.1.1. Assume that the initial storage of water in the river segment is 10 mm in depth.

(a) Determine the time at which the change in storage of the river segment is increasing or decreasing, at its maximum.
(b) Calculate the storage change (in mm) in the river segment during the time periods of [0, 4 hr], and [6, 8 hr].
(c) Determine the amount of water (in mm) that is "lost" or "gained" in the river segment over the time period of 12 hr.
(d) What is the storage volume (in mm) at the end of the 12th hour?

9.1.3 There are two reservoirs, A and B, connected in series. Reservoir A is located upstream and releases its water to reservoir B. The surface area of reservoir A is half of the surface area of B. In the past one year, the two reservoirs received the same amount of rainfall of 100 cm and evaporated 30 cm of water. However, during the same period, reservoir A experienced a change in storage of 20 cm whereas storage in reservoir B remained constant. Please clearly state any assumption used in the calculation.

(a) Determine the outflow volume from reservoir A to B during the past year.
(b) Determine the outflow volume from reservoir B during the past year.
(c) How big is the flow rate from reservoir B as compared with that of reservoir A?

9.2.1 The storage-outflow characteristics for a reservoir are given below. Determine the storage-outflow function $2S/\Delta t + Q$ versus $Q$ for each of the tabulated values using $\Delta t = 1.0$ hr. Plot a graph of the storage-outflow function.

| Storage ($10^6$ m$^3$) | 70 | 80 | 85 | 100 | 115 |
|---|---|---|---|---|---|
| Outflow (m$^3$/s) | 0 | 50 | 150 | 350 | 700 |

9.2.2 Route the inflow hydrograph given below through the reservoir with the storage-outflow characteristics given in problem 9.2.1 using the level pool method. Assume the reservoir has an initial storage of $70 \times 10^6$ m$^3$.

| Time (h) | 0 | 1 | 2 | 3 | 4 | 5 | 6 | 7 | 8 |
|---|---|---|---|---|---|---|---|---|---|
| Inflow (m$^3$/s) | 0 | 40 | 60 | 150 | 200 | 300 | 250 | 200 | 180 |
| Time (h) | 9 | 10 | 11 | 12 | 13 | 14 | 15 | 16 | |
| Inflow (m$^3$/s) | 220 | 320 | 400 | 280 | 190 | 150 | 50 | 0 | |

9.2.3 Rework problem 9.2.2 assuming the reservoir storage is initially $80 \times 10^6$ m$^3$.

9.2.4 Write a computer program to solve problems 9.2.2 and 9.2.3.

9.2.5 Rework example 9.2.2 using a 1.5-acre detention basin.

9.2.6 Rework example 9.2.2 using a triangular inflow hydrograph that increases linearly from zero to a peak of 90 cfs at 120 min and then decreases linearly to a zero discharge at 240 min. Use a 30-min routing interval.

9.2.7 Consider a reservoir with surface area of 1 km$^2$. Initially, the reservoir has a storage volume of 500,000 m$^3$ with no flow coming out of it. Suppose it receives, from the beginning, a uniform inflow of 40 cm/h continuously for 5 hr. During the time instant when the reservoir receives the inflow, it starts to release water simultaneously. After 10 hr, the reservoir is empty and outflow becomes zero thereafter. It is also known that the outflow discharge reaches its peak value at the same time instant when the inflow stops. For simplicity, assume that the variation in outflow is linear during its rise as well as during its recession.

(a) Determine the peak outflow discharge in m$^3$/s.
(b) Determine the time when the total storage volume (in m$^3$) in the reservoir is maximum and its corresponding total storage volume.
(c) What is the total storage volume (in m$^3$) in the reservoir at the end of the eighth hour?

9.2.8 A rectangular reservoir equipped with an outflow-control weir has the following characteristics: $S = 5 \times h$ and $Q = 2 \times h$, in which $S$ is the storage (m$^3$/s-day), $Q$ is the outflow discharge (in m$^3$/s), and $h$ is the water elevation (in m). With an initial water elevation being 0.25 m, route the following inflow hydrograph to determine:

(a) the percentage of reduction in peak discharge by the reservoir; and
(b) the peak water surface elevation.

| Time | 6:00 am | 9:00 am | 12:00 nn | 3:00 pm | 6:00 pm |
|---|---|---|---|---|---|
| Inflow (m$^3$/S) | 30 | 120 | 450 | 300 | 30 |

9.2.9 A rectangular detention basin is equipped with an outlet. The basin storage-elevation relationship and outflow-elevation relationship can be described by the following simple equations:

Storage-elevation relation: $S = 10 \times h$;
Outflow-elevation relation: $Q = 2 \times h^2$

in which $S$ is the storage (in m$^3$/s-hr), $Q$ is the outflow discharge (in m$^3$/s), and $h$ is the water elevation (in m). With an initial water elevation being 0.25 m, route the following inflow hydrograph to determine:

(a) the percentage of reduction in peak discharge by the reservoir; and
(b) the peak water surface elevation.

| Time | 1:00 pm | 2:00 pm | 3:00 pm | 4:00 pm | 5:00 pm | 6:00 pm |
|---|---|---|---|---|---|---|
| Inflow (m$^3$/s) | 5 | 20 | 75 | 50 | 15 | 5 |

9.2.10 To investigate the effectiveness of a flood control reservoir, a 100-year design flood hydrograph is used as an input in the routing exercise. The reservoir has a surface area of 250 hectares and its only outlet is an uncontrolled spillway located 5 m above the datum. The design flood hydrograph is given in the following table and other physical characteristics of the reservoir are provided in the Figures P9.2.10*a* and *b*. Assuming that the initial reservoir level is 4 m above the datum, determine

the effectiveness of the reservoir in terms of the reduction in inflow peak discharge.

| Time (hr) | 0 | 3 | 6 | 9 | 12 | 15 | 18 | 21 |
|---|---|---|---|---|---|---|---|---|
| Inflow ($m^3/s$) | 50 | 200 | 400 | 600 | 300 | 200 | 100 | 50 |

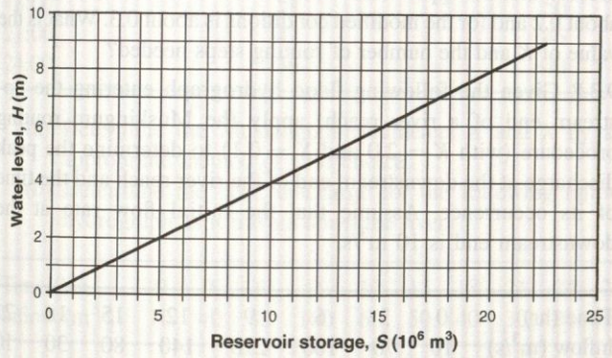


(*a*)

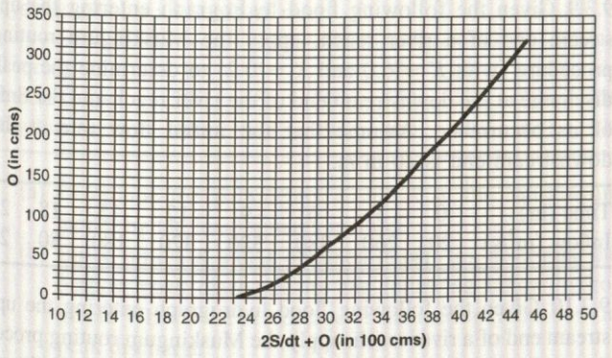


(*b*)

**Figure P9.2.10** (*a*) Reservoir water level storage curve; (*b*) Reservoir routing curve.

9.2.11 To investigate the effectiveness of a flood control reservoir, a 100-year design flood hydrograph is used as input in the routing exercise. The reservoir has only one flow outlet located on the spillway crest with the elevation of 104 m. The reservoir has the elevation-storage-discharge relationship shown in Table 9.2.11(a). Given the design flood hydrograph as shown in Table 9.2.11(b) and assuming that the initial reservoir elevation level is at 103 m, determine the effectiveness of the reservoir in terms of the reduction in inflow peak discharge. (Note: 1 hectare = 0.01 $km^2$)

**Table 9.2.11(a)** Reservoir Elevation-Storage-Outflow Relation

| Elevation (m) | 100 | 101 | 102 | 103 | 104 | 105 | 106 | 107 |
|---|---|---|---|---|---|---|---|---|
| Storage ($\times 10^5 m^3$) | 50 | 60 | 70 | 80 | 92 | 105 | 120 | 140 |
| Outflow ($m^3/s$) | 0 | 0 | 0 | 0 | 8 | 17 | 27 | 40 |

**Table 9.2.11(b)** Inflow Hydrograph

| Time (hr) | 0 | 12 | 24 | 36 | 48 | 60 | 72 | 84 |
|---|---|---|---|---|---|---|---|---|
| Inflow ($m^3/s$) | 10 | 20 | 30 | 40 | 30 | 25 | 15 | 10 |

9.2.12 The Kowloon Bywash Reservoir (KBR) is located on the upstream of the Lai Chi Kok area. It is a small reservoir equipped with a tunnel with a maximum capacity of 2 $m^3/s$ delivering reservoir water to the downstream Tai Po Road water treatment plant. There is an uncontrolled spillway with the crest elevation at 115 m. The stage-volume-outflow relationships of KBR are shown in the attached table and Figure P9.2.12*a*. Further, the reservoir routing curve, i.e., $2S/\Delta t + O$ vs. $O$, for $\Delta t = 1$ hr is shown in the Figure P9.2.12*b*.

| Elevation (mPD) | Outflow ($m^3/s$) | Storage ($m^3$) | $2S/\Delta t + O$ ($m^3/s$) |
|---|---|---|---|
| 109.73 | 2.00 | 531,000 | 297.0 |
| 112.78 | 2.00 | 679,182 | 379.3 |
| 115.06 | 2.00 | 801,442 | 447.2 |
| 115.22 | 4.02 | 809,759 | 453.9 |
| 115.37 | 12.11 | 818,107 | 466.6 |
| 115.52 | 22.21 | 826,488 | 481.4 |
| 115.67 | 36.36 | 834,901 | 500.2 |
| 115.83 | 51.50 | 843,347 | 520.0 |
| 115.98 | 69.72 | 851,824 | 543.0 |
| 116.13 | 89.93 | 860,333 | 567.9 |
| 116.28 | 114.20 | 868,874 | 596.9 |
| 116.44 | 136.43 | 877,447 | 623.9 |
| 116.59 | 162.72 | 886,051 | 655.0 |
| 116.74 | 193.03 | 894,688 | 690.1 |
| 116.89 | 228.40 | 903,355 | 730.3 |

Consider the inflow hydrograph given in the table below. Determine the peak outflow discharge from the KBR and the corresponding water surface elevation and the storage volume. Assume that the initial storage in the reservoir is 500,000 $m^3$.

| Time (hr) | 1 | 2 | 3 | 4 | 5 | 6 | 7 |
|---|---|---|---|---|---|---|---|
| Inflow ($m^3/s$) | 10 | 80 | 200 | 150 | 100 | 60 | 20 |

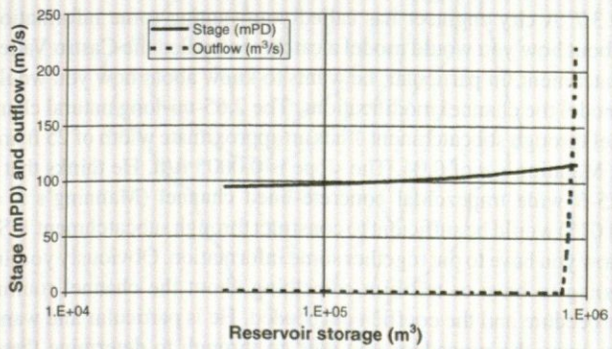


(*a*)

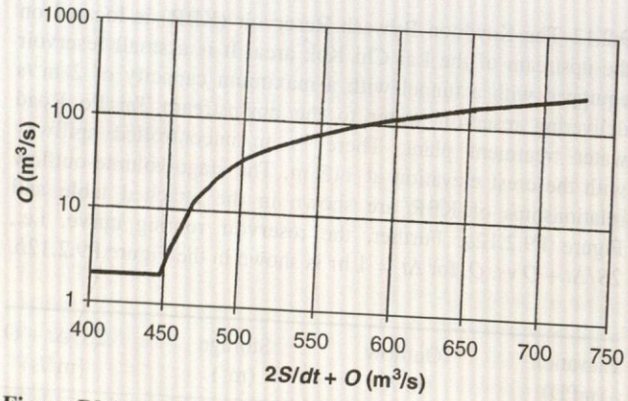


**Figure P9.2.12** (*a*) Stage-Storage-Outflow relationship; (*b*) Reservoir routing curve

9.3.1 Rework example 9.3.4 using $\Delta t = 2$ hr.

9.3.2 Rework example 9.3.4 assuming $X = 0.3$.

9.3.3 Rework example 9.3.4 assuming $K = 1.4$ hr.

9.3.4 Calculate the Muskingum routing $K$ and number of routing steps for a 1.25-mi long channel. The average cross-section dimensions for the channel are a base width of 25 ft and an average depth of 2.0 ft. Assume the channel is rectangular and has a Manning's $n$ of 0.04 and a slope of 0.009 ft/ft.

9.3.5 Route the following upstream inflow hydrograph through a downstream flood control channel reach using the Muskingum method. The channel reach has a $K = 2.5$ hr and $X = 0.2$. Use a routing interval of 1 hr.

| Time (h) | 1 | 2 | 3 | 4 | 5 | 6 | 7 |
|---|---|---|---|---|---|---|---|
| Inflow (cfs) | 90 | 140 | 208 | 320 | 440 | 550 | 640 |
| Time (h) | 8 | 9 | 10 | 11 | 12 | 13 | 14 |
| Inflow (cfs) | 680 | 690 | 630 | 570 | 470 | 390 | 360 |
| Time (h) | 15 | 16 | 17 | 18 | 19 | 20 | |
| Inflow (cfs) | 330 | 250 | 180 | 130 | 100 | 90 | |

9.3.6 Use the U.S. Army Corps of Engineers HEC-HMS computer program to solve Problem 9.3.5.

9.3.7 A city engineer has called you wanting some information about how you would model a catchment called the Castro Valley catchment. In particular, he wants to know about how you would model the channel modifications. The 2.65-mi-long natural channel through subcatchment 1 has an approximate width of 25 ft and a Manning's $n$ of 0.04. The slope is 0.0005 ft/ft. He thinks that a 25-ft wide trapezoidal concrete-lined channel (Manning's $n$ = 0.015) would be sufficient to construct through subcatchment 1. So now you have to put together some information. Obviously you are going to have to tell him something about the channel routing procedure and the coefficients needed. He is particular and wants to know the procedure you will go through to determine these, including the number of routing steps. The natural and the concrete channels can be considered as wide-rectangular channels for your calculations so that the hydraulic radius can be approximated as the channel depth. At this time you don't know any peak discharges because you have not done any hydrologic calculations but yet you still need to approximate the $X$ and $K$ for the $C_1$, $C_2$, and $C_3$ and the number of steps for the routing method. You have decided that the approximate value of $X$ for natural conditions is about 0.2 and for the modified conditions is about 0.3. What is the value of $K$ and the number of routing steps needed?

9.3.8 Given the following flood hydrograph entering the upstream end of a river reach, apply the Muskingum routing procedure (with $K = 2.0$ and $X = 0.1$) to determine the peak discharge at the downstream end of the river reach and the time of its occurrence. Assume that the initial flow rate at the downstream end is 10 $m^3/s$.

| Time (hr) | 0 | 3 | 6 | 9 | 12 | 15 | 18 | 21 |
|---|---|---|---|---|---|---|---|---|
| Inflow ($m^3/s$) | 10 | 70 | 160 | 210 | 140 | 80 | 30 | 10 |

9.3.9 Given the following flood hydrograph entering the upstream end of a river reach, apply the Muskingum routing procedure (with $K = 6.0$ and $X = 0.2$) to determine the peak discharge at the downstream end of the river reach and the time of its occurrence. Assume that the initial flow rate at the downstream end is 20 $m^3/s$.

| Time (hr) | 0 | 3 | 6 | 9 | 12 | 15 | 18 | 21 |
|---|---|---|---|---|---|---|---|---|
| Inflow ($m^3/s$) | 20 | 260 | 380 | 580 | 320 | 180 | 80 | 20 |

9.3.10 Given the following flood hydrograph entering the upstream end of a river reach, apply the Muskingum routing procedure (with $K = 5.0$ hr and $X = 0.2$) to determine the peak discharge at the downstream end of the river reach and the time of its occurrence. Assume that the initial flow rate at the downstream end is 10 $m^3/s$.

| Time (hr) | 0 | 2 | 4 | 6 | 8 | 10 | 12 |
|---|---|---|---|---|---|---|---|
| Inflow ($m^3/s$) | 10 | 150 | 400 | 350 | 200 | 80 | 10 |

9.3.11 The table given below lists the inflow hydrograph.

| Time (hr) | 1 | 2 | 3 | 4 | 5 | 6 |
|---|---|---|---|---|---|---|
| Instantaneous discharge ($m^3/s$) | 5 | 40 | 100 | 75 | 30 | 10 |

(a) Determine the percentage of attenuation in peak discharge as the hydrograph travels a distance of 10 km downstream using the Muskingum method with $X = 0.1$ and $K = 2.0$ hr. Assume that the initial outflow rate is 5 $m^3/s$.

(b) Also, it is known that the channel bank-full capacity 10 km downstream is 50 $m^3/s$, determine the overflow volume (in $m^3$) of outflow hydrograph exceeding 50 $m^3/s$.

9.3.12 From a storm event, the flood hydrographs at the upstream end and downstream end of a river reach were observed and are tabulated below.

| Time (hr) | Inflow ($m^3/s$) | Outflow ($m^3/s$) |
|---|---|---|
| 09:00 | 15 | 15 |
| 12:00 | 35 | 30 |
| 15:00 | 63 | 42 |
| 18:00 | 54 | 56 |
| 21:00 | 42 | 45 |
| 24:00 | 36 | 40 |

(a) Determine the Muskingum parameters $K$ and $X$ by an appropriate method of your choice.
(b) Determine the peak discharge for the following inflow hydrograph as it travels down the river.

| Time (hr) | 0 | 3 | 6 | 9 | 12 | 15 | 18 | 21 | 24 | 27 |
|---|---|---|---|---|---|---|---|---|---|---|
| Inflow ($m^3/s$) | 10 | 40 | 80 | 100 | 60 | 50 | 40 | 30 | 20 | 10 |

9.3.13 The following table contains observed inflow and outflow hydrographs for a section of river.

| Time (hr) | 0 | 1 | 2 | 3 | 4 | 5 | 6 |
|---|---|---|---|---|---|---|---|
| Inflow ($m^3/s$) | 200 | 400 | 700 | 550 | 400 | 300 | 200 |
| Outflow ($m^3/s$) | 200 | 215 | 290 | 410 | 440 | 420 | 380 |

(a) Determine the parameters $K$ and $X$ in the Muskingum model by the least-squares method.
(b) Based on the $K$ and $X$ obtained in part (a), determine the outflow peak discharge for the following inflow hydrograph. What is the percentage of attenuation (reduction) in peak discharge?

| Time (hr) | 0 | 0.5 | 1.0 | 1.5 | 2.0 | 2.5 | 3.0 |
|---|---|---|---|---|---|---|---|
| Inflow ($m^3/s$) | 100 | 400 | 300 | 200 | 100 | 100 | 100 |

9.3.14 From a storm event, the flood hydrographs at the upstream end and downstream end of a river reach are tabulated below.

| Time (hr) | Inflow ($m^3/s$) | Outflow ($m^3/s$) |
|---|---|---|
| 09:00 | 15 | 15 |
| 12:00 | 35 | 30 |
| 15:00 | 63 | 42 |
| 18:00 | 54 | 56 |
| 21:00 | 42 | 45 |

(a) Determine the Muskingum parameters $K$ and $X$ by the least-squares method of your choice.
(b) Based on the estimated values of $K$ and $X$ from part (a), determine the outflow peak discharge at the downstream end of the river reach for the following inflow hydrograph.

| Time (hr) | 0 | 2 | 4 | 6 | 8 |
|---|---|---|---|---|---|
| Flow rate ($m^3/s$) | 20 | 70 | 50 | 40 | 30 |

9.3.15 Given the following flood hydrograph entering the upstream end of a river reach, apply the Muskingum routing procedure (with $K = 4.0$ hr and $X = 0.2$) to determine:

(a) the peak discharge at the downstream end of the river reach;
(b) the time of its occurrence; and
(c) the percentage of peak flow attenuation.

Assume that the initial flow rate at the downstream end is 10 $m^3/s$.

| Time (hr) | 0 | 2 | 4 | 6 | 8 | 10 | 12 |
|---|---|---|---|---|---|---|---|
| Inflow ($m^3/s$) | 10 | 250 | 570 | 320 | 180 | 70 | 10 |

9.3.16 Consider the following flood hydrograph entering the upstream end of a river reach. Apply the Muskingum routing procedure (with $K = 6.0$ and $X = 0.2$) to:

(a) determine the peak discharge at the downstream end of the river reach; and
(b) find the time to peak at the downstream section.

Assume that the initial flow rate at the downstream end is 50 $m^3/s$.

| Time (hr) | 0 | 3 | 6 | 9 | 12 | 15 | 18 | 21 |
|---|---|---|---|---|---|---|---|---|
| Inflow ($m^3/s$) | 50 | 150 | 300 | 500 | 300 | 150 | 100 | 50 |

9.3.17 The Castro Valley watershed has a total watershed area of 5.51 $mi^2$ and is divided into four subcatchments as shown in Figure P9.3.17. The following table provides existing characteristics of the subcatchments.

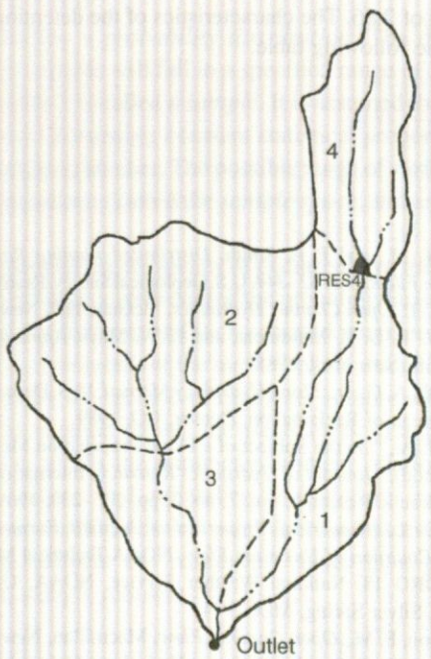


**Figure P9.3.17** Castro Valley watershed

| Subcatchment number | Area ($mi^2$) | Watershed length ($L$) (mi) | Length to centroid ($L_{CA}$) (mi) | SCS curve number |
|---|---|---|---|---|
| 1 | 1.52 | 2.65 | 1.40 | 70 |
| 2 | 2.17 | 1.85 | 0.68 | 84 |
| 3 | 0.96 | 1.13 | 0.60 | 80 |
| 4 | 0.86 | 1.49 | 0.79 | 70 |

Parameters for Snyder's synthetic unit hydrograph for existing conditions are $C_p = 0.25$ and $C_t = 0.38$. The Muskingum $K =$ 0.3 hr for area 3 and $K = 0.6$ hr for area 1. The Muskingum $X$ for each stream reach is 0.2. The rainfall to be used is the 100-year return period SCS type I storm pattern with a total rainfall of 10 in. Use the HEC-HMS model to determine the runoff hydrograph at the outlet of the watershed.

9.3.18 For the watershed described in problem 9.3.17, a residential development will be considered for area 4. This development will increase the impervious area so that the SCS curve number will be 85. The unit hydrograph parameters will change to $C_t = 0.19$ and $C_p = 0.5$. The natural channel through area 1 will be modified so that the Muskingum routing parameters will be $K = 0.4$ hr and $X = 0.3$. Use the HEC-HMS model to determine the change in the runoff hydrographs for area 4 and for the entire watershed.

9.3.19 Refer to problems 9.3.17 and 9.3.18. A detention basin is to be constructed at the outlet of area 4 with a low-level outlet and an overflow spillway (ogee type). The low-level outlet is a 5-ft-diameter pipe (orifice coefficient = 0.71) at a center line elevation of 391 ft above mean sea level (MSL). The overflow spillway has a length of 30 ft, crest elevation of 401.8 ft (above MSL), and a weir coefficient of 2.86. The characteristics of the detention basin are given in the following table.

| Reservoir capacity (ac-ft) | Elevation (ft above MSL) |
|---|---|
| 0 | 388.5 |
| 6 | 394.2 |
| 12 | 398.2 |
| 18 | 400.8 |
| 23 | 401.8 |
| 30 | 405.8 |

Use the HEC-HMS model to determine the runoff hydrograph at the watershed outlet for the developed conditions with the detention basin. Graphically show a comparison of the runoff hydrograph for the undeveloped, developed, and developed conditions with the detention basin.

9.3.20 Use the HEC-HMS model to solve problems 9.3.17, 9.3.18, and 9.3.19 considering the three as plans 1, 2, and 3 and solve through one simulation.

9.5.1 Determine the $\partial Q/\partial x$ on the time line $j+1$ for the linear kinematic wave model. Consider a 100-ft-wide rectangular channel with a bed slope of 0.015 ft/ft and a Manning's $n = 0.035$. The distance between cross-sections is 3000 ft and the routing time interval is 10 min. $Q_i^{j+1} = 1000$ cfs, $Q_i^j = 800$ cfs, and $Q_{i+1}^j = 700$ cfs. Use the linear kinematic wave (conservation form) approach to compute $\partial Q/\partial x$ on time line $j+1$.

9.5.2 Develop a flow chart of the linear kinematic wave (conservation form) method.

9.6.1 Determine the $\partial Q/\partial A$ using $Q_i^{j+1}$ and $Q_{i+1}^j$ for the Muskingum–Cunge model. Consider a 100-ft-wide rectangular channel with a bed slope of 0.015 ft/ft and a Manning's $n = 0.035$. The distance between cross-sections is 2000 ft and the routing time interval is 10 min. Given are $Q_i^{j+1} = 1000$ cfs, $Q_i^j = 800$ cfs, and $Q_{i+1}^j = 700$ cfs. Next compute $K$ and $x$ and then the routing coefficients.

9.6.2 Develop a flowchart of the Muskingum–Cunge method.

## REFERENCES


Alley, W. M., and P. E. Smith, *Distributed Routing Rainfall-Runoff Model, Open File Report 82–344*, U.S. Geological Survey, Reston, VA, 1987.

Chow, V. T., *Open Channel Hydraulics*, McGraw-Hill, New York, 1959.

Chow, V. T., D. R. Maidment, and L. W. Mays, *Applied Hydrology*, McGraw-Hill, New York, 1988.

Cudworth, A. G., Jr., *Flood Hydrology Manual*, U. S. Department of the Interior, Bureau of Reclamation, Denver, CO, 1989.

Cunge, J. A., "On the Subject of a Flood Propagation Method (Muskingum Method)," *Journal of Hydraulics Research*, International Association of Hydraulic Research, vol. 7, no, 2, pp. 205–230, 1969.

Fread, D. L., *Numerical Properties of Implicit Form-Point Finite Difference Equation of Unsteady Flow*, NOAA Technical Memorandum NWS HYDRO 18, National Weather Service, NOAA, U.S. Dept. of Commerce, Silver Spring, MD, 1974.

Henderson, F. M., *Open Channel Flow*, Macmillan, New York, 1966.

Hewlett, J. D., *Principles of Forest Hydrology*, University of Georgia Press, Athens, GA, 1982.

Lighthill, M. J., and G. B. Whitham, "On Kinematic Waves, I: Flood Movement in Long Rivers," *Proc. Roy. Soc. London* A, vol. 229, no. 1178, pp. 281–316, 1955.

Masch, F. D., *Hydrology*, Hydraulic Engineering Circular No. 19, FHWA-10-84-15, Federal Highway Administration, U.S. Department of the Interior, McLean, VA, 1984.

Strelkoff, T., "The One-Dimensional Equations of Open-Channel Flow," *Journal of the Hydraulics Division*, American Society of Civil Engineers, vol. 95, no. Hy3, pp. 861–874, 1969.

U.S. Army Corps of Engineers, "Routing of Floods Through River Channels," *Engineer Manual*, 1110–2–1408, Washington, DC, 1960.

U.S. Army Corps of Engineers, Hydrologic Engineering Center, *HEC-1, Flood Hydrograph Package, User's Manual*, Davis, CA, 1990.

Woolhiser, D. A., R. E. Smith, and D. C. Goodrich, *KINEROS, A Kinematic Runoff and Erosion Model: Documentation and User Manual*. U. S. Department of Agricultural Research Service, ARS-77, Tucson, AZ, 1990.

# Chapter 10

# Probability, Risk, and Uncertainty Analysis for Hydrologic and Hydraulic Design

## 10.1 PROBABILITY CONCEPTS

This section very briefly covers probability concepts that are important in the probabilistic, risk, and uncertainty analysis for hydrologic and hydraulic design and analysis. Table 10.1.1 provides definitions of the various probability concepts needed for analysis. Many hydraulic and hydrologic variables must be treated as random variables because of the uncertainties involved in the respective hydraulic and hydrologic processes. As an example, the extremes that occur are random hydrologic events and can therefore be treated as such.

A *random variable* $X$ is a variable described by a *probability distribution*. The distribution specifies the chance that an observation $x$ of the variable will fall in a specified range of $X$. A set of observations $x_1, x_2, \ldots, x_n$, of the random variable $X$ is called a *sample*. It is assumed that samples are drawn from a population (generally unknown) possessing constant statistical properties, while the properties of a sample may vary from one sample to another. The possible range of variation of all of the samples that could be drawn from the population is called the *sample space*, and an *event* is a subset of the sample space.

A *probability distribution* is a function representing the frequency of occurrence of the value of a random variable. By fitting a distribution to a set of data, a great deal of the probabilistic information in the sample can be compactly summarized in the function and its associated parameters. Fitting distributions can be accomplished by the method of moments or the method of maximum likelihood (see Chow et al., 1988). Between the two methods, the method of moments is more widely used, primarily for its computational simplicity. The method relates the parameters in a probability distribution model to the statistical moments to which the parameter-moment relationships for commonly used distributions in frequency analysis and reliability analysis are immediately available (see Table 10.1.2). In practice, the true mechanism that generates the observed random process is not entirely known. Therefore, to estimate the parameter values in a probability distribution model by the method of moments, sample moments are used.